Preparation of polymer-clay nanocomposites via dispersion polymerization using tailor-made polymeric surface modifiers

by

Nagi Greesh

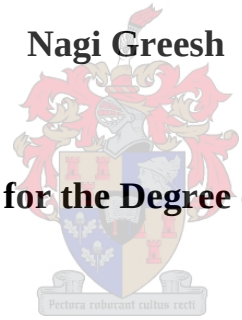

Dissertation presented for the Degree of Doctor of philosophy

(Polymer Science)

University of Stellenbosch

Promoter: Dr. P. C. Hartmann

Co promoter: Prof. R. D. Sanderson

December 2011

Declaration

I, Nagi Greesh, hereby declare that the work contained in this dissertation is my own original work and that I have not previously in its entirely or in part submitted it at any university for a degree.

December 2011

Stellenbosch

_____

Nagi Greesh

Abstract

Fully exfoliated polystyrene-clay nanocomposites were prepared via free radical polymerization in dispersion polymerization, in a mixture of ethanol and water. Sodium montomorillonite clay (MMT) was pre-modified using 3-(trimethoxysilyl) propyl methacrylate (MPTMS) before being used in a dispersion polymerization process. The particles obtained were not completely stable and TEM images showed that most of the clay platelets were distributed in the dispersing phase.

A second objective included, the preparation of low molecular weight of polystyrene (PS) and amphiphilic block copolymers of poly(styrene-b-2-hydroxyethyl acrylate) (PS-b-PHEA)using reverse iodine transfer polymerization (RITP) living/controlled free radical polymerization.The reaction kinetic profile of the RITP process for styrene and 2-Hydroxyethyl acrylate (HEA) was also studied. The formation of the block copolymer PS-b-PHEA was confirmed by GPC and gradient HPLC. The resulting PS-I and (PS-b-PHEA)-I were chemically modified by dimethylethylamine and triethylamine respectively, ended with PS and PS-b-PHEA has quaternary ammonium end-chain functionality (PS-cationic and (PS-b-PHEA)-cationic). The obtained functional polymers (PS-cationic) and (PS-b-PHEA)-cationic) were then grafted onto MMT via a simple ion-exchange process to offer MMT with polymer chains on the surface (PS-MMT) and (PS-b-PHEA)-MMT). Furthermore, the ability of the interaction ofPS-b-PHEA with MMT by adsorption via several functional groups was also investigated.

The third objectiveincluded the use of this new class of pre-modified clay PS-MMT in the preparation of PCNs as stabilizers, the clay particles were encapsulated into PS latexes with a partially exfoliated structure at 100% CEC, upon stoppage of the polymerization process, and the final dispersion found to be stable for up to 5 wt% of clay filler loading. The thermal and thermo-mechanical properties of PS-nanocomposites were found to be dependent on both nanocomposites morphology, and clay loading.

(PS-b-PHEA)-MMT was also used as stabilizers in the preparation of PS via dispersion polymerization. PS colloidal particles obtained were found to be armoured by (PS-b-PHEA)-MMT layers, with particles sizes in the micro-size range, with fair stability were obtained for clay loadings up to 5%. Analysis of the structure and thermo-mechanical properties of the resulting PCNs revealed the efficiency of the clay surface pre-modification in stabilizing the system throughout the heterophasic polymerization process.The melt flow properties of final PCNs were found to be strongly dependent on the clay loading, with shift observed from liquid-like viscoelastic to solid-like viscoelastic behaviour as the clay content increased due to percolation of the clay network within the PS matrix taking place upon film formation above T_g.

Opsomming

Die eerste doelwit was die voorbereiding van ten volle geëksfolieerde polistireen-klei nanosamestellings deur vrye radikaal polimerisasie in dispersie-polimerisasie, in 'n mengsel van etanol en water. Natrium montmorilloniet klei (MMT) is gemodifiseer deur gebruik te maak van 3-(trimetoksiesiliel) propiel metakrilaat (MPTMS), voordat dit gebruik is in die dispersie-polimerisasie. Die bekomde partikels was nie heeltemal stabiel nie. Transmissie elektronmikroskopie (TEM) resultate het getoon dat die meeste van die klei plaatjies in die dispersie-fase versprei is.

Die tweede doelwit was die voorbereiding van polistireen (PS) met ‘n lae molekulêre massa, gevolg deur die vorming van amfifiliese blok kopolimere van poli(stireen-b-2-hidroksie-etiel akrilaat) (PS-b-PHEA) met behulp van omgekeerde jodium oordrag polimerisasie (RITP) lewendige/gekontroleerde vrye radikaal polimerisasie. Die reaksie kinetiese profiel van die RITP proses was bestudeer met betrekking tot stireen en 2-hidroksie-etiel akrilaat (HEA). Die vorming van die blok kopolimeer PS-b-PHEA is bevestig deur GPC en gradiënt HPLC. Die gevolglike PS-I en (PS-b-PHEA)-I was chemies gewysig deur onderskeidelik dimetieletielamien en trietielamien, waardeur PS en PS-b-PHEA een kwaternêre ammonium ketting-endfunksionaliteit bekom het (PS-kationies en (PS-b- PHEA)-kationies). Laasgenoemde twee funksionele polimere was toe gekoppel aan MMT deur 'n eenvoudige ioon-ruilingsproses wat MMT met polimeerkettings op die oppervlak (PS-MMT) en (PS-b-PHEA)-MMT) tot gevolg het. Die interaksie van PS-b-PHEA met MMT deur middel van adsorpsie van verskeie funksionele groepe is ook ondersoek.

Die derde doel was gerig op die gebruik van hierdie nuwe klas gemodifiseerde klei PS-MMT as stabiliseerders vir die voorbereiding van polimeer-klei-nanosamestellings (PCNs). Die 100% CEC gemodifiseerde klei deeltjies is ge-inkapsuleer in die PS emulsies met 'n gedeeltelik geëksfolieërde struktuur, na afloop van die polimerisasie

proses. Die finale dispersie was stabiel tot en met ‘n klei inhoud van 5 wt%. Daar is gevind dat die termiese en termo-meganiese eienskappevan die PS-nanosamestellings afhanklik is van beide die morfologie en die klei inhoud.

(PS-b-PHEA)-MMT was ook gebruik as stabiliseerder in die voorbereiding van PS deur dispersie polimerisasie. Daar is gevind dat die PS kolloïdale partikels wat verkry is, versterk was deur (PS-b-PHEA)-MMT lae. Partikel groottes was in die mikro-grootte gebied, en voldoende stabiliteit is verkry vir ‘n klei inhoud van tot 5%. Analise van die struktuur en die termo-meganiese eienskappe van die bekomde PCNs het getoon dat die vooraf modifisering van die klei oppervlak doeltreffend was in die stabilisering van die sisteem gedurende die heterofase polimerisasie proses. Daar is ook gevind dat die smelt vloei eienskappe van die finale PCNs sterk afhang van die klei inhoud; 'n verskuiwing vanaf vloeistof-agtige viskoelastiese tot vaste-agtige viskoelastiese gedrag is waargeneem soos die klei-inhoud verhoog. Hierdie verskynsel was te danke aan perkolasie van die klei netwerk binne die PS matriks wat plaasvind tydens film vorming by ‘n hoër temperatuur as die glasoorgangstemperatuur (Tg).

Acknowledgements

Firstly, I would thank **Allah**, without whom this thesis would certainly not have been possible, and this degree not obtained. Thank you Allah for the prayers that were answered. You inspired- but most of all, thank you for the strength to persevere. I love You with all my heart.

Secondly, the Department of Chemistry and Polymer Science, the UNESCO centre for Macromolecules, MONDI packaging (South Africa), and Centre of Macromolecules and Materials Science (Libya) for their financial support and giving me the opportunity to study in this filed.

To my supervisor, Dr. Patrice Hartmann, for his guidance and his belief in me to always exert myself beyond the norm and to reach for the sky. He has broken the mould of immaturity and has sculptured a strong independent character within myself. For this I am eternally grateful.

To my co supervisor Prof. R.D. Sanderson, for the chance he gave to me to do something different and individual, and giving me the opportunity to finish it. Thank you Doc for the constant encouragement and your eternal optimism.

Dr. Margie Hurndall, is thanked for the time spent helping me write my thesis.

To all my Libyan friends, we have been together since we did our first degrees and now at PhD level we are still together, we were very great team, people I am going to miss you.

Lastly, **To my beloved parents, my sweet wife and my brothers and sisters,** who have stood by me through all the good and bad times. Thank you for giving me life and walking the distance with me.

List of contents

Chapter 5: Functionalization of Montmorillonite by Functional block copolymer

Chapter 6: Preparation of PS-clay nanocomposites via Dispersion Polymerization Using PS-MMT as Stabilizer

Chapter 8: Conclusions and recommendations

List of figures

Chapter 2

Chapter 3

Chapter 4

Chapter 5

Chapter 6

Chapter 7

List of tables

Chapter 2

Chapter 3

Chapter 5

Chapter 6

Chapter 7

List of publications

- Nagi Greesh, Patrice C. Hartmann and Ronald D. Sanderson. "Preparation of Polystyrene-Clay Nanocomposites by Free-radical Polymerization in Dispersion" *Molecular Materials and Engineering*, 2009, 294,787-794

- Nagi Greesh, Patrice C. Hartmann and Ronald D. Sanderson. "*Preparation of Polystyrene-Clay Nanocomposites via Dispersion Polymerization Using Oligomeric Styrene-Montmorillonite as Stabilizer*" Polymer international Accepted

- Nagi Greesh, Patrice C. Hartmann and Ronald D. Sanderson. "*Preparation of Polystyrene Colloid Particles Armoured by Clay Platelets via dispersion polymerization"* Polymer Accepted

- Nagi Greesh, Patrice C. Hartmann and Ronald D. Sanderson"*Preparation of Oligomeric (Styrene-b-2-Hydroxyethyl acrylate) Block Copolymer using Reverse Iodine Transfer Polymerization (RITP)*" Submitted to Applied Polymer science

- Nagi Greesh, Patrice C. Hartmann and Ronald D. Sanderson. "*Functionalization of Montmorillonite by End-Chain mono- Cationic Polystyrene and End-chain mono-Cationic Poly(Styrene-b-2-Hydroxethyl acrylate)*" submitted to Journal of Colloid and Interface Science

List of abbreviations

AMPS	2-acrylamido-2-methyl-1-propanesolphunicacid
AIBN	2,2azobis(isobutyronitrile)
BA-I	Iodo-terminated poly(butyl acrylate
°C	Degree Celsius
CTAB	Cetyltrimethylammonium bromide
CEC	Cation exchange capacity
CO_2	Carbon dioxide
d	Interlayer distance
DLS	Dynamic light scattering
DMA	Dynamic mechanical analysis
DMEA	N,N-dimethylethylamine
DMF	N,N-dimethylformamide
DHB	2,5-dihydroxybenzoic acid
FT-IR	Fourier Transform Infrared
ITP	Iodine transfer polymerization
G’	Storage modulus
G”	Loss modulus
GPC	Gel permeation chromatography

HEA	2-Hydroxyethayl acrylate
HPLC	High-performance liquid chromatography
HPC	Hydroxypropyl cellulose
LVE	Linear viscoelastic
MMT	Montmorillonite clay
MPTMS	3-(trimethoxysilyl) propyl methacrylate
M_n	Number average molecular mass
M_W	Weight average molecular weight
M_W/M_n	Polydispersity index
NMP	Nitroxide-mediated polymerization
NMR	Nuclear magnetic resonance
PCNS	Polymer-clay nanocomposites
PBA	Poly(butyl acrylate)
PEO	Poly(ethylene oxide)
PS	Poly(polystyrene)
PS-b-PHEA	Poly(styrene-b-2-hydroxyethyl acrylate
PS-cationic	Cationic polystyrene
PS-b-PHEA-cationic	Cationic poly(styrene-b-2-hydroxyetyl acrylate)
PS-co-BA	Poly(styrene-co-butyl acrylate)
PS-I	Iodo-polystyrene
(PS-b-PHEA)-I	Iodo-poly(styrene-b-2-hydroxyetyl acrylate)

PS-MMT	Poly(styrene) grafted to clay
(PS-b-PHEA)-MMT	Poly(styrene-b-2-hydroxyetyl acrylate) grafted to clay
PHEA	Poly(2-hydroxyethyl acrylate)
PVA	Poly(vinyl alcohol)
RAFT	Reversible addition-fragmentation chain transfer polymerization
RITP	Reverse iodine transfer polymerization
SAXS	Small angle scattering
SEM	Scanning electron microscopy
TEA	Triethylamine
TEM	Transmission electron microscopy
TGA	Thermogravimetric analysis
Tg	Glass transition temperature
THF	Tetrahydrofuran
UV	Ultraviolet
WAXD	Wide angle X-ray diffraction
Wt	Weight
XRD	X-ray diffraction

Introduction and Objectives

1.1 Introduction

Often polymeric materials are requiredto exhibit certain properties to satisfy specific applications. One of the ways in which the properties of a polymer can be modified is by the addition of a second selected component.[1,2] New composite materials can then be produced with improved properties. Inorganic fillers are commonly used as a second component in polymers to reduce the cost and to modify a variety of physical properties, such as stiffness, strength, thermal stability, etc.[3-5]Different types of fillers are presently being used in industry, such as glass fibres, mineral fillers, metallic fillers, etc. In conventional composite materials these types of fillers range in size from several microns to a few millimetres.[3,6,7]

Clay is one of the most abundant natural and inexpensive inorganic filler materials. Clay was introduced in the nanotechnology field as a new type of filler to produce polymer-clay nanocomposites (PCNs).[2,3,8-11] Depending on the ordering and degree of clay dispersion in a polymer matrix there are three types of nanocomposites that can be distinguished (i.e. conventional composites, intercalated and exfoliated nanocomposites).[10,12]

The preparation of PCNs requires a good compatibility between the clay surface and the polymers or monomers.[3,10,11] The swellable clays, such as montmorillonite (MMT) are hydrophilic and therefore incompatible with hydrophobic polymers or monomers.[13,14] Furthermore, the clay platelets are bound to each other by Van der waals forces, which make the interlayer in the clay very narrow. The hydrophilicity of clay can be changed by surface modification.[10,13] The surface modification of clay can be typically performed by ion exchange of surface inorganic cations (e.g. Na^+, K^+, Ca^{2+}) by organic cationic

surfactants. Polymer and oligomers with quaternary ammonium have been also used to modify the clay surface to obtain polymer-modified clay.[10,11,15-19] Most of these polymers have been prepared by conventional polymerization, but the resultant modified polymer has only limited applications. The study presented in this thesis based on the preparation of polymers using Reverse Iodine Transfer living/controlled Polymerization, (RITP). RITP is a simple and fast method to prepare polymers with controlled molecular weight.[20-22] Another advantage of using RITP in this particular study is that the resultant polymer (i.e. iodine-functionalized polymers), iodine can easily be replaced by quaternary ammonium groups in order to obtain the desired polymer structure (i.e. cationic polymer) that can be used to modify the clay in order to obtain a polymer-modified clay. Polymersgrown from clay surfaceshave been widely reported. In most casescontrolled free radical polymerization systems, such as atom transfer radical polymerization ARTP[23-25] and reversible addition fragmentation polymerization RAFT[25-28] were used. To date the combination of RITP technology and clay nanotechnology has not been reported.

Many researchers have focused on the preparation of PCNs latexes using emulsion and miniemulsion polymerization, and some studies showed that clay can be successfully exfoliated under these conditions.[13,29-34] Dispersion polymerization is one type of technique used to produce a polymer latex. It is a simple and fast method to obtain monodisperse polymer particles of range of 1-20 µm, in very good yields.[35] The polymerization of a monomer in dispersion polymerization carried out in the presence of a second polymer soluble in the reaction medium.[36]Because this second polymer can act as a steric stabilizer to prevent the flocculation of growing particles it must be amphiphilic,[37] it must contain both an anchor segment, with affinity for the final polymer particles, and a solvent soluble segment. Three types of steric stabilizers have been used: homopolymers, block and graft copolymers, and macromonomers.[38] To date there are only few articles that reported on the preparation of PCNs via dispersion polymerization, and only intercalated and partially exfoliated structures have been obtained.[39]

Over the past decade, another highly interesting research area in the nanocomposites field is the use of organically modified clay as stabilizers. Some researcher groups prepared PCNs latex particles via Pickering emulsion polymerization or inverse emulsion polymerization and suspension polymerization.[40,41] The degree of hydrophobicity of the solid particles plays an important role. In aqueous emulsion, if the particles are too hydrophobic they will remain in the oil phase, and if the particles are too hydrophilic, they will remain in the aqueous phase.[42,43] Once again, the treatment of a clay surface with organic modifier is an essential requirement to obtain stable polymer latex. Most recently, many researchers have focused on preparing polymers brushes from the clay surface, and then successfully used them as stabilizers to obtain stable polymer latexes in emulsion, miniemulsion and suspension polymerizations.[23,40,41] According to the literatures, stable polymer latex can be obtained by the generation of armoured polymer particles (i.e. where the clay platelets are on the polymer surface), by reducing of the interfacial tension between the colloidal particles and water.[23,40,41,44] Furthermore, the encapsulation of inorganic particles on to polymer latex particles also results in good polymer latex stability.[27,45,46] To date, only polymer-clay latexes obtained via emulsion, miniemulsion and suspension techniques have been reported, while the preparation of PCNs latexes via dispersion polymerization in polar medium has not been reported yet.

1.2 Objectives

The overall objective is to check a new route to exfoliate clays into polymers using dispersion polymerization in a mixture of ethanol and water. In this study the clay platelets are used as fillers to improve the thermal and mechanical properties of the final PCNs, and as steric stabilizers in dispersions polymerization after modification with low molecular weight polymers prepared using RITP.

Therefore there were three main objectives:

1- Synthesis of functional polymer and amphiphilic copolymer using RITP.
2- The modification of MMT using the synthesized functional polymer and copolymer, in order to obtain polymer-modified clay.
3- The use of the polymer-modified clay as stabilizers in dispersion polymerization.

Accordingly, the specific tasks envisaged were the following:-

- Syntheses of fully exfoliated polystyrene-clay nanocomposites via dispersion polymerization in polar medium (ethanol/water), using 3-(trimethoxysilyl) propyl methacrylate (MPTMS) as organic modifier. Characterization of the PCN latex obtained in terms of its colloidal properties, structure, polymer matrix and composite morphology, thermal stability and thermo-mechanical properties.

- Synthesis of polystyrene (PS) and poly (2-hydroxyethyl acrylate) (PHEA) using controlled/living polymerization via RITP and study the ability of the styrene and HEA monomers to be polymerized in a controlled manner in the RITP process. Determine the final polymer composition using ^{1}H-NMR and MALDI-TOF. Preparation of amphiphilic block copolymers of poly(styrene-b-2-hydroxyethyl acrylate) (PS-b-PHEA) using RITP, and determine the living nature of the RITP process using GPC and HPLC.

- Preparation of cationic PS and cationic PS-b-PHEA via polymer modification by Menshutkin reaction[47] between iodine-PS and N.N-dimethylethylamine, iodine-PS-b-PHEA and triethylamine, respectively. Characterization of cationic PS and cationic PS-b-PHEA by FT-IR, ^{1}H-NMR, and MALD-TOF. Use of the cationic PS and cationic PS-b-PHEA to modify MMT, to obtain polymer-modified clay (PS-MMT) and ((PS-b-PHEA)-MMT). Characterization of PS-MMT and (PS-b-PHEA)-MMT using FT-IR, TGA and SAXS. Determinations of PS-b-PHEA ability to surface modify via adsorption onto clay to obtain (PS-b-PHEA)-MMT and characterize using FT-IR, TGA and SAXS.

- Preparation of PCNs via dispersion polymerization, using PS-MMT as stabilizer. Determine the effect of clay's hydrophobicity on the stability and morphology of polystyrene latexes, by using three different concentrations of PS-cationic (i.e. 25%, 65% and 100% CEC) to control the clay hydrophilicity. Characterization of the polymer latex in terms of monomer conversion, polymer particle sizes and

polymer latex morphology. Study of the morphology of the PCNs. Determination of the thermal stability of the synthesized nanocomposites using TGA, and comparison their thermal stability to that of the pure polymer. Determination of the mechanical properties and $T_g$of the synthesised nanocomposites using DMA and comparison with those of the virgin polymer.

- Preparation of a PS latex armoured by clay layers using (PS-b-PHEA)-MMT as stabilizer. Characterize the PCNs latex obtained in terms of colloidal properties and structure. Determination of the effect of (PS-b-PHEA)-MMT loading on the thermal stability and thermo-mechanical properties of the polymer matrix using TGA and DMA, respectively. The melt rheology properties of PCNs were also investigated.

1.3 Layout of dissertation

This dissertation is written in the "publication style". Chapters 3-7 have been either published or submitted as in their present form. The first and last chapters contain introductions objectives, and conclusions, respectively, as relevant to the entire study, Chapter 2 presents historical and background to the entire study.

1.3.1 Chapters layout

Chapter 1 contains a brief introduction to PCNs and the objectives of this study are described.

Chapter 2 presents an important overview in the literature background on various methods of synthesis of PCNs, focusing on dispersion polymerization, and on the techniques commonly used for the characterizationof PCNs. General methods used to modify clay are also described, and the use of clay platelets as stabilizers of colloidal particles is reviewed. The need for the research undertaken in this study is highlighted.

Chapter 3 describes the synthesis of PS-nanocomposites via free-radical polymerization using dispersion polymerization in polar medium (ethanol/water), and physico-chemical characterization the nanocomposites obtained. The modification of clay was carried out

using MPTMS prior being used in the polymerization systems. The effect of clay loadings on particle sizes and distribution of polystyrene colloidal particles were determined.

Chapter 4 describes the synthesis of PS, PHEA and amphiphilic block copolymer of PS-b-PHEA via RITP, with the aim of achieving product with predetermined molecular weight and molecular weight distribution.

Chapter 5 describes the preparation of cationic polystyrene (PS-cationic) by polymer modificationby Menshutkin reaction[47] between iodine-PS macroinitiator and N.N-dimethylethylamine. PS-cationic was then used to modify the clay surface via an ion-exchange process in order to obtain polystyrene- modified clay (PS-MMT). Cationic PS-b-PHEA ((PS-b-PHEA)-cationic) was also obtained by polymer modification between iodine-(PS-b-PHEA) and triethylamine. (PS-b-PHEA)-cationic was used to modify MMT surface via ion-exchange process in order to obtain (PS-b-PHEA)-MMT. Furthermore, the amphiphilic block copolymer of PS-b-PHEA was adsorbed directly onto the clay and the formation of (PS-b-PHEA)-MMT was fully characterized using TGA, FT-IR and SAXS.

Chapters 6 and 7 describe the synthesis and characterization of PCNs obtained by making use of dispersion polymerization. PS-MMT and (PS-b-PHEA)-MMT were used in dispersion polymerization as stabilizers.

Chapter 8 presents conclusions to this study and recommendations for future work.

1.3 References

1. Nalwa, H. S., Polymer/clay Nanocomposites. In *Encyclopedia of Nanoscience and Nanotechnology*, American Scientific Publishers: California, **2004**; Vol. 8, pp 791-843.

2. Paul, D. R.; Robeson, L. M. *Polymer* **2008,** 49, 3187-3204.

3. Utracki, L. A.; Kamal, M. R. *The Arabian Journal for Science and Engineering* **2002,** 27, 43-67.

4. Pramoda, K. P.; Liu, T.; Liu, Z.; He, C.; Sue, H. *Polymer Degradation and Stability* **2003,** 81, 47-56.

5. Vuorinen, A.; Dyer, S.; Lassila, L.; Vallittu, P. *Dental Materials* **2008,** 24, 708-713.

6. Eitan, A.; Fisher, F. T.; Andrews, R.; Brinson, L. C.; Schadler, L. S. *Composites Science and Technology* **2006,** 66, 1162-1173.

7. Okada, A.; Usuki, A. *Journal of Materials Research* **1995,** 3, 109-117.

8. Rosorff, M., Polymer-Clay Nanocomposites. In *Nano Surface Chemistry*, Marcel Dekker Inc: New York and Basel, **2002**; pp 653-673.

9. Okamoto, M. *Rapra Review Reports* **2003,** 14, 1-40.

10. Alexandre, M.; Dubois, P. *Materials Science and Engineering: A* **2000,** 28, 1-63.

11. Ray, S.; Okamoto, M. *Progress in Polymer Science* **2003,** 28, 1539-1641.

12. Lebaron, P. C.; Wang, Z.; Pinnavaia, T. J. *Applied Clay Science* **1999,** 15, 11-29.

13. Noh, M. W.; Lee, D. C. *Polymer Bulletin* **1999,** 42, 619-626.

14. Yariv, S.; Cross, H., Organo-Clay Complexes and Interactions. In Marcel Dekker, Inc: New York and Basel, **2002**; pp 1-101.

15. Su, S.; Jiang, D.; Wilkie, C. *Polymer Degradation and Stability* **2004,** 83, 333-346.

16. Su, S.; Jiang, D.; Wilkie, C. *Polymer Degradation and Stability* **2004,** 84, 279-288.

17. Biasci, L.; Aglietto, M.; Ruggeri, G.; Ciardelli, F. *Polymer* **1994,** 35, 3296-3304.

18. Huskic, M.; Zagar, E.; Zigon, M.; Brnardic, I.; Macan, J.; Ivankovic, M. *Applied Clay Science* **2009,** 43, 420-424.

19. Huskic, M.; Brnardic, I.; Zigon, M.; Ivankovic, M. *Journal of Non-Crystalline Solids* **2008,** 354, 3326-3331

20. Lacroix-Desmazes, P.; Severac, R.; Boutevin, B. *Macromolecules* **2005,** 38, 6299-6309.

21. Lacroix-Desmazes, P.; Severac, R.; Boutevin, B. *Polymeric Preprints* **2003,** 44, 683-684.

22. Enriquez-Medrano, F.; Guerrero-Santos, R.; Hernandez-Valdez, M.; Lacroix-Desmazes, P. *Journal of Applied Polymer Science* **2010,** 119, 2476-2484.

23. Yang, Y.; Liu, L.; Zhang, J.; Li, C.; Zhao, H. *Langmuir* **2007,** 23, 2867-2873.

24. Yang, Y.; Zhang, J.; Liu, L.; Li, C.; Zhao, H. *Journal of Polymer Science Part A: Polymer Chemistry* **2007,** 45, 5759-5769.

25. Tasdelen, M.; Kreutzer, J.; Yagci, Y. *Macromolecular Chemistry and Physics* **2010,** 211, 279-285.

26. Samakande, A.; Sanderson, R.; Hartmann, P. *Journal of Polymer Science Part A: Polymer Chemistry* **2008,** 46, 7114-7126.

27. Samakande, A.; Sanderson, R.; Hartmann, P. *Polymer* **2009,** 50, 42-49

28. Samakande, A.; Juodaityte, J. J.; Sanderson, R. D.; Hartmann, P. C. *Macromolecular Materials and Engineering* **2008,** 293, 428-437.

29. Choi, Y. S.; Wang, K. H.; Xu, M.; Chung, I. J. *Chemistry of Materials* **2001,** 14, 2936-2939.

30. Choi, Y. S.; Choi, M. H.; Wang, K. H.; Kim, S. O.; Kim, Y. K.; Chung, I. J. *Macromolecules* **2001,** 34, 8978-8985.

31. Zeng, C.; Lee, L. J. *Macromolecules* **2001,** 34, 4098-4103.

32. Qutubuddin, S.; Fu, X.; Tajuddin, Y. *Polymer Bulletin* **2002,** 48, 143-149.

33. Xu, M.; Choi, Y. S.; Kim, Y. K.; Wang, K. H.; Chung, I. J. *Polymer* **2003,** 44, 6387-6395.

34. Khatana, S.; Dhibar, A.; Ray, S.; Khatua, B. *Macromolecular Chemistry and Physics* **2009,** 210, 1104-1113.

35. Saenz, J. M.; Asua, J. M. *Journal of Polymer Science Part A: Polymer Chemistry* **1996,** 34, 1977-1992.

36. Kawaguchi, S.; Winnik, A.; Ito, K. *Macromolecules* **1996,** 29, 4465-4471.

37. Kawaguchi, S.; Winnik, M.; Ito, K. *Macromolecules* **1995,** 28, 1159-1167.

38. Gibanel, S.; Heroguez, V.; Forcada, J. *Journal of Polymer Science Part A: Polymer Chemistry* **2007,** 39, 2767-2777.

39. Zhao, Q.; Samulski, E. T. *Polymer* **2005,** 47, 663-671.

40. Zhang, J.; Chen, K.; Zhao, H. *Journal of Polymer Science Part A: Polymer Chemistry* **2008,** 46, 2632-2639.

41. Wu, Y.; Zhang, J.; Zhao, H. *Journal of Polymer Science Part A: Polymer Chemistry* **2008,** 47, 1535-1543.

42. Voorn, D.; Ming, W.; van Herk, A. M. *Macromolecules* **2006,** 39, 4654-4656.

43. Bourgeat-Lami, E.; Lang, J. *Journal of Colloid and Interface Science* **1999,** 210, 281-289.

44. Putlitz, B.; Landfester, K.; Fischer, H.; Antonietti, M. *Advanced Materials* **2001,** 13, 500-504.

45. Voorn, D.; Ming, W.; van Herk, A. M. *Macromolecular Symposia* **2006,** 245, 585-590.

46. Tiarks, F.; Landfester, K.; Antonietti, M. *Macromolecular Chemistry and Physics* **2001,** 202, 51-60.

47. Smith, M.; March, J., March's Advanced Organic Chemistry In Wiley: New Jersey, **2007**; pp 395-656.

Chapter 2

Polymer-clay Nanocomposites: Theoretical Background

2.1 Introduction

Polymer materials can be filled with different inorganic synthetic and/or natural compounds in order to improvecertain properties such as heat resistance, mechanical strength and impact resistance, or to reduce other properties, like electrical conductivity or permeability for gases such as oxygen or water vapour.[1]The degree of reinforcement depends on the rigidity and aspect ratio of the filler itself, and the force adhesion between filler and polymer matrix. Some of the nanoparticles studied to date included nanofibres, carbon nanotubes, graphene sheets and clays.[2-4] The advantages of using clays as fillers for polymers are their availability, low cost, and high aspect ratio (i.e. surface to volume or length to thickness with platelets).[2]Typically there are several methods used to prepare polymer-clay nanocomposites (PCNs) such as solution, melt blending, template, and in-situ intercalative polymerization.

There are many reports on the synthesis of PCNs by in situ intercalative polymerization, such as emulsion[5], miniemulsion[6] and suspension.[7] However, only a very few articles report on the preparation of PCNs using dispersion polymerization, and there only intercalated morphology was observed.[8] Dispersion polymerization is known as an useful method to prepare monodisperse polymer particles, with sizes ranging from 1 to 10 μm. Micron-size monodisperse polymer particles are used in wide variety of applications, such as toners, column backing materials for chromatography, and biomedical and biochemical analysis.[9,10]

2.2Types and structures of clay minerals

Clay minerals are called layered silicates because of their stacked structure of 1-nm silicate sheets with a variable basal distance.[11] Generally, there are two building blocks

that can form the silicate layer clays, as shown in Fig. 2.1, the silica (Si) being tetrahedral and the alumina (Al) being octahedral.[11]

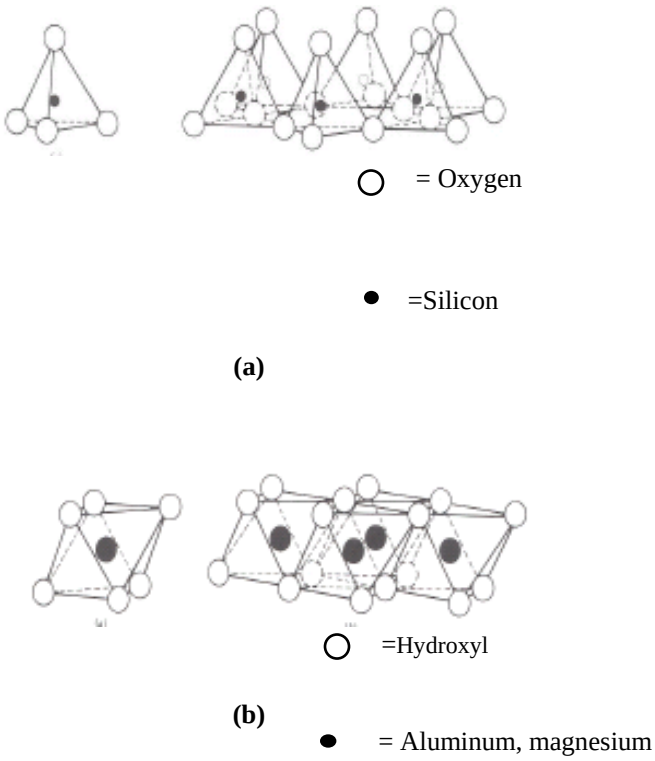

Fig. 2.1: a) Silica tetrahedron and tetrahedral units arranged in a hexagonal network, and b) cation octahedron and octahedral units arranged in a sheet.[11]

The silica tetrahedral groups are arranged to form a sheet of tetrahedron units, and the alumina octahedral units are joined together to form a sheet of octahedral units. Depending on the number and combination of structural units (tetrahedral and octahedral sheets), the clay minerals can be divided into two types, 1:1 and 2:1 phyllosilicates.[11,12]

(i) 1:1 phyllosilicates:"Non-swelling" clays such as kaolinite consist of units of single sheets of silica tetrahedra between alumina octahedral sheets.[13]

(ii) *2:1 phyllosilicates*: These are known as "swelling" clays, where the layer of minerals is composed of one central octahedral sheet sandwiched between two tetrahedral sheets, condensed in one unit layer designated as 2:1. The most common clays that have a 2:1 structure are smectites (e.g. montmorillonite, saponite, etc.), mica, and chlorites.[13]

The layered silicates used to form nanocomposites belong to the same structure of 2:1 phyllosilicates. Their crystal lattice consists of two-dimensional, 1-nm thick layers, which are made up of two tetrahedral sheets of silica fused to an edge-shaped octahedral sheet of alumina or magnesia. Depending on the particular silicate the lateral dimensions of the layers can be about 300 Å or more. The layers organize themselves to form stacks with regular Van der Waals gaps in between them, called the interlayer or the gallery.[1,11,12,14-16]

Naturally the layers undergo isomorphic substitution within them, which includes replacement of one ion for another of similar size (for example, Al^{3+} is replaced by Mg^{2+}or by Fe^{2+}, or Mg^{2+} is replaced by Li^{+}). This leads to a change in the total charge and the location of the charge on the mineral.[11,12,17,18] Isomorphic substitution within the layer generates negative charges that are normally counterbalanced by hydrated alkali or alkaline earth cations (such as Na^{+}, K^{+} and Ca^{2+}) residing in the interlayer.[15,16] Because of the relatively weak forces between the layers, interaction of various molecules, and even polymers, with the layers surface are possible.

Ion-exchange reactions with cationic surfactants, including primary, tertiary and quaternary ammonium or phosphonium, render the normally hydrophilic silicate surface organophilic, which makes possible the intercalation of many non-polar polymers. The role of the alkyl ammonium cations in the organosilicates is to reduce the surface energy of the inorganic host and improve the wetting characteristics with polymers.[11,12,19-21]

The commonly used layered silicates are montmorillonite (MMT), hectorite and saponite.[15,16] Details of the structure and chemistry of these layered silicates are given in Fig. 2.2 and Table 2.1.

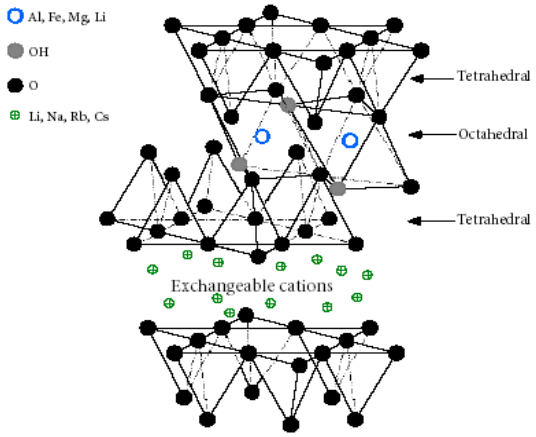

Fig. 2.2: Structure of 2:1 phyllosilicates.[19]

All of these silicates are characterized by a large active surface area (700-800 m^2/g in the case of MMT), a moderate negative surface charge (cation exchange capacity) and layer morphology.[1,19] The layer charge indicated by the chemical formula is only to be regarded as an average over the whole crystal because the charge varies from layer to layer (within certain links). Only a small proportion of the charge-balancing cations are located at the external crystal surface, with the majority being present in the interlayer space.[22]

Table 2.1: Formula of commonly used 2:1 layered phyllosilicates[12]

2:1 phyllosilicate	General formula
Montmorillonite	$M_x (Al_{4-x} Mg_x) Si_8 O_{20} (OH)_4$
Hectorite	$M_x (Mg_{6-x} Li_x) Si_8 O_{20} (OH)_4$
Saponite	$M_x (Mg_x) (Si_{8-x} Al_x) O_{20} (OH)_4$

The cations are exchangeable for others in aqueous solution. The presence of the cations in the galleries of silicate makes the silicate layers completely hydrophilic, and completely compatible with hydrophilic polymers such as poly(ethylene oxide) (PEO) and poly(vinyl alcohol) (PVOH).[16] On the other hand, these silicate layers are poorly compatible with hydrophobic polymers as the stacks of clay platelets are held tightly together by electrostatic forces.[16,23]

Fig. 2.3 shows that the counterions are attracted to the net negative charge within the clay platelets. The counterions can be shared by two neighbouring platelets, resulting in stacks of platelets that are held tightly together. This makes the penetration of polymers or monomer(s) into the galleries of silicate more difficult. For these reasons, the clay must be treated before it can be used to make nanocomposite materials.[23]

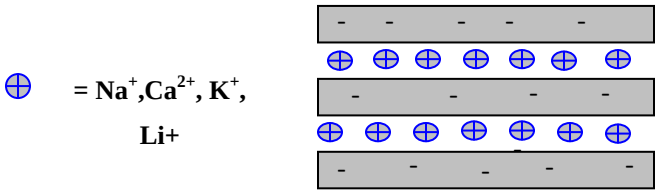

Fig. 2.3: The arrangement of charges on the surface of silicate layers.

2.3 Modification of clay

The mechanical properties of nanocomposites are affected by the dispersion state of silicate particles in the polymer matrix.[24] PCNs usually have improved mechanical and thermal properties when the dispersion of silicate layers in the polymer matrix is high (exfoliated structure).[12,24-26]There are two main issues to be addressed to prepare successfully polymer-clay nanocomposites. The first one is the high hydrophilicity of silicate layers that makes them incompatible with hydrophobic polymers. The second is the narrow basal spacing of silicate layers that makes the penetration of polymer into the silicate interlayer very difficult.[12,26] In order to overcome these problems, the clay surface must be modified.

The modification of clay to render it 'organophilic' is an essential requirement for the successful formation of PCNs. Bergaya and Lagaly[27] have reported different ways to modify 2:1 clay minerals: (1) ion exchange with organic cations, (2) adsorption, (3) binding of inorganic and organic cations, (4) grafting of organic compounds, (5) reaction with acids (6) physical treatment such as by ultrasound and plasma and (7) reaction with silane compounds. Ion exchange with organic cations, absorption and reaction with silane compounds will be discussed in more detail in the following three sections respectively.

2.3.1 Ion-exchange with organic cations

A popular and relatively easy method of modifying the clay surface, making it more compatible with an organic matrix, is ion exchange.[27] The cations are not strongly bound to the clay surface, so small cationic molecules can replace exchangeable cations present on the clay surface.

The most common cationic surfactants used in ion-exchange reactions for the synthesis of PCNs are primary, secondary, and quaternary alkyl ammonium or alkylphosphonium cations.[16] The exchange of inorganic cations by organic ions in clay galleries not only makes the organoclay surface compatible with the monomer or polymer matrix but also decreases the interlayer cohesive energy of clay platelets by expanding the d-spacing, i.e. more room is created for polymer chains to enter into these spaces. This facilitates the penetration of polymers or monomers into the clay galleries.[12,15,28] Fig 2.4 shows the surface modification of MMT clay via ion-exchange reaction.

Depending on the charge density of the clay and the ionic surfactant, different arrangements of the ions are possible. In general, the longer the surfactant chain length and the higher the charge density of the clay, the further apart the clay layers will be forced. This is expected, since both of these parameters contribute to increasing the volume occupied by the intergallery surfactant. [15]

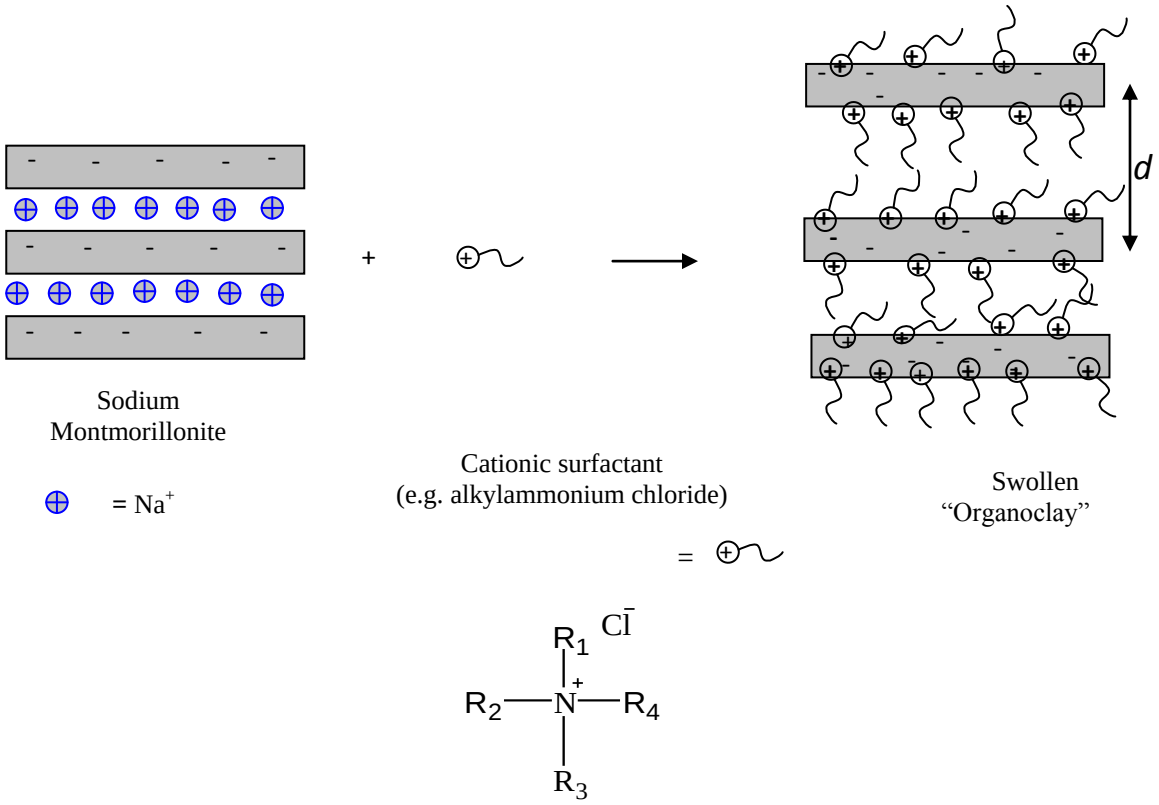

Fig. 2.4: Schematic representation of clay surface treatment by an ion-exchange reaction.

The total number of replaceable small inorganic cations is governed by the moderate negative surface charge called the cation exchange capacity (CEC), i.e. the maximum number of exchangeable sites. Different types of clays have different CEC values they range from 80-120 meq/100 g of clay (milliequivalent per 100 g of clay).[19]

The morphology and properties of nanocomposites are often greatly influenced by the properties of the organic cations used as clay modifiers. Zhang *et al*.[29] investigated the effects of reactive intercalating agents (clay modifiers) with different lengths of alkyl chains on the morphology and properties of polystyrene-nanocomposites (PS-nanocomposites). They synthesized different PS-nanocomposites by using ion-exchange reactions, using four different surfactants. Exfoliated structures were obtained when reactive surfactants that had polymerizable groups were used, while intercalated structures were obtained when non-reactive surfactants were used.

Surfactants used for the synthesis of PS-nanocomposites range from alkyl to aromatic-containing ammonium surfactants.[29,30] The polar head of a surfactant clay modifier plays an important role in terms of the structure of nanocomposites. Intercalated structures were obtained with a surfactant having a methyl group (CH_3)in the polar head, while exfoliated PS-nanocomposite were achieved with a surfactant having a benzyl in the polar head group. Both of these nanocomposites structures were achieved under similar conditions, using suspensionpolymerization. The presence of the benzyl group improved the compatibility with styrene (St) so that formation of the exfoliated structure was easier. PS-clay nanocomposites with organo-MMT-containing benzyl units similar to St show a higher thermal stability than other PS-organo-MMT nanocomposites. This indicates that the structure and properties of the surfactant used in the preparation of organo-MMT, plays a very important role in determining the properties of the final PCNs.[31]

The clay surface also can be modified using oligomers or polymers. The preparation and the use of oligomerically-modified clay to obtain PCNs have been extensively reported.[32] For example butadiene-modified clay was prepared by ion-exchange between sodium montmorillonite (Na^+-MMT) and a butadiene surfactant. The butadiene surfactant was obtained from the reaction between vinylbenzyl chloride grafted polybutadine with a tertiary amine. Then nanocomposites of PS, high impact polystyrene, acrylonitrilebutadienestyrene terpolymer, poly(methyl methacrylate), polypropylene and polyethylene were prepared by melt blending this modified clay with the virgin polymers.[33] The ion exchange of cationic surfactants onto a homo-ionic MMT dispersed in water was found to be independent of the size of the hydrophilic polar head group of the cationic surfactant, and its pH.[22]

2.3.2 Modification by adsorption

There are several reasons why researchers in the field of nanocomposites sought alternative methods to modify clay surfaces. The low thermal stability of quaternary ammonium compounds commonly used to modify the clay surface generally leads to decomposition products that impart undesirable colour and odour, with subsequently poorer composite properties.[34] In addition, the commercial availability of quaternary

ammonium compounds is limited. In order to obtain fully exfoliated nanocomposites the modifier should be thermodynamically compatible with the polymer. Here, in order to produce nanocomposites, alternative methods to modify the clay are used. The physicochemical properties of mineral clay allow the interaction between clay and non-cationic organic molecules to take place.

Interactions between organic molecules and clay are very common in nature. Such interactions include cation exchange (explained in the previous section), and adsorption of polar and non-polar molecules.[13] The organic molecules that have partial negative charge can interact with exchangeable cations via the formation of ion-dipole bonds. Therefore such organic molecules can be used as clay modifiers. This phenomenon was first applied with different types of glycols.[34] The organic polar molecules can be adsorbed by mineral clay by the formation of a coordination bond between the exchangeable cation and the organic molecules or by proton transfer from interlayer water to the organic molecules, or vice versa.[13]

Neutral molecules penetrate into the interlayer spaces of clay when the energy that results from the adsorption process is sufficient to overcome the interaction between silicate layers. Clay can form interlayer complexes with many types of uncharged molecules. The presence of water molecules in the interlayer space of the clay (see Fig. 2.5) leads to the creation of some competition between water molecules and uncharged organic molecules for ligand positions around the exchangeable cations. The adsorption of uncharged organic molecules increases as the concentration of organic molecules increases and as the volume of water in the system is lowered.

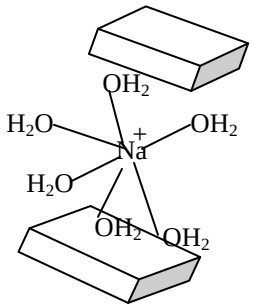

Fig. 2.5: Representation of the arrangement of water molecules around Na^+ ions.[13]

Some studies have been carried out on the interaction between clay and organic molecules, such as amide compounds. The interaction between amides and Na^+-MMT was investigated by Tahoun and Mortland.[35] When amides are adsorbed by Na^+-MMT they can be partially protonated. The degree of protonation depends on the acid strength of exchangeable cations and the polarization of the adsorbed water by the cations. Both functional groups of an amide (carbonyl and amine) form hydrogen bonds with water molecules. In this case water molecules works as bridges between the amide molecules and exchangeable cations in the silicate interlayer. The interaction between urea molecules and clay was studied by Mortland.[36] Molecular urea is bound to the exchangeable cation via water molecule bridges. The carboxylic group (C=O) of the urea molecules coordinates the metallic cation. Greesh *et al.*[37] studied the adsorption of 2-acrylamido-2-methyl-1-propanesulfonic acid (AMPS) and found that AMPS can adsorb onto the surface of the clay galleries in two ways: first, by formation of hydrogen bonds between the amido groups and water molecules surrounding the exchangeable cations and second by formation of ion-dipole interactions between the sulfonate groups and the interlayer exchangeable cations.

Not only the small molecules can be adsorbed onto clay, but also some polymer molecules such as poly(vinyl alcohol) (PVOH) and polyacrylamide (PAM) bonded with clay surface by various interactions such as hydrogen bonding and ion-dipole bonding.[38-40]Stutzmann and Siffert [41], using IR spectroscopy, studied the adsorption mechanism and fine structure of complexes obtained between Na^+-MMT and acetamide or polyacrylamide. The adsorption takes place on the external surface of the clay particles. The organic molecules are protonated on the surface and adsorbed by electrostatic force. There are two adsorption possibilities: strong, irreversible adsorption, which corresponds to the formation of chemisorbed molecules, or the more important adsorption of molecules retained by the formation of hydrogen bonds.

2.3.3 Reaction with silane compounds

The hydroxyl groups on the edges of clay platelets can react with silane compounds to yield ether linkages. The grafting of silane into clay mainly occurs at the external surface

of the clay and is highly dependent on the accessible surface area. Accordingly, there is no change in the interlayer distance. However, He *et al.*[42] studied the grafting of silane compounds onto clay and demonstrated that the grafting process occurs in two basic steps: first, the silane molecules interact into the clay interlayer and, second, a condensation reaction takes place between these silane molecules and clay surface. Fig. 2.6 shows the interaction between silane and a clay surface.

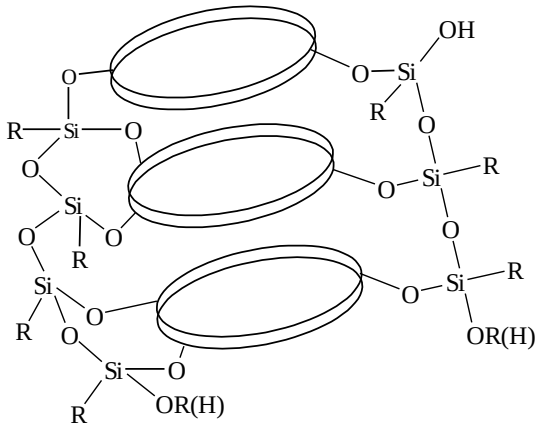

Fig.2.6: Schematic representation of the coupling reaction of trifunctional silane molecules on clay.[43]

Herrera *et al.*[43] modified laponite clay with silane compounds and found that the silane molecules can potentially react with laponite particles via a condensation reaction between the surface hydroxyl groups located on the clay edges and the alkoxy groups of the silane molecules, giving rise to the formation of Si-O-Si covalent bonds and increase in d-spacing of laponite from 12 Åto 17Å after the modification with 3-(trimethoxysilyl) propyl methacrylate (MPTMS). They explained these results as following: The silylation reaction produces siloxane polymers able to penetrate the external part of the interlaminate space and partially push the clay sheets apart.[43]

2.4 Polymer clay-nanocomposite structure

Depending on the nature of the components used (layer silicate, organic cation and polymer matrix) and the method of preparation, three different types of nanocomposite

structures can be obtained when the clay particles are dispersed in a monomer or polymer matrix (see Fig 2.7).[12]

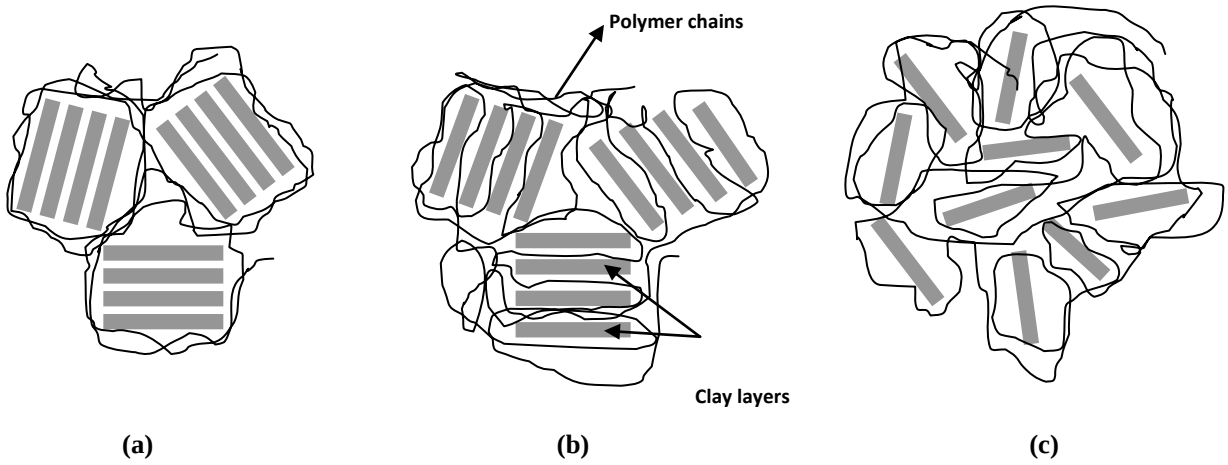

Fig. 2.7: Types of nanocomposite structures: (a) conventional, (b) intercalated and (c) exfoliated.[44] (Note: (a) layers number 500-1000, (b) layers number up to 1000 but can also tend toward a single figure depending on the extent of intercalation, and (c) individual layers loosened from 1000 sheets per single clay particle.)

Conventional composites: This type of composite contains clay tactoids, with the layers aggregated in an un-intercalated face-to-face form. In this case the clay tactoids are dispersed simply as a segregated phase, as illustrated in Fig. 2.7(a). The polymer chains are unable to intercalate between the silicate sheets. In this case there is no change in the d-spacing of the clay, which is around 1.15 nm.[23] This results in the composites having poor mechanical properties.[15,44,45]

Intercalated nanocomposites: Here the polymer is located in the clay galleries, expanding the clay structure, but retaining some long-distance order between the platelets. Only a few polymer chains penetrate in between clay galleries, as illustrated in Fig. 2.7(b). This type of nanocomposite shows a slight improvement in mechanical and thermo-mechanical properties relative to the pure polymer,[15,19,45] with substantial improvement in thermal stability.[46]

Exfoliated nanocomposites: This type of structure can be formed when all individual clay layers are fully separated from each other, and are no longer close enough to interact with one another. The average distances between the segregated layers are dependent on the

clay loading, and they are evenly distributed throughout the polymer matrix. Exfoliated nanocomposites show greater homogeneity than intercalated nanocomposites.[15,19,44]

Exfoliated PCNshave improved mechanical performance. The homogeneous dispersion of clay into the polymer matrix provides an enormous surface area, and leads to a high interfacial area between platelets and the polymer matrix.[19]This very large interfacial area leads to restrictions in free volume, chain mobility and conformation, relaxation behaviour, and thermal transitions.[47]Polymer chains that are close to the clay interface have lower free volume than the bulk polymer, explaining why nanocomposites have unusual properties, such as increased toughness, and improved barrier properties.[1]

2.5 Methods used to synthesise polymer-clay nanocomposites

Depending on the starting materials and synthesis techniques, the methods used to synthesize nanocomposites are divided into four main groups: solution, melt blending, template, and in-situ intercalative polymerization.

2.5.1 Solution method

Here the organoclay and the polymer are dissolved in a polar organic solvent. The polymer chains migrate between the silicate layers, due to the weak forces between thesilicate layers the solvent separates the layers, thereby allowing the polymer to adsorb onto the surfaces of individual silicate platelets. The solvent is then allowed to evaporate, leaving a nanocomposite behind. The final structure depends on the thermodynamics ofthe multi-component mixture and the rates of diffusion and adsorption of polymers into the silicate system.[12,19,48] A schematic representation of the solution method is shown in Fig. 2.8.

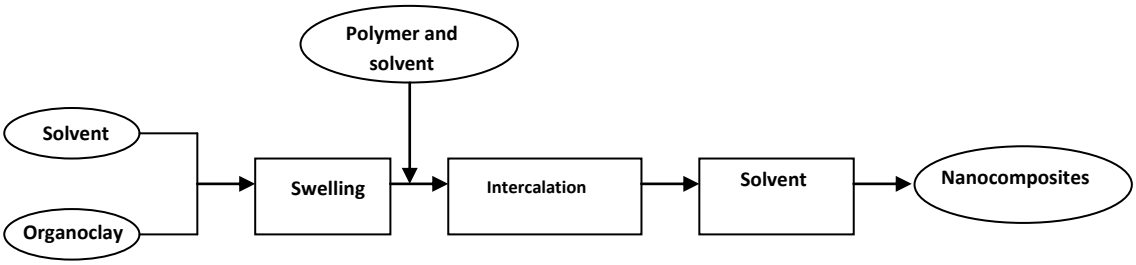

Fig. 2.8 : Schematic representation of the preparation of nanocomposites via the solution method

This route can be used to synthesize nanocomposites from polymers with low or no polarity. From a commercial point of view, however, this route involves the use of large volumes of organic solvents, which is environmentally unfriendly and economically prohibitive.[19,49]It is also believed that a small quantity of solvent remains in the final product at the polymer-clay interface, and this will lead to the creation of weaker interfacial interaction between the polymer and the clay surfaces and later emissions problems.[12]

2.5.2 Melt blending synthesis

The melt blending process involves mixing the layered silicate, by annealing statically or under shear, with the polymer while heating the mixture above the softening point of the polymer. During the annealing process the polymer chains diffuse from the bulk polymer melt into the galleries between the silicate layers.[15,19,49-52]

The technique of melt blending is particularly attractive due to its versatility and compatibility with existing processing infrastructure and is beginning to be used for commercial applications.[53] The structure of nanocomposites formed via polymer melt intercalation depends upon the thermodynamic interaction between the polymer and the silicate as well as the transportation of polymer chains from the bulk melt into the silicate interlayer.[54]A schematic representation of the melt blending process is shown in Fig. 2.9.

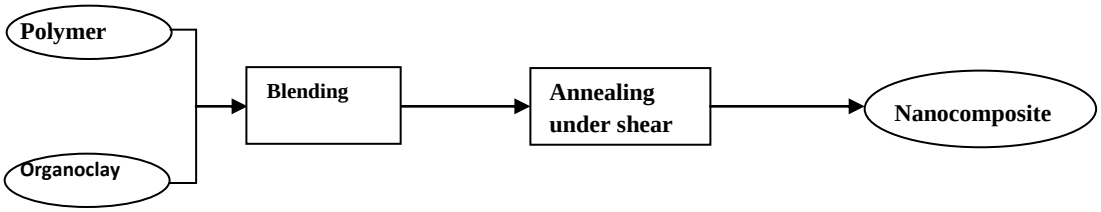

Fig. 2.9: Schematic representation of the preparation of nanocomposites via the melt blending method.

The use of the melt intercalation method to synthesize nanocomposite materials is limited for the following two reasons:

First, during high-temperature processing the low thermal stability of the clay modifier leads to a decrease in the distance between clay sheets due to degradation of the clay modifier during processing. This also leads to a loss in hydrophobicity of the clay surface, and it becomes hydrophilic again.[55,56] This was confirmed by Park *et al*.[57] who discovered that the interlayer distance of clay galleries decreased as the temperature increased to 200-280ºC due to degradation of surfactant in the clay gallery, which leads to interruption of intercalation between polymer and the clay.

Second, this method seems unsuitable for producing certain polymers, such as amorphous PS, even though PS can be intercalated into the clay via weak interaction between the phenyl group of polystyrene and the clay surface. Upon heating, this interaction becomes weaker between PS and clay, and leads to a decrease in the interlayer spacing.[58]

2.5.3 Template method

This method is useful for water soluble monomers or polymers. For in situ hydrothermal crystallization of the polymer-hectorite clays it involves creating a 2 wt% gel of silica sol, magnesium hydroxide sol, lithium fluoride, and polymer in water.This method is used with water soluble polymers, and refluxing is typically carried outfor 2 days [59]. The selected modifiers are usually positively charged, to encourage incorporation into the gallery space via electrostatic interaction. Used of this method leads to the layered silicate

being highly dispersed in a one-step process.[19,59]This method is far less well developed for layered silicates and thus is of no significance in the present study.

2.5.4 In situ intercalative polymerization

A schematic representation of the in situ intercalative process is shown in Fig. 2.10. In this method the layered silicate is swollen within the liquid monomer or monomer solution so the polymer formation can occur between the intercalated sheets. Polymerization can be initiated either by heat or radiation, or by free-radical initiator.[12,15-17,19,22,60]

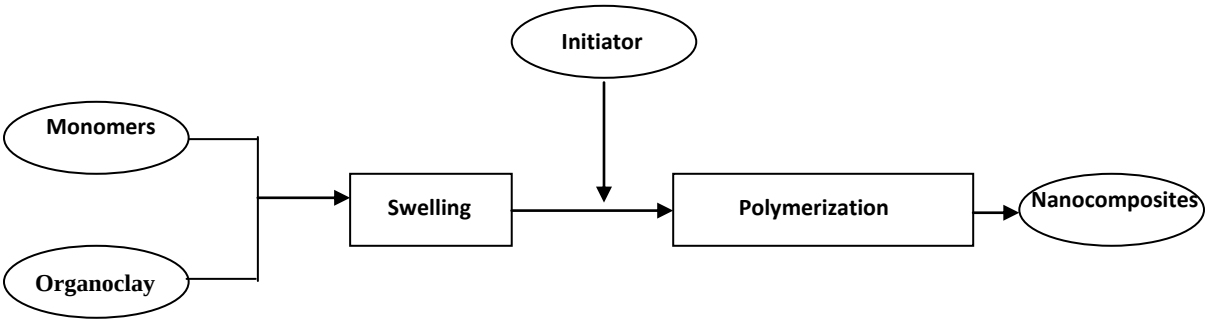

Fig. 2.10: Schematic representation of the preparation of nanocomposites via in situ polymerization.

In the case of using a monomer solution, the polarity of the solvent has a significant effect. In order to ensure a high monomer concentration inside the clay galleries the solvent should have the ability to interact with the polar surface of the clay. Akelah and Moet[61] modified Na^{+}-MMT and Ca^{2+}-MMT using (vinyl benzyl) trimethyl ammonium chloride, then the modified clay was dispersed in three different solvents, acetonitrile, acetonitrile/toluene and acetonitrile/THF. Styrene was added to the dispersed clay and polymerized. They obtained an intercalated structure with different interlayer distances, depending on the solvent used. Acetonitrile was found to be the best solvent.

In general in-situ intercalative polymerization relies on a suitable choice of the organic modifier and the type of clay. The practical advantages of this method are that the layered silicate can be used without modification[45] and it is simple to vary the clay loading.

The low viscosity and small size of the monomers, compared to polymers, allows them to penetrate more easily inside the galleries of silicate layers. Another advantage of in situ intercalative polymerization is that the silicate is combined with polymer at relatively low temperature,[62] which reduces the problem of polymer degradation during the process, and no decomposition of surfactants takes place. Minimal quantities of solvents are used (in cases where monomer solutions are used) as opposed to very dilute solutions used for the solution technique.[30]

It is also the only method that can be used for dispersed polymerization methods (i.e. polymerization in emulsion, miniemulsion, suspension and dispersion). Emulsion, miniemulsion and suspension have been extensively used for the synthesis of nanocomposites,[7,63] and there are a few reports of the preparation of PCNs in dispersion polymerization.[64,65]

2.5.4.1 Preparation of nanocomposites using dispersion free radical polymerization

Dispersion polymerization is a simple and fast (i.e. single step) technique used to prepare monodisperse polymer particles of a range of sizes between 1 and 20μm in very good yields.[9,66-70]Dispersion polymerization may be defined as a type of precipitation polymerization in which the polymerization is carried out in the presence of a suitable polymeric stabilizer that is soluble in the reaction medium. A schematic representation of the mechanism of polymerization in dispersion is shown in Fig. 2.11.

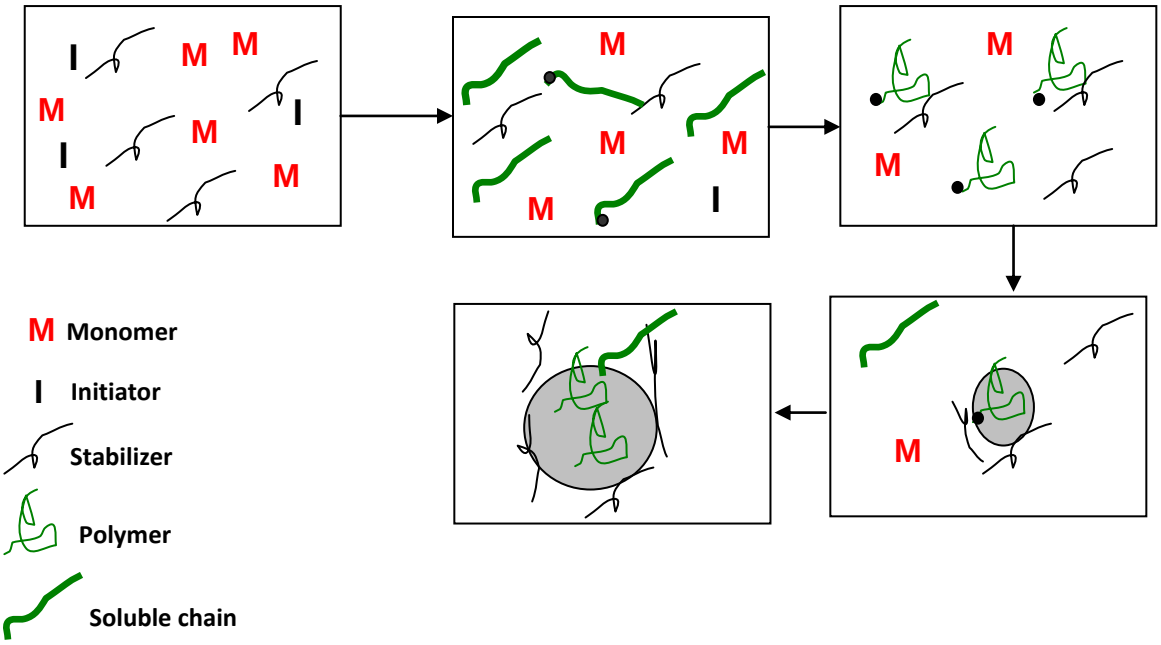

Fig. 2.11: Schematic description of dispersion polymerization.[71]

The continuous phase is chosen to be a solvent for the monomer to be polymerized and a non-solvent for the resultant polymer.[72-74] A steric stabilizer is used to produce a colloidally stable dispersion, without which the polymerization would afford macroscopic particles of polymer of uncontrolled size.[75] The dispersion polymerization process takes place in a homogenous medium of monomers, free radical initiator, and polymeric stabilizer dissolved in a suitable solvent. As the temperature is raised the initiator decomposes and generates free radicals, which initiate chain growth by the addition of monomers. The growing chain remains in solution until a critical chain length is reached, and then precipitates. This is called nucleation. These unstable nano-size particles aggregate into large particles of about 200 nm and stabilize themselves against further aggregation by adsorbing the stabilizer from the medium. These particles grow by capturing small nuclei and oligomeric radicals from the continuous phase, and polymerizing the absorbed monomer inside the particles. This continues until all of the oligomeric radicals and nuclei generated in the reaction medium are consumed [76].

Dispersion polymerization has been widely used for the preparation of a variety of polymers, such as PS,[72,77] poly(butyl acrylate) (PBA),[78] polyacrylamides,[70] poly(styrene-co-butyl acrylate) (PS-co-BA),[75] and poly(methyl methacrylate) (PMMA) .[79] However, there are only a few articles reporting on the use of the dispersion polymerization method in the field of a nanotechnology.[64,65]

Zhao and Samulski[80] prepared a partially exfoliated PMMA nanocomposite using dispersion polymerization in supercritical carbon dioxide (CO_2). The clay was modified using a fluorinated surfactant. They found that the modified clay not only acts as inorganic filler but also as a stabilizer for the growth of PMMA particles. In another study, Zhao and Samulski [64] synthesized PMMA and PS nanocomposites via dispersion polymerization in supercritical CO_2 in the presence of clay that was surface modified using aminopropyl-terminated poly(dimethysiloxane) surfactant. The morphology of the nanocomposites obtained was strongly dependent on the concentration of the organically and the type of polymer involved. In the case of PMMA an exfoliated structure was obtained, whereas in the case of PS a nanocomposite with a partially exfoliated morphology was obtained. Lami and Lang [81]successfully encapsulated silica particles by polymerizing St using dispersion polymerization in polar medium (ethanol/water) with3-(trimethoxysilyl) propyl methacrylate (MPTMS) chemically attached to the silica particles. Park *et al.*[82] synthesized PMMA encapsulated silica by dispersion polymerization in supercritical CO_2. The silica particles were modified using MPTMS before being used in dispersion polymerization. Dispersion polymerization of styrene was used by Liu *et al* [83]tograft PS from silica particles. The surface of the silica particles was first treated withMPTMS, followed by radical copolymerization of St monomers. Zerda *et al.*[84] also used supercritical CO_2 as a reaction medium for the preparation of highly filled PCNs.

This study focuses on the preparation of PCNs via dispersion polymerization in polar medium (ethanol/water, 85:15). One of the most important advantages is that water is used as a part of dispersion medium. Water makes the galleries of layered silicates wide without any chemical treatment.[23] Na^+-MMT clay swells due to the presence of hydration

water molecules around the inorganic cations (Na^+) [13], potentially favouring insertion of monomers into the galleries.[17] However, a particular attention must be given to homogenously disperse clay in dispersion polymerization where the dispersion medium is not pure water, but rather a mixture water/aliphatic alcohol.[17,85]

2.5.4.2 Clay platelets as stabilizers in in-situ intercalative polymerization

Surfactants are widely used for many different applications because of their remarkable ability to influence the properties of surfaces and interfaces. Surfactants are able to reduce the interfacial tension between oil and water by adsorbing at the liquid–liquid interface. At the interface, the hydrophobic part penetrates into the oil phase, and the hydrophilic " polar head" points towards the aqueous phase.[86]

Not only molecular surfactants (small molecular surfactants or amphiphilic copolymers) but also solid particles can stabilize emulsions. An emulsion stabilized by particles instead of surfactant molecules is called a Pickering emulsion.[87-89] The efficiency of solid particles in stabilizing emulsions depends on many parameters, such as particle size, interparticle interactions, and particle wettability. The stabilization of Pickering emulsions by various types of particles, such as inorganic particles, semiconducting nanoparticles, colloidal particles and polymer micelles has been reported in literature.[89,90]

For environmental and economic reasons (clays are non-pollutants and inexpensive raw materials, contrary to surfactants), the stabilization of emulsions by clay and clay minerals could be valuable to industry to formulate surfactant free emulsions.[91] Classical emulsions (O/W) have been successfully stabilized by montmorillonite, laponite platelets, double layered hydroxides, and mixtures of clay minerals to improve the colloidal stabilization. Bon and Clover[92]investigated Pickering, miniemulsion polymerization using laponite clay as the stabilizer and showed that Pickering miniemulsion polymerization was successful for a variety of hydrophobic monomers (i.e., styrene, butyl (meth)acrylate, octyl acrylate, and 2-ethyl hexyl acrylate). The laponite-stabilized miniemulsion polymerizations yielded armored latexes, of which the surfaces of the particles were covered with clay.[92] Voorn *et al.*[93] demonstrated that surfactant-free

inverse emulsion polymerization can be successfully carried out by using organically modified clay platelets as stabilizing particles.

The surface of most of the 2:1 phyllosilicates such as bentonite and montmorillonite is hydrophilic, hence clay would not spontaneously adsorb onto the interface of oil and water mixture. In order to achieve a favorable (oil/clay/water) triphasic contact angle of about 90º, which is pre-requisite to a thermodynamically-driven successful Pickering stabilization, the clay should be partially organoically modified in order to slightly decrease its hydrophilic nature to an extend by which the affinity of the clay surface for the oil phase and the water phase would be almost equal.[86,94]

Introducing polymer brushes on the surface of clay layers is a versatile way to improve the assembly of clay particles at fluid–fluid interface and to obtain stable colloid particles. Yang *et al*[95] synthesized PS and poly(2-(dimethyamino)ethyl methacrylate) (PDMAEMA) mixed polymer brushes on the surface of clay layers via in-situ free radical polymerization. The polymerization was initiated by a cationic ammonium free radical initiator that was ion exchanged onto the surface of clay layers. The resulting polymer brushes on the clay surface were successfully used to produce stable PS latexes in Pickering suspension polymerization where the polymer particles were completely covered by clay particles.

Because the stability of Pickering emulsions is strongly dependent on interfacial tensions between particles and liquids, the grafting of polymer chains (polymer brushes) on the surface of particles will further reduce the interfacial tensions between particles and liquids, and the stability of the emulsions will be improved.[96] Yang *et al*[97] reported the synthesis of amphiphilic poly[methyl methacrylate-b-2-(dimethylamino) ethyl methacrylate] (PMMA-b-PDMAEMA) block copolymer brushes on the surface of clay layers by in situ atom transfer radical polymerization (ATRP) and the preparation of poly(methyl methacrylate) (PMMA) colloid particles with clay layers on the surface by Pickering emulsion polymerization. Wu *et al*[86] prepared hydrophobic PS brushes on the edges of clay using ATRP, and then successfully used PS-modified clay as stabilizers in

suspension polymerization of PS, TEM images showed the clay particles surrounding the polymer particles.

The present study focuses on another preparation of polymer latexes in dispersion polymerization using clay as stabilizer. Dispersion polymerization carried out in the presence of second polymer (i.e. steric stabilizer) in order to prevent flocculation of growing particles,[98] the stabilizers usually used in dispersion polymerization are: homopolymer, block and graft copolymers and macromonomers.[76,99]

Most block copolymers have been synthesized using meticulous and time-consuming living ionic polymerizations,[100] but recently attempts have been made to synthesize block copolymers using other simple techniques. Among them, controlled/living radical polymerization has been a particularly useful technique for the preparation of well-defined polymer structures. The three main techniques capable of inducing living behaviour are nitroxide-mediated polymerization (NMP),[101] atom transfer radical polymerization (ATRP),[102] and reversible addition-fragmentation chain transfer polymerization (RAFT).[103]

RAFT [104-107] and ATRP [8,107] have been employed to grow polymer from clay surface to produce polymer-modified clay, used in emulsion polymerization as stabilizers. The more recent ITP (iodine transfer polymerization) and RITP (reverse iodine transfer polymerization) methods have not yet been used in the nanotechnology field.

The present study deals with the modification of clay surface using functional polymers prepared by RITP, and the use of the subsequent polymer-modified clay as stabilizers in dispersion polymerization process.

2.5.4.3 Reverse iodine transfer polymerization

A new technique in the field of living/controlled free radical polymerization (LRP/CRP) namely RITP, has recently been developed by Lacroix-Desmazes *et al*.[108-111] RITP is based on the use of molecular iodine (I_2) as control agent. In RITP (Fig 2.12), the radicals provided by the decomposed initiator react preferably with iodine or propagate with a few monomer units before reacting with iodine to form in situ the iodinated transfer

agents (A-I and A-M*n*-I respectively). Once all the iodine has been consumed, the core equilibrium of degenerative chain transfer between active and dormant chains takes place.[110]

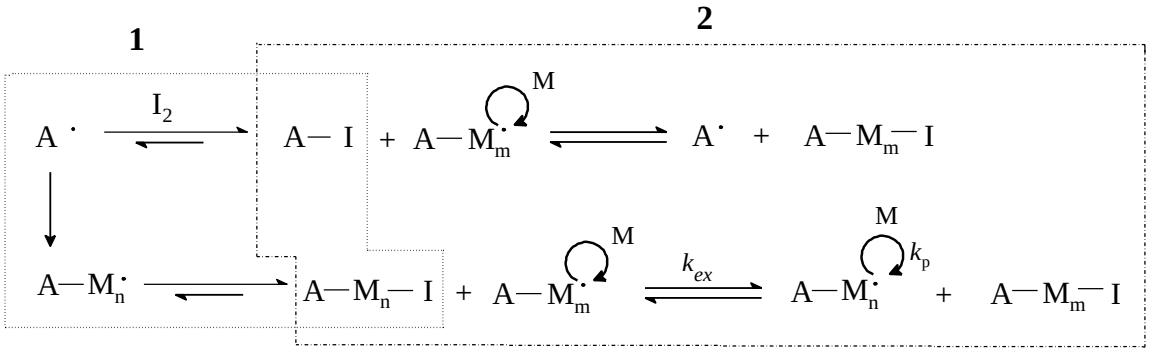

·A: radical from the initiator, I_2: molecular iodine, M: monomer unit, and n: number-average degree of polymerization.

Fig. 2.12 : Simplified mechanism of reverse iodine transfer polymerization (RITP).[110]

One molecule of iodine will control two polymer chains. So, in this process, the molecular weight of the polymer is controlled by the molar ratio between the quantity of monomer and twice the quantity of iodine initially added (eq 2.1).

$$M_{n,theor} = \frac{m_{mono}.C}{2n_{I_2}} + M_{A-I} \quad (2.1)^{110}$$

Where m_{mono} is mass of monomer and C% is conversion, $M_{A\text{-}I}$ stand for molecular weight of A-I adduct, while A stands for the radical fragment from the initiator, and n_{I_2} is number of moles of iodine.

The advantage of using RITP is that the transfer agents are generated in situ in the reaction medium.[112] Moreover, RITP is practically easier to perform than other polymerization methods, since only molecular iodine needs to be added to the reaction.

RITP has already been successfully used to polymerize applied to a wide range of monomers such as acrylates,[108] styrene,[113] MMA,[110,114] and copolymers of vinylidene chloride and methyl acrylate.[109] However, the use of RITP in the field of PCNs has not been reported yet.

In the present study RITP was used to prepare iodo-terminated polystyrene (PS-I) and block copolymers of poly(styrene-b-2-hydroxyethyl acrylate) (PS-b-PHEA).

2.6 Characterization of the structures of nanocomposites

The techniques most commonly used for characterization of the nanocomposite structures are X-ray diffraction and transmission electron microscopy.[115]

Three different nanocomposites structures can be distinguished, depending on the ordering and the dispersion of clay layers inside the polymer matrix, namely conventional, intercalated and exfoliated.[23]

2.6.1 X-ray diffraction

X-ray diffraction (XRD) allows the determination of the space between structural layers of silicate (the distance between the basal layers of the MMT clay, or of any layered material), using Bragg's law:

$$n\lambda = 2d \sin \theta \quad 2.2$$

where λ corresponds to the wavelength of the X-ray radiation used in the diffraction experiment, d is the spacing between diffractional lattice planes and θ is the measured diffraction angle.[116]

Intercalation and exfoliation change the dimensions of gaps between the silicate layers, so an increase in layer distance indicates that a nanocomposite has formed. A reduction in diffraction angle value corresponds to an increase in the silicate layer distance.[117] X-ray diffraction has been used to look at changes in *d*-spacings when nanocomposite materials are prepared. The *d*-spacing observed by XRD for nanocomposite materials has been used to describe the nanoscale dispersion of the clay in the polymer.[118] Fig. 2.13 shows

typical X-ray diffraction patterns of the three type of layered silicate polymer composites structures.[19]

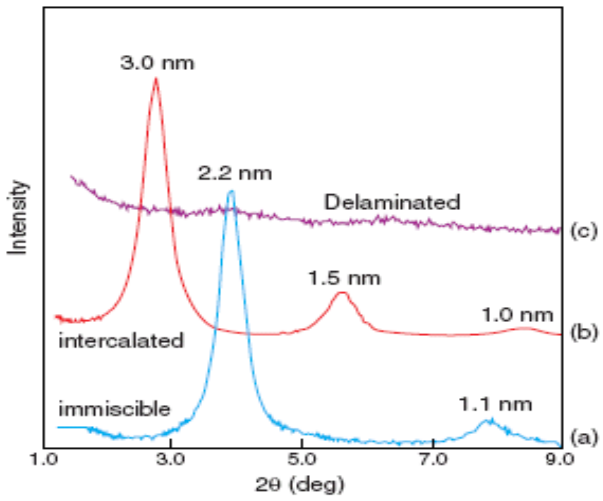

Fig. 2.13: X-ray patterns of three layered silicate structures: (a) conventional, (b) intercalated, (c) exfoliated.[19]

Conventional (immiscible)materials exhibit no change in *d*-spacing respective to pristine clay, meaning that no polymer has entered the gallery and that the spacing between clay layers is unchanged. *Intercalated* nanocomposites exhibit an increased of *d*-spacing, indicating that polymer chainshave entered the gallery, have expanding the layers. *Exfoliated* (delaminated) materials show no diffraction peak, suggesting that a great amount of polymer has entered the gallery spacesand disordered the plates.[12,23,118-120]

Although XRD is a most useful technique for measuring the *d*-spacing of ordered immiscible and ordered intercalated nanocomposites,[12] it may be insufficient for themeasurement of disordered and exfoliated materials that give no XRD peaks. More specifically, the absence of a peak may be misinterpreted in cases where no peak is seen.[115,120]

Many factors, such as concentration and order of the clay, can influence the XRD patterns of layered silicates. Therefore, the lack of a diffraction peak obtained from XRD patterns of clay containing polymer materials cannot prove, or disprove alone, the existence of exfoliated clay platelets in the nanocomposite. Furthermore, XRD relates

only to the degree of dispersion of clay sheets with respect to each other in the polymer matrix, and does not give information with respect to interaction between the organic and inorganic phase in the composite materials.[120]

2.6.2 Transmission electron microscopy (TEM)

TEM is a very powerful tool for the analysis of PCNs as it can qualitatively describe how the layered silicate filler is dispersed in the polymer. When nanocomposites have formed, the cross section of the individual of the silicate sheets of microtomed samples are seen as dark lines.[12,19,120]

Very thin cross-sections (40-50 nm) of the nanocomposite are required in order to get a good quality image. For this reason the nanocomposite needs to be microtomed.[115]

2.7 Determination the properties of PCNs

The incorporation of layered silicates in a polymer matrix generally leads to improvements in the properties of the composites materials obtained.[12,16,19] Amongst those properties, an expected large increase in modulus (tensile or Young's modulus and flexural modulus) of nanocomposites with filler contents sometimes as low as 1 wt% has drawn muchattention.[18,121] Improvementsin thermal stability and fire retardancy are other interesting properties displayed by nanocomposites. PCNs have also been studied and used for their superior barrier properties against gas and vapour transmission. Finally, depending on the type of polymeric materials, nanocomposites can also display interesting properties in the terms of ionic conductivity or thermal expansion.

The following sections describe how the presence of clay particles in a polymer matrix can affect the thermal and mechanical properties of polymers.

2.7.1 Thermo-mechanical properties of PCNs

Dynamic mechanical analysis consists in measuring the viscoelastic properties of a material when exposed to cyclic deformation as a function of temperature. There are three main parameters that are used to express DMA results: (i) the storage modulus (G^{I}), which is a measure of elastic response to the deformation; (ii) the loss modulus (G^{II}),

which is a measure of the non-reversibleplastic response, and (iii) tanδ, i.e. the ratio of G^{II}/G^{I}. Tan δ can be used for the determination of energy absorption through molecular mobility after the glass transition temperature (T_g).[16]

When polymer chains are intercalated in the silicate gallery or when the silicate layers are partially exfoliated in the polymer matrix, interactions between the polymer and the surface of the silicate layers become stronger.Sluggish motions of chain segments of polymer chains brings about an increase of the $T_g$relative to the corresponding neat polymer, which can lead thermo-mechanical behaviour similar to cross-linked polymer systems.[122]

The interaction between the polymer matrix and silicate layers at the interface can hinder the mobility of polymer chain segments at or near the interface, leading to improved mechanical properties. In general, higher G^{I} values for nanocomposites below the T_g (i.e. glassy state) and in the rubbery region, relative to pristine polymers and conventional composites, are obtained. This can be attributed to the large aspect ratio of the structural hierarchy on the nanoscale level. The incorporation of small quantities of polar comonomers during the synthesis of PCNs not only affects the resultant nanocomposite structure, but the mechanical properties as well due to enhanced interaction between the polymer matrix and the clay nanofiller.[16,123]

Intercalated polystyrene-clay nanocomposites containing 17.2 wt% of Na^{+}-MMT, synthesized by emulsion polymerization, did not show any improvement in the storage modulus but rather a shift towards high temperatures and broadening of the tan □ peak relative to the pristine polystyrene.[124] This implies that the clay only restricted the segmental motion of the polystyrene matrix, resulting in an increase of the glass transition temperature.[124] However, enhanced storage modulus was obtained by Xu *et al*.[23] who used a small amount of the polar specialty monomer 2-acrylamido-2-methyl-1-propanesulfonic acid (AMPS) to modify Na^{+}-MMT, followed by synthesis of poly(styrene-co-methyl methacrylate)/clay nanocomposites by emulsion polymerization.

In the PCNs obtained, the storage modulus was found to be increasing with an increase in the clay loading.

Choi *et al.*[45] synthesized exfoliated and intercalated poly(styrene-co-acrylonitrile) copolymer nanocomposites using AMPS as clay modifier. They found interesting results in terms of mechanical properties of nanocomposites. The exfoliated poly(styrene-co-acrylonitrile)/clay nanocomposite obtained were found to have a higher storage modulus than the intercalated structure. It was also found that the T_g values for exfoliated nanocomposites increased with the content of silicate, but the intercalated nanocomposites had lower T_g values than pure poly(styrene-co-acrylonitrile). They suggested that the decrease in glass transition temperature for intercalated structures was related to the molecular weight distribution of the polymer matrix. A polymer with broad molecular weight distribution may contain a low molecular weight portion, with the apparent increased concentration of chain ends reducing the glass transition temperature in similar a manner like plasticizers do.

Qutubuddin and Fu[125] synthesized fully exfoliated polystyrene using vinylbenzyldimethyldodecyl ammonium as clay modifier. They found a decrease in T_g from 100°C in the pure polymer to 94°C in the polystyrene nanocomposite containing 7.6 wt% clay. They attributed this decrease of theT_g to a decrease in molecular weight resulting from hindered diffusion of the polymerization initiator (hindered by the high viscosity of the styrene- swollen clay), giving faster termination, as well as the restricted propagation of styrene chains by the impervious clay platelets.

2.7.2Thermal stability of PCNs

Thermogravimetric analysis is used primarily for determining the thermal stability of a polymer. TGA is an old technique, but has been applied to polymers only since the 1960s.[126] The most widely used TGA method is based on continuous measurement of weight on a sensitive balance (thermobalance) as the sample temperature is increased in air or an inert atmosphere. This is referred as non-isothermal TGA. Data are recorded as

thermograms giving a measurement of weight loss as a function of temperature as the sample decomposes into volatile products.

Weight loss may also arise from evaporation of residual moisture or solvent, but at temperatures higher than 100°C it generally results from polymer decomposition. TGA has been also used for determining volatilities of plasticizers and other additives.[126]

In general, PCNs show improved thermal stability relative to the pristine polymers, regardless of the experimental environment.[126,127] Generally, the incorporation of silicate in the polymer matrix enhances the thermal stability by acting as a superior insulator and mass transport barrier to the volatile products generated during decomposition.[49]

The improvement in thermal stability of PCNs was first reported by Blumstein,[128] when he studied the thermal stability of PMMA loaded with montmorillonite clay. He showed that when PMMA was inserted between lamellae of montmorillonite clay the material was still thermally stable under conditions that would otherwise degrade pure PMMA. He proposed that the stability of the PMMA-clay nanocomposites is due not only to its structure, but also to restricted thermal motion ofthe PMMA in the gallery.

Very small amounts of clay are required for an improvement in thermal stability relative to the pristine polymers.[46] Doh and Cho [129] observed that the maximum thermal stability of their intercalated polystyrene-clay nanocomposites was achieved when only 0.3 wt% clay was used. They used dimethylbenzyloctadecylammonium-modified MMT clay.

Xu *et al*.[23] synthesized poly(styrene-co-methylmethylacrylate) using 2-acrylamido-2-methyl-1-propanesulphonic acid (AMPS) as clay modifier. TGA results showed that as the clay content increased, the onset temperature of thermal decomposition of the nanocomposite moved slightly towards a higher temperature. They also found that the exfoliated nanocomposite with 3 wt% silicate showed a 7°C increase in decomposition temperature at 20% weight loss, resulting from the heat-barrier effect of the clay platelets.

TGA results have been also reported as being environment dependent. Poly(ethylene-co-vinyl acetate) synthesized by melt intercalation showed better thermal stability in a nitrogen environment than in air, and the thermal stability increased with an increasing amount of clay. In air, the nanocomposites showed a significant delay of weight loss, probably due to the barrier effect to diffusion of both the volatile thermo-oxidation products and oxygen from the gas phase to polymer.[49]

The chemical structure of surfactants used for the modification of clay has a significant effect on the extent of thermal stability of the polystyrene-clay nanocomposites. When nanocomposites are utilized in high-temperature applications, the low thermal stability of the surfactants, which are usually used to render the layered silicates organophilic, can be a limiting factor. Zhang *et al.*[29] used three surfmer-modified clays and non-reactive surfactant-modified clay to prepare polystyrene-clay nanocomposites and discovered that surfmer-based nanocomposites had superior thermal stability relative to non-reactive surfactant-based nanocomposites.

The organoclay has two opposing functions affecting the thermal stability of the PCNs. One is its barrier effect, which should improve the thermal stability, and the other is the catalytic effect towards the degradation of the polymer matrix, which decreases the thermal stability. When adding a low fraction of clay to the polymer matrix, the clay layers should be well dispersed. The barrier effect is predominant, but with increasing loading the catalyzing effect rapidly increases and becomes dominant, so that the thermal stability of the nanocomposite decreases.[29]

Exfoliated polystyrene nanocomposites have been found to exhibit better properties relative to the other types of composites.[12,19,49,130] Thermal stability is one such property. This enhanced stability has been attributed to the high thermal stability of clay and its excellent barrier properties, which prevent heat from being, transmitted quickly, thereby limiting the continuous decomposition of the nanocomposites. Many researchers have observed that exfoliated polystyrene-clay nanocomposites show exceptional thermal stability.[125,131-133] Exfoliated structures have hugely improved thermal properties

compared to conventional and intercalated materials, due to the homogeneous dispersion of the clay layers through the polymer matrix and the high surface area of clay layers.[24]

The clay acts as a heat barrier, which enhances the overall thermal stability of the system, as well as assists in the formation of char after thermal decomposition. In the early stages of thermal decomposition the clay shifts the decomposition to higher temperatures. After that, this heat barrier effect results in a reverse thermal stability. In other words, the stacked silicate layers can hold accumulated heat, which can be used as a heat source to accelerate the decomposition process, in conjunction with the heat flow supplied by the outside heat source.[16,49]

2.8 References

1. Giannelis, E. P.; Krishnamooti, R.; Manias, E. *Advances in Polymer Science* **1999,** 138, 107-147.

2. Utracki, L. A., Polymer-Containing Polymeric Nanocomposites. In Rapra Technology Limited: U.K, 2004; Vol. 1, pp 1-430.

3. Okada, A.; Usuki, A. *Journal of Materials Research* **1995,** 3, 109-117.

4. Messersmith, P. B. *Journal of Materials Research* **1992,** 7, 2599-2607.

5. Yang, W.; Ko, T.; Wang, S.; Shin, P.; Chang, M.; Jiang, G. *Polymer Composites* **2008,** 29, 409-414.

6. Li, H.; Yu, Y.; Yang, Y. *European Polymer Journal* **2005,** 41, 2016-2022.

7. Wang, D.; Zhu, J.; Yao, Q.; Wilkie, C. A. *Chemistry of Materials* **2002,** 14, 3837-3843.

8. Yang, Y.; Wu, D.; Li, C.; Liu, L.; Cheng, X.; Zhao, H. *Polymer* **2006,** 47, 7374-7381.

9. Xu, Z.; Deng, Z.; Li, X.; Yi, C. *Journal of Polymer Science Part A: Polymer Chemistry* **2005,** 43, 2368-2376. .

10. Kawaguchi, S.; Ito, K. *Advances in Polymer Science* **2005,** 175, 299-328.

11. Utracki, L. A.; Kamal, M. R. *The Arabian Journal for Science and Engineering* **2002,** 27, 43-67.

12. Ray, S.; Okamoto, M. *Progress in Polymer Science* **2003,** 28, 1539-1641.

13. Yariv, S.; Cross, H., Organo-Clay Complexes and Interactions. In Marcel Dekker, Inc: New York and Basel, 2002; pp 1-101.

14. Lee, S.; Kim, J. *Journal of Polymer Science: Part B: Polymer Physics*, **2004,** 42, 246-252.

15. Lebaron, P. C.; Wang, Z.; Pinnavaia, T. J. *Applied Clay Science* **1999,** 15, 11-29.

16. Nalwa, H. S., Polymer/clay Nanocomposites. In *Encyclopedia of Nanoscience and Nanotechnology*, American Scientific Publishers: California, 2004; Vol. 8, pp 791-843.

17. Noh, M. W.; Lee, D. C. *Polymer Bulletin* **1999,** 42, 619-626.

18. Luckham, P. F.; Rossi, S. *Advances in Colloid and Interface Science* **1999,** 82, 43-92.

19. Alexandre, M.; Dubois, P. *Materials Science and Engineering: A* **2000,** 28, 1-63.

20. Burnside, S. D.; Giannelis, E. P. *Chemistry of Materials* **1995,** 7, 1597-1600.

21. Messersmith, P. B.; Giannelis, E. P. *Chemistry of Materials* **1994,** 6, 1719-1725.

22. Rosorff, M., Polymer-Clay Nanocomposites. In *Nano Surface Chemistry*, Marcel Dekker Inc: New York and Basel, 2002; pp 653-673.

23. Xu, M.; Choi, Y. S.; Kim, Y. K.; Wang, K. H.; Chung, I. J. *Polymer* **2003,** 44, 6387-6395.

24. Xu, M.; Choi, Y. S.; Wang, K. H.; Kim, J. H.; Chung, I. *Macromolecular Research* **2003,** 11, 410-417.

25. Meneghetti, P.; Qutubuddin, S. *Langmuir* **2003,** 20, 3424-3430.

26. Choi, Y. S.; Chung, I. J. *Macromolecular Research* **2003,** 11, 425-430.

27. Bergaya, F.; Lagaly, G. *Applied Clay Science* **2001,** 19, 1-3.

28. Fischer, H. *Materials Science and Engineering A* **2003,** 23, 763-772.

29. Zhang, W. A.; Chen, D. Z.; Xu, H. Y.; Chen, X. F.; Fang, Y. E. *European Polymer Journal* **2003,** 39, 2323-2328.

30. Sadhu, S.; Bhowmick, A. K. *Journal of Applied Polymer Science* **2004,** 92, 698-709.

31. Xie, W.; Hwu, J.; George, J.; Thand, M.; Pan, W. P. *Polymer Engineering and Science* **2003,** 43, 214-222.

32. Su, S.; Jiang, D.; Wilkie, C. *Polymer Degradation and Stability* **2003,** 83, 333-346

33. Su, S.; Jiang, D.; Wilkie, C. *Polymer Degradation and Stability* **2004,** 84, 279-288.

34. Beall, G. W.; Goss, M. *Applied Clay Science* **2004,** 27, 179-186.

35. Tahoun, S. A.; Mortland, M. M. *Soil Science* **1966,** 10, 314-321.

36. Mortland, M. M. *Clay Minerals* **1966,** 6, 143-156.

37. Greesh, N. G.; Hartmann, P. C.; Cloete, V.; Sanderson, R. D. *Journal of Colloid and Interface Science* **2008,** 319, 2-11.

38. Deng, Y.; Dixon, J. B.; White, G. N. *Soil Science Society of America Journal* **2006,** 70, 297-304.

39. Deng, Y.; Dixon, J. B.; White, G. N.; Loeppert, R. H.; Juo, A. S. R. *Colloids and Surfaces A: Physicochemical and Engineering Aspects* **2006,** 281, 82-91.

40. Bussetti, S.; Ferreiro, E. *Clays and Clay Minerals* **2004,** 52, 334-340.

41. Stutzmann, T.; Siffert, B. *Clays and Clay Minerals* **1977,** 25, 392-406.

42. He, H.; Duchet, J.; Galy, J.; Gerard, J. *Journal of Colloid and Interface Science* **2005,** 288, 171-176.

43. Negrete-Herrera, N.; Letoffe, J. M.; Putaux, J. L.; David, L.; Bourgeat-Lami, E. *Langmuir* **2004,** 20, 1564-1571.

44. Chen, B. *British Ceramic Transactions* **2004,** 6, 241-249.

45. Choi, Y. S.; Xu, M.; Chung, I. J. *Polymer* **2003,** 44, 6989-6994.

46. Gilman, J. W.; Jackson, C. L.; Morgan, A. B.; Harris, R. *Chemistry of Materials* **2000,** 12, 1866-1873.

47. Froio, D.; Ziegler, D.; Orroth, C.; Thellen, C.; Lucciarini, J.; Ratto, J. A. *ANTEC* **2004**, 2422-2426.

48. Yano, K.; Usuki, A.; Okada, A.; Kurachi, T.; Kamigaito, O. *Journal of Polymer Science Part A: Polymer Chemistry* **1993,** 31, 2493-2498.

49. Okamoto, M. *Rapra Review Reports* **2003,** 14, 1-40.

50. Manias, E.; Chen, H.; Krishnamooti, R.; Genzer, J.; Kramer, E. J.; Giannelis, E. P. *Macromolecules* **2000,** 33, 7955-7966.

51. Vaia, R.; Jandt, K. D.; Kramer, E. J.; Giannelis, E. P. *Chemistry of Materials* **1996,** 8, 2628-2635.

52. Giannelis, P. E. *Advanced Materials* **1996,** 8, 29-40.

53. Fornes, T. D.; Yoon, P. J.; Hunter, D. L.; Keskkula, H.; Paul, D. R. *Polymer* **2002,** 43, 5915-5933.

54. Huang, J.; Zhu, Z.; Yin, J.; Qian, X.; Sun, Y. *Polymer* **2001,** 42, 873-877.

55. Gilman, J.; Awad, W.; Davis, R.; Shields, J.; Harris, R.; Davis, C.; Morgan, A.; Sutto, T.; Callahan, J.; Trulove, P.; Delong, H. *Chemistry of Materials* **2002,** 14, 3776-3785.

56. Xie, W.; Xie, R.; Pan, W.; Hunter, D.; Koene, B.; Tan, L.; Vaia, R. *Chemistry of Materials* **2002,** 14, 4837-4845.

57. Park, C. I.; Park, O. O.; Lim, J. G.; Kim, H. J. *Polymer* **2001,** 42, 7465 -7475.

58. Gilman, J. W. *Applied Clay Science* **1999,** 15, 31-49.

59. Carrado, K. A.; Xu, L. *Chemistry of Materials* **1998,** 10, 1440-1445.

60. Qutubuddin, S.; Fu, X.; Tajuddin, Y. *Polymer Bulletin* **2002,** 48, 143-149.

61. Akelah, A.; Moet, A. *Journal of Materials Science Letters* **1996,** 31, 3589-3596.

62. Choi, Y. S.; Ham, H. T.; Chung, I. J. *Polymer* **2003,** 44, 8147-8154.

63. Samakande, A.; Hartmann, P. C.; Cloete, V.; Sanderson, R. D. *Polymer* **2007,** 48, 1490-1499.

64. Zhao, Q.; Samulski, E. T. *Polymer* **2006,** 47, 663-671.

65. Bourgeat-Lami, E.; Lang, J. *Journal of Colloid and Interface Science* **1999,** 210, 281-289.

66. Paine, A.; Winnik, F. *Langmuir* **1989,** 5, 903-910.

67. Saenz, J. M.; Asua, J. M. *Journal of Polymer Science Part A: Polymer Chemistry* **1996,** 34, 1977-1992.

68. Ho, C. H.; Nhen, S. A.; Amiridis, M. D.; Van, J. W. *Journal of Polymer Science Part A: Polymer Chemistry* **1997,** 35, 2907-2915.

69. Liu, J.; Chew, C.; Wang, S.; Gan, L.; Lin, J.; Tan, K. *Polymer* **1998,** 39, 283-289.

70. Song, B.; Cho, M.; Yoon, K.; Lee, D. *Journal of Applied Polymer Science* **2003,** 87, 1101-1108.

71. Shay, J. S.; English, R. J.; Spontak, R. J.; Balik, C. M.; Khan, S. A. *Macromolecules* **2000,** 33, 6664-6671.

72. Liu, J.; Gan, L. M.; Chew, C. H.; Quek, C. H.; Gong, H.; Gan, L. H. *Journal of Polymer Science Part A: Polymer Chemistry* **1997,** 35, 3575-3583.

73. Horak, D. *Journal of Polymer Science Part A: Polymer Chemistry* **1999,** 37, 3785-3792.

74. Kim, O.; Lee, K.; Kim, K.; Lee, B. H.; Choe, S. *Polymer* **2006,** 46, 1953-1959.

75. Lee, K.; Seo, H. *Korea Polymer Journal* **1998,** 6, 405-413.

76. Jayachandran, K. N.; Chatterji, P. R. *Journal of Macromolecular Science: Part C: Polymer Reviews* **2001,** 41, 79-94.

77. Ahmed, S. F.; Poehlein, G. W. *Industrial & Engineering Chemistry Research* **1997,** 36, 2597-2604.

78. Wang, D.; Dimonie, V.; E. David Sudol; EL-aasser, M. *Journal of Applied Polymer Science* **2002,** 84, 2692 - 2709.

79. Lee, J. M.; Shim, S. E.; Choe, S. *Industrial & Engineering Chemistry Research* **2006,** 12, 648-651.

80. Zhao, Q.; Samulski, E. T. *Macromolecules* **2005,** 38, 7967-7971.

81. Bourgeat-Lami, E.; Lang, J. *Journal of Colloid and Interface Science* **1998,** 197, 293-308.

82. Park, E. J.; Kim, W. S.; Hwang, H. S.; Park, C.; Lim, K. T. *Macromolecular Symposia* **2007,** 249, 196-201.

83. Liu, P.; Liu, W.; Xue, Q. *Designed Monomers and Polymers* **2004,** 7, 253-260.

84. Zerda, A. S.; Caskey, T. C.; Lesser, A. J. *Macromolecules* **2003,** 36, 1603-1608.

85. Choi, Y. S.; Choi, M. H.; Wang, K. H.; Kim, S. O.; Kim, Y. K.; Chung, I. J. *Macromolecules* **2001,** 34, 8978-8985.

86. Wu, Y.; Zhang, J.; Zhao, H. *Journal of Polymer Science Part A: Polymer Chemistry* **2008,** 47, 1535-1543.

87. Pickering, S. U. *Journal of the Chemical Society, Transactions* **1907,** 91 2001-2021.

88. Cauvin, S.; Colver, P.; Bon, F. *Macromolecules* **2005,** 38, 7887-7889.

89. Binks, B. P. *Current Opinion in Colloid & Interface Science* **2002,** 7, 21-41.

90. Zhang, J.; Chen, K.; Zhao, H. *Journal of Polymer Science Part A: Polymer Chemistry* **2008,** 46, 2632-2639.

91. Guillota, S.; Bergayaa, F.; Azevedoa, C.; Warmonta, F.; Tranchant, J. *Journal of Colloid and Interface Science* **2009,** 333, 563-569

92. Bon, S.; Colver, P. *Langmuir* **2007**, 8316-8322.

93. Voorn, D.; Ming, W.; van Herk, A. M. *Macromolecules* **2006,** 39, 2137-2143.

94. Khatana, S.; Dhibar, A.; Ray, S.; Khatua, B. *Macromolecular Chemistry and Physics* **2009,** 210, 1104-1113.

95. Yang, Y.; Zhang, J.; Liu, L.; Zhao, H. *Journal of Polymer Science Part A: Polymer Chemistry* **2007,** 45, 5759-5769.

96. Liu, L.; Zhang, J.; Wu, C.; Zhao, H. *Macromolecular Rapid Communications* **2008,** 29, 45-51.

97. Yang, Y.; Liu, L.; Zhang, J.; Li, C.; Zhao, H. *Langmuir* **2007,** 23, 2867-2873.

98. Riess, G.; Labbe, C. *Macromolecular Rapid Communications* **2004,** 25, 401-435.

99. Jung, H.; Song, K.; Lee, K.; Lee, B.; Choe, S. *Journal of Colloid and Interface Science* **2007,** 308, 103-141.

100. Cho, Y.; Yang, J.; Lee, J. *Materials Science and Engineering A* **2004,** 24, 293-304.

101. Georges, M.; Vergin, R.; Kazmair, P.; Hamer, G. *Macromolecules* **1993,** 26, 2987-2995.

102. Wang, J.; Matyjaszewski, K. *Macromolecules* **1995,** 28, 7901-7911.

103. Moad, G.; Chiefari, J.; Chong, Y.; Krstina, J.; Mayadunne, R.; Postma, A.; Rizzardo, E.; Thang, S. *Polymer International* **2000,** 49, 993-1002.

104. Samakande, A.; Juodaityte, J.; Sanderson, R.; Hartmann, P. *Macromolecular Materials and Engineering* **2008,** 293, 428-437.

105. Samakande, A.; Sanderson, R.; Hartmann, P. *Polymer* **2009,** 50, 42-49

106. Samakande, A.; Sanderson, R.; Hartmann, P. *Journal of Polymer Science Part A: Polymer Chemistry* **2008,** 46, 7114-7126.

107. Tasdelen, M.; Kreutzer, J.; Yagci, Y. *Macromolecular Chemistry and Physics* **2010,** 211, 279-285.

108. Lacroix-Desmazes, P.; Severac, R.; Boutevin, B. *Macromolecules* **2005,** 38, 6299-6309.

109. Lacroix-Desmazes, P.; Severac, R.; Boutevin, B. *Polymeric Preprints* **2003,** 44, 683-684.

110. Boyer, C.; Lacroix-Desmazes, P.; Robin, J.; Boutevin, B. *Macromolecules* **2006,** 39, 4044-4053.

111. Enriquez-Medrano, F.; Guerrero-Santos, R.; Hernandez-Valdez, M.; Lacroix-Desmazes, P. *Journal of Applied Polymer Science* **2010,** 119, 2476-2484.

112. Tonnar, J.; Lacroix-Desmazes, P.; Boutevin, B. *Macromolecules* **2007,** 40, 6076-6081.

113. Nottelet, B.; Lacroix-Desmazes, P.; Boutevin, B. *Polymer* **2007,** 48, 50-57.

114. Shin, H.; Oh, H.; Lee, K.; Lee, B.; Choe, S. *Polymer* **2009,** 50, 4299-4307.

115. Causin, V.; Mareigo, C.; Ferrara, G. *Polymer* **2005,** 46, 9533-9537.

116. Ginnelis, P. E. *Chemistry of Materials* **1996,** 8, 29-40.

117. Poreter, D.; Metcalfe, E.; Tomas, M. J. K. *Fire and Materials* **2000,** 24, 45-52.

118. Haraguchi, K.; Jun, H.; Matsuda, K.; Takehisa, T.; Elliott, E. *Macromolecules* **2005,** 38, 3482-3490.

119. Kim, Y. K.; Choi, Y. S.; Wang, K. H.; Chung, I. J. *Chemistry of Materials* **2002,** 14, 4990-4995.

120. Morgan, A. B.; Gilman, J. W. *Journal of Applied Polymer Science* **2003,** 87, 1329-1338.

121. Wang, H.; Chang, K.; Chu, H. *Polymer International* **2005,** 54, 114-119.

122. Zhang, Y.; Lee, J.; Jang, H.; Nah, C. *Composites: Part B* **2004,** 35, 133-138.

123. Manias, E.; Chen, H.; Krishnamooti, R.; Genzer, J.; Kramer, E. J.; Giannelis, E. P. *Macromolecules* **2002,** 33, 7955-7966.

124. Noh, M. W.; Lee, D. C. *Polymer Bulletin* **1999,** 42, 619-626.

125. Qutubuddin, S.; Fu, X. *Polymer* **2001,** 42, 807-813.

126. Stevens, M. P., *Polymer Chemistry : An Introduction*. Oxford University Press: New York, 1990; p 171.

127. Jang, B. N.; Wilkie, C. A. *Polymer* **2005,** 46, 9702-9713.

128. Blumstein, A. *Journal of Polymer Science, Part A: Polymer Chemistry* **1965,** 3, 2653-2661.

129. Doh, J.; Cho, I. **1998,** Polymer Bulletin, 511-518.

130. Biswas, M.; Ray, S. *Advances in Polymer Science* **2001,** 155, 170-221.

131. Yei, D. R.; Kuo, S. W.; Su, Y. C.; Chang, F. C. *Polymer* **2004,** 45, 2633-2640.

132. Zhang, W. A.; Chen, D. Z.; Xu, H. Y.; Chen, X. F.; Fang, Y. E. *European Polymer Journal* **2003**, 2323-2328.

133. Wilkie, A.; Zhang, J. *Polymer Degradation and Stability* **2004,** 83, 301-307.

Chapter 3

Preparation of Polystyrene-Clay Nanocomposites by Free-radical Polymerization in Dispersion

Abstract

Fully exfoliated polystyrene-clay nanocomposites were prepared via free radical polymerization in dispersion polymerization, for the first time, in a mixture of ethanol and water. Sodium montomorillonite clay was pre-modified using 3-(trimethoxysilyl) propyl methacrylate before being used in a dispersion polymerization process. The objective of this study was to determine the impact of the clay concentrations on the monomer conversion, the polymer molecular weight, and the morphology and thermal stability of the nanocomposites prepared via dispersion polymerization. Dynamic light scattering and scanning electron microscopy revealed that the particle size decreased and became more uniformly distributed with increasing clay loading. X-ray diffraction and transmission electron microscopy revealed that nanocomposites at low clay loading yielded exfoliated structures, while intercalated structures were obtained at higher clay loading.

Chapter 3

Preparation of Polystyrene-Clay Nanocomposites by Free-radical Polymerization in Dispersion

3.1 Introduction

The preparation of uniform polymer particles of micrometer size has attracted a great deal of interest.[1,2] Latexes with narrow particle size distribution have found a wide variety of applications, such as in toners, column packing materials for chromatography, solid supports for organic and biopolymer synthesis, and in biochemical analysis.[2-5] These particles are difficult to obtain because their size lies between the size of the particles produced by conventional emulsion polymerization (0.06–0.7 μm) and suspension polymerization (50–1000 μm).

Dispersion polymerization is a simple and fast (i.e. single step) technique used to prepare monodisperse polymer particles of intermediate range of sizes (1–20 μm) in very good yield.[5-10] Dispersion polymerization may be defined as a type of precipitation polymerization in which the polymerization is carried out in the presence of a suitable polymeric stabilizer that is soluble in the reaction medium. The continuous phase is chosen to be a solvent for the monomer to be polymerized and a non-solvent for the resultant polymer.[3,11,12] A steric stabilizer is used to produce a colloidally stable dispersion, without which the polymerization would afford macroscopic particles of polymer of uncontrolled size.[13] The dispersion polymerization process takes place in a homogenous medium of monomers, free radical initiator, and polymeric stabilizer dissolved in a suitable solvent. At elevated temperature the initiator decomposes and generates free radicals, which initiate chain growth by the addition of monomers. The growing chain remains in solution until a critical chain length is reached, and then it

precipitates. This step is refered to as nucleation. These unstable nano-size particles aggregate into large particles of about 200 nm in diameter and stabilize themselves against further aggregation by adsorbing the stabilizer from the medium. These particles grow by capturing small nuclei and oligomeric radicals from the continuous phase, and polymerizing the absorbed monomer inside the particles. This continues until all of the oligomeric radicals and nuclei generated in the reaction medium are consumed.[14]

Dispersion polymerization has been widely used for the preparation of a variety of polymers, such as polystyrene (PS),[3,4] poly(butyl acrylate) (PBA),[15] polyacrylamides,[9] poly(styrene-co-butylacrylate) (PS-co-BA),[13] and poly(methyl methacrylate) (PMMA).[16]However, there are only a few articles reporting on the use of the dispersion polymerization method in the field of nanotechnology.[17,18]

Polymer-clay nanocomposites (PCNs) is one of the most rapidly growing fields in nanotechnology because PCN materials exhibit excellent mechanical, thermal and gas barrier properties relative to the corresponding neat polymers.[19] Among the few recent articles that report on the use of dispersion polymerization to prepare clay-containing nanocomposite materials, only intercalated or partially exfoliated structures have been obtained. Zhao and Samulski[20] prepared a partially exfoliated PMMA nanocomposite using dispersion polymerization in supercritical carbon dioxide (CO_2). The clay was modified using a fluorinated surfactant. They found that the modified clay not only acts as an inorganic filler but also as a stabilizer for the growth of PMMA particles by free-radical polymerization of PMMA. In another study Zhao and Samulski[17] synthesized PMMA and PS nanocomposites via dispersion polymerization in supercritical CO_2 in the presence of clay that was surface modified using aminopropyl-terminated poly(dimethysiloxane) surfactant. The morphology of the nanocomposites obtained was strongly dependent on the concentration of the organoclay and on the type of polymer involved. In the case of PMMA an exfoliated structure was obtained whereas in the case of PS a nanocomposite with a partially exfoliated morphology was obtained. Lami and Lang[21]successfully encapsulated silica particles by polymerizing styrene using dispersion polymerization in polar medium (ethanol/water), with 3-(trimethoxysilyl) propyl

methacrylate(MPTMS) chemically attached to the silica particles. Park *et al.*[22] synthesized PMMA encapsulated silica by dispersion polymerization in supercritical CO_2. The silica particles were modified using MPTMS before being used in dispersion polymerization. Dispersion polymerization of styrene was used by Liu *et al.*[23]tograft PS from silica particles. The surface of the silica particles was first treated withMPTMS followed by radical copolymerization of styrene monomers. Zerda *et al.*[24] also used supercritical CO_2 as a reaction medium for the preparation of highly filled PCNs.

To the best of the aurthor's knowldege there are no reports of PCNs prepared via dispersion polymerization in polar medium. The present work reports for the first time, the preparation of fully exfoliated PCNs using dispersion polymerization in polar medium (ethanol/water, 85:15), and the impact of the clay loading on particle size, morphology and thermal properties of the nanocomposite materials prepared.

3.2 Experimental

3.2.1 Materials

Sodium montmorillonite (Na-MMT) (Cloisite-NA+) was obtained from Southern Clay Products, Inc. (USA), as a fine powder with an average particle size of less than 13 μm^3 by volume in the dry state, and with a cation exchange capacity (CEC) of 92.6 milliequivalents (meq)/100 g clay. Stabilized styrene monomer was obtained from Aldrich. The stabilizer was removed by washing three times with a 3 wt% potassium hydroxide solution and then purifying by distillation under reduced pressure at 30 ^{o}C. 3-(Trimethoxysilyl) propyl methacrylate 98% was obtained from Aldrich and used as received. The initiator 2,2-azobis(isobutyronitrile) (AIBN) was obtained from Aldrich and recrystallized before use. Hydroxypropyl cellulose (HPC) and MPTMS were purchased from Aldrich and used as received.

3.2.2 Functionalization of MMT by MPTMS

Na-MMT (6 g) was suspended in toluene (200 mL) and the required quantity of MPTMS (4.4 g), corresponding to about 1.5 meq of coupling agent per gram MMT, was

introduced into the reaction flask. The reaction mixture was stirred for four days at ambient temperature. The grafted Na-MMT then was washed four times with 150 mL toluene in order to remove unreacted MPTMS. The crude product was dried at 40 °C in a vacuum oven. It was then suitable for use in the dispersion polymerization.

3.2.3 Dispersion polymerization

The silane functionalized MMT was utilized as seed particles. The polymerizations were carried out in a 250 ml three-necked round-bottom flask equipped with a baffle stirrer, a reflux condenser, a nitrogen inlet, and a rubber septum, at 75 °C. In a typical procedure, MPTMS-MMT (1 – 10 wt % relative to 10 g monomer) was suspended in a dispersion medium containing ethanol and water (85/10). HPC (0.015 g) was dissolved in ethanol (5 mL). The monomer phase was prepared by dissolving AIBN (0.004 g) in styrene monomer (10 g), and then purging with nitrogen for 20 min. The solution of stabilizer/dispersion medium was first charged into the reactor, followed by purging with nitrogen gas for 20 min. The mixture was stirred and heated to 75 °C. The monomer phase was then added all at once. Polymerization was carried out for 6 h. On completion of the reaction the reactor was cooled by immersion in an ice bath for 10 min. Small quantities of the dispersion were regularly sampled, the product was dried in a vacuum oven at 25 °C for 24 h, and then analyzed by small angle X-ray diffraction (SAXS), transmission electron microscopy (TEM) and thermogravimetric analysis (TGA).

3.2.4 Characterization

SAXS measurements were performed at 298 K, in a transmission configuration. A copper rotating anode X-ray source (functioning at 4 kW) with a multilayer focusing "Osmic" monochromator giving high flux (10^8 photons/sec) and punctual collimation was used. An "image plate" 2D detector was used. Diffraction curves were obtained, giving diffracted intensity as a function of the wave vector *q*. The d spacing was calculated using the formula: $d = 2\pi/q$ (where q is the wave vector; associated with Bragg's peak position).[25,26]

TEM analysis was carried out at an accelerating voltage of 120 kV. Prior to analysis, samples of PCNs were stained with OsO_4, then embedded in epoxy resin and cured for 24 h at 60 ºC. The embedded samples were cut into slices of a nominal thickness of 100 nm, using an ultramicrotome with a diamond knife on a Reichert Ultracut S ultramicrotome, at room temperature. The sections were transferred from water at room temperature onto a 300-mesh copper grid.

TGA was carried out using a TGA-50 SHIMADZU thermogravimetric instrument, with a TA-50 WSI thermal analyzer, connected to a computer. Samples (10–15 mg) were degraded in a nitrogen atmosphere, using a nitrogen flow rate of 50 mL/min and a heating rate of 20 °C/min.

Gel permeation chromatography (GPC) was performed using a Waters 600E system controller equipped with a Waters 610 fluid unit pump, a Waters 410 differential refractometer as detector, and a column set of a PLgel 5 mm guard 50×7.5 mm and a PLgel 5 mm mixed-C 300×7.5 mm column (Polymer Laboratories, USA). Measurements were carried out at 30 ºC, using THF as eluent and a flow rate of 1 mL/min. The GPC column was first calibrated with 10 samples of polystyrene standards. Prior to analysis samples were vigorously stirred in THF for a week to ensure that all components were fully dissolved. The samples were then filtered through a 0.45-µm filter membrane, five times, thus only the components soluble in THF were analyzed.

The sizes of the PS particle prepared in dispersion polymerization were determined by scanning electron microscopy (SEM), using a Leo® 1430VP scanning electron microscope. Prior to imaging, the samples were sputter-coated with gold. Samples were quantified by EDS analysis using an Oxford Instruments® 133keV detector and Oxford INCA software.

Dynamic light scattering (DLS) was also used to determine the particle size. Latex samples were prepared by dissolving a few drops of latex in deionized water. DLS measurements (Malvern Instruments, USA) were carried out at 25 ºC on a Malvern-Nano instrument fixed at 90 degrees. The instrument system was calibrated using

nanospheresize standards of polymer microsphereres in water, with a mean dimeter of 60 nm.

3.3 Results and Discussion

3.3.1 Modification of clay

FT-IR spectra of MPTMS, neat Na-MMT and MPTMS modified Na-MMT were recorded, and shown in Fig.3.1.

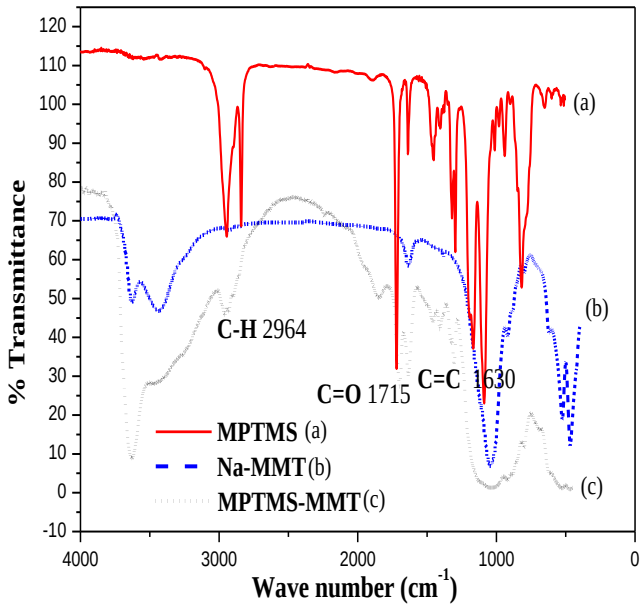

Fig. 3.1: FT-IR spectra of MPTMS, Na-MMT and MPTMS-MMT.

The FT-IR spectrum of Na-MMT shows absorption bands at 620, 3432 and 1640 cm^{-1}, corresponding to the Al-O, Si-O and OH stretching, respectively.[27,28]The appearance of new bands in the FT-IR spectrum of clay modified by MPTMS (MPTMS-MMT) indicates the presence of MPTMS in the clay. The band at 2964 cm^{-1} is related to the C-H stretching of MPTMS. Other new bands in the FT-IR spectrum of MPTMS-MMT can be seen at 1715 cm^{-1}, corresponding to the (C=O stretching) of MPTMS, and at 1360 cm^{-1}, corresponding to the (C=C stretching) of MPMTS. The FT-IR spectrum of MPTMS-MMT was found to be similar to spectra of MPTMS-MMT reported in literature.[21,29-31]

In order to gain quantitative insight into the extent to which the grafting process took place, TGA was used to determine the amount of MPTMS that was chemically anchored on the clay after extensive washing. Fig.3.2 shows the TGA thermograms before and after the grafting of the MPTMS molecules onto theclay.

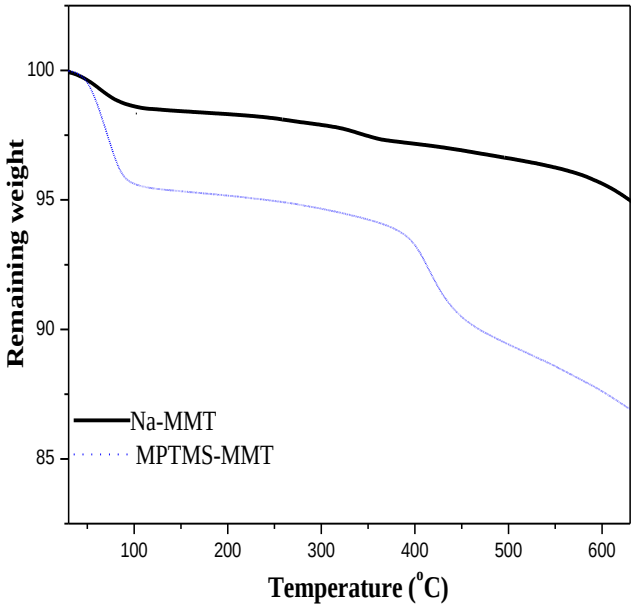

Fig. 3.2: TGA thermograms of Na-MMT and MPTMS-MMT.

The weight loss of pure clay between 20 and 100 ºC corresponds to the removal of water coordinated with Na^+ from the interlayer.[32] The difference between the weight loss of the unmodified and the modified clay confirmed the grafting of MPTM onto clay. The grafted amount was determined using equation (3.1),[30] using the weight loss $W_{200-600}$differencebetween 200 and 600 ºC,corresponding to the MPTMS degradation.[30]

$$Grafted\ amount\ (meq/g) = 10^3\ (W_{200-600}) / (100 - W_{200-600})\ M \quad (3.1)$$

where M (g/mol) is molecular weight of the grafted silane molecules. Accordingly, only 33.5 meq/100 g MPTMS was experimentally found to be grafted onto the clay.

The changes in the interlayer distance (*d* spacing) before and after the modification process were monitored using SAXS measurements. The SAXS patterns of the clay materials before and after grafting are shown in Fig. 3.3.

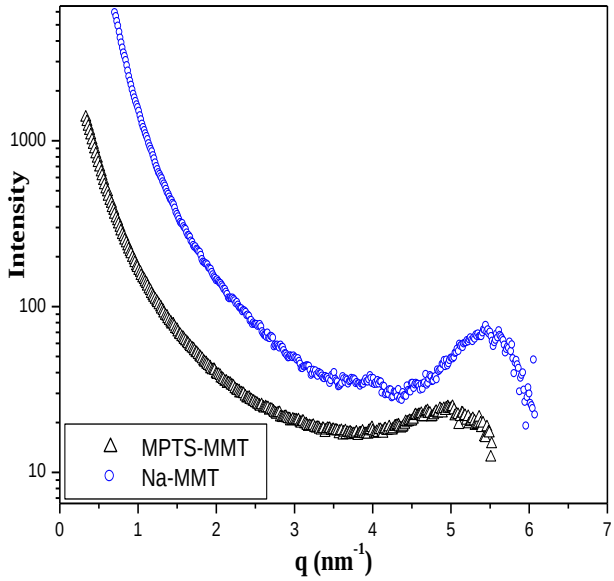

Fig. 3.3: SAXS patterns of Na-MMT and MPTMS.

The *d* spacing for neat Na^+-MMT, namely 1.18 nm, was found to be comparable to the values reported in the literature.[33] An increased interlayer distance was found for the modified clay relative to the unmodified clay. Such an increase in *d*-spacing of MPTMS-MMT relative to pure MMT shows that insertion of MPTMS also occured between clay platelets, and not only on the external surface of the clay. This is in accordance with the findings of He *et al.*[34] who studied the grafting of silane compounds onto clay and demonstrated that the grafting process occurs in two basic steps: first, the silane molecules are intercalated into the clay interlayer and, second, the condensation reaction takes place between silane molecules and the clay layer surface. On the contrary, Shimizu *et al.*[29] suggested that the silane molecules could only react at the "broken" edges of the clay layer rather than with the interlayer surface. Negrete-Herrera *et al.*[30] modified laponite clay with silane compounds and found that the silane molecules could potentially react with laponite particles through a condensation reaction between the surface

hydroxyl groups located on the clay edges and the alkoxy groups of the silane molecules, giving rise to the formation of Si-O-Si covalent bonds. Wu *et al*[35] prepared PS brushes on the edges of clay sheets using edge modification by silane, followed by polymerization using atom transfer radical polymerization (ATRP).

3.3.2 Polymerization and latex characterization

The effects of varying amounts of organoclay on the molecular weight, monomer conversion, polymer particle size, and latex viscosity of synthesized PCNs were investigated. The results are tabulated in Table 3.1.

Table 3.1. Effects of added organoclay on the conversion, average molecular weight, polydispersity of PS particle sizes and viscosity of PS nanocomposites

Organoclay (wt % relative to styrene)	Conversion (%)	$\overline{M}_w \times 10^3$ (g/mol)	$\overline{M}_n \times 10^3$ (g/mol)	$\overline{M}_w / \overline{M}_n$	Viscosity (η) $\times 10^{-2}$ (Pa.s)	Particle size (nm)
0	82	595	141	4.22	0.153	1320
1	75	411	126	3.26	0.245	1050
3	68	347	68	5.10	0.376	731
5	64	424	138	3.07	0.620	331
7	68	333	107	3.10	0.670	261
10	68	311	124	2.50	1.600	254

The general trend shows a decrease in the molecular weight and the conversion as the clay loadings increases. Different results were reported by Zhao and Samulski.[17] who synthesized PS/clay nanocomposites using dispersion polymerization in supercritical CO_2 and found that the molecular weight of PS did not change noticeably as the clay concentration increased. Yan *et al*.[36] on the other hand, found that the conversion and the molecular weight of PS nanocomposites prepared in supercritical CO_2 increased significantly upon increasing the clay loading. The discrepancy between the various reports and the results of this study shows that the clay loading can not be considered as being the main factor impacting on the polymerization conversion and molecular weight.

Fig. 3.4 shows a particle size analysis of colloidal suspensions of neat PS and PS/clay nanocomposites prepared using different clay loadings using dynamic light scattering (DLS).

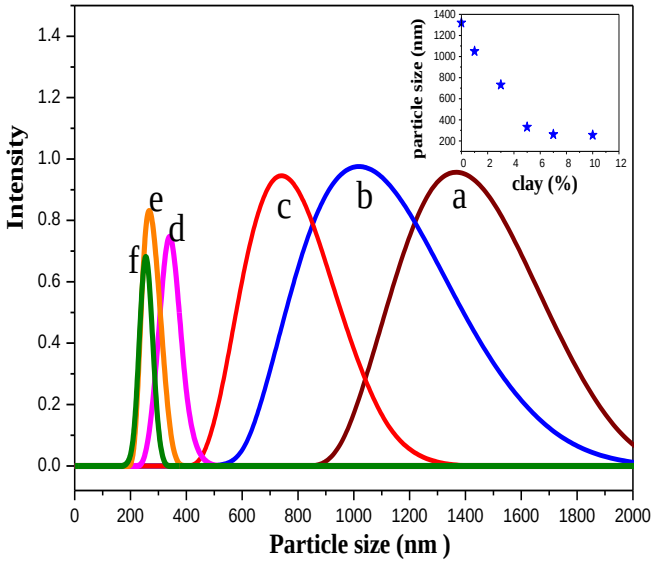

Fig. 3.4: DLS size distribution graph of PS and PS/clay nanocomposites with (a) 0 wt%, (b) 1 wt%, (c) 3 wt%, (d) 5 wt%, (e) 7 wt% and (f) 10 wt% clay loading, respectively. The insert shows the evolution of the mean particle size as a function of the percentage clay loading in the original feed.

DLS shows that the neat PS has an average particle diameter of about 1.3 – 1.4 µm, with a broad distribution. On the other hand, in the case of PCNs, the average diameter of PS particles decreased, and became more uniformly distributed (i.e. narrow distribution) as the concentration of clay increased from 1 wt% to 10 wt% loadings. The PS/clay nanocomposite particles obtained were also characterized using SEM (see Fig.3.5). The particle size decreased and became more uniformly distributed as the clay content increased, confirming DLS measurements.

The findings of this study are in agreement with those of Zhao and Samulski,[17] who prepared PMMA nanocomposites via dispersion polymerization in supercritical CO_2, and observed similar effects of clay on the particle size of the PMMA particles obtained. It is however worth mentioning that the morphology of PS prepared without MPTMS-modified clay was found to be ill-defined (cf. Fig.3.5 e), it had large particle sizes and non-uniform size distribution, as measured by DLS.

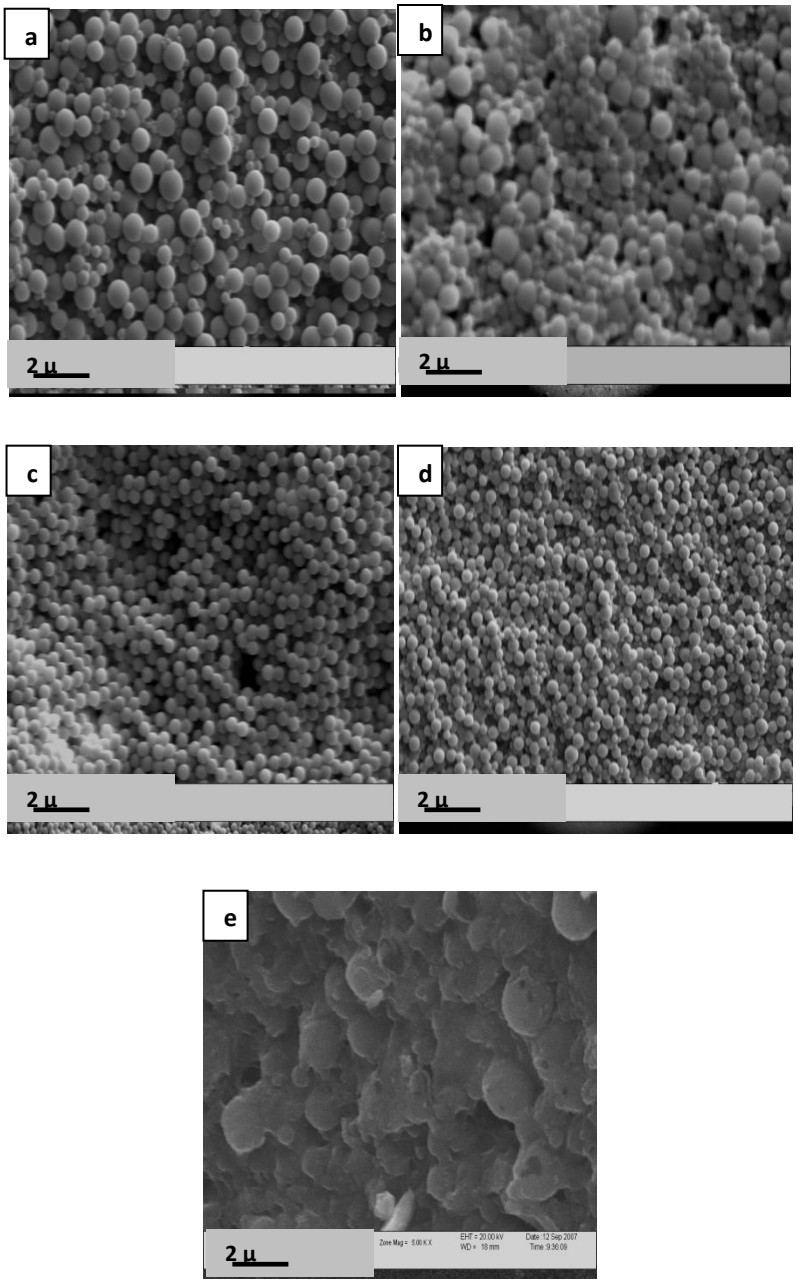

Fig. 3.5: SEM images of PS nanocomposites (a–d) containing 1 wt%, 3 wt%, 7 wt% and 10 wt% clay loadings, respectively, and (e) neat PS.

Although here the MPTMS-clay is meant to act as a stabilizer in styrene polymerization, the decrease in particle size with increasing MPTMS-clay loading is not consistent with what is usually observed when common stabilizers are used in typical dispersion polymerizations.[13]It is proposed that the difference is related to the dispersion

polymerization mechanism described earlier in Section 3.1. As nucleation in the early stage of the polymerization is intrinsically unstable, and aggregates into larger particles, they then start to stabilize themselves against further aggregation by adsorption of MPTMS-MMT from the medium.[7] Therefore, the number of formed nuclei increased with increasing MPTMS-MMT concentration which led to many small particles. Yang *et al*.[37]also prepared PS colloid particles armoured by clay layers with mixed polymer brushes in suspension polymerization and observed that the clay layers had a similar effect on the particle size and distributions. Fig.3.6 shows an example of a TEM image of a PS/clay nanocomposite latex prepared at 7 wt% clay loading. The clay particles appear as relatively thick platelets surrounding the polymer particles, and they are not evenly distributed inside the particles.

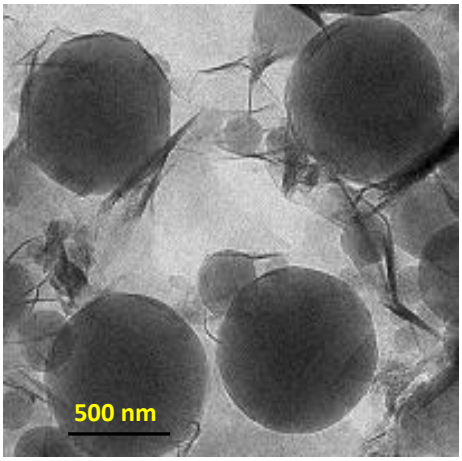

Fig. 3.6: TEM image of PS/clay nanocomposite particle prepared at 7 wt% clay loading.

Furthermore, the viscosity of the reaction medium substantially increased with increasing MMT clay loading, as shown in Table 3.1. This reduced the movement of small nuclei and oligomeric radicals from the continuous phase into the polymer particles, therefore hindering the polymerization inside the particles and resulting in smaller particles size.

3.3.3 Material characterization

3.3.3.1 The morphology of nanocomposites

SAXS has been widely used to characterize the layered structure of PCNs as the change in 2θ is correlated to changes in the interlayer distance of the clay.[38]

Fig. 3.7 shows the SAXS patterns of nanocomposites synthesized using different MPTMS-clay loadings (1–10 wt %).

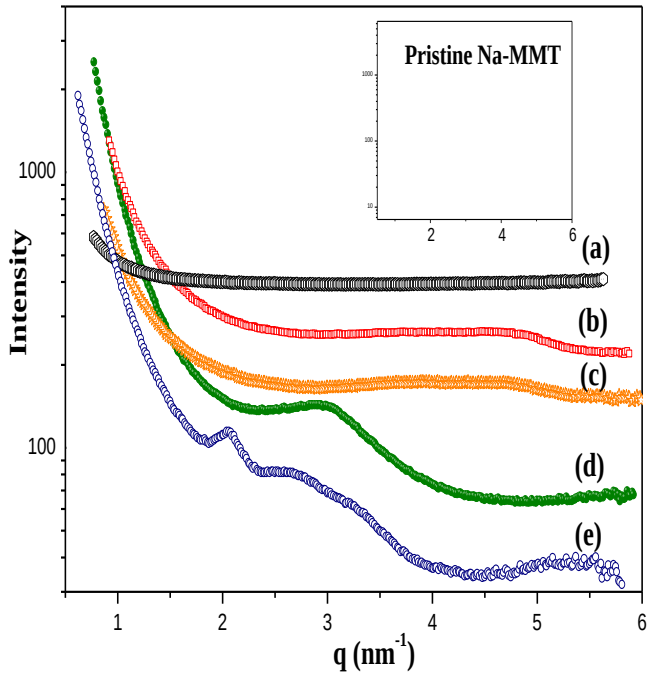

Figure 3.7 SAXS patterns of PS/clay nanocomposites containing (a) 1 wt%, (b) 3 wt%, (c) 5 wt%, (d) 7 wt% and (e) 10 wt% clay loading, respectively.

The final morphology of the nanocomposites prepared is undoubtedly influenced by the MPTMS-clay content. At 1wt% clay loading no peak in SAXS patterns was distinguishable, as seen in Fig. 3.7 a. This may be due to either the absence of periodically stacked MMT layers (i.e. an exfoliated structure) or due less likekly to the detection limit of the measuring system. The formation of a fully exfoliated structure of PS/clay nanocomposite at 1 wt% clay loading was confirmed by TEM (cf. Fig. 3.8 a), where all the silicate layers appear as dark lines that are completely separate from each other. On the other hand, broad peaks were observed as the clay loading increased,

indicating that exfoliated-intercalated (*partially exfoliated*) structures were obtained at 3 wt% and 5 wt% MPTMS-clay loadings. This was consistent with TEM results (see Fig. 3.8 b), showing that some of the clay platelets are still stacked to each other, as seen by the darkest areas, while some individual clay layers are well dispersed in the polymer matrix. At 7 wt% and 10 wt% MPTMS-clay loadings diffraction peaks corresponding to *d*-spacings of between 2.04 and 3.05 nm appeared (cf. Fig. 3.7 d and e), showing intercalated structures, as confirmed by TEM (cf. Fig. 3.8 c and d).

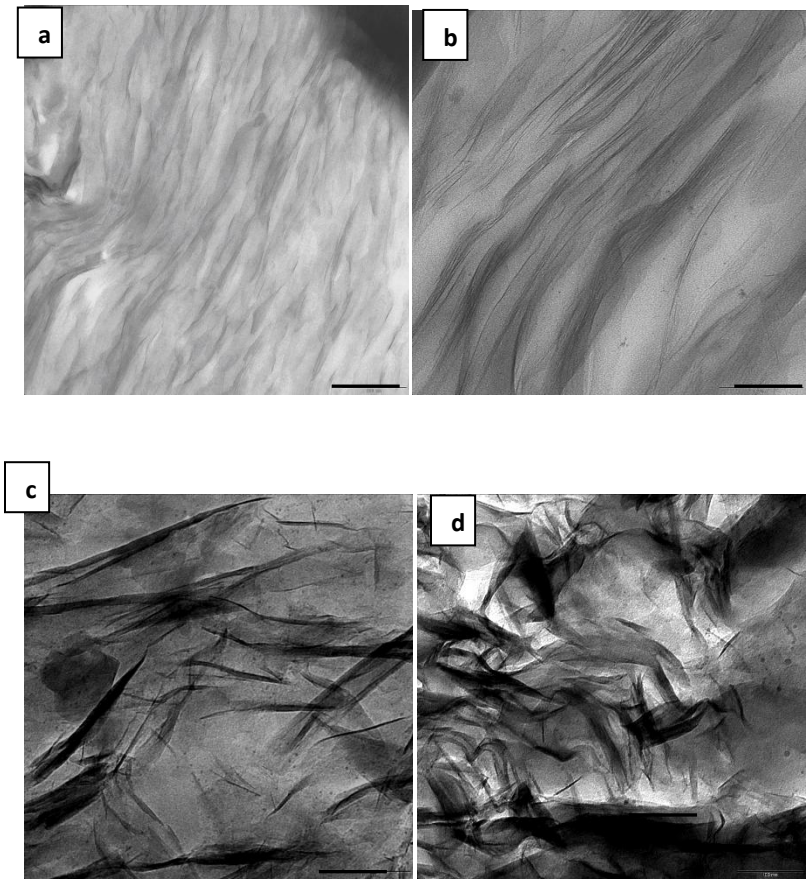

Fig. 3.8: TEM images of PS containing (a) 1 wt%, (b) 5 wt%, (c) 7 wt% and (d) 10 wt% clay loadings, respectively. Bar = 100 nm

SAXS and TEM data clearly show that the nanocomposite structure is strongly dependent on the clay/polymer ratio. These results are consistent with those of other researchers

who obtained exfoliated structures in emulsion polymerization at low clay loading and intercalated structures at high clay loading[39-42],showing that the clay loading is a critical factor affecting the morphology and properties of PCNs. There is however no universal trend relating to the way that the percentage of clay affects the morphology and properties. In one of our previous studies, we investigated the effect of clay loading on the morphology and properties of poly(styrene-*co*-butyl acrylate) nanocomposites prepared by polymerization in emulsion.[43] Exfoliated PCNs were obtained at 10 wt% clay loading, whereas an intercalated morphology was obtained for a clay loading ofabout 1 wt%. Among the few articles reporting on the morphology of nanocomposites prepared using dispersion polymerization, Zhao and Samulski[17] obtained exfoliated structures with PMMA and intercalated structures with PS (prepared under similar conditions). They interpreted the discrepancy between the observed morphologies as being due to the difference in the interaction between polymers and clay, where PMMA interacts with clay via hydrogen bonding and PS interacts with clay via weaker van der Waals forces. Yan *et al*.[36] also obtained only intercalated structures for PS/clay nanocomposites prepared via dispersion polymerization in supercritical CO_2.

3.3.3.2 Thermal stability of nanocomposites

The thermal stabilities of the PS/clay nanocomposites were studied by TGA and compared to neat PS under similar conditions as shown in Fig. 3.9. All synthesized PS/clay nanocomposites were found to be thermally more stable than the neat PS. The temperature of onset of decomposition shifted toward higher temperature as the amount of MPTMS-modified clay increased.

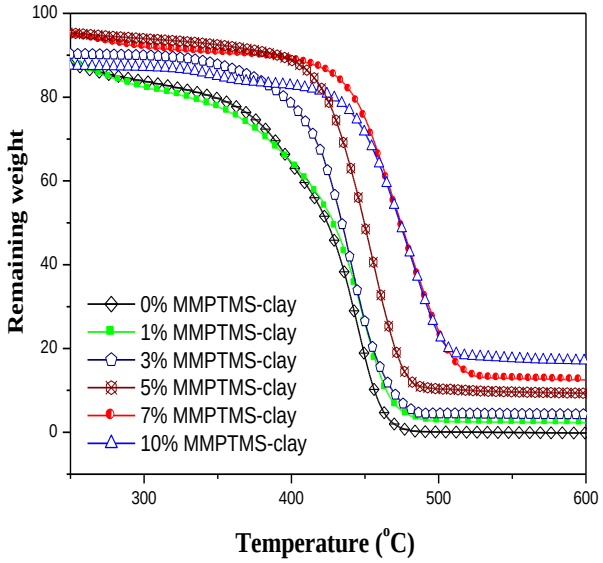

Fig. 3.9:Thermal stability of PS/clay nanocomposites at different clay loadings and 0 wt% clay as reference.

The improvement in thermal stability due to the presence of clay is generally attributed to the formation of clay char that acts as a mass transport barrier and an insulator between the bulk polymer and the surface, where the combustion of the polymer takes place.[19,44]The presence of clay also hinders the diffusion of volatile decomposition products within the nanocomposites.[19] The enhancement of the thermal stability of nanocomposites has also been attributed to the restricted thermal motion of polymer chains inside the clay galleries.[45] The thermograms show that both the dispersion states of clay within the polymer matrix and the clay loading have a effect on the thermal stability. The nanocomposites with 10 wt% clay (*intercalated*) show higher thermal stability relative to the nanocomposites with 1 wt% clay (*exfoliated*). It is generally reported that exfoliated nanocomposite structures have higher thermal stability than intercalated structures.[33,46] However, contradictory results have been also reported by Giannelis,[47] who synthesized exfoliated and intercalated poly(ethylene imine)/clay nanocomposites, with the same clay loading in emulsion polymerization, and found higher thermal stabilities for intercalated structures relative to the exfoliated morphologies. Samakande *et al.*[48] observed similar results with PS/clay nanocomposites prepared by free-radical polymerization in bulk. In the present work it is clear that the contribution of both factors,

namely an increase in clay loading and a higher degree of intercalation, led to the improvement of the PS/clay nanocomposite's thermal stability as the clay loading increased.

3.3.3.3 Thermo-mechanical properties of nanocomposites

The response of a material to cyclic deformation as a function of temperature was measured by dynamic mechanical analysis (DMA). There are three main parameters that can be determined via DMA: (i) the storage modulus (G'), which is a measure of elastic response to the deformation, (ii) the loss modulus (G''), which a measure of the plastic response and (iii) Tan δ the ratio $\frac{G''}{G'}$.[49]

For temperatures below the T_g all nanocomposites that were synthesized, showed a higher storage modulus plateau relative to that of the neat polymer, as shown in Table 3.2. The enhancement in storage modulus is caused by the high aspect ratio of dispesersed clay and the interaction between the polymer chains and clay layers, resulting in a decrease in the polymer sgements mobility near the polymer-clay interface. Fig. 3.10 shows the variation in storage modulus and tan δ as a function of temperature for pure PS, and its nanocomposites with various morpholgies (intercalated and exfoliated).

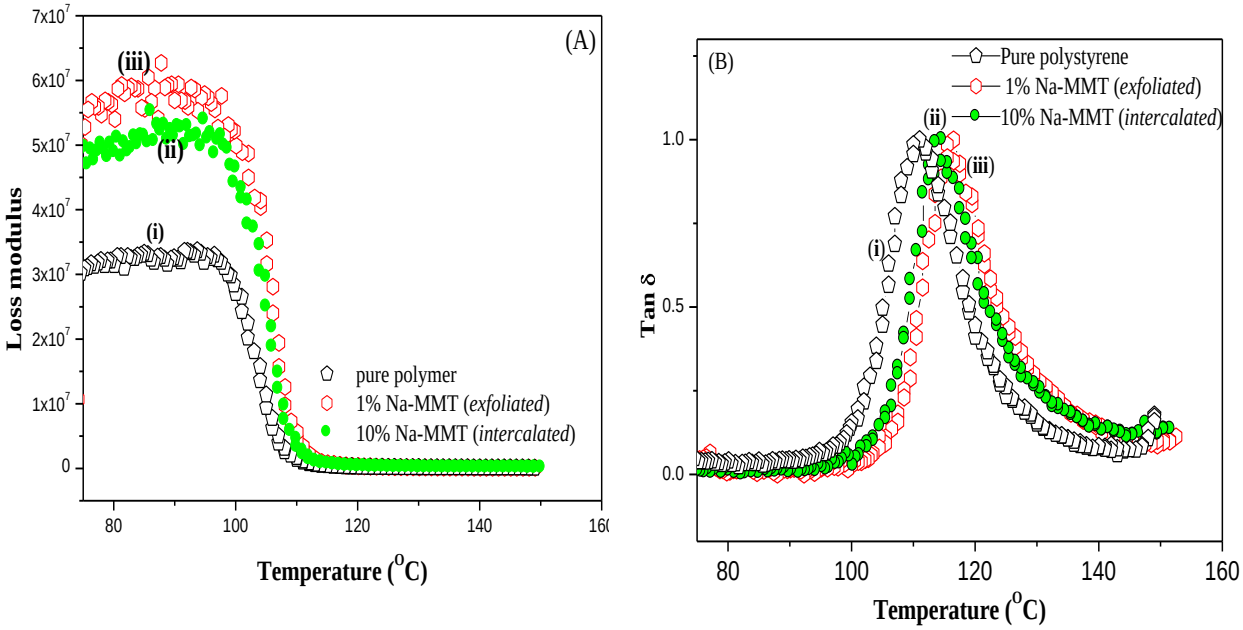

Fig. 3.10: Variation of (A) storage modulus and (B) tan δ vs. temperature for (i) pure PS, and nanocomposites with (ii) 10 wt% clay loading (intercalated), and (iii) 1 wt% clay loading (exfoliated).

The exfoliated PS-nanocomposites at clay loadings 1-5 wt% showed a higher storage modulus relative to intercalated nanocomposites at higher clay loadings (7 wt% and 10 wt%). This is due to homogenous dispersion of clay in the polymer matrix and a higher interface area between polymer matrix and the clay filler taking place in the exfoliated PCN. Exfoliated clay platelets have a flexible, sheet-type structure, whose thickness is in the order of 1 nm and lateral dimensions (length and width) range from several hundreds of nanometres to a few microns. On the other hand, conventional composites contain clay particles with micron-scale dimensions. Therefore the mechanical properties are strongly affected by the dispersion state of clay particles through the polymer matrix.[50]

Table 3.2. T_g values and storage modulus of nanocomposite

Sample	% clay	G^I x 10^7 (Pa) @ T<T_g	T_g(ºC)
PS standard	0	3.07	101
PS/clay nanocomposites	1	5.60	113
	5	5.00	115
	7	4.83	117
	10	4.80	115

All $T_g$values were obtained from the onset of the tan δ curve. Fig. 3.10 (B) shows that tan δ peaks for nanocomposites shifted to higher temperature relative to that for pure polymer. This trend has been reported before, and is attributed to a restricted chain mobility brought about by the clay nanofiller, i.e. the clay layers act in similar way as cross-linkers in the nanocomposites systems, leading to the restriction of motion.[51]

3.4 Conclusions

Fully exfoliated PS/clay nanocomposites were successfully synthesized for the first time via dispersion polymerization in polar medium (ethanol/water). The particle size and molecular weight of the PS/clay nanocomposites were affected by the MPTMS-clay loading. The particles size decreased and the distribution narrowed as the clay loading increased. Exfoliated structures were obtained at low clay loading, while intercalated structures predominated at increasing clay loading. All synthesized PS/clay nanocomposites were found to be thermally more stable than the neat PS. Intercalated, high clay loading PCNs were found to be thermally more stable than exfoliated structures with low clay loading. The prepared nanocomposites also exhibited enhanced mechanical properties, which were dependent on the extent of clay dispersion.

3.4 References

1. Ober, C. K.; Lokt, K. P. *Macromolecules* **1987,** 20, 268-273.

2. Bulmus, V.; Tuncel, A.; Piskin, E. *Journal of Applied Polymer Science* **1996,** 60, 697-704.

3. Liu, J.; Gan, L. M.; Chew, C. H.; Quek, C. H.; Gong, H.; Gan, L. H. *Journal of Polymer Science Part A: Polymer Chemistry* **1997,** 35, 3575-3583.

4. Ahmed, S. F.; Poehlein, G. W. *Industrial & Engineering Chemistry Research* **1997,** 36, 2597-2604.

5. Saenz, J. M.; Asua, J. M. *Journal of Polymer Science Part A: Polymer Chemistry* **1996,** 34, 1977-1992.

6. Paine, A.; Winnik, F. *Langmuir* **1989,** 5, 903-910.

7. Ho, C. H.; Nhen, S. A.; Amiridis, M. D.; Van, J. W. *Journal of Polymer Science Part A: Polymer Chemistry* **1997,** 35, 2907-2915.

8. Liu, J.; Chew, C.; Wang, S.; Gan, L.; Lin, J.; Tan, K. *Polymer* **1998,** 39, 283-289.

9. Song, B.; Cho, M.; Yoon, K.; Lee, D. *Journal of Applied Polymer Science* **2003,** 87, 1101-1108.

10. Xu, Z.; Deng, Z.; Li, X.; Yi, C. *Journal of Polymer Science Part A: Polymer Chemistry* **2005,** 43, 2368-2376. .

11. Horak, D. *Journal of Polymer Science Part A: Polymer Chemistry* **1999,** 37, 3785-3792.

12. Kim, O.; Lee, K.; Kim, K.; Lee, B. H.; Choe, S. *Polymer* **2006,** 46, 1953-1959.

13. Lee, K.; Seo, H. *Korea Polymer Journal* **1998,** 6, 405-413.

14. Jayachandran, K. N.; Chatterji, P. R. *Journal of Macromolecular Science: Part C: Polymer Reviews* **2001,** 41, 79-94.

15. Wang, D.; Dimonie, V.; Sudol, E.; El-aasser, M. *Journal of Applied Polymer Science* **2002,** 84, 2692-2709.

16. Lee, J. M.; Shim, S. E.; Choe, S. *Industrial & Engineering Chemistry Research* **2006,** 12, 648-651.

17. Zhao, Q.; Samulski, E. T. *Polymer* **2006,** 47, 663-671.

18. Bourgeat-Lami, E.; Lang, J. *Journal of Colloid and Interface Science* **1999,** 210, 281-289.

19. Ray, S.; Okamoto, M. *Progress in Polymer Science* **2003,** 28, 1539-1641.

20. Zhao, Q.; Samulski, E. T. *Macromolecules* **2005,** 38, 7967-7971.

21. Bourgeat-Lami, E.; Lang, J. *Journal of Colloid and Interface Science* **1998,** 197, 293-308.

22. Park, E. J.; Kim, W. S.; Hwang, H. S.; Park, C.; Lim, K. T. *Macromolecular Symposia* **2007,** 249, 196-201.

23. Liu, P.; Liu, W.; Xue, Q. *Designed Monomers and Polymers* **2004,** 7, 253-260.

24. Zerda, A. S.; Caskey, T. C.; Lesser, A. J. *Macromolecules* **2003,** 36, 1603-1608.

25. Lebaron, P. C.; Wang, Z.; Pinnavaia, T. J. *Applied Clay Science* **1999,** 15, 11-29.

26. Wang, H.; Chang, K.; Chu, H. *Polymer International* **2005,** 54, 114-119.

27. Choi, Y. S.; Ham, H. T.; Chung, I. J. *Polymer* **2003,** 44, 8147-8154.

28. Xu, M.; Choi, Y. S.; Kim, Y. K.; Wang, K. H.; Chung, I. J. *Polymer* **2003,** 44, 6387-6395.

29. Shimizu, I.; Yoshino, A.; Okabayashi, H.; Nishioc, E. *Journal of the Chemical Society, Faraday Transactions 1: Physical Chemistry in Condensed Phases* **1997,** 93, 1971-1979.

30. Negrete-Herrera, N.; Letoffe, J. M.; Putaux, J. L.; David, L.; Bourgeat-Lami, E. *Langmuir* **2004,** 20, 1564-1571.

31. Voorn, D.; Ming, W.; van Herk, A. M. *Macromolecules* **2006,** 39, 4654-4656.

32. Xi, Y.; Martens, W.; He, H.; Frost, R. L. *Journal of Thermal Analysis and Calorimetry* **2005,** 81, 91-97.

33. Alexandre, M.; Dubois, P. *Materials Science and Engineering: A* **2000,** 28, 1-63.

34. He, H.; Duchet, J.; Galy, J.; Gerard, J. *Journal of Colloid and Interface Science* **2005,** 288, 171-176.

35. Wu, Y.; Zhang, J.; Zhao, H. *Journal of Polymer Science Part A: Polymer Chemistry* **2008,** 47, 1535-1543.

36. Yan, C.; Ma, L.; Yang, J. *Journal of Applied Polymer Science* **2005,** 98, 22-28.

37. Yang, Y.; Zhang, J.; Liu, L.; Li, C.; Zhao, H. *Journal of Polymer Science Part A: Polymer Chemistry* **2007,** 45, 5759-5769.

38. Chen, J.; Poliks, M. D.; Ober, C. K.; Y. Zhang; Wiesner, U.; Giannelis, E. *Polymer* **2002,** 43, 4895-4904.

39. Qutubuddin, S.; Fu, X.; Tajuddin, Y. *Polymer Bulletin* **2002,** 48, 143-149.

40. Meneghetti, P.; Qutubuddin, S. *Langmuir* **2003,** 20, 3424-3430.

41. Choi, Y. S.; Xu, M.; Chung, I. J. *Polymer* **2003,** 44, 6989-6994.

42. Choi, Y. S.; Chung, I. J. *Macromolecular Research* **2003,** 11, 425-430.

43. Greesh, N.; Hartmann, P.; Sanderson, R. *Macromolecular Materials and Engineering* **2009,** 294, 206-212.

44. Wang, J.; Du, J.; Zhu, J.; Wilkie, C. A. *Polymer Degradation and Stability* **2002,** 77, 249-252.

45. Blumstein, A. *Journal of Polymer Science, Part A: Polymer Chemistry* **1965,** 3, 2653-2661.

46. Fischer, H. *Materials Science and Engineering A* **2003,** 23, 763-772.

47. Giannelis, P. E. *Advanced Materials* **1996,** 8, 29-40.

48. Samakande, A.; Hartmann, P. C.; Cloete, V.; Sanderson, R. D. *Polymer* **2007,** 48, (6), 1490-1499.

49. Nalwa, H. S., Polymer/clay Nanocomposites. In *Encyclopedia of Nanoscience and Nanotechnology*, American Scientific Publishers: California, 2004; Vol. 8, pp 791-843.

50. Gopakumar, T.; Lee, J.; Kontopoulou, M.; Parent, J. *Polymer* **2002,** 43, 5483 - 5491

51. Luo, J.; Daniel, M. *Combustion Science and Technology* **2003,** 63, 1607-1616.

Chapter 4

Preparation of Oligomeric (Styrene-b-2-Hydroxyethyl acrylate) Block Copolymer using Reverse Iodine Transfer Polymerization (RITP)

Abstract

Reverse iodine transfer polymerizations (RITP) of 2-hydroxyethyl acrylate (HEA) were performed in N,N-dimethylformamide at 70 °C using AIBN as initiator. Poly(2-hydroxyethyl acrylate) (PHEA) with M_n=3300 g/mol and M_w/M_n< 1.5 were obtained. Homopolymerization of styrene in RITP was also carried out under similar conditions using toluene as solvent. The resulting iodo-polystyrene (PS-I) was used as a macroinitiator for the synthesis of amphiphilic block copolymers based on HEA with controlled well-defined structure. Poly (styrene-b-2-hydroxyethyl acrylate) with M_n= 12980 g/mol and polydispersity index (M_w/M_n)= 1.4was obtained, copolymer composition was characterized using ^{1}H-NMR and FT-IR, while SEC and gradient HPLC were used to confirm the formation of block copolymer and the living character of polymer chains.

Preparation of Oligomeric (Styrene-b-2-Hydroxyethyl acrylate) Block Copolymer using Reverse Iodine Transfer Polymerization (RITP)

4.1 Introduction

It is well known that diblock and triblock copolymers can constitute effective stabilizers in heterophase polymerization methods.[1,2] It can be inferred that amphiphilic block copolymers, in which one segment can anchor to the surface of polymer particles and other segment can extend into the continuous phase, can provide a steric barrier to prevent the coagulation of polymer particles.[3-7] Therefore, control over the molecular weight and molecular weight distribution of block copolymers is important for achieving successful dispersion polymerization. This chapter describes the synthesis of amphiphilic block copolymers of poly (styrene-b-2-hydroxyethyl acrylate) PS-b-PHEA using reverse iodine transfer polymerization (RITP) living/controlled radical polymerization (LRP/CRP). The application of using PS-b-PHEA as stabilizer in dispersion polymerization is described in Chapter 7 of this dissertation.

The field of LRP/CRP has grown rapidly in the past decade.[8] A variety of well-controlled polymers have been successfully prepared by various CRP methods, including Atom Transfer Radical Polymerization (ATRP),[9]Reversible Addition-Fragmentation chain Transfer (RAFT),[10]Nitroxide-Mediated Polymerization (NMP),[11]and Reverse Iodine Transfer Polymerization (RITP).[12] RITP is a new CRP methodthat was recently developed by Lacroix-Desmazes *et al.*[13] the mechanism of which was described earlier, in Chapter 2, Section 2.5.4.3.

The advantages of RITP are that the transfer agent is generated in situ in the reaction medium, therefore in RITP the synthesis or storage of the transfer agents is not

required.[14] Moreover, RITP is practically easier than other polymerization methods, since only molecular iodine needs to be added to the reaction to achieve control the polymerization.

RITP has been successfully applied to a wide range of monomers such as acrylates,[13] styrene,[15,16] methyl methacrylate (MMA),[17,18] and copolymers of vinylidene chloride and methyl acrylate.[19]

This chapter describes for the first time the use of RITP forthe homopolymerization of HEA, and the subsequent copolymerization with styrene monomer to form block copolymers of PS-b-PHEA. PHEA is an acrylate polymer that is rubbery at room temperature. Because of its high affinity for water, it has been used in hydrophilic polymeric gel for applications such as agricultural, coating and biomedical applications.[20]The synthesis of PHEA and subsequent amphiphilic block copolymers with well-defined structures has been reported using different CRP methods, such as ATRP,[21] and NMRP.[22] For instance, HEA was polymerized by Coca *et al* [21] using the ATRP method. The polymerization exhibited first-order kinetics and the number average molecular weights increased with conversion, while polydispersities remained low throughout the polymerization (M_w/M_n~1.2). Reactions were conducted in bulk and in 1:1 (v/v) aqueous solutions.

Muhlebach *et al.* [23] synthesized amphiphilic block copolymers by CRP. They reported the block copolymerization of butyl acrylate (BA) and 2-trimethylsilyl-oxyethyl acrylate (TMS-HEA) by ATRP. Diblock and triblock copolymers with predefined block lengths and low polydispersities were obtained, when using methyl-2-bromopropionate as initiator and CuBr as catalyst. Hydrolysis of TMS groups led to block copolymers with (BA) and HEA units, which were characterized by size exclusion chromatography (SEC), nuclear magnetic resonance spectroscopy(NMR), and Fourier transform infrared spectroscopy (FT-IR). Recently, NMP was also used to synthesizePHEA in bulk, in organic solvent (N,N-dimethylformamide),and controlled polymerization was obtained with polydispersity indiceslower than 1.3. Amphiphilic block copolymers of PBA-b-PHEA) with different molecular weights and block composition were also

studied.[22]Khutoryanski *et al.*[24] synthesized amphiphilic copolymers based on PHEA and P(vinyl butyl ether) and studied their interaction with poly (carboxylic acids).

To the best of the author's knowledge there are only few articles reported on the preparation of block copolymers using RITP. Lacroix-Desmazes *et al.*[13] confirmed the living nature of RITP by preparation of a poly(methyl acrylate)-b-polystyrene block copolymer, where they used iodo-terminated poly(methyl acrylate) (PMA-I) as macroinitiator and added styrene as a second block. Tonnar *et al.*[14] successfully synthesized a poly(butyl acrylate-b-styrene) block copolymer in seeded emulsion polymerization using RITP, by using an iodo-terminated PBA-I as macroinitiator. Recently, Enriquez-Medrano *et al*[25] used difunctional initiator to simplify the synthesis of triblock copolymers of poly(styrene-butyl acrylate-styrene) by RITP in only two steps starting with the formation of the central block using 2,5-di(2-ethylhexanoylperoxy)-2,5-dimethylhexane as a difunctional initiator and then resuming the polymerization to grow the external blocks in a second step.

This chapter reports on the preparation of PS-b-PHEA block copolymersvia RITP. Iodo-terminated PS (PS-I) was synthesized first and then used as macroinitiator to grow the second PHEA block.

4.2 Experimental

4.2.1 Materials

Commercial HEA (HEA, Aldrich, 96%) contains impurities, such as ethylene glycol, acrylic acid and ethylene glycol diacrylate. The presence of diacrylates leads to cross linking, and acrylic acid may inhibit the polymerization. Therefore, the polymerization of unpurified or poorly purified monomer may be incomplete and/or slow or lead to insoluble solids. HEA was therefore purified by dissolving in water (25% by volume) and then washing the solution 10 times with hexane to extract diacrylates. The aqueous solution was then salted (200 g NaCl), and monomer was separated from aqueous phase by ether extraction (4 times) to remove acrylic acid which remained in the water phase. Finally, magnesium sulfate (3 wt%) drying agent was used to remove traces of water

before evaporation of the ether phase on a rotary evaporator. The purified monomer was distilled under vacuum immediately prior its use in polymerization. Stabilized styrene monomer was obtained from Aldrich. The stabilizer was removed by washing three times with a 3 wt% potassium hydroxide solution. The styrene was then purified by distillation under reduced pressure at 30 °C. The initiator 2,2-azobis(isobutyronitrile) (AIBN) was obtained from Aldrich and recrystallized from methanol.

4.2.2 Homopolymerization of HEA and styrene

In a typical procedure of HEA polymerization by the RITP process, HEA (6g, 51.7 mmol) DMF (12 mL) AIBN (335 mg, 2.04 mmol) and iodine (304 mg, 1.20 mmol) were introduced in a Schlenk flask. After three freeze-thaw pump cycles the flask was heated to 75 ºC in an oil bath. The polymerization was conducted in the dark, under an argon atmosphere with magnetic stirring for 24 h. Samples for analysis purpose were continuously withdrawn from the reactor with a glass syringe through a septum and under positive nitrogen flushing.

The RITP of styrene was performed in a similar way, except that the solvent used was toluene. Furthermore, in the case of styrene polymerization by RITP, a higher molecular weight was targeted. In a typical procedure the stoichiometry used was: styrene (6g, 57.6 mmol), toluene (12 mL) AIBN (0.0272 g, 0.17 mmol) and iodine (0.025g, 0.1mmol).

4.2.3 Block copolymerization of HEA and styrene

Block copolymers of PS-b-PHEA were prepared by the macroinitiator method. Iodo-polystyrene (PS-I), prepared according to procedure above, was used as macroinitiator (after removal of excess monomer from the first block). The macroinitiator was directly heated with HEA monomer at 75 ºC to afford the block copolymer. In a typical procedure, PS-I macroinitiator (1.6 g, 0.02 mol) was dissolved in DMF and mixed with HEA (1.3 g, 0.0112 mol) and AIBN (0.0001g, 6.02×10^{-7} mol) in a Schlenk tube. After degassing by freeze-vacuum-thaw cycles, the polymerization was conducted in the dark with stirring at 75 °C for 48 h. The resultant copolymer was then precipitated in a cold mixture of ethanol and diethyl ether, and then dried in a vacuum oven at 30 °C for 3 days.

The block copolymer was characterized by the following techniques: NMR, FT-IR, SEC and High Performance Liquid Chromatography (HPLC).

4.2.4 Characterization

NMR analysis was performed at 20 ºC using a Varian VXR-unity 300 MHz. FT-IR spectra were recorded with a Perkin Elmer 1650 transform infrared spectrophotometer, using an average of 32 scans. SEC was performed using a Waters 600E system controller equipped with a Waters 610 fluid unit pump, a Waters 410 differential refractometer as detector, an a column set of PLgel 5 µm 50 × 7.5 mm and a PLgel 5 µm mixed-C 300 × 7.5 mm column. Measurements were carried out at 30 °C, using THF as eluent and a flow rate of 1 mL/min.

Matrix-Assisted Laser Desorption/Ionisation time- of Flight mass spectrometry (MALDI-TOF) were recorded on a Voyager-DE STR (Applied Biosystems, Farmingham) equipped with a nitrogen 337 nm laser in the reflector mode, at 25 kV accelerating voltage and with delayed extraction. The matrix used was 2,5-dihydroxybenzoic acid (DHB)(Aldrich)and potassium trifluoro acetate (KTFA) (Aldrich) was used as the cationizing agent. For each analysis the analyte sample was prepared by first making up the following concentration of the matrix, KTFA, and sample, in DMF, separately: 35 mg/mL matrix; 5 mg/mL KTFA; 1 mg/mL sample, before mixing them in the ratio of 4:1:4 and hand spotting on the target plate. 1000 laser shots were performed for each spectrum.

Separation of block copolymers by chemical composition in this study was performed using a dual pump HPLC comprising of the following units: Waters 2690 separation module (Alliance), Agilent 1100 series variable wavelength detector, PL-ELS 1000 detector. Data were recorded and processed using PSS WinGPC unity (Build 2019) software. The separation was done through a bare silica column (Nucleosil C18 5mm(250 mm x 4.6 mm)) at 30 °C. The samples were prepared in THF at a concentration of 5 mg/mL.

4.3 Results and discussion

4.3.1 Homopolymerization of HEA

Due to the insolubility of high molecular weight PHEA in common solvents, due to intermolecular hydrogen bonding,[20] only low molecular weights of PHEA were targeted.The homopolymerization of HEA in DMF proceeded with 80% conversion being achieved within 10 hours $M_{n(SEC)}$ =3300 g/mol, $M_{n(theor)}$ = 2193 g/mol and PDI 1.5. Scheme 4.1 shows the homopolymerization of HEA by RITP.

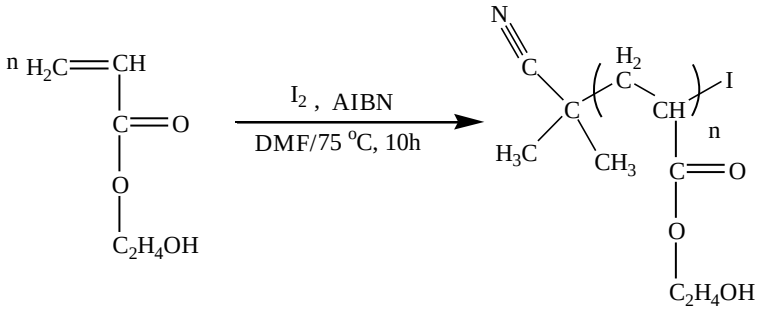

Scheme 4.1: Homopolymerization of HEA via RITP.

HEA was polymerized in DMF so as to allow a relatively low viscosity and a good dissipation of the heat of the reaction.[21] DMF was also the selected solvent due to its ability to dissolve both the initiator and the monomer. Fig. 4.1 (i) shows that $M_n$increased linearly as a function of monomer conversion, indicating a constant number of growing chains throughout the polymerization,showing that the polymerization occurred in a controlled manner.[26]

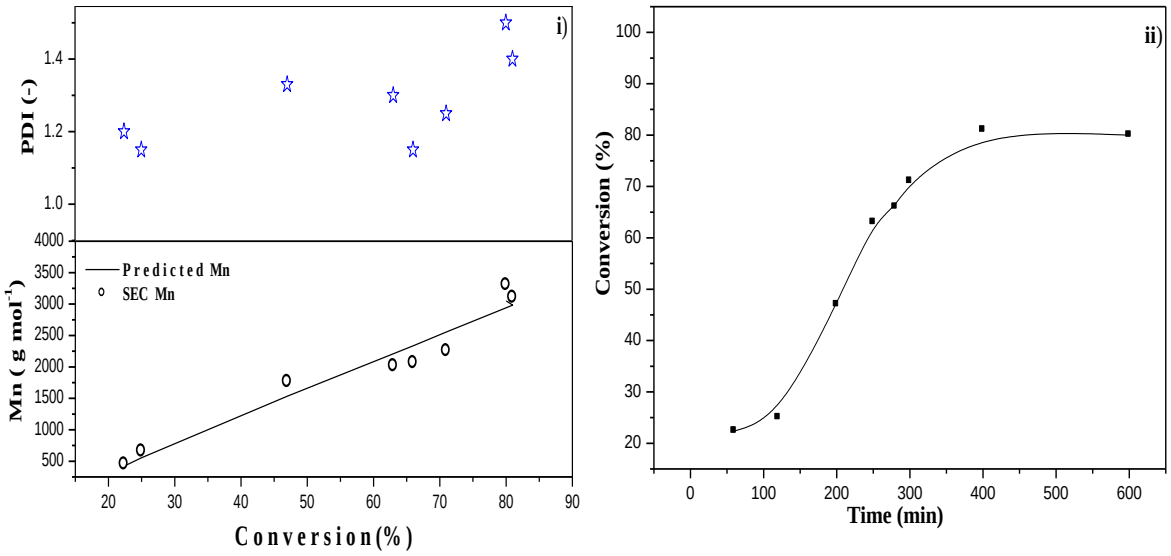

Fig. 4.1: HEA polymerized by RITP: (i) $M_{n(exp)}$, $M_{n\ (theory)}$, and PDI versus conversion, and (ii) conversion (%) versus time.

The evolution of monomer conversion with time clearly shows that the RITP polymerization of HEA is relatively fast and the inhibition period took less than 2h. This could be due to a slight accelerating effect of the polar solvent DMF.[21] This is in agreement with the polymerization of HEAusing ATRP in DMF, whereby a similar solvent effect was observed.[20] In the RITP process, during the inhibition period, the free radicals predominantly react with iodine to form in situ the reversible chain transfer agent. When all the iodine is consumed, at the end of the inhibition period, the degenerative transfer equilibrium takes place. The [initiator]/[I_2] ratio is the determining parameter controlling the duration of inhibition period.[13,17] The [initiator]/[I_2] ratio must be higher than 1.5 to achieve high yields of polymerization. Below 1.5 the polymerization yield has been reported to be generally low.[13,14,17] The theoretical inhibition time can be calculated by Equation 4.1.[17]

$$time^{inhibition}_{(theoretical)} = \frac{-\ln(\frac{1-[I_2]_0}{f.[AIBN]_0})}{k_d} \quad (4.1)$$

Where $[I_2]_0$ and $[AIBN]_0$ are initial concentrations of iodine and initiator, respectively, k_d is the decomposition rate constant of the initiator (k_d=7.5x 10^{-4} s^{-1}at 75ºC)[27], and f is the initiator efficiency (f =0.7 for AIBN) in DMF.[28] It was found that the experimental and

theoretical inhibition times of RITP of HEA at 75 °C are in fair agreement. This correlates well with findings obtained by Boyer *et al*[17]who studied the RITP mechanism of methyl methacrylate (MMA). The consumption of monomer is very low until the concentration of molecular iodine becomes negligible, since the rate of reaction between radicals and iodine is much higher than the rate of propagation of the monomer. Hence, there is direct correlation between the inhibition period and the presence of free iodine in the reaction medium. Moreover, this inhibition period can be divided into two stages, the first stage being when the concentration of the A-I adduct builds up, and a second stage corresponding to the formation of very short A-M_n-I oligomers. Thus, all the iodine is consumed, whereas only few percent of HEA are being consumed during the inhibition period. However, it is worth mentioning that this behaviour is not the same for all polymers prepared by RITP. A typical counter example is for the RITP-mediated polymerization of styrene, where the inhibition period is influenced by both concentrations of monomer and iodine due to the formation of styrene-iodine complex.[29]

The $M_{n,SEC}$ was found to increase linearly as a function of the conversion, and the PDI remained below 1.5. The theoretical molecular weight was calculated according to the following equation.[17]

$$M_{n,theor} = \frac{m_{mono}.C\%}{2n_{I_2}} + M_{A-I} \quad (4.2)$$

Where m_{mono} is mass of monomer and C% is conversion, n_{I_2} is the number of moles of iodine, $M_{A\text{-}I}$ stand for molecular weight of A-I adduct, while A stands for the radical fragment from the initiator. The experimental M_n values measured via SEC were in good agreement with the theoretical M_n at low conversion. However, deviation of experimental M_n from the prediction occurred at higher conversion, indicating a partial loss of control which could be due to the occurrence of chain transfer to polymer. However, overall RITP of HEAtakes place in a controlled manner.

The ^{1}H-NMR spectrum of PHEA purified by precipitation, is shown in Fig 4.2. Only traces of ethylenic protons were found at ~ 5.72 and 6.3 ppm indicating the negligible residual of monomer.

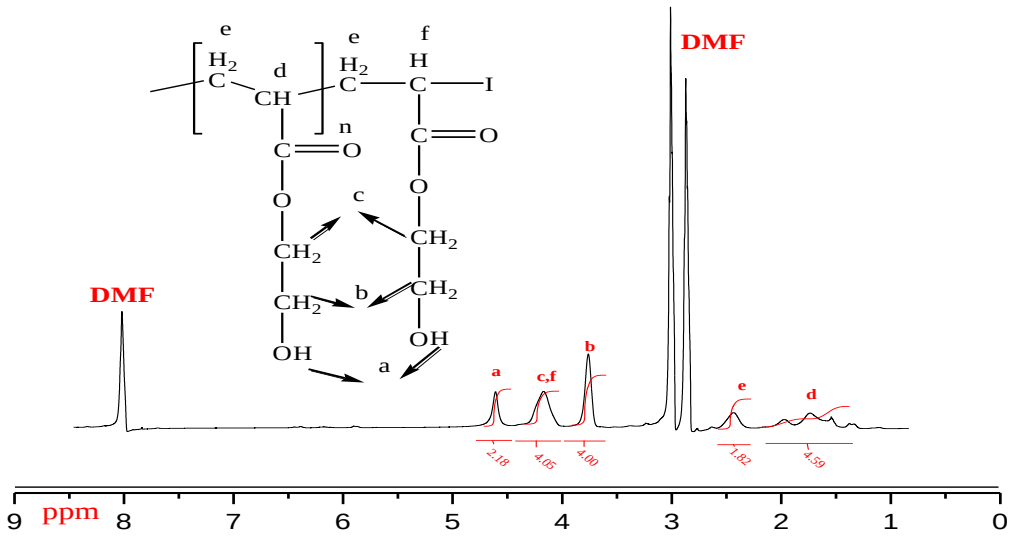

Fig. 4.2: ^{1}H-NMR spectrum in DMF-d^{7} of PHEA polymerized in DMF by RITP

The signal at 4.8 ppm comes from the resonance of the proton of the hydroxyl group (a), while the signals at 4.07 and 3.7 ppm correspond to the CH_2 protons of the hydroxyethyl group (c and b). The methine at β position from the iodo group (f) is expected to give a signal at 4.05 ppm. This is however overlapped with the resonance of methylene protons (c). A similar NMR spectrum of PHEA was also observed when prepared by ATRP, as reported by Coca *et al.*[21] They also found that the signal of the methine proton at the bromine end chain overlapped with the signal of the resonance of the methylene protons from the hydroxyethylgroup. The PHEA structure was further analyzed using MALDI-TOF which is a powerful analytical method to elucidate the structures of low to medium molecular weight polymers synthesized via CRP.[30]

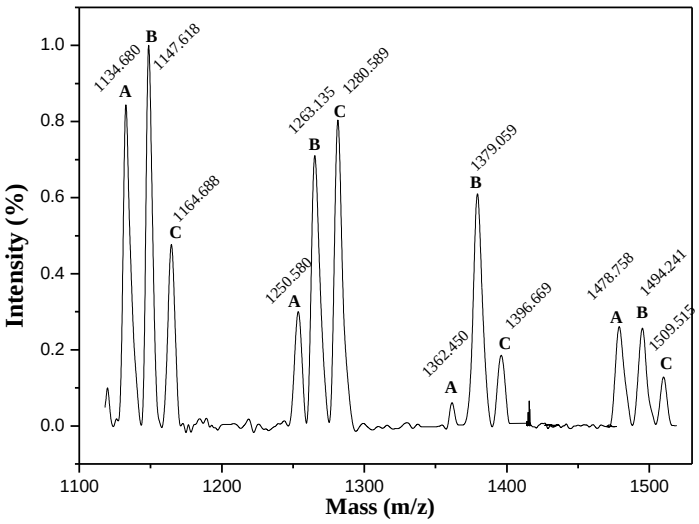

Fig. 4.3: MALDI-TOF spectrum of PHEA via RITP.

Fig. 4.3 shows a MALDI-TOF analysis of a low molecular weight PHEA prepared by RITP. Focusing on the zone m/z=1100-1500,three different series (A, B, and C) are distinguished. The expected A-M_n-I structure cationized using Na^+ appears at m/z= 1147.618, 1263.135 and 1379.059, with a strong intensity (as seen in the distributions (B)). The distributions (C) at m/z= 1164.688, 1280.589 and 1396.669 can be attributed to the adsorption of PHEA with one water molecule, giving the structure PHEA(H_2O), because this polymer has a high affinity for water. The complexation of water molecules in MALDI-TOF analysis of polymers has been reported by Ladaviere*et al.*[31] The distributions (A) at m/z= 1134.680, 1250.580 and 1362.450 could be due to elimination of HI from A-M_n-I polymer chains at high temperature (150 °C) or during the MALDI-TOF analysis, resulting in an unsaturated chain end as shown in Scheme 4.2.

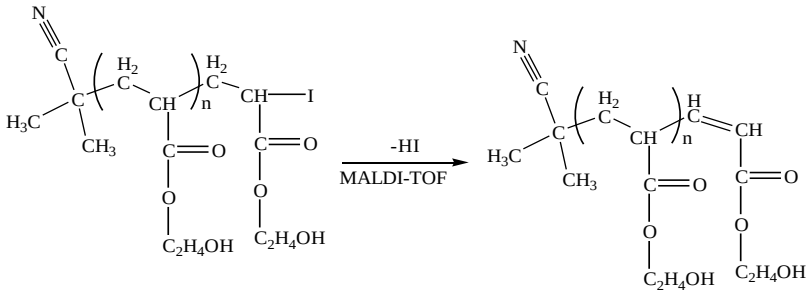

Scheme 4.2: Elimination reaction of PHEA during MADI-TOF analysis.

A similar elimination of hydrogen halide has been observed and reported for PHEA prepared via ATRP and terminated by bromine.[21]Nonaka *et al*[32] prepared poly(methyl methacrylate) (PMMA) via ruthenium-mediated CRP. The polymer chains were terminated by chlorine, although the elimination of HCl from terminal chlorine was not observed during MALDI-TOF analysis, probably due to the higher stability of C-Cl covalent bond relative to C-Br or C-I. In summary, A-M_n-I was the major product in the sample, further confirming the relevance of the mechanism of RITP presented in Section 2.5.4.3.

4.3.2 Homopolymerization of styrene

The homopolymerization of styrene via RITP in toluene proceeded with 57% conversion being achieved within24 hours: $M_{n(SEC):}$12980, $M_{n\ (theor):}$ 14400 and PDI 1.4. Fig. 4.4 shows the evaluation of M_n and PDI as a function of monomer conversion.

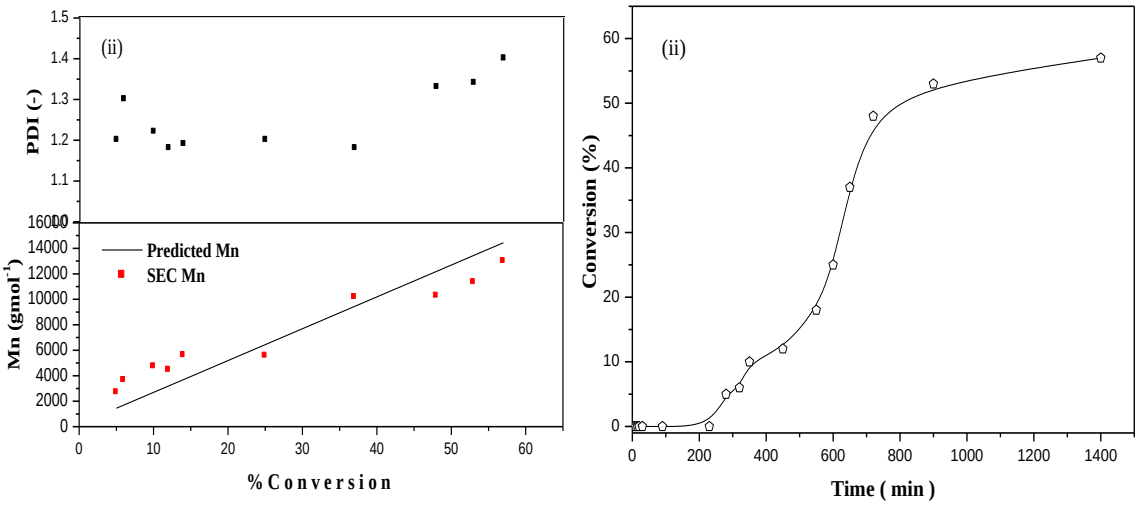

Fig. 4.4: Styrene polymerized by RITP: (i) $M_{n(exp)}$, $Mn_{(theor)}$ and PDI versus conversion, and (ii) conversion versus time.

The number average molecular weight M_n increased linearly with the conversion, and was found to correlate well with the theoretical $M_{n,\ predicted}$. The PDI remained in an acceptable range for reverse iodine transfer polymerization of styrene.[16,29] The plot of conversion as a function of time depicted in Fig 4.4 (ii) shows the presence of an inhibition periodof about 4 h. These results corresponds well with the results of studies

conducted by Tonnar *et al*.[29] who found in the early stages of styrene polymerization via RITP an inhibition period of about 4 h. This is shorter than the theoretical inhibition period, calculated by Equation 4.1 (k_d is 0.00014285 s^{-1} at 80°C).[27] The calculated theoretical inhibition period is significantly longer (18 h) than the experimental inhibition time observed,which is not consistent with the observation made for RITP of HEA and other acrylates such as methyl acrylate[13] and methyl methacrylate.[17] Tonnar *et al*[29]studied the inhibition period for RITP of styrene, and found that the only hypothesis that can explain the shorter inhibition than expected is due to the formation of styrene diiodide (Scheme 4.3). The formation of a charge transfer complex has also been reported as a possible reason for shorting the duration of the inhibition period.[15]

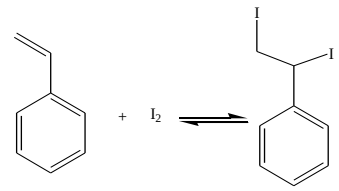

Scheme 4.3 : Reversible addition of iodine onto styrene.

Since the formation of styrene diiodide is reversible, iodine can be liberated after the end of observed inhibition period. The liberated iodine thus reacts immediately with radicals present in the reaction medium creating new transfer agents, this hypothesis accounts for the shorter inhibition period while keeping a good correlation between theoretical and experimental molecular weight.

Clearly, the mechanism of RITP of styrene is a little bit more complicated than for HEA. The complexity of the RITP mechanism for styrene is due to the complexity of the chemistry between iodine and the styrene, whereby many different reactions can occur including addition of iodine onto the styrene double bond (yielding styrene diiodide),[13] iodine acting as initiator of cationic polymerization of styrene, formation of a charge transfer complex between iodine and styrene, or due to the ability of iodine to form complexes with donor compounds such as benzene rings and derivatives.[33]

Notwithstanding the complicated mechanism of RITP polymerization of styrene, it remains a straightforward and simple technique to prepare PS with a relatively well-defined structure.

Fig. 4.5 shows a typical ^{1}H-NMR spectrum of a low molecular weight PS prepared via RITP. The signal at 4.5 - 4.8 ppm corresponds to the methine proton baring the iodine chain end. This confirms the PS-I structure, which is consistent with that referenced in the literatures.[34,35] This also confirms the structure of the polymer according to the mechanism of RITP previously described in Section 2.5.4.2.

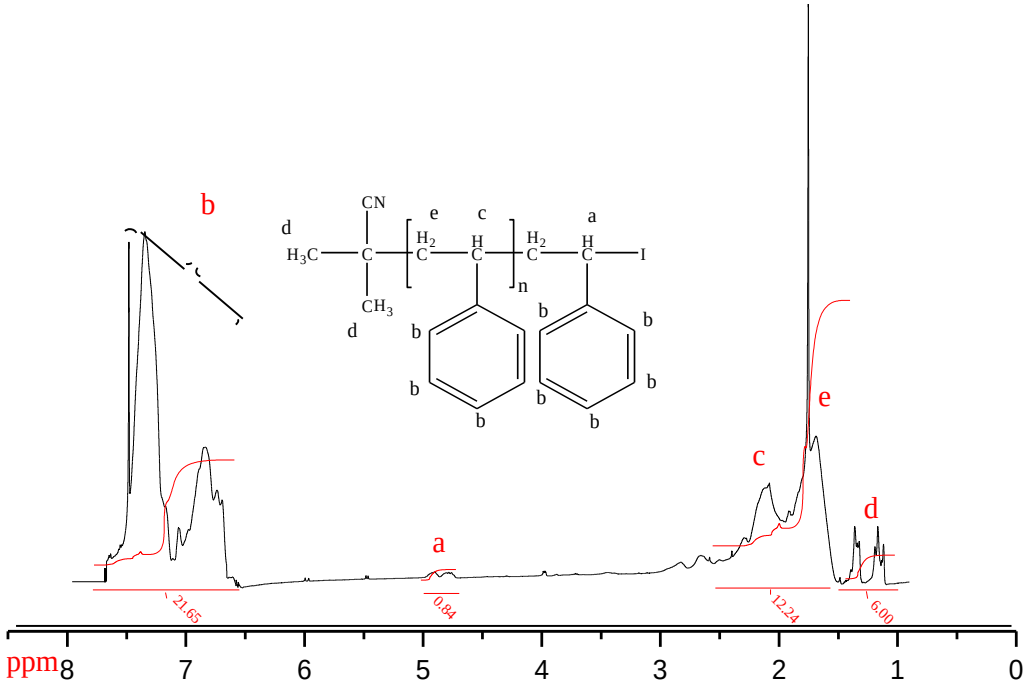

Fig. 4.5: ^{1}H-NMR spectrum in $CDCl_3$ of PS prepared by RITP

The protons *d* of the two methyl groups of the radical initiator (-C-(CN) $(CH_3)_2$) appear at 1.20 ppm, peaks at 6.5- 7.5 is corresponded to the aromatic protons, thus it is possible to calculated the molecular weight by ^{1}H-NMR spectroscopy using the integral of the methine proton (Fig 4.5 (a))at the iodine chain end (4.5-4.8) and the integral of aromatic protons in the polymer chain (Fig. 4.5 (b)). The results show that: $M_{n,theor}$ = 700 g mol $^{-1}$, $M_{n,\ SEC}$ = 607 g mol^{-1}, PDI = 1.31 and $M_{n,NMR}$ 590 g mol^{-1}. From ^{1}H-NMR it is also

possible to evaluate the iodine functionality of chains F^{iodine}(i.e. the proportion of chains end-capped with iodine) using Equation 4.3.[17]

$$F^{iodine} = \frac{\int(-CHI^{a}-)}{\int\frac{(-C(CN)(CH_3{}^{d})_2}{6}} \frac{\frac{0.84}{6.00}}{\frac{6.00}{6.00}} = 0.84 \quad (4.3)$$

The iodine functionality determined by ^{1}H-NMR is about 84%, indicating that most of the PS chains were end-capped with iodine. Thus PS-I prepared here was used as a macroinitiator to synthesize PS-b-PHEA block copolymer.

4.3.3 Preparation of amphiphilic block copolymer

PS-b-PHEA was prepared using PS-I as a macroinitiator, and addingthe second monomer (i.e. HEA). During the preparation of PS-I macroinitiator, the conversion was kept below 50% in order to avoid loss of livingness by loss of iodine-capped ends, and the temperature was kept low (< 40 °C) when polymers were dried under vacuum.

The obtained block copolymer was characterized using ^{1}H-NMR and FT-IR spectroscopy. A typical ^{1}H-NMR spectrum of PS-b-PHEA prepared via RITP is shown in Fig. 4.6.

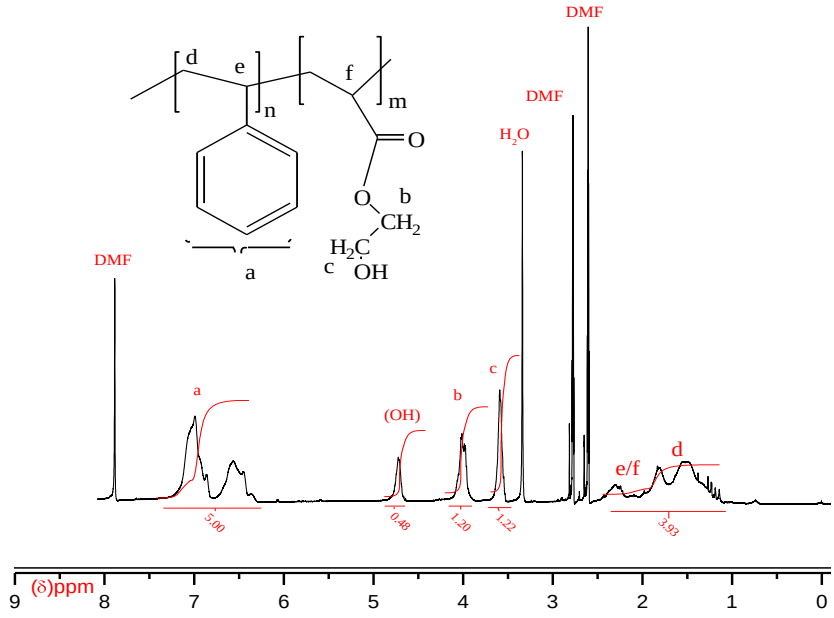

Fig. 4.6: ^{1}H-NMR spectrum in DMF-d^{7} of PS-b-PHEA prepared via RITP

The signals at 6.50-7.30 ppm are related to the protons of the aromatic styrene groups. The strong signals at 3.55 and 4.05 ppm are ascribed to the methylene (–CH_2)protons of the hydroxyethyl group (c and b) and the signal at 4.8 ppm corresponds to the –OH of hydroxyethyl group. The presence of peaks belonging to styrene and HEA in the ^{1}H-NMR spectrum indicated that copolymerization took place.However, it is worth mentioning that ^{1}H-NMR does not allow differentiating between a blend containing two homopolymers from a copolymer containing both monomer units.

The methylene proton linked to iodine is expected to resonate at 4.05 ppm, which overlapped with the other –CH_2 (b) from hydroxethyl substitutes. The relative amounts of styrene and HEA monomer units incorporated into the copolymer were determined using ^{1}H-NMR, by integration of specific peaks belonging to styrene (a) and HEA monomer units (b, c). The following Equation was used:

$$PS\% = \frac{\frac{\int a}{5}}{\frac{\int a}{5} + \frac{\int b + c}{4}} \times 100\% \qquad (4.4)$$

where PS% is the percentage of PS in the copolymer, a and b, c are the integration of the peaks of styrene and HEA respectively. PS-b-PHEA contained 62% styrene and 38% 2-hydroxyethyl acrylate, which in agreement with the theoretical ratio.

FT-IR spectroscopy analysis of PHEA, PS and PS-b-PHEA are shown in Fig. 4.7. In the FT-IR spectrum of PHEA a carbonyl band (C=O stretching) appeared at 1719 cm^{-1}, an aliphatic band (C-H stretching) was observed at 2949 cm^{-1} and an aliphatic (C-H bending) at 1447 cm^{-1}. The broad band at 3500 cm^{-1} corresponds to O-H stretching, and O-H bending can be seen at 1394 cm^{-1}. The ester group of the polymer (C-O stretching) shows bands in the FT-IR spectrum at 1162 cm^{-1}. Bands belonging to ethylenic double bond at 1633 cm^{-1} had completely disappeared; this FT-IR spectrum of PHEA was found to be consistent with the literature.

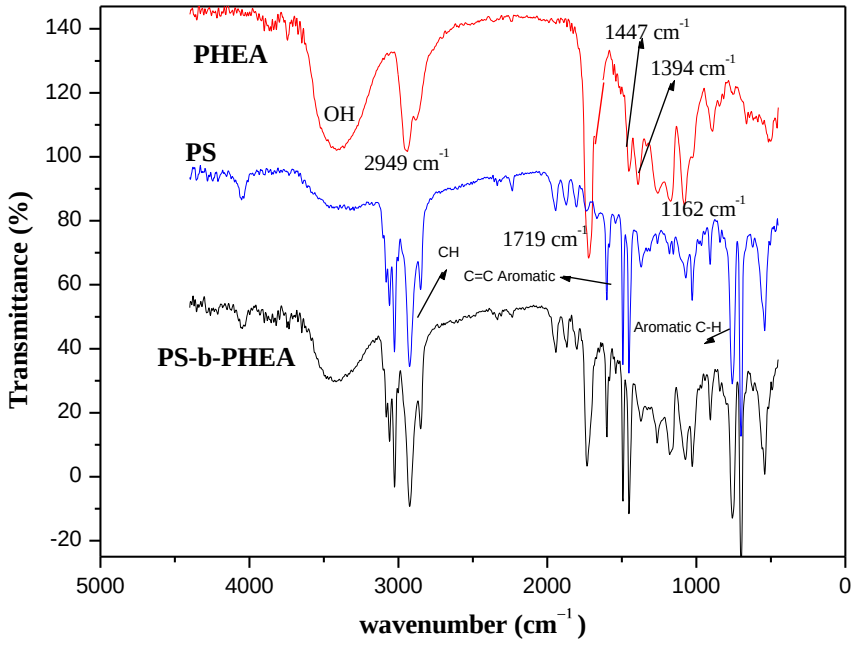

Fig. 4.7: FT-IR spectra of PS, PHEA and PS-b-PHEA.

In the FT-IR spectrum of PS the aromatic (C=C stretching) band appeared at 1602 cm^{-1}, the aromatic (C-H) bands was observed at 740 cm^{-1},and aliphatic band (C-H stretching) appeared at 3024 cm^{-1}. The FT-IR spectrum of PS-b-PHEA exhibited all bands belonging to bothblocks: HEA (i.e. C=O stretching at 1719 cm^{-1}) and styrene aromatic ring (i.e.

C=C stretching at 1602^{-1} cm), giving an indication of the copolymerization of styrene HEA using the RITP method, the characteristic bands of double bonds disappeared in the spectrum of copolymer, for example, 1633 cm^{-1} for HEA.[20] However, it is worth mentioning that FT-IR spectroscopy does not allow differentiating between a blend containing two homopolymers from a copolymer containing both monomer units.

The copolymer was further characterized by UV-Vis spectroscopy.The six-membered aromatic ring of the styrene monomer units were expected to absorb UV light in the region between 280 nm to 300 nm. The UV spectra of the PS, PHEA and PS-b-PHEA are presented in Fig.4.8 UV-analysis of the PS-b-PHEA showed that copolymer had strong absorption of UV light in the wavelength region where the styrene units absorb, whereas no absorption in this region was observed for PHEA.

A calibration curve was built from standard solutions of increasing concentration of PS in DMF, in order to determine the normal extinction coefficient of PS in DMFat a given wavelength of 255 nm.A plot of absorbance versus concentration of PS, (in mol/L), was constructed as shown in Fig 4.8. The linear relationship between concentration (C) (mol/L) and absorbance (A) shows that solutions of PS in DMF follow the Beer-Lambert law. From this calibration extinction coefficient (ε) can be determined via Equation 4.5:

$$A = \varepsilon.C.b \quad (4.5)$$

Where A absorbance, ε is extinction coefficient (L. $mol^{-1}.cm^{-1}$), and b is the length of curette (cm). ε was determined from the slope of linear curve in Fig 4.8 and was found to be 555 L mol^{-1} cm^{-1}.

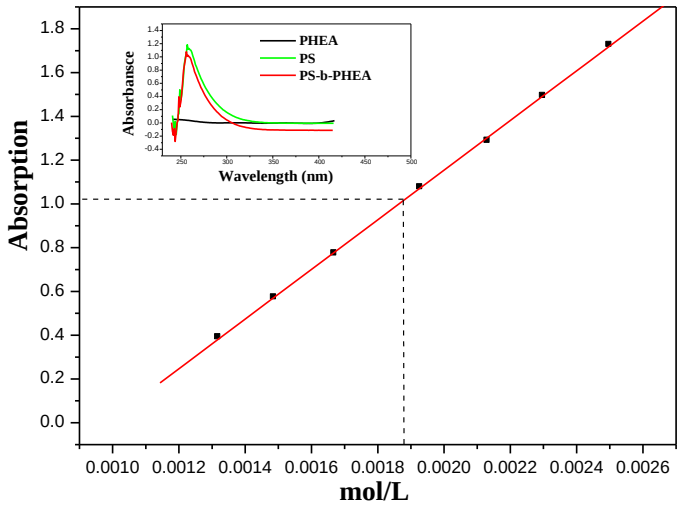

Fig. 4.8: Calibration curve for the determination of the percentage of styrene and HEA into PS-b-PHEA (the insert shows the UV/Vis spectra of PS, PHEA and PS-b-PHEA).

Samples of a known mass of PS-b-PHEA were dissolved in DMF (concentration of 0.003 mol/L)and itsabsorbancewas measured. The actual apparent concentration in terms of PS units in the solution was calculated from the Beer-Lambert law and found to be equal to

$$C_{PSunits} = \frac{A}{\varepsilon.b} = \frac{1.04}{555 \times 1} = 0.00187 \text{ mol/L}$$

The amount of styrene units in the copolymer was about 62%, which was found to be in agreement with the copolymer composition determined via ^{1}H-NMR spectroscopy.

^{1}H-NMR and FT-IR spectroscopy results showed the presence of both species (i.e. PS segment and HEA segment) within the copolymer. However, these techniques again do not allow to differentiae if the obtained product was indeed a pure block copolymer or a mixture of homopolymerization products, namely PS, PHEA and PS-b-PHEA block copolymer.

4.3.4 Block copolymer structure characterization

A combination of SEC and gradient HPLC characterization techniques were used to confirm the formation of block copolymer as well as the livingness of the PS-I macroinitiator. PS-b-PHEA block copolymers were prepared by sequential RITP

polymerization of styrene followed by HEA. The macroinitiator PS-I was prepared first via RITP of styrene, until a conversion of 50% was reached. The resulting PS-I macroinitiator has a $M_{n(SEC)}$=7.100 g/mol and PDI of 1.5. The theoretical molecular weight of the final block copolymer obtained was calculated using Equation 4.5.

$$M_{n,theor} = M_{n(1)} + \frac{m_{(2)}}{n_{(1)}} \times C_2 \quad (4.5)$$ [14]

Where $M_{n(1)}$ is the number average molecular weight of the first block (i.e. PS-I), $m_{(2)}$ is the mass of second monomer (i.e. HEA), $n_{(1)}$ is the number of moles of the macroinitiator and C_2 is the conversion of HEA.

The molecular weight of the block copolymer was found to increases monotonically with conversion, while the PDI decreased. The final molecular weight of block copolymer was found : $M_{n,theo}$ =11305 g mol^{-1}, $M_{n,SEC}$ =13000 mol^{-1}, PDI= 1.4. Fig. 4.9 shows an example of SEC traces of a block copolymer after extraction of unreacted monomers.

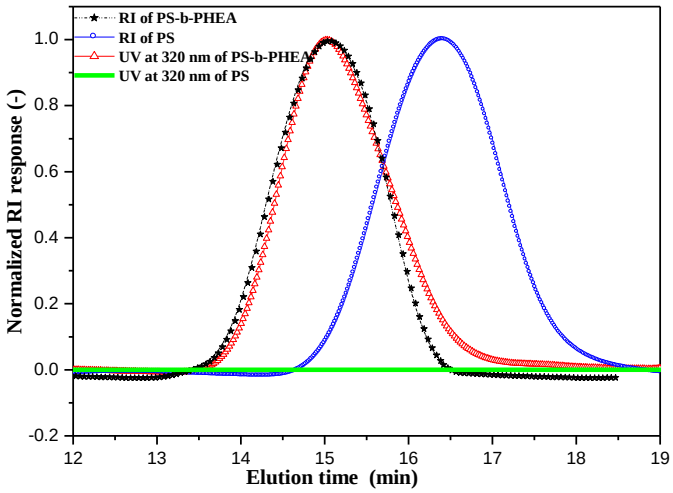

Fig. 4.9: SEC traces of PS-b-PHEA.

SEC instrument equipped with a dual detector system (RI and UV) was used to characterize the block copolymers.The UV detector was set up at a wavelength of 320 nm, which is the wavelength of absorption of C=O chromophore groups of the PHEA block only. It is noted that the entire molecular weight distribution shifts toward higher

molecular weights compared to the macroinitiator, indicating that the molecular weight of thePS macroinitiator increased due to chain extension. This confirmed that most of the PS chains had a "living" character as they took part in the formation of the desired block copolymer. Moreover, the overlapping of the RI and UV signals proved that almost all polymer chains had integrated HEA monomer units. These results agree very well with those obtained by Lacroix-Desmazes *et al.*[13] who prepared a block copolymer of poly(methyl acrylate)-b-polystyrene via RITP and characterized the block copolymers using SEC with a dual detectors (refractive index and UV). They reported unimodal distribution with visible shift of the iodo terminated macroinitiator toward higher molecular weights. Tonnar *et al.*[14] also synthesized a block copolymer of poly(styrene-b-butyl acrylate) via RITP in aqueous phase, and observed similar results including the living character of the polymerization via RITP.

However, it is well known that block copolymers preparedby free-radical polymerization, using a monomer and a low molecular weight macroinitiator, may display heterogeneity in terms of both molecular mass and chemical composition.[36,37] Therefore, the characterization of these materials by a single technique such as SEC can be inaccurate due to the effects of both the molecular mass and chemical composition on the specific hydrodynamic volume of each block.[38,39] Gradient elution high performance liquid chromatography, also known as gradient polymer elution chromatography (GPEC) is a good technique for separating copolymers on the basis of their chemical composition.[40] A block copolymer may often in fact contain homopolymer, unreacted macroinitiator as well as copolymer. In this study the GPEC separation of PS-b-PHEA was performed in toluene/DMF binary system. Linear gradients were used here, as shown in Fig. 4.10. PS homopolymer is readily soluble in toluene and therefore unretained on the stationary phase. The block copolymer is however insoluble in the starting gradient composition. The retention process in the case of the PS-b-PHEA copolymer, using toluene/DMF system on silica relies on initial precipitation, followed by adsorption-retention after re-dissolution of the block copolymer in the solvent gradient.

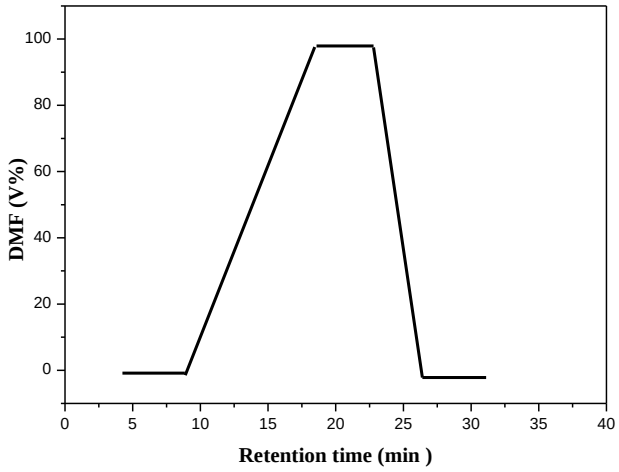

Fig. 4.10: Gradient elution profile considered for separation of PS-b-PHEA block copolymer (stationary phase: Nucleosil 100 Si-5µm, eluent toluene / DMF.

Separation is a function of component polarity: Here PS is less polar than PHEA, therefore the separation whereby PS eluts first is not due to the stationary phase but rather due to the solvent gradient. Indeed, the reverse stationary phase should already retain more PS than PHEA, PS is expected to elute first in a low polarity solvent (toluene), followed by PHEA. PS and PHEA homopolymer standards were used to identify their retention times in the elution profile. Fig. 4.11 shows the retention times of these homopolymers under the selected conditions, PS was found to elute between 3 and 5 min, while PHEA eluted between 17 and 19 min.

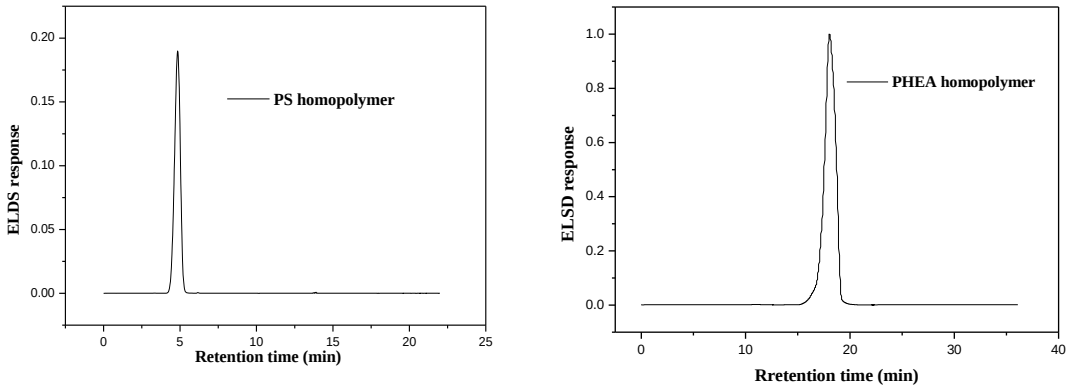

Fig. 4.11: HPLC elution chromatogram of PS (left) and PHEA (right).

Fig. 4.12 shows the gradient HPLC chromatograph for a typical PS-b-PHEA copolymer. It shows that very good separation into three fractions was obtained.

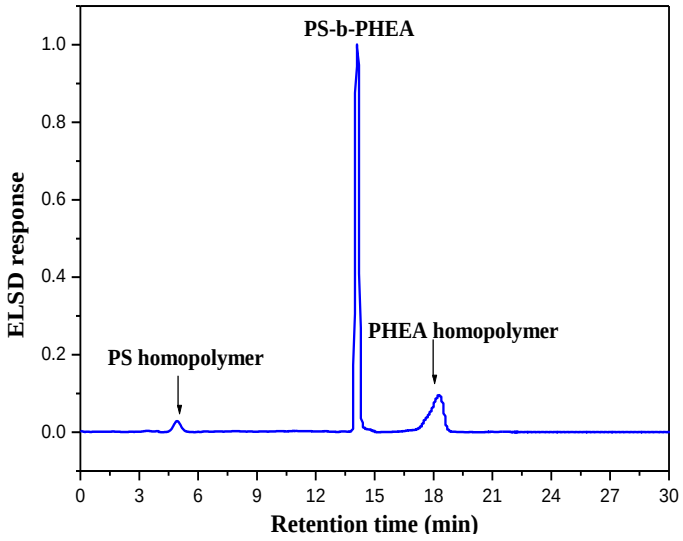

Fig. 4.12: Gradient HPLC chromatogram of PS-b-PHEA block copolymer.

The assignment of the peaks was carried out by comparison of the chromatographic behaviour of PS and PHEA homopolymer using a reversed phase column (Nucleosil CN 100Å). The three elution peaks are assigned to sample constituents PS, PHEA and PS-b-PHEA respectively. PS homopolymer elutes first, followed by the block copolymer PS-b-PHEA and finally the homopolymer of PHEA elutes last.

The presence PS homopolymer may be due to the presence of PS dead chains devoid of iodo end group at the beginning of the block copolymerization process. The presence of PHEA homopolymer is probably due to direct initiation of HEA in the presence of the free-radical initiator to form PHEA-I resulting from the reaction between this HEA radical and iodine arising from PS-I during the copolymerization reaction. As mentioned earlier, a very few articles discussed the preparation of block copolymers via RITP[13,14] and the characterization of PS-b-PHEA copolymers by HPLC has not been reported before.

HPLC results prove that the block copolymerization between styrene and HEA by RITP was successful although small amount of PS and PHEA homopolymers were found.

4.4 Conclusions

This study showed that controlled/living polymerization of styrene and HEA by RITP was successfully achieved. The reaction kinetic profile of the RITP process for styrene has however found to be different from HEA. The observed inhibition time was shorter for HEA than for styrene. The structure of polymers produced was analyzed by ^{1}H-NMR, FT-IR and MALDI-TOF, and found to be in good agreement with the theoretical A-M_n-I expected structure, showing that RITP can be used for the synthesis of functional PS-I and PHEA-I polymers with controlled molecular weights. Finally, from a PS-I (PS macroinitiator end-capped with iodine) and upon addition of a second monomer, the amphiphilic block copolymer PS-b-PHEA was successfully synthesized, illustrating the living nature of the RITP process. The successful formation of the block copolymer PS-b-PHEA was confirmed by GPC and gradient HPLC.

These results demonstrate the potential of the RITP process for industrial development of controlled radical polymerization to synthesize block copolymers in a versatile cost and effective manner.

4.5 References

1. Jayachandran, K. N.; Chatterji, P. R. *Journal of Macromolecular Science: Part C: Polymer Reviews* **2001,** 41, 79-94.

2. Jialanella, G.; Firer, E.; Piirma, I. *Journal of Polymer Science, Part A: Polymer Chemistry* **1992,** 30, 1925-1932.

3. Winzor, C.; Mrazek, Z.; Winnik, M.; Croucher, M.; Riess, G. *European Polymer Journal* **1994,** 30, 121-128.

4. Watanabe, S.; Kobayashi, T.; Sumitomo, H.; Murata, M.; Masuda, Y. *Polymer Bulletin* **2010,** 65, 543-550.

5. Galia, A.; Pierro, P.; Filardo, G. *Journal of Supercritical Fluids* **2004,** 32, 255-263.

6. Zhu, Y.; Ford, W. *Macromolecules* **2008,** 41, 6089-6093.

7. Shay, J. S.; English, R. J.; Spontak, R. J.; Balik, C. M.; Khan, S. A. *Macromolecules* **2000,** 33, 6664-6671.

8. Braunecker, W.; Matyjaszewski, K. *Progress in Polymer Science* **2007,** 32, 93-146.

9. Wang, S.; Matyjaszeweski, K. *American Chemical Society* **1995,** 117, 5614-5622.

10. Chierfari, J.; Ercole, Y.; Jeffery, J.; Le, T.; Mayadunne, R. *Macromolecules* **1998,** 31, 5559-5567.

11. Geoges, K.; Veregin, N.; Kazmaler, M.; K. *Macromolecules* **1993,** 26, 2987-2995.

12. Tonnar, J.; Lacroix-Desmazes, P.; Boutevin, B. *Macromolecular Rapid Communications* **2006,** 27, 1733-1738.

13. Lacroix-Desmazes, P.; Severac, R.; Boutevin, B. *Macromolecules* **2005,** 38, 6299-6309.

14. Tonnar, J.; Lacroix-Desmazes, P.; Boutevin, B. *Macromolecules* **2007,** 40, 6076-6081.

15. Nottelet, B.; Lacroix-Desmazes, P.; Boutevin, B. *Polymer* **2007,** 48, 50-57.

16. Oh, H.; Shin, H.; Jung, H.; Lee, B.; Choe, S. *Journal of Colloid and Interface Science* **2009,** 353, 459-466

17. Boyer, C.; Lacroix-Desmazes, P.; Robin, J.; Boutevin, B. *Macromolecules* **2006,** 39, 4044-4053.

18. Shin, H.; Oh, H.; Lee, K.; Lee, B.; Choe, S. *Polymer* **2009,** 50, 4299-4307.

19. Lacroix-Desmazes, P.; Severac, R.; Boutevin, B. *Polymeric Preprints* **2003,** 44, 683-684.

20. Vargun, E.; Usanmaz, A. *Journal of Polymer Science Part A: Polymer Chemistry* **2005,** 43, 3957-3965.

21. Coca, S.; Jasieczek, C.; Beers, K.; Matyjaszewski, K. *Journal of Polymer Science Part A: Polymer Chemistry* **1998,** 36, 1417-1424.

22. Bian, K.; Cunningham, M. *Macromolecules* **2005,** 38, 695-701.

23. Muchlebach, A.; Gaynor, S.; Matyjaszewski, K. *Macromolecules* **1998,** 31, 6046-6052.

24. Khutoryanski, V.; Mun, A.; Nurkeeva, S.; Akmetkaliera, T.; Shmakov, S.; Lee, C.; Park, K. *Journal of Polymer Science Part B: Polymer Physics* **2006,** 44, 196-204.

25. Enriquez-Medrano, F.; Guerrero-Santos, R.; Hernandez-Valdez, M.; Lacroix-Desmazes, P. *Journal of Applied Polymer Science* **2010,** 119, 2476-2484.

26. Valetova, N.; Semyonycheva, L.; Artemov, A.; Grishin, D. *Applied Organometallic Chemistry* **2005,** 19, 977-974.

27. Hook, P. J. V.; Tobolsky, V. A. *American Chemical Society* **1958,** 80, 779-782.

28. Moad, G.; Rizzardo, E.; Solomon, J.; Willing, I. R. *Macromolecular Rapid Communications* **1984,** 5, 793-798.

29. Tonnar, J.; Severac, R.; Lacroix-Desmazes, P. *Polymeric Preprints* **2008,** 49, 68-72.

30. Barner-Kowollik, C.; Davis, P.; Stenzel, H. *Polymer* **2004,** 45, 7791-7799.

31. Ladaviere, C.; Lacroix-Desmazes, P.; Delolme, F. *Macromolecules* **2009,** 42, 70-84.

32. Nonaka, H.; Ouchi, M.; Kamigaito, M.; Sawamoto, M. *Macromolecules* **2001,** 34, 2083 -2088.

33. Yamada, H.; Kojima, J. *Journal of the American Chemical Society* **1960,** 82, 1543-1547.

34. Benjamin, N.; Lacroix-Desmazes, P. *Polymer* **2007,** 48, 50-57

35. Goto, A.; Ohno, K.; Fukuda, T. *Macromolecules* **1998,** 31, 2809-2814.

36. Mortesen, K.; Gasser, U.; Gursel, S.; Sherer, G. *Journal of Polymer Science Part B: Polymer Physics* **2008,** 46, 1660-1668.

37. Suggs, L.; Payne, R.; Yaszemski, M.; Alemany, L.; Mikos, A. *Macromolecules* **1997,** 30, 4318-4323.

38. Murgasova, R.; Hercules, D. *Analytical and Bioanalytical Chemistry* **2002,** 373, 481-489.

39. Falkenhagen, J.; Much, H.; Stauf, W.; Muller, A. *Macromolecules* **2000,** 33, 3687-3693.

40. Gao, H.; Louche, G.; Sumerlin, B. S.; Jahed, N.; Golas, P.; Matyjaszewski, K. *Macromolecules* **2005,** 38, 8979-8982.

Functionalization of Montmorillonite by Functional block copolymer

Abstract:

Iodo-terminated polystyrene (PS-I) and poly(styrene-b-2.Hydroxyethyl acrylate) (PS-b-PHEA-I) were synthesized by reverse iodine transfer polymerization (RITP). The resulting polymers were reacted at room temperature with dimethylethylamine (DMEA) and triethylamine (TEA) respectively,affording PS and PS-b-PHEAwith quaternary ammonium chain-end functionality (PS-cationic and (PS-b-PHEA)-cationic). The results new polymers structure was analyzed by FT-IR, MALDI-TOF and ^{1}H-NMR.

PS-cationic and (PS-b-PHEA)-cationicwere successfully used for the modification of montmorillonite clay surface(MMT), as was confirmed by Fourier transform spectroscopy(FT-IR), thermogravimetric analysis (TGA), and Small a321ngle x-ray scattering (SAXS).

The complete ion-exchange was never obtained even when an excess amount of cationic polymers were used. This is due to bulkiness of the oligomeric PS-cationic and (PS-b-PHEA)-cationic. Furthermorethe mol% (relative to CEC) of (PS-b-PHEA)-cationicincorporated into the clay galleries was found to be greater than the amount of PS-cationic, due to the more hydrophilic character of (PS-b-PHEA)-cationic relative to PS-cationic, allowing (PS-b-PHEA)astronger interaction with clay from different functional groups such as the ester groups and hydroxyls groups and ether groups, via hydrogen bonds and ion-dipole interactions respectively, as well as via ion-exchange.

Functionalization of Montmorillonite by Functional block copolymer

5.1 Introduction

Surface modification of clay is attractive because it allows the creation of new materials, that can be used for applications requiring certain rheological behavior of organoclays, in various solvent systems, in areas such as oil well drilling fluids, paint, grease, cosmetics and personal care products.[1,2]Over the past two decades the use of organoclays in polymer-clay nanocomposites (PCNs)has emerged as interesting field.[3-5]The most common clay used in the preparation of PCNs is montmorillonite (MMT), this is due to its high aspect ratio and high surface area relative to others clays.[1,5,6] The preparation of organoclays is relativelysimple; it is achieved by surface modification with organic compounds via at least one of the following methods: ion-exchange with organic cations, or direct adsorption of organic compounds.[3,7-10]

In the ion-exchange reaction, alkaline earth cations situated in between clay sheets are replaced by cationic surfactants with long hydrophobic chains, affording a clay surface with hydrophobic character.[3] Cationic surfactants such as alkyl ammonium and alkyl phosphonium are commonly used to render the clay surface hydrophobic and to increase the *d*-spacing clay galleries, prior to clay being used for the preparation of PCNs.[9,11,12]

Besides small organic molecules such as cationic surfactants, the interactions of clay with large organic species such as polymers and oligomers have been studied. Huskic *et al.*[13] successfully modified the MMT surface by cationic polyester synthesized from N-octyl- or N-methyldiethanolamine and organic acid chlorides with varying chain length, as was confirmed by thermogravimetric analysis (TGA) and small angle X-ray diffraction (SAXS). Oligomeric chains of polyoxypropylene amine derivatives were also used to

modify MMT via ion-exchange, and the basal spacing of oligomeric-modified clay was found to be dependent on the structure and the amount of modifier used.[14]The preparation and use of oligomerically-modified clay to obtain PCNs have been extensively reported.[13,15-17] For example butadiene-modified clay was prepared by ionic exchange between MMT and butadiene surfactant. Then nanocomposites of polystyrene (PS), high impact polystyrene (HPS), poly(methyl methacrylate) (PMMA), polypropylene (PP) and polyethylene (PE) were prepared by melt blending this modified clay with the virgin polymers.[18]Zhang *et al.*[19] modified MMT with an oligomeric surfactant containing styrene and lauryl acrylate units along with a small amount of vinylbenzyl chloride to permit the formation of an ammonium salt as a way to bind to clay. This modified clay was then used to synthesize PE and PP nanocomposites by melt blending this modified clay with neat polymers.[19]

Uncharged molecules with selected functional groups, such as esters, carboxylic, hydroxyl and amino groups are able to form ion-dipole interactions with the exchangeable cations present in the clay galleries, hence also affording organoclays.[10,20] Polar organic molecules can be adsorbed by clay minerals by the formation of coordination bonds with the exchangeable cations, or by proton transfer from the interlayer water molecules surrounding the inorganic cations to the organic molecules, or by proton transfer from the organic molecules to the interlayer water molecules surrounding the inorganic cations.[21] Deng *et al.*[22]studied the interaction between polyacrylamide (PAM) and MMT, the main bonding between the polymer and clay are ion-dipole interaction between exchangeable cations and the carbonyl (C=O) oxygens of amides group (–CONH–), or by H-bonding between the amide groups and water molecules present in the hydration shells of exchangeable cations. Greenland *et al.*[23] found that polyvinyl alcohol (PVOH)strongly and irreversibly adsorbs onto MMT through hydrogen bonds between the hydroxyl groups of the polymer and the oxygenatoms present on the MMT galleries surface.

To date, most reports on the use of modification of clay by polymers and oligomers have focused on the use of polymers or oligomerswith uncontrolled molecular

weight,[13,18,24,25]although the synthesis of cationic polymer and cationic amphiphilic copolymer with control manner were reported, for instance Save *et al*[26] used benzyl dithiobenzoate RAFT agent to synthesize amphiphilic diblock copolymers poly(styrene-b-vinylbezyl chloride) quaternized with N,N-dimethyldodecylamine as well as poly(styrene-b-vinylbenzyl chloride) quaternized with triethylamine. These amphiphilic copolymers were used as electrosteric stabilizer of latexes in emulsion polymerization of styrene.

This present study describes the modification of MMT by PS ended with one quaternary ammonium group (PS-cationic) and cationic amphiphilic blocks copolymer of poly(styrene-b-2-hydroxyethyl acrylate) with quaternary ammonium group ((PS-b-PHEA)-cationic), prepared ina controlled manner using reverse iodine transfer polymerization (RITP), as described in the previous chapter. The resulting iodo-polystyrene (PS-I) was reacted with N,N-dimethylethylamine (DMEA) at room temperature to obtain PS with one quaternary ammonium end group(PS-cationic). Then PS-cationic was simply ion-exchanged with clay in suitable solvent, leading to organically modified (PS-MMT).

(PS-b-PHEA)-I was reacted with triethylamine (TEA) in order to obtain (PS-b-PHEA)-cationic, that can ion-exchange with inorganic cationic inside the clay galleries to obtain (PS-b-PHEA)-MMT. Furthermore, PS-b-PHEA can also interact directly with clay via the adsorption mechanisms, by the creation of hydrogen bonds between the hydroxyl groups of the PS-b-PHEA and the oxygens of MMT surface, or ion-dipole interaction between exchangeable cations and the carbonyl (C=O) oxygens of the ester groups of PS-b-PHEA block.Eventually, these interactions also ended with PS-b-PHEA molecules attached with clay surface ((PS-b-PHEA) -MMT).

PS-MMT and (PS-b-PHEA)-MMT were fully characterized using Fourier transform spectroscopy(FT-IR), thermogravimetric analysis (TGA), and Small angle x-ray scattering (SAXS). The main purpose of the preparation of PS-MMT and (PS-b-PHEA)-MMT is to use them as stabilizers in dispersions polymerization,as described later in Chapters 6 and 7.

5.2 Experimental

5.2.1 Materials

Sodium montmorillonite (MMT), Cloisite-NA^+ was obtained from Southern Clay Products (USA) as a fine powder with an average particle size of less than 13 μm^3 by volume in the dry state, and with a cation exchange capacity (CEC) of 92.6 milliequivalents (meq) per 100 g clay. PS and PS-b-PHEA were synthesized using the RITP technique, as described in Sections 4.2.2 and 4.2.3. DMEA was obtained from Fluka and used as received. Dry tetrahydrofuran (THF,HPLC grade) was obtained from (Sigma Aldrich) and distilled over lithium aluminium tetrahydride. All the other solvents (p.a. grade or higher) were obtained from Sigma Aldrich and used as received.

5.2.2 Characterization

NMR spectra were recorded using a Varian VXR-Unity 300 MHz instrument at 20°C, FT-IR spectra were recorded with a Perkin Elmer 1650 instrument using an average of 32 scans.

Thermogravimetric analysis**(**TGA) of the organoclay was carried out using a TGA-50 SHIMADZU thermogravimetric instrument using a TA-50 WSI thermal analyzer connected to a computer. Samples (10-15 mg) were degraded in nitrogen (flow rate 50 mL/min) at a heating rate of 5 °C/min.

SAXS measurements were performed at 298 K. Small angle X-ray diffraction (SAXS) measurements were carried out in a transmission configuration. A copper rotating anode X-ray source (functioning at 4 kW) with a multilayer focusing “Osmic” monochromator giving high flux (10^8 photons/sec) and punctual collimation was used. An “image plate” 2D detector was used.

Matrix-assisted laser desorption/ionisation-time of flight mass spectrometry (MALDI-TOF) spectrawere recorded using a Voyager-DE STR (Applied Biosystems, Framingham) equipped with a nitrogen 337 nm laser in the reflector mode at 25

kV accelerating voltage and with delayed extraction. The matrix was trans-2-(3-(4-tert-butylphenyl)-2-methyl-2-propenylidene) malononitrile (Aldrich). The analyte sample was prepared by first preparing a range of samples with the following concentrations of the matrix, sample, in DMF, separately: 35 mg/mL matrix; 1 mg/mL sample, before mixing them in the ratio of 4:1 and hand spotting on the target plate. One thousand laser shots were performed for each spectrum.

5.2.3 Synthesis of cationic polystyrene (PS-cationic)

The synthesis of iodo-polystyrene (PS-I) via RITP was describedin Section 4.2.2. Due to the weak bond energy of the carbon-iodine bond (220 KJ/mole)[27] the replacement of iodine at the chain ends with other functional groups become simple and easy.

In typical procedure iodo-polystyrene (PS-I) (30g, 0.0042 mole)with average M_w of 7100 g $mol^{-1}$was dissolved in dry THF and stirred with a magnetic stirrer. A two-fold mole excess of DMEA was added drop wise to the PS-I solution and stirred at room temperature (25ºC) in the dark for 48 h. The resultant polymer (PS-cationic) was then precipitated in cooled methanol, the excess DMEA was removed by redissolving the PS six times in THF, and precipitating in cooled methanol followed by drying in a vacuum oven at 30 °C for 48 h.

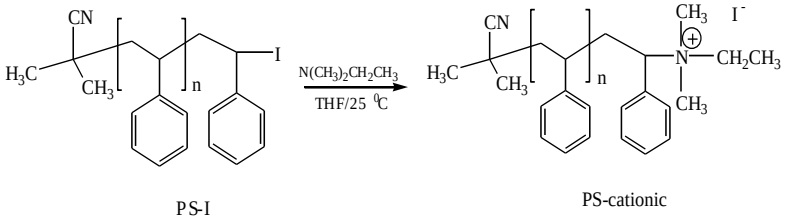

Scheme 5.1: Synthesis of PS-cationic.

5.2.4 Modification of MMT by PS-cationic

MMT (2 g) was introduced to a 250-mL flask containing (150 mL) of THF. The mixture was stirred at room temperature until the aggregation of the clay in the THF was no longer observed. Various quantities of PS-cationic ($M_{n\ SEC}$ 7100 g/mol)(3.28, 6.57, 9.86, 13.14, 17.08 and 19.71g) were added to the reaction mixture, and stirringwas continued for an additional 48 h at room temperature.

PS-MMT was separated from THF by centrifugation of the mixture at 4400 rpm (for 30 min), followed by redispersion in THF (100 mL) to remove any unreacted PS-cationic. This procedure was repeated six times, until the washing THF was free of PS. This was confirmed by measuring the UV adsorption of the centrifuged washing THF (to monitor the concentration of unreacted PS in the solution).

In further experiments the modification of clay using PS-cationic was similarly carried out in toluene in order to determine the effect of the solvent medium in the modification process.

5.2.5 Synthesis of cationic block copolymer ((PS-b-PHEA)-cationic)

In a typical procedure iodo-block copolymer ((PS-b-PHEA)-I) (10 g, 0.0015 mole)with average M_w of 6329 g $mol^{-1}$was dissolved in dry DMF and stirred with a magnetic stirrer. A two-fold mole excess of TEA was added dropwise to the (PS-b-PHEA)-I solution and stirred at room temperature (25ºC) in the dark for 48 h. The resultant polymer ((PS-b-PHEA)-cationic) was then precipitated in cooled methanol/diethyl ether solution, the excess of TEA was then removed by redissolving the PS-b-PHEA six times in DMF, and precipitating in cooled methanol/diethyl ether followed by drying in a vacuum oven at 30 °C for 48 h.

5.2.6 Modification of MMT by (PS-b-PHEA)-cationic

The modification of MMT using (PS-b-PHEA)-cationic was carried out under similar conditions used to modify the clay with PS-cationic. DMF was used as a solvent. In a typical procedure different amount of PS-b-PHEA ($M_{n\ SEC}$ 6329 g/mol) (1.5, 3.0115 and

6.023g) was dissolved in 200 ml DMF and the added drop-wise to the suspension of clay in water. The mixture was stirred for 48 h. (PS-b-PHEA)-MMT was separated from DMF by centrifugation of the mixture at 4400 rpm (for 30 min), followed by redispersion in DMF (100 mL) to remove any unreacted (PS-b-PHEA)-cationic and precipitate in cooled methanol/ diethyl ether and dried in vacuum oven at 35 °C for 3 days.

5.3Results and discussion

5.3.1 Characterization of PS-cationic

Fig. 5.1 shows a typical ^{1}H-NMR spectrum of a low molecular weight PS prepared using RITP and Fig. 5.2 shows a typical ^{1}H-NMR spectrum of PS-cationic obtained from the reaction of PS-I with DMEA.

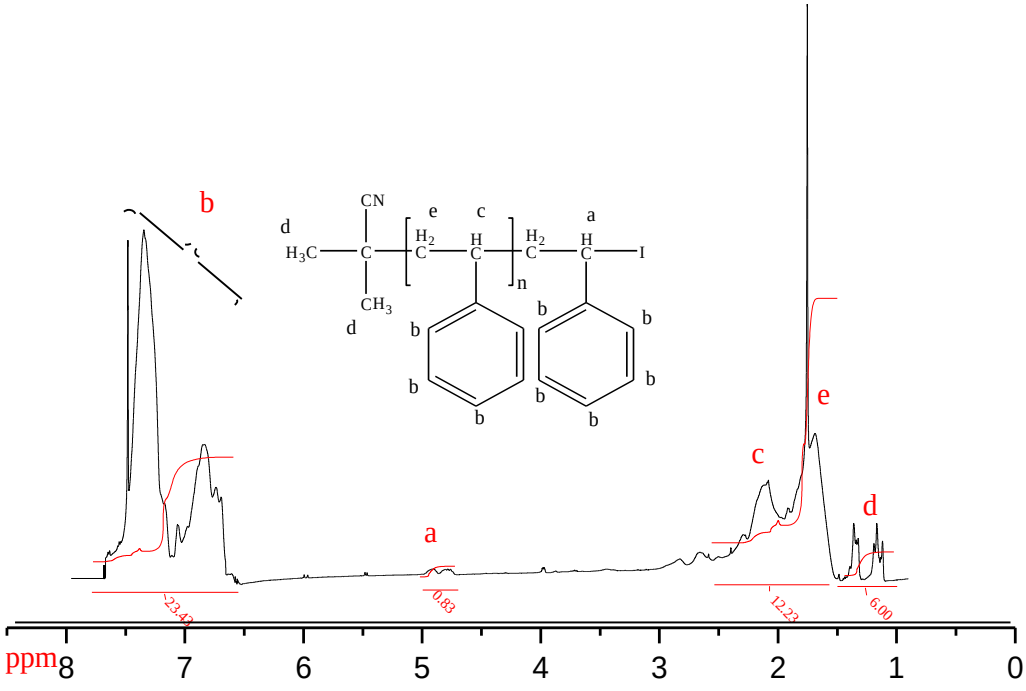

Fig. 5.1: ^{1} H-NMR spectrum of PS-I prepared by RITP ($CDCl_3$ solvent).

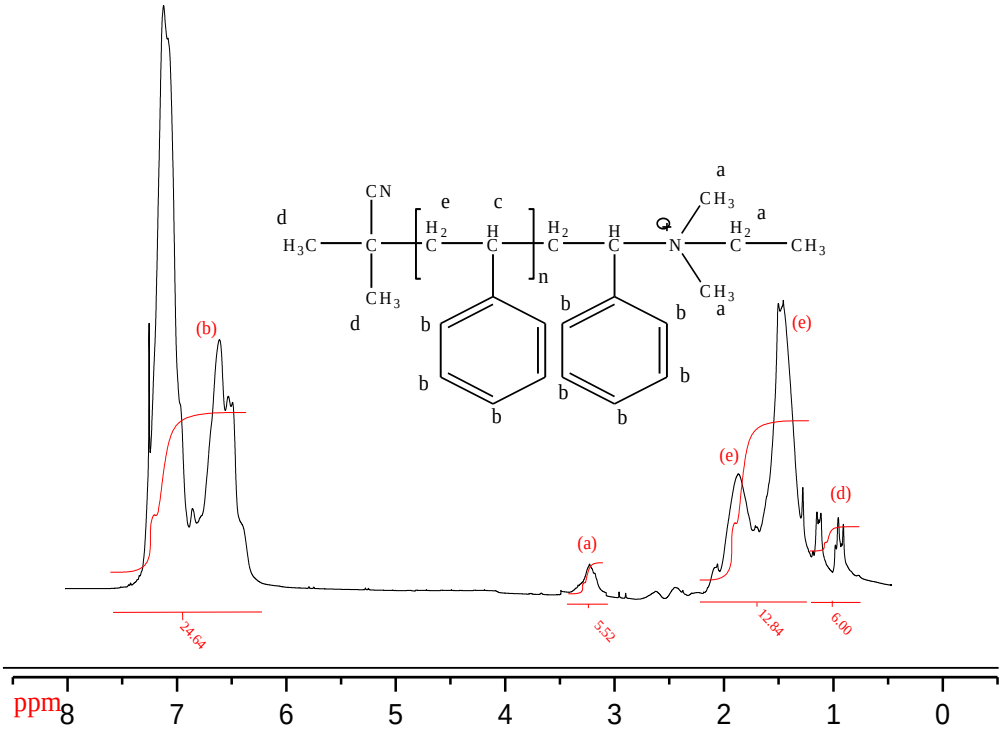

Fig. 5.2: ^{1}H-NMR spectrum of PS-Cationic ($CDCl_3$solvent)

The signal at 4.5-4.8 ppm in Fig. 5.1 corresponds to the methine proton in the β position from the iodogroup, in Fig. 5.2 this signal disappears after the reaction of PS-I with DMEA, indicated that the iodine was removed, and a new signal appears at 3.25-3.38 ppm, this is related to the protons of the methyl groups of the quaternary ammonium group at the chain ends. This proves that the replacement of the iodo group by the quaternary ammonium group was successful, resulting in PS chains with one positively charged chain end (i.e. PS-cationic).

FT-IR spectra of PS-I and PS-cationic were recorded and shown in Fig.5.3. The spectrum shows the characteristic transmission bands of the PS-I and PS-cationic. The position and functional groups responsible for them are outlined in Table 5.1.

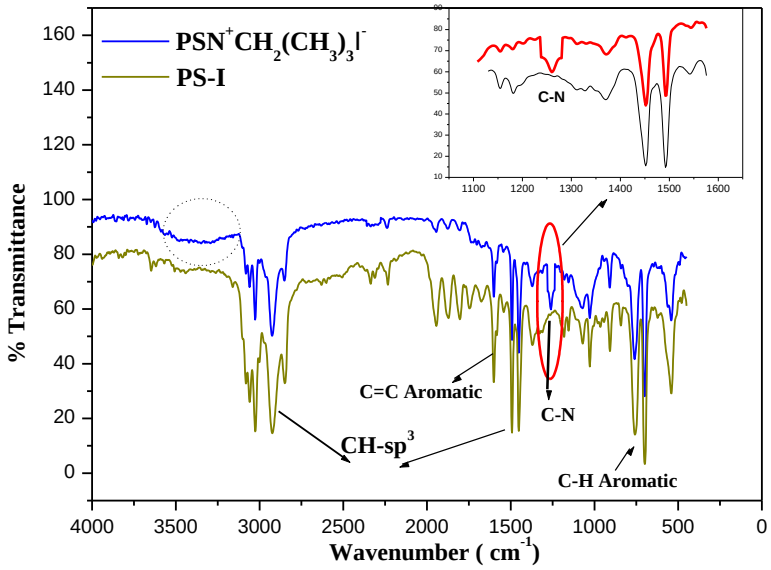

Fig. 5.3: FT-IR spectra of PS-I and PS-cationic.

Table 5.1: FT-IR data of the functional groups of PS-I and PS-cationic.

Functional group	PS wavelength	PS-cationic wavelength	Band mode
Ring	700	700	Bend
CH	1028	1030	Bend
CH	1070	1070	Bend
CH	1160	1160	Bend
CH	1182	1180	Bend
CN	-	**1260**	Bend
Ring	1450	1450	Stretching
Ring	1493	1493	Stretching
Ring	1606	1606	Stretching
CH	2845,2924,3064,3084	2845,2930,3063,3084	Stretching

In the FT-IR spectrum of PS-cationic the absorption band of the (C–N stretching) at 1260 cm^{-1} which is related to the presence of quaternary ammonium group on the polymer chain ends, [28]in addition the broad band at 3150-3300 is related to the stretching and deformation vibrations of the CH_3 groups in dimethyl ethyl ammonium ($(CH_3)_2CH_2CH_3N^+$) as was referenced in the literature,[29] confirmed the replacement of iodine by the quaternary ammonium group.

MALDI-TOF it is a powerful analytical method used to determine the structure of polymers synthesized using CRP.[30] Fig. 5.4 shows a typical MALDI-TOF spectrum of PS-cationic. The analysis was performed in reflectron mode using 2,5-dihydroxybenzoic acid (DHB) as matrix. The three major populations were identified at 998.23, 1102.749 and 1206.652 and were attributed to A-$(PS)_n$-$N^+(CH_3)_2CH_2CH_3$where A stands for the fragment from the initiator polymer chains. Other strong populations at 1014.3, and 1118.708 correspond to A-M_n-N $(CH_3)_2CH_2CH_3(H_2O)$ results from the adsorption of water molecule due to the polarity of quaternary ammonium groups.The complexation of water molecules in MALDI-TOFF analysis of polymer has been reported by Ladaviere*et al,*[31] who study the structure of PS prepared using Nitroxide-Mediate Polymerization (NMP).In summary, A-$(PS)_n$-$N^+(CH_3)_2CH_2CH_3$was the major product in the sample, further confirming the structure of PS-cationic.

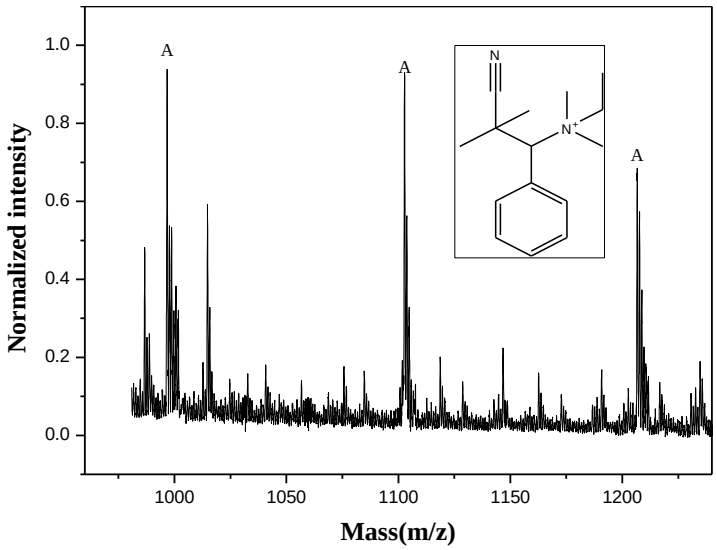

Fig: 5.4 MALDI-TOF spectrum of PS-cationic.

It was also noted that there was change in the colour of the polymer solution after the reaction of PS-I with DMEA (see Fig. 5.5).

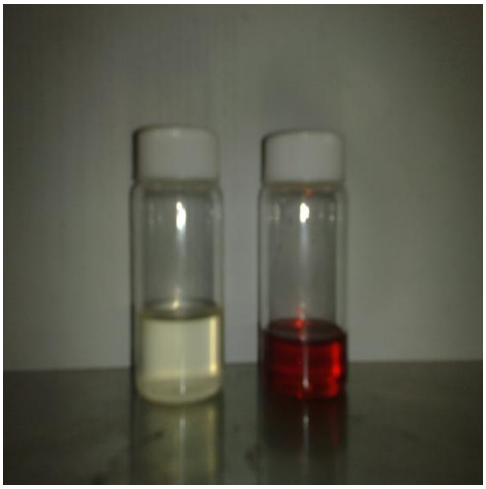

Fig. 5.5: Photograph of PS-I (right) solution and PS-cationic solution (left).

Fig. 5.5 shows PS-I and PS-$N^{+}(CH_3)_2CH_2CH_3$solutions after 3 days of dissolving in THF. Ared colour appears when PS-I is dissolved in THF due to small amount of free iodine (I_2) released in the solution, while PS-cationic (with quaternary ammonium end group)

has no colour. This provides further proof that the quarterisation reaction took place, (as was already determined by ^{1}H-NMR and MALDI-TOF analysis).

5.3.2 Modification of MMT by PS-cationic

The clay was modified with different PS-cationic concentrations;the concentration of organic modifier (e.g. PS-cationic) is given as % CECin order to relate to cationic surfactants generally used to prepare modified clay. The CEC represent the amount of surface anionic changes for which counter cation can be substituted by another cationic species (e.g. cationic surfactant) given in miliequivalent (i.e. m mol) per hundred grams of clay.

In order to remove all unadsorbed PS-cationic from the external clay surface the PS-MMT samples were washed with THF and centrifuged to separate the PS-MMT from the THF. This procedure was repeated until the washing THF was found to be free of PS, as confirmed by UV absorbance at 255 nmof the washing THF. Fig. 5.6 shows the change in UV absorbance of the THF after washes as a function of the number of washings.

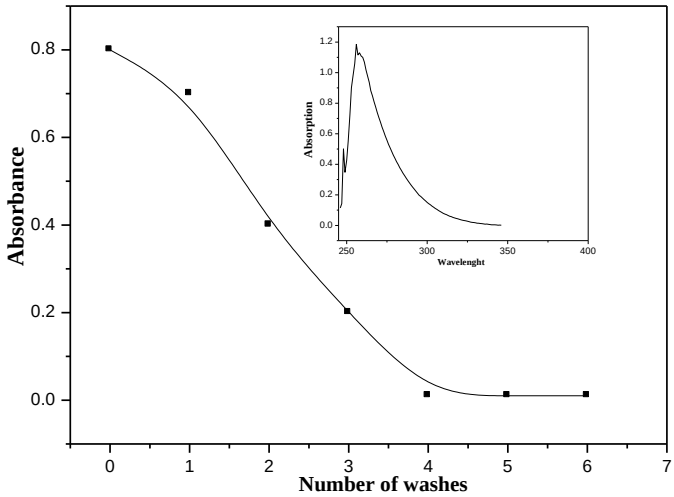

Fig. 5.6: UV absorbance of THF vs. number of washing cycles for 100% CEC PS-cationic. (the insert shows the UV/Vis spectra of PS-cationic.

Styrene units were expected to absorb UV-light at 255 nm,The UV absorbance value decreased with subsequent washings until it became constant after washing the modified

clay 5-6 times, indicating that this number of washing (5-6) times under these experimental conditions were necessary for a complete removal of unreacted PS. Therefore the characterization of PS-MMT by other analytical methods, SAXS, TGA and FT-IR, will be only related to the PS localized inside the clay galleries.

5.3.2.1 Characterization of PS-MMT by TGA

TGA was used to determine the amount of PS-cationic incorporated inside the clay galleries via ion exchange.[3,10,32]Various quantities of PS-cationic (M_n = 7100 g/mol) were used to modify the clay surface (25%, 65%, 100%, 130% and 150% relative to CEC of the clay). The decomposition behaviour of all samples was examined by TGA analysis results as shown in Fig. 5.7. Clay minerals are thermally more stable in comparison toorganic molecules. These minerals will begin to lose structural hydroxyl groups at 600^{o}C while still maintaining the layer structure up to 800^{o}C.[33] The weight loss of pure clay between 20 °C and 100 °C corresponds to the removal of water from the interlayer galleries. The weight loss of MMT in the temperature range 100 °C to 600 °C is about 2.6%, and can be attributed to the desorption of hydrogen-bonded water molecules and some of the hydroxyl groups from the tetrahedral sheets of clay.[34,35]

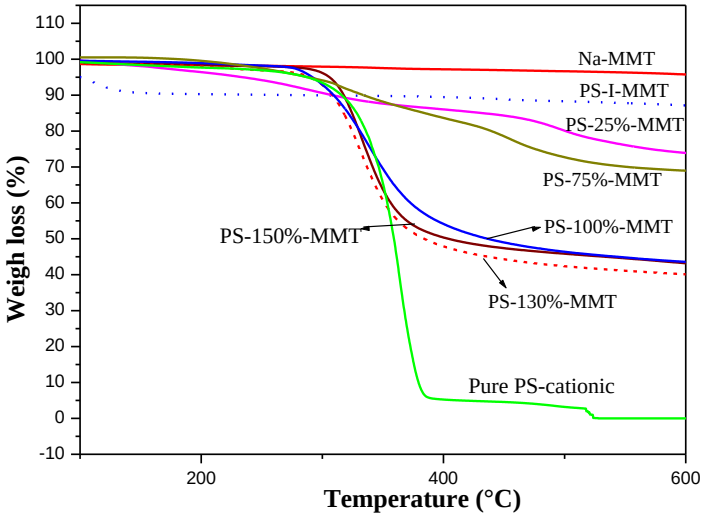

Fig. 5.7: Thermal gravimetric curves of: pristine MMT, pure PS and PS-MMT with various clay Modifier amount.

In general, all the PS-MMT samples decompose in a similar fashion. At temperatures between 260 and 600 °C, the organic modifier (PS) in thegalleries decomposes. TGA analysis of neat PS-cationic was also performed.

The difference in weight loss between pure clay and clay modified by PS-cationic (in THF) indicated that PS-cationic was successfully ion-exchanged at the surface of clay.The difference between the percentage weight loss of the virgin clay and the modified clay is attributed to the amount of cationic organic species ion-exchanged.[36-41]The amount of PS loaded in the clay was determined from the difference between the residual weight difference between PS-MMT and pristine clay measured at 600°C as seen in Fig.5.7 and summarized in Table 5.2.The clay was modified using PS-I,and the decomposition behaviour of the sample is also represented in the figure.

Table 5.2: Initial PS-cationic concentrations and the quantities of PS-cationic inside clay galleries

Initial concentration of PS-cationic		Weigh loss at 600 °C (%)	Quantities of PS-cationic into clay galleries		
Rel. to CEC of clay [a] (%)	Feed mass (g)		Mass [b] %	Exp mass (g)	Exp %CEC
Pure Clay	0	4.02	0	0	0
25% in THF	3.28	26.45	22.53	2.28	17.00
75% in THF	9.85	51.23	44.98	4.43	34.35
100% in THF	13.13	56.18	39.80	5.25	40.13
100% of PS-I	13.13	13.022	9.002	1.18	8.95
130% in THF	17.08	59.95	37.03	5.85	44.00
150% in THF	19.71	56.18	39.80	5.25	40.13

[a] Relative to cation exchange capacity of clay

[b] Percentages of PS ion exchanged with clay

Table 5.2 shows that PS-cationic and PS-I used to modify the clay with similar amount (i.e. 100% CEC).Clearly, the amount of PS incorporated inside clay galleries was greater when PS-cationic was used as modifier than when using PS-I.This confirmed that PS-

cationic indeed interacted with the clay only via ion-exchange, while there is not any interaction between MMT and PS-I as expected.

The quantity of PS bound to the clay surface increases with an increase in PS-cationic. The curve for 75% CEC falls between the curves for 25% CEC and 100% CEC, while curves for 130% CEC and 150% CEC almost overlap the curve for 100% CEC, indicating that PS incorporated into clay reached a maximum when the concentration of the initial PS reached 100% CEC. According to TGA results shown in the Table 5.2,complete cation exchange was never obtained, even with an excess PS-cationic (i.e. 130% CEC and 150% CEC). This may be explained on the basis of steric hindrance of PS-cationic chains caused by the size of the head group preventing complete cation exchange from being achieved. This is in agreement with the findings ofBiasci *et al.*[36]who functionalized MMT by methyl methacrylate polymers containing side-chain ammonium cations. They found that even with an excess amount of polymers the complete cation exchange was not obtained due to the bulkiness of head group.

The molar mass value of the PS-cationic used as modifierwas fairly high for clay surface modifier,and thus could hinder the mobility and diffusion of PS-cationic chains into clay galleries during the ion-exchange process, which also effected the achievement of complete ion-exchange.This is in disagreement with deductions made by Huskic *et al.*[13] they successfully modified a MMT surface by a cationic polyester (M_w= 1620 g mol^{-1}) via ion-exchange, and concluded that complete ion-exchange reaction was obtained.

Unlike common alkyl ammonium cations in clay modification, most polymeric cationic compounds are not water soluble, hencethe need for an organic solvent as a carrier to facilitate the ion-exchange process.[25]Furthermore, according to findings of Amarasinghe *et al.*[42] solvents polarity has a large influence on expansion of the clay interlayer. Non-polar solvents such as toluene are unable to make any strong interaction with polar interlayer water molecules, or negatively charge clay sheets, thus has no influence on the clay interlayer spacing. On the other hand an intermediate polarity solvent, such as methanol, which has both hydrogen bonding and donor and acceptor characteristics, interacts with the clay structure by creating hydrogen bonds with both oxygen and the

interlayer water, lead to an increase in the *d*-spacing, and hence facilitates the clay modification.

The effect of the solvent polarity on the degree of the clay modification was investigated. The modification of clay was carried out using either THF or toluene as a solvent modification medium. The amount of PS-cationic incorporated in both cases was determined by TGA. Results in Fig. 5.8 show thatthe weight loss at 600ºC of PS-MMT prepared in toluene was only 8%, while the weight loss of PS-MMT prepared in THF was about 55%. This indicated that the quantity of PS inside clay was significantly greater when the modification was carriedout in THF.

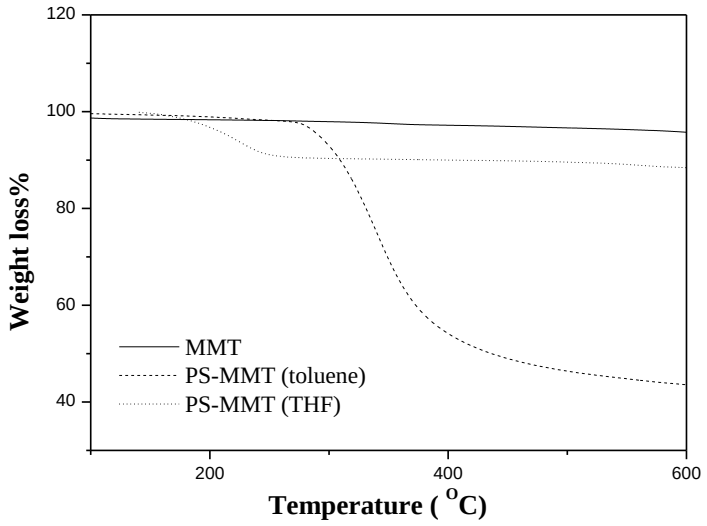

Fig. 5.8: Thermal gravimetric curves for PS-MMT prepared in toluene and THF

There are two possible reasons for this:

- The quaternary ammonium in PS-cationic chains is a polar group; therefore in non-polar medium (e.g. toluene) it is less solvated and will tend to remain surrounded by the PS chain,hence becoming less accessible for interacting with the clay surface. On the other hand, the quaternary ammonium groups of PS in THF are close to the surface and bind to the clay via ion-exchange.Scheme5.2 illustrates the behavior of PS-cationic in different solvent (THF and toluene).

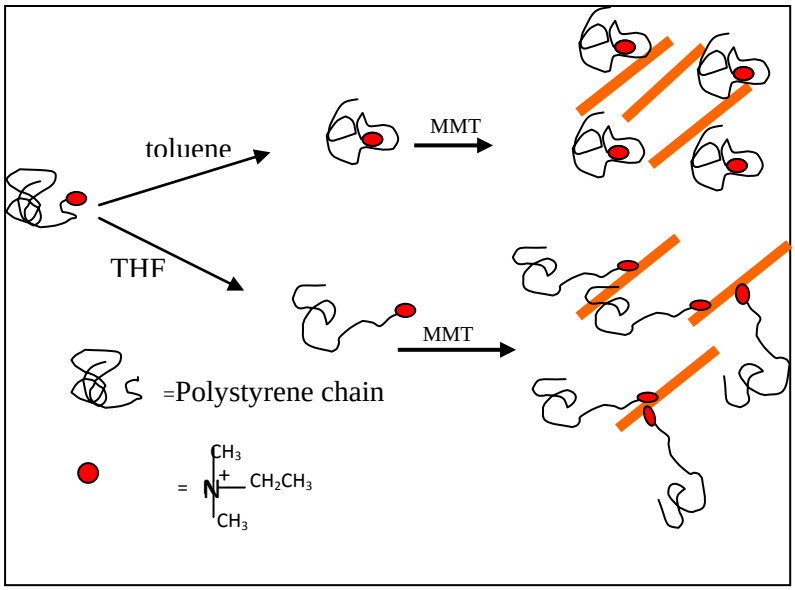

Scheme 5.2: Schematic representation of the effect of polarity of the solvent medium on clay modification

- According to Amarasinghe *et al.*[42] who studied the effect of solvent polarity on clay modification, due to the polarity of THF facilitates the insertion of PS molecules inside clay galleries. Fig. 5.9 (a) and (b) shows TEM image of PS-MMT prepared from PS-cationic either dispersed in THF or intoluene.

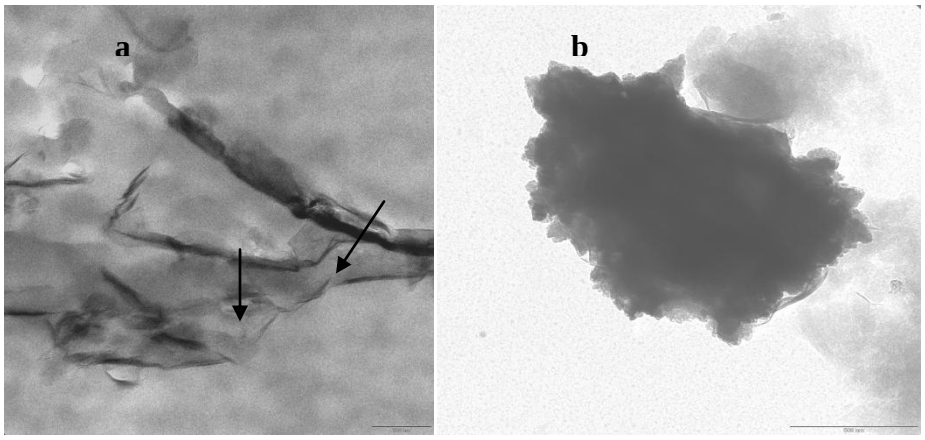

Fig. 5.9: TEM image of PS-MMT dispersed in THF (a) and of PS-MMT dispersed in toluene (b)

Fig. 5.9 (a) depicts a TEM image of PS-MMT dispersed in THF, as indicated by arrowhead, the stacked clay particles can be seen. Fig 5.9 (b) shows a TEM image of PS-

MMT dispersed in toluene, the aggregation of polymer particles around the clay can be seen. Toluene is a good solvent for PS chains but yields poor interaction with hydrophilic clay surface.

5.3.2.2 Characterization of PS-MMT by FT-IR

FT-IR spectra of neat MMT and PS-MMT were recorded and compared as illustrated in Fig. 5.10.

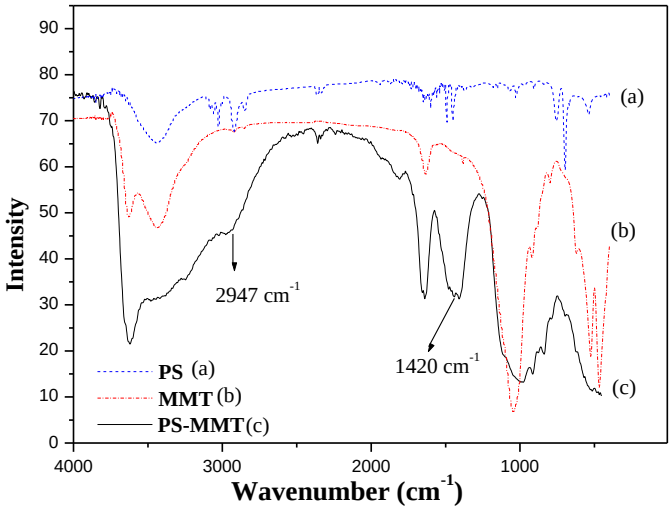

Fig. 5.10: FT-IR spectra of neat MMT and PS-MMT.

The FT-IR spectrum of MMT shows absorption bandsat 3432, 3630 and 1640 cm^{-1}, corresponding to the OH stretching of the silicate layers.[32] The sharp band at 1043 cm^{-1} is related to the stretching of Si–O bonds of the silicate layer.[32,43] The band at 620 cm^{-1} is related to the Al–O of the silicate layers. The appearance of newbands in the FT-IR spectrum of clay modified by PS-cationic (see Table 5.3) is an indication of the presence of PS within MMT.

Table 5.3 FT-IR data of the functional groups of MMT, PS, and PS-MMT

Assigned groups (cm^{-1})	MMT wavelength (cm^{-1})	PS wavelength (cm^{-1})	PS-MMT wavelength (cm^{-1})
Al-O	620		620
Si-O	526,463,1043		526,460,1040
O–H	1640,3432,3630		1651,3434,3634
C=C ring		1602,1491,1451	1430
C–H		2845,2924,3024,3064	2947,2850

The bands at 2947 and 2850 cm^{-1} are related to C–H stretching of PS molecules. Other new bands in the FT-IR spectrum of PS-MMT can be seen at 1430 cm^{-1},corresponding to the aromatic C=C stretching.

5.3.2.3Study of the *d*-spacing of PS-MMT using SAXS

SAXS has been used to study changes in the basal spacing of MMT before and after modification.[44] The *d* spacing can be calculated according to Bragg's law: $d = 2\pi/q$ (where q is a wave vector and its value corresponds to the associated Bragg peak position).[3] The quantities of PS-cationic that were used to modify the clay surface were calculated relative to the CEC of the MMT that was used (i.e. 92.6 meq/100 mg). Fig. 5.11 shows SAXS patterns for MMT modified using different PS-cationic concentrations. SAXS patterns for unmodified clay MMT and MMT modified using PS-I were also shown in the figure.

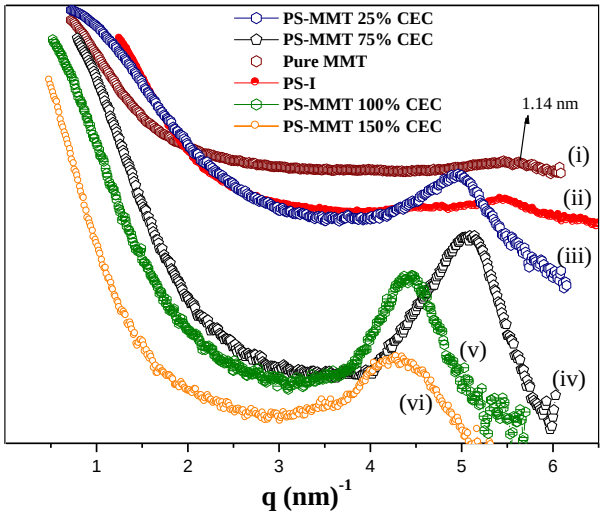

Fig. 5.11: SAXS patterns of (i) pristine MMT, and PS-MMT modified using different concentrations of PS-cationic: (iii) 25%, (iv) 75%, (v) 100% and (vi) 150% CEC of clay and (ii) Clay modified by PS-I.

The SAXS pattern of pristine MMT (Fig. 5.11(i)) shows that the pristine MMT has an interlayer spacing of d = 1.14 nm, which is in agreement with the literature.[32,45] The SAXS patterns of PS-MMT samples (Fig. 5.11(iii-vi)) show that the XRD peak positions shifted toward lower qvalues, and according to Bragg's law, the interlayer spacing of PS-MMT samples increased compared to that of pristine MMT.

The increase in the interlayer distances of PS-MMT samples relative to pure clay confirmed the insertion of PS chains into the clay galleries as observed by TGA (see Section 5.3.2.1). This confirms that the ion-exchange interaction took place. Similar results was obtained by Huskic *et al.*[24] who modified MMT using cationic polyester, the *d*-spacing increased after the modification process, indicating the insertion of polyester into clay galleries via ion-exchange. Yoon *et al.* [14] used oligomeric polyoxypropylene amine derivatives to modify MMT via ion-exchange. The basal spacing of oligomeric-modified clay was found to be dependent on the structure and the amount of the modifier.

Fig. 5.11 (ii) shows no significant change in the SAXS peak position when PS-I 100% CEC of was used.This is in agreement with TGA results, and the author's expectations,

as there is no driving force leading to the insertion of PS inside the clay galleries.This serves as further proof that PS-cationic interacts with MMT via ion-exchange.

The interlayer distance was found to increase with increasing PS-cationic concentrations, up to 100% CEC no further increase in *d*-spacing was observed for PS loadings higher than 100% CEC. This is in good agreement with the TGA results, which indicated that there is a limit in terms of the amount of PSthat interacts withthe clay surface after washing, due to the bulkiness of the PS chains head group and to the high molecular weight of the PS used. This is in agreement with findings of Huskic *et al.*[24] who found that the *d*-spacing of MMT increased from 1.14 to 1.82 nm after modification with a cationic polyester, and it remained constant even when an excess of cationic polyester was added, as complete ion exchange was obtained.

The change in interlayer distance as a function of PS concentration could result from a change in the conformation of the PS chains inside the clay galleries, as has been reported for other organic modifiers, and it depends on the molecule's chemical structure of the organic modifier, chain length, concentration and temperature.[3,46]The chains of the organic modifiers are thought to lie either parallel to the host layers, forming mono- or bi-layers, or radiate away from the surface, forming extended (paraffin-type) mono- or bi-molecular arrangements[3,5] This is further supported by the changes seen in the shape of SAXS diffraction peaks with changing PS concentrations (see Fig 5.11). It is known that on XRD diffractograms a narrow peak indicates that clayplatelets are regularly packedwhile a broad peak indicates heterogeneity of packing, with a relatively undefined *d*-spacing.[47] In other words, this means that the relatively narrow diffraction peaks observed for 75 and 100% CEC in Fig 5.11, indicate a rather regular packing of PS chains on the clay surface. The broad peaks inFig 5.11 show a relative disorder existing during the transition between the flat-type and paraffin-type of packing.

5.3.2.4Study of the morphology of PS-MMT using TEM

TEM was used hereto image the clay in polymer,TEM images of PS-MMT prepared using different PS-cationic concentrations (50% and 150% CEC) are shown in Fig. 5.12

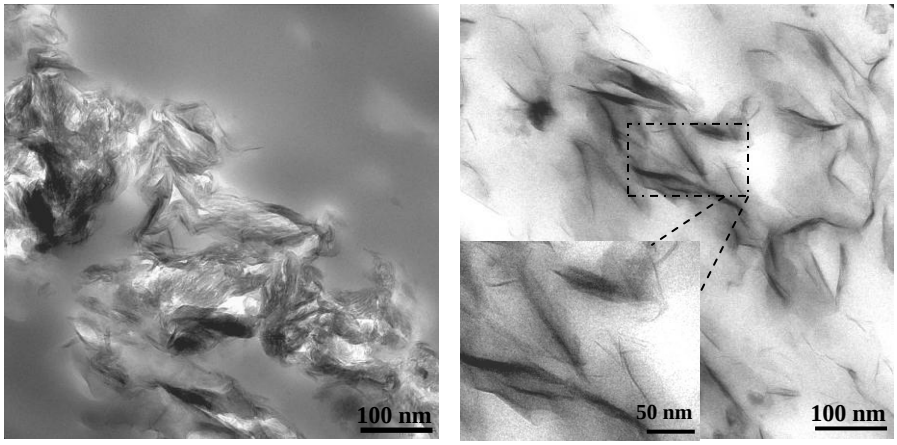

Fig. 5.12: TEM images of PS-MMT prepared at different PS-cationic concentrations: (a) 50% CEC and (b) 150% CEC.

TEM image of 50% CEC in Fig. 5.12 (a) shows that the clay platelets are highly packed to each other. They appear as thick dark lines in the image, suggesting that there is only an intercalated structure, this was expected due to the limited amount of polymer chains in between the clay interlayer galleries. In the case of 150%CEC, the clay platelets still appear as groups. Image recorded at higher magnification did show small regions where the clay platelets are separate, but most clay layers remain packed to each other (i.e. *Intercalated structure*). This is in agreement with findings of Su *et al.*[16] who prepared an oligomeric ammonium salt of copolymer of styrene with a quaternaized vinylbenzyl chloride, and observed a few single clay layers appearing to be exfoliated or mixture of exfoliation and intercalation. On the other hand, after Su *et al.*[18] prepared butadiene-modified clay via ion exchange reaction between butadiene surfactant and MMT, only a highly intercalated structure was observed in the TEM image. A TEM image of MMT modified using 100% CEC PS-I is shown in Fig 5.13.

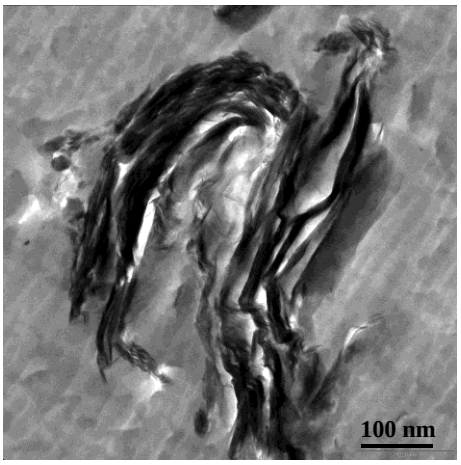

Fig. 5.13: TEM images of PS-MMT prepared using 100% CEC PS-I.

The dark spots represent the clayaggregates which are poorly dispersed inthe matrix. From this result, together with the fact that there wasparticularly no change in the position of the characteristic diffraction peak of clay (see Fig 5.11 (ii)), it can beconcluded that a conventional microcomposite of unmodified montmorillonite was obtained.

From these observationsand those made from X-ray patterns of the polymer-modified clays, it can beconcluded that,indeed the PS-cationic chains interacted with the clay via ion-exchange,and resulted in PCNs that had only intercalated morphology.

5.3.3 Characterization of (PS-b-PHEA)-cationic

The positively charged amphiphilic diblock copolymer ((PS-b-PHEA)-cationic) was obtained by the chemical reaction between (PS-b-PHEA)-I and triethylamine. Fig. 5.14 shows a typical ^{1}H-NMR spectrum of (PS-b-PHEA)-cationic.

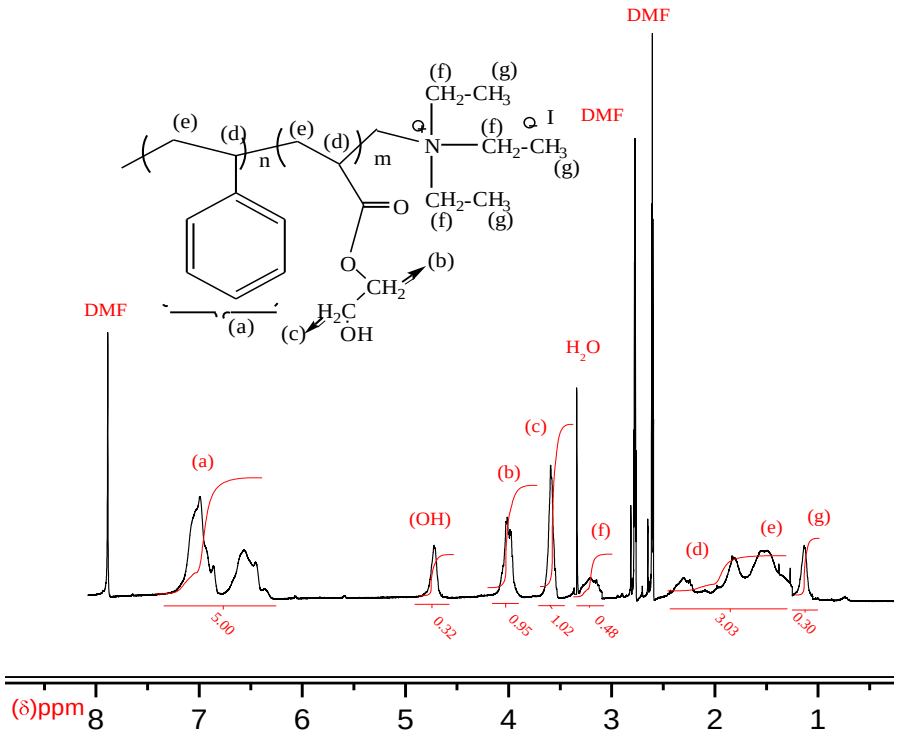

Fig. 5.14: H^1-NMR spectrum of (PS-b-PHEA)-cationic

Peaks at 6.20-7.30 ppm are ascribed to aromatic protons. The strong signals at 3.55 and 4.05 ppm are ascribed to the methylene ($^{-}CH_2$)protons of the hydroxyethyl group (c and b) and the signal at 4.8 ppm corresponds to the ^{-}OH of hydroxyethyl group.Peaks at 3.15-3.36 ppm (2H, $–N(\underline{CH_2}CH_3)_3$)and 1-1.24 ppm (9H, $–N(CH_2\underline{CH_3})_3$) are ascribed to the methylene and methyl protons of $–N^{+}(CH_2CH_3)_3$) I^{-}respectively, confirming the successful quaternizetion of PS-b-PHEA.

5.3.4Modification of montmorillonite by (PS-b-PHEA)-cationic copolymer

Block copolymer of PS-b-PHEA was previously synthesized using RITP as described in Chapter 4, (PS-b-PHEA)-I was quaternized by reaction with an excess TEA to obtain (PS-b-PHEA)-cationic.

(PS-b-PHEA)-cationic was used to modify the clay surface by the ion-exchange process, however, the ion-exchange reaction is probably not the only type of interactions that take

place between PS-b-PHEA and MMT, because the presence of hydroxyl and carbonyl ester groups on the main chains of (PS-b-PHEA)-cationic, allows (PS-b-PHEA) to interact directly with a clay surface via the creation of several types of bonds, such as the ion-dipole interaction between exchangeable cations of MMT galleries, and the carbonyl (C=O) oxygen of ester groups as was reported for poly(acrylamide) PAM[48] or via hydrogen bonds between the hydroxyl groups of the copolymer and the oxygen atoms of MMT surface as was reported for the adsorption of PV(OH).[23] In order to investigate the ability of the interaction of PS-b-PHEA with a clay via an adsorption process, non-cationic-PS-b-PHEA (i.e. (PS-b-PHEA)-I) was also used as a modifier.

In general, low molecular weight of (PS-b-PHEA)-cationic was used in this study in order to modify clay surface for two specific reasons: (i) to ensure that (PS-b-PHEA) penetrates easily in between clay galleries, and (ii) because the (PS-b-PHEA)-MMT will be used as a stabilizer in dispersion polymerization, it is well know that a block copolymer with only low molecular weight should be used as stabilizer, as reported by Baines *et al.*[49] who successfully synthesized PS latexes particlesby dispersion polymerization in methanol only when a low molecular weight (< 10000 g/mol)poly(2-(dimethylamino)ethyl methacrylate-b-alkyl methacrylate) block copolymers were used.

After modification the (PS-b-PHEA)-MMT was washed five times with DMF to remove all un-bonded (PS-b-PHEA), and then (PS-b-PHEA)-MMT was characterized using FT-IR, TGA and SAXS.

5.3.4.1 Characterization of (PS-b-PHEA)-MMT by FT-IR

FT-IR spectrum of PS-b-PHEA, (PS-b-PHEA)-MMT and pristine clay (MMT) were recorded as seen in Fig. 5.15 and Table 5.3. The appearance of new bands in the FT-IR spectrum of clay modified by (PS-b-PHEA)-cationic (see Table 5.4) is a qualitative indication that the ion-exchange process was indeed successful.

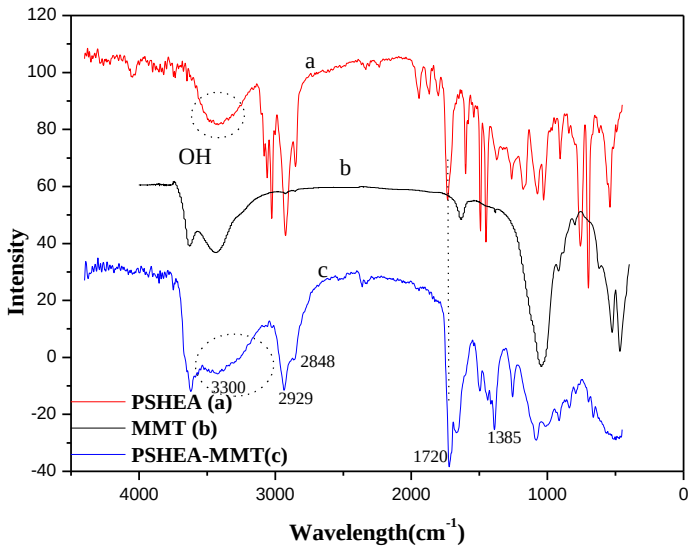

Fig. 5.15: FT-IR spectra of: (a) PS-b-PHEA and (b) pristine MMT and (c) (PS-b-PHEA)-MMT.

Table 5.4: FT-IR date of the functional groups of MMT, PS-b-PHEAand (PS-b-PHEA) -MMT

Assigned groups (cm^{-1})	MMT wavelength (cm^{-1})	PS-b-PHEA wavelength (cm^{-1})	(PS-b-PHEA)-MMT wavelength (cm^{-1})
Al-O	620		620
Si-O	526,463,1043		526,460,1040
O-H	1640,3432,3630	1298,3400	1651,34300,3634
C=C Ring		1385,1602,1491,1451	1430
C-H		2845,2924,3024,3064	2848,2929,2850
C=O		1754	1720
C-O-C		1203	1237

New strong bands related to (C−Hstretching) bonds of the copolymer appeared at 2929 cm^{-1} and 2848 cm^{-1} in the FT-IR spectrum of (PS-b-PHEA)-MMT. Another new band at 1720 cm^{-1} relative to (C=O stretching) group in HEA segments in PS-b-PHEA, however, the C=O band was shifted to 1720 $cm^{-1}$from its original wavelength at 1754 cm^{-1}in PS-b-PHEA, this indicated that PS-b-PHEA probably also had interacted with MMT via an adsorption mechanism, in accordance to thefindings of Yariv *et al*[50]and Tahoun *et al*, [51] who found that compounds containing C=O groups, such as aldehydes, ketones, carboxylic acids, esters, and amides, etc., behave similarly when adsorbed on swelling clay minerals, the C=O group is either bound to the exchangeable metallic cation through a water molecule bridge via hydrogen bonding,as seen in Scheme 5.3 (a), or it is directly linked to the cation via ion-dipole interaction,as seen in Scheme 5.3 (b). When the interaction between a C=O group and the cation is via water bridge, the shift of the C=O stretching band to lower frequency relative to the position in the spectrum of the neat compound, is less than 30-40cm^{-1}.[51] When the C=O group is directly coordinated to the cation, the shift of C=O stretching band depends on the strength of the bond, as the degree of covalency of this bond increases,this band appears at a lower frequency.[10,50] This in agreement with findings of Deng *et al,*[22] who studied the interactions between polyacrylamide and clay using FT-IR. They concluded that the most likely interactions taking place between the C=O groups of the amide and the water molecules surrounding the exchangeable cations leading to shifts of FT-IR bands to lower wavelengths.

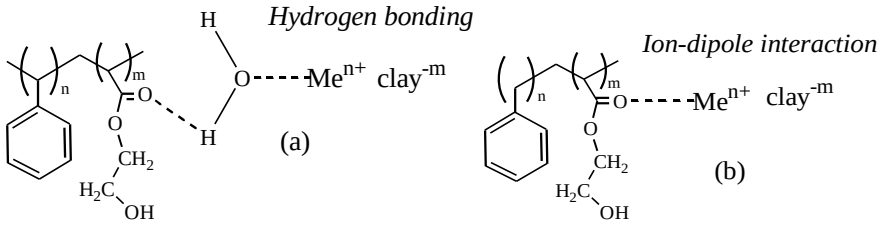

Scheme 5.3: Interaction between PS-b-PHEA and clay via (a) hydrogen bonding between carbonyl groups of PS-b-PHEA and the exchangeable cations through water molecules, and (b) directly via ion-dipole interaction

The band at 1385 cm^{-1} is related to C=C stretching of styrene aromatic groups. The FT-IR spectrum of pure PS-b-PHEA exhibited a strong OH band at 3400 cm^{-1}. This band shifted to a lower wavelength 3300 cm^{-1} in the FT-IR spectrum of (PS-b-PHEA)-MMT and also became broader. This is related to formation of hydrogen bonds between the OH of PS-b-PHEA and the oxygen of the water molecules surrounded the exchangeable cations onto clay galleries as seen in Scheme 5.4, this is in accordance with the findings of Greenland *et al.* [23] who suggested that the hydroxyl groups of PVOH bonded to the exchangeable cations through the water molecules.

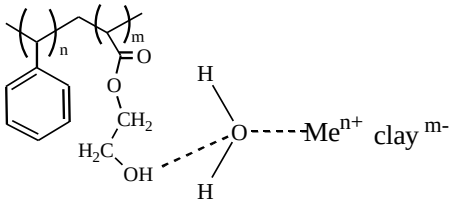

Scheme 5.4: Interaction of PS-b-PHEA and clay via hydrogen bonding between the hydroxyl groups of PS-b-PHEAand water inside the clay galleries.

The presence of hydroxyl groups on the clay'sedgesoffer other possible interaction between the copolymer and the clay surface, via formation of hydrogen bonding between the carbonyl of the ester groups of the copolymer chains and the hydroxyl groups on the clay's edges as seen in the Scheme 4.5. Compounds containing C=O groups, such as aldehydes, ketones, carboxlic acids, esters, polyacrylamide and polyacrylates etc. behave similarly when adsorbed onto swelling clay minerals.[10,50]

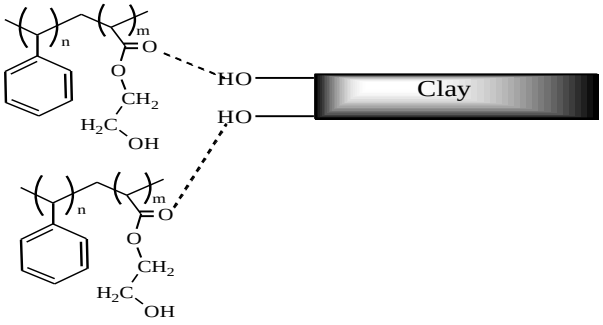

Scheme 5.6: Interaction of PS-b-PHEA and clay via hydrogen bonding between hydroxyl groups of PS-b-PHEA, and hydroxyl groups on the clay's edges.

Table 5.3 shows that, the band belonging to C-O-C of PS-b-PHEA at 1203 cm^{-1}underwent 30 cm^{-1} shift up after the adsorption of PS-b-PHEA into clay.This is most likely caused by two kinds of interactions between HEA segments and the exchangeable cations: (1) PS-b-PHEA forms hydrogen bonds with water molecules in the hydration shell of exchangeable cations (Scheme 5.7 a) or (2) PS-b-PHEA directly bonds to the exchangeable cations through ion-dipole interactions or coordination (Fig 5.7 b), these types of interaction were reported by Deng *et al.*[48] who studied the bonding mechanism of PEO into clay using FT-IR.

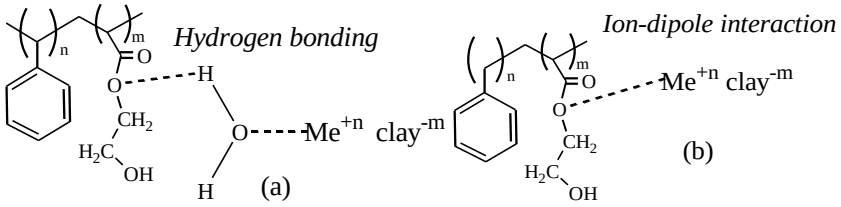

Scheme 5.7 Two possible bonding mechanisms between PS-b-PHEA and MMT: (a) Water bridge: oxygen atoms of PS-b-PHEA forms hydrogen bonding with water in the hydration shell of exchangeable cations (b) direct ion-dipole interaction between the oxygen atoms of PS-b-PHEA and exchangeable cations.

The absence of other new bands that were expected to be seen in FT-IR spectra of (PS-b-PHEA)-MMT is due to the complexity of the FT-IR spectrum of the clay itself, overlapping with the FT-IR bands of PS-b-PHEA. However, the appearance of the new bands in the FT-IR spectrum of (PS-b-PHEA)-MMT relative to the virgin clay is a qualitative indication that the interaction between PS-b-PHEA molecules and clay was successful by both ways: ion-exchange and the adsorption mechanism.

5.3.4.2 Amounts of (PS-b-PHEA)-cationic inside clay

TGA was used to determine the amount of (PS-b-PHEA)-cationic successfully incorporated into the clay, Fig 5.16 shows the TGA thermograms of unmodified clay and (PS-b-PHEA)-MMT prepared at different (PS-b-PHEA)-cationic concentrations, MMT was also modified using (PS-b-PHEA)-I using 100% CEC (PS-b-PHEA)-I. The TGA curve for the pure copolymer showed a weight loss at 100 ºC. This is due to the loss of

water absorbed by PS-b-PHEA, which has high capacity for water uptake, as reported elsewhere.[52,53]

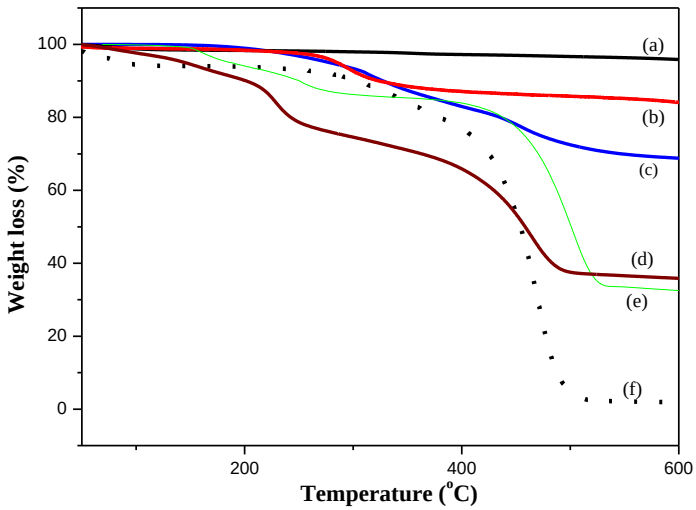

Fig. 5.16: TGA thermograms of (a) pristine MMT, and MMT modified using (PS-b-PHEA)-cationicin different concentrations: (b) 25% CEC, (c) 50% CEC, (d) 100% CEC, (e) is MMT modified by (PS-b-PHEA)-I, and (f) pure PS-b-PHEA.

The difference in the residual weight loss between unmodified clay and (PS-b-PHEA)-MMT indicates that the PS-b-PHEA was successfully incorporated with clay surface, as FT-IR results did indicate. The amount of (PS-b-PHEA) incorporated into clay tabled in table 5.5.

Table 5.5: Initial PS-b-PHEA concentrations and the quantities of PS-b-PHEA inside clay galleries as determined by TGA

Initial concentration of PS-b-PHEA -cationic		Weigh loss at 600 °C	Quantities of PS-b-PHEA in clay galleries		
Rel. to CEC of clay [a] (%)	Feed mass (g)		Mass [b] %	Exp mass (g)	Exp % CEC
Pure clay	0	4.02	0	0	0
25%	1.50	22.17	18.17	0.27	4.50
50%	3.01	33.13	29.11	1.57	26.35
100%	6.02	70.41	66.37	3.97	65.55
(PS-b-PHEA)-I (100% CEC)	6.02	65.64	61.62	3.68	60.85

[a] Relative to cation exchange capacity of clay

[b]Percentages of (PS-b-PHEA)adsorbed onto clay

The quantities of PS-b-PHEA incorporated into clay were determined from the difference in the weight loss found between unmodified clay and PS-b-PHEA at 600 °C. The weight loss of MMT is due to the loss of chemisorbed water.[35] The weight loss measured for (PS-b-PHEA)-MMT is due to the decomposition of PS-b-PHEA and adsorbed water in the clay. Three different PS-b-PHEA concentrations were used (25%, 50% and 100% CEC), and as was expected, the amount of PS-b-PHEA incorporated into clay increased with the initial amount of PS-b-PHEA. In general all (PS-b-PHEA)-MMT samples decomposed in a similar fashion. At temperature between 220 and 520 ºC the organic constituent (PS-b-PHEA) into MMT decomposes.

According to the results shown in Fig 5.16(e) and Table 5.5, (PS-b-PHEA)-I was also had strongly incorporated within MMT galleries via adsorption process by creation of hydrogen bonding and ion-dipole interaction confirmed by the FT-IR results.

It should noted that,although PS-cationic and (PS-b-PHEA)-cationic does undoubtedly interact with the clay surface via ion exchange reaction,the mol% (relative to CEC) of (PS-b-PHEA)-cationicincorporated into the clay galleries was found to be greater than the amount of PS-cationic. This is due to the more hydrophilic character of (PS-b-PHEA)-cationic relative to PS-cationic, allowing (PS-b-PHEA) to stronger interaction with clay from different functional groups such as the ester groups and hydroxyls groups and ether groups, via hydrogen bonding and ion-dipole interactions respectively, as well as via ion-exchange. The complete ion-exchange was never obtained; this is also due to bulkiness of the oligomeric (PS-b-PHEA)-cationic copolymer.

5.3.4.3 Study of *d*-spacing of (PS-b-PHEA)-MMT by SAXS

SAXS measurements allow monitoring the changes in the basal spacing of clay, as the organic molecules insert inside the clay galleries. The *d*-spacing (interlayer distance) of clay was calculated as described in Section 5.2.2.Fig. 5.17 shows the SAXS patterns of unmodified clay, and clay modified with (PS-b-PHEA)-I and (PS-b-PHEA)-cationic.

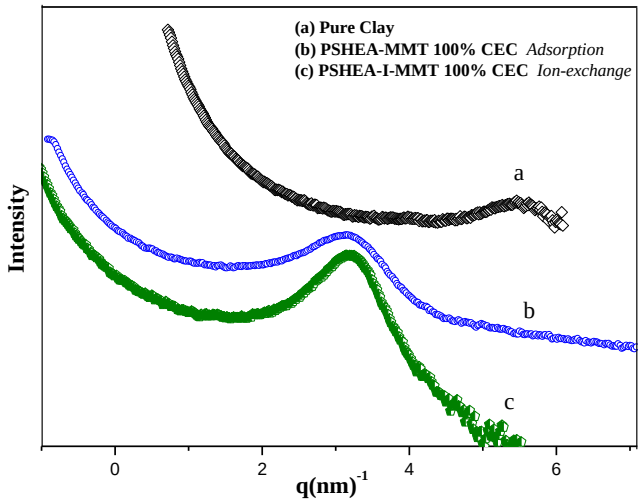

Fig. 5.17: SAXS patterns of (a) neat MMT,(b)(PS-b-PHEA)-MMT using 100% CEC (PS-b-PHEA)-I, and (c) (PS-b-PHEA)-MMT using 100% CEC (PS-b-PHEA)-cationic.

Fig 5.16 shows that the SAXS diffraction peak position of modified clay shifted towards lower (q) values (i.e. high interlayer distance, as calculated using Bragg's law) when compared to pristine clay.

The significant increases in the *d*spacing of modified clay in Fig. 5.17 (b) relative to that for pure clay in Fig. 5.17 (a), indicated that the (PS-b-PHEA)-I molecules wereundoubtedly inserted inside the clay galleries,and were not just adsorbed on the external surface.[33](PS-b-PHEA)-I could interact with the exchangeable cations as well through the water molecules via ion-dipole interaction, the increases of *d*-spacing of MMT was reported of for several non-cationic polymers that adsorbed into MMT, such as PVOH,[23] PAM[22] and PEO.[48] Interaction between C-O-C groups and exchangeable cations via hydrogen bonding with water bridge or directly via ion dipole interaction with exchangeable cations, increases the *d*-spacing, as was confirmed by Deng *et al.*[48] who studied the adsorption of PEO using SAXS. The *d*spacing of modified clay using (PS-b-PHEA)-cationic in Fig. 5.17 was also increased due to both processes: the ion-exchange and adsorption of (PS-b-PHEA) molecules inside clay galleries.

(PS-b-PHEA)-MMT shows a relatively broad diffraction peak due the heterogeneity of the PS-b-PHEA chains packing, with relatively undefined *d*-spacing.[47] It is known that during the adsorption processes the organic molecules replace water and became coordinated to cations or occupy sites in a second sphere of coordination around the cations, being bonded to cations through bridging water molecules[10]. However, PS-b-PHEA is an amphiphilic polymer and has a high capacity for water uptake; therefore during the adsorption processes the water molecules remained on the clay galleries and are not expulsed by PS-b-PHEA, hence this could increase the heterogeneity of molecules inside clay galleries.

The diffraction peak of (PS-b-PHEA)-MMT prepared using (PS-b-PHEA)-cationic appears less broad than when prepared using (PS-b-PHEA)-I. This indicates that the terminal quaternary ammonium cationic group born by (PS-b-PHEA)-cationic, allows a more regular packing of the PS-b-PHEA oligomeric copolymer chains. This effect is likely to be driven by the additional capability of (PS-b-PHEA)-cationic to interact with the clay surface via ion exchange.

5.4 Conclusions

This study showed for the first time, the modification of MMT using polymer (PS) and amphiphilic oligomeric block copolymer (PS-b-PHEA) which were prepared by the "RITP" controlled/living polymerization method.

PS-cationic was synthesized by a simple reaction between PS-I and DMEA. Analysis by FT-IR, ^{1}H-NMR and MALDI-TOF indicated the replacement of iodine from the PS end chains by a quaternary ammonium group. PS-cationic was successfully used for MMT surface modification, performed in THF, as was confirmed by SAXS, TGA, and FT-IR analysis. The attachment between PS-cationic and clay was strongly dependent on the polarity of the modification medium, the modification of clay by PS-cationic was only successful in polar medium,and it was unsuccessful in non-polar solvent.

(PS-b-PHEA)-cationic was also obtained by reaction of (PS-b-PHEA)-I with TEA. The interaction of (PS-b-PHEA)-cationic with claywas found to be occurring via both ion-

exchange process and adsorption. (PS-b-PHEA)-cationic can adsorbed onto the surface of clay galleries in several ways: by formation of H-bonding, Van der Waals forces, and ion exchange. These interactions lead to an increase in the basal spacing relative to pristine MMT (1.14 nm for virgin MMT up to 2.09 nm for modified clay).

5.5References

1. Paiva, L.; Morales, A.; Diaz, F. *Applied Clay Science* **2008,** 42, 8-24.

2. Jordan, J. W. *Physical and Colloid Chemistry* **1949,** 53, 294-306.

3. Ray, S.; Okamoto, M. *Progress in Polymer Science* **2003,** 28, 1539-1641.

4. Nalwa, H. S., Polymer/clay Nanocomposites. In *Encyclopedia of Nanoscience and Nanotechnology*, American Scientific Publishers: California, 2004; Vol. 8, pp 791-843.

5. Alexandre, M.; Dubois, P. *Materials Science and Engineering: A* **2000,** 28, 1-63.

6. Lebaron, P. C.; Wang, Z.; Pinnavaia, T. J. *Applied Clay Science* **1999,** 15, 11-29.

7. Okamoto, M. *Rapra Review Reports* **2003,** 14, 1-40.

8. Morgan, A. B.; Gilman, J. W. *Journal of Applied Polymer Science* **2003,** 87, 1329-1338.

9. Choi, Y. S.; Xu, M.; Chung, I. J. *Polymer* **2003,** 44, 6989-6994.

10. Yariv, S.; Cross, H., Organo-Clay Complexes and Interactions. In Marcel Dekker, Inc: New York and Basel, 2002; pp 1-101.

11. Fischer, H. *Materials Science and Engineering A* **2003,** 23, 763-772.

12. Choi, Y. S.; Ham, H. T.; Chung, I. J. *Polymer* **2003,** 44, 8147-8154.

13. Huskic, M.; Zagar, E.; Zigon, M.; Brnardic, I.; Macan, J.; Ivankovic, M. *Applied Clay Science* **2009,** 43, 420-424.

14. Yoon, K.; Sung, H.; Hwang, Y.; Noh, S.; Lee, D. *Applied Clay Science* **2007,** 38, 1-8.

15. Breen, C. *Applied Clay Science* **1999,** 15, 187-219

16. Su, S.; Jiang, D.; Wilkie, C. *Polymer Degradation and Stability* **2004,** 83, 333-346.

17. Zhang, J.; Jiang, D.; Wang, D.; Wilkie, C. *Polymer Degradation and stability* **2006,** 91, 2665-2674.

18. Su, S.; Jiang, D.; Wilkie, C. *Polymer Degradation and Stability* **2004,** 84, 279-288.

19. Zhang, J.; Jiang, D.; Wilkie, C. *Thermochimica Acta* **2005,** 430, 107-113.

20. Nasser, A.; Gal, M.; Gerstl, Z.; Mingelgrin, U.; Yariv, S. *Journal of Thermal Analysis and Calorimetry* **1997,** 50 257 - 268

21. Grim, R. E., *Applied Clay Mineralogy*. McGraw-Hill: New York. Toronto . London, 1962; p 312-422.

22. Deng, Y.; Dixon, J. B.; White, G. N.; Loeppert, R. H.; Juo, A. S. R. *Colloids and Surfaces A: Physicochemical and Engineering Aspects* **2006,** 281, 82-91.

23. Greenland, D. *Journal of Colloid Science* **1963,** 18, 647-664.

24. Huskic, M.; Brnardic, I.; Zigon, M.; Ivankovic, M. *Journal of Non-Crystalline Solids* **2008,** 354, 3326-3331

25. Zhang, J.; Manias, E.; Wilkie, C. *Journal of Nanoscience and Nanotechnology* **2008,** 8, 1567-1615.

26. Save, M.; Manguian, M.; Chassenieux, C.; Charleux, B. *Macromolecules* **2005,** 38, 280-289.

27. Lacroix-Desmazes, P.; Severac, R.; Boutevin, B. *Polymeric Preprints* **2003,** 44, 683-684.

28. Pavia, D.; Lampman, C.; Kriz, G., *Introduction to Spectroscopy* Thomson Learning, Inc: New York 2001; p 1-203.

29. Pigorsch, E. *Starch* **2009,** 61, 129-138.

30. Barner-Kowollik, C.; Davis, P.; Stenzel, H. *Polymer* **2004,** 45, 7791-7799.

31. Ladaviere, C.; Lacroix-Desmazes, P.; Delolme, F. *Macromolecules* **2009,** 42, 70-84.

32. Xu, M.; Choi, Y. S.; Kim, Y. K.; Wang, K. H.; Chung, I. J. *Polymer* **2003,** 44, 6387-6395.

33. He, H.; Duchet, J.; Galy, J.; Gerard, J. *Journal of Colloid and Interface Science* **2006,** 295, 202-208.

34. Zheng, H.; Zhang, Y.; Peng, Z. *Journal of Applied Polymer Science* **2004,** 92, 638-646.

35. Xi, Y.; Martens, W.; He, H.; Frost, R. L. *Journal of Thermal Analysis and Calorimetry* **2005,** 81, 91-97.

36. Biasci, L.; Aglietto, M.; Ruggeri, G.; Ciardelli, F. *Polymer* **1994,** 35, 3296-3304.

37. Fornes, T. D.; Hunter, D. L.; Paul, D. R. *Macromolecules* **2004,** 37, 1793-1798.

38. Qutubuddin, S.; Fu, X. *Polymer* **2001,** 42, 807-813.

39. Kawasami, M.; Hasegawa, N.; M. Kato; Usuki, A.; Okada, A. *Macromolecules* **1997,** 30, 6333-6338.

40. Samakande, A.; Hartmann, P. C.; Cloete, V.; Sanderson, R. D. *Polymer* **2007,** 48, 1490-1499.

41. Xu, M.; Choi, Y. S.; Kim, Y. K.; Wang, K. H.; Chung, I. J. *Polymer* **2003,** 44, 6387-6395.

42. Amarasinghe, P.; Katti, K. S.; Katti, D. R. *Journal of Colloid and Interface Science* **2009,** 337, 97-105.

43. Choi, Y. S.; Ham, H. T.; Chung, J. *Chemistry of Materials* **2004,** 16, 2522-2529.

44. Yermiyahu, Z.; Lapides, I.; Yariv, S. *Applied Clay Science* **2005,** 30, 33-41.

45. Badran, A.; Youssef, A.; El-Hakim, A. A. *Polymer Bulletin* **2004,** 53, 9-17.

46. Vaia, R. A.; Teukolsky, R. K.; Giannelis, E. P. *Chemistry of Materials* **1994,** 6, 1017-1022.

47. Lee, S. Y.; Kim, S. J. *Journal of Colloid and Interface Science* **2002,** 248, 231-238.

48. Deng, Y.; Dixon, J.; White, G. *Colloid Polymer Science* **2006,** 284, 347-356.

49. Baines, F.; Dionisio, S.; Billingham, N. C.; Armes, S. *Macromolecules* **1996,** 29, 3096-3102.

50. Yariv, S. *Thermochimica Acta* **1996,** 274, 1-35.

51. Tahoun, S. A. *United Arab Republic Journal of Chemistry* **1971,** 14, 123-132.

52. Vargun, E.; Usanmaz, A. *Journal of Polymer Science Part A: Polymer Chemistry* **2005,** 43, 3957-3965.

53. Bouzouia, F.; Diamoum, S. *Journal of Applied Polymer Science* **2008,** 110, 3574-3581.

Chapter 6

Preparation of PS-Clay Nanocomposites via Dispersion Polymerization Using PS-MMT as Stabilizer

Abstract:

This study describes the preparation of PS-clay nanocomposite colloidal particles via free-radical polymerization in dispersion. Montmorillonite clay (MMT) was pre-modified using different concentrations of PS-cationic so that the effect of the degree of modification on the morphology of colloidal PS particles could be studied. The morphology of PS-nanocomposite latexes was strongly affected by the degree of clay modification. The clay platelets were encapsulated inside PS latex only when the clay surface became highly hydrophobic. The morphology of PS-nanocomposites was found to range from partially exfoliated to intercalated depending on the percentage of clay loading. The impact of PS-MMT concentration on the monomer conversion, the polymer molecular weight, the thermal stability and the thermo-mechanical properties of the final PS-nanocomposites were determined.

Chapter 6

Preparation of PS-Clay Nanocomposites via Dispersion Polymerization Using PS-MMT as Stabilizer

6.1 Introduction

Over the past two decades polymer-clay nanocomposites (PCNs) have emerged as attractive engineering materials due to their unique properties and broad range of application.[1-3] Montmorillonite (MMT) and other clays are naturally hydrophilic, which makes them poorly suited for mixing and interacting with most polymers. Moreover, the stacks of clay platelets are held tightly together by electrostatic forces which further hinder penetration of monomers or polymer into the clay galleries. Hydrated cations present at the surface of clay platelets can be replaced by organic cations, thus making the clay more organophilic , and hence compatible with non polar species, including synthetic polymer matrix.[1,4-6]

PCNs may be prepared using various processes, e.g template synthesis, melt intercalation, and in situ intercalative polymerization.[7] In situ intercalative polymerization has been successfully performed by polymerization in suspension,[8] in solution,[8] in bulk,[9] in emulsion[10,11] and in dispersion polymerization.[12-14]

An increasing number of recent research report on achieving a dispersion of inorganic nanoparticle inside polymer latex particles using in situ intercalative polymerization in heterogeneous media.[15-20]This technique of polymer encapsulation is becoming more and more popular since polymer-encapsulated particles offer very interesting potential applications, such as adhesives, textiles coating, optics and electronics.[18,21] Hydrophobic nanoparticles can usually disperse in the monomer phase without any former treatment, as described for the polystyrene (PS) encapsulation of organic phthalocyanine blue pigments,[22] or carbon-black particles.[23,24] On the other hand, in order to encapsulate

hydrophilic inorganic particles within hydrophobic polymer matrix, the hydrophobization of the inorganic particles by surface treatment is necessary, prior they can be used in the process.[14] Although the encapsulation of inorganic particles has been extensively studied, most inorganic particles used were spherical with a narrow size distribution.[15] It is well known that clay particles have a platy morphology with a broad size distribution, resulting in more difficulties in the dispersion and the encapsulation of these particles in monomer droplets hence in the final polymer latex particles.[17]

Several researchers have attempted to synthesize polymer encapsulated clay nanocomposites via suspension, emulsion or miniemulsion polymerization.[17,25]Huang and Brittain[26] synthesized poly(methyl methacrylate) (PMMA) layered silicate nanocomposites by suspension polymerization and emulsion polymerization. They simply mixed unmodified clay into the aqueous phase prior mixing it with water-based polymer latex. The nanoclay particles were not encapsulated and the final suspension was reported as poorly stabilized. Negrete- Herrera *et al.*[27] synthesized water-based PCNlatexesby first chemically modifying laponite clay minerals using silane agents (methacryloxy propyl mono-, di-and trimethylethoxysilane) before the polymerization and then proceededwith seeded emulsion polymerization. However, the stabilityof the final latex was not reported. Samakande *et al.*[28] encapsulated clay particles inside a PS latex via RAFT mediated miniemulsion polymerization. The clay was pre-modified using cationic RAFT agents via a simple ion-exchange reaction, and then the miniemulsion polymerization was carried out. A stable latex with narrow PS particle size distribution was obtained.

Besides emulsion and miniemulsion polymerization, dispersion polymerization has also been used for the encapsulation of inorganic materials in polymer particles.[14,29] Dispersion polymerization also leads to composite particles dispersed in the polymerization medium, however, the main difference between dispersion polymerization and other heterophase polymerization method is the nature of the dispersion medium which is usually a mixture of water and an aliphatic alcohol.[30] Such a dispersion medium is selected in order to allow both monomer and initiator to be soluble,

where the forming polymer is insoluble, hence precipitates in a controlled manner.[31,32] This type of polymerization has already been used to encapsulate organic particles inside polymer latexes as reported by Bourgeat-Lami *et al.*[14] They found that the encapsulation of silica particles by PS could be achieved in dispersion polymerization with the aid of a coupling agent chemically attached onto the surface of the silica particles.

Earlier, in Chapter 3 the preparation of PS-nanocomposites by conventional dispersion polymerization was described. The clay was surface modified by an organo silane compound before use in the polymerization. The nanoclay particles were not encapsulated inside the polymer latex and the final latex was not stable.[12]As dispersion polymerization is a simple and fast method that allows the preparation of monodisperse polymer particles of a sizerange of (1-20 µm)[33,34] it could potentially be suitable for the encapsulation of large particles such as MMT.

For the preparation of PS-nanocomposites via dispersion polymerization described in this chapter, the clay particles were first modified using low molecular weight PS (M_n = 7100 g/mol) bearing quaternary ammonium end groups (PS-cationic). The subsequent modified PS-MMT was then used as a stabilizer in the polymerization of styrene in dispersion. Various degrees of surface modification were evaluated in terms of the ability of the modified clay to stabilize the dispersion polymerization. Prior to polymerization, the clay surface was modified with 25%, 65% and 100 % CEC of clay. The effects of clay hydrophobicity on the morphologies and stability of PCNs dispersion were subsequently evaluated. Morphology, thermal stability and thermo-mechanical properties of the PCNs materials were studied after film formation.

6.2 Experimental

6.2.1 Materials

Styrene (99% Aldrich) was purified by washing three times with a 3% potassium hydroxide aqueous solution, followed by distillation at 40 °C under reduced pressure. The initiator 2, 2-azo-bis-isobutyronitrile (AIBN) was obtained from Aldrich and re-crystallized from methanol before use. PS-MMT was prepared according to the

procedures described in Section 5.2.4. Deionized water was obtained from a Millipore Milli-Q-purification water system. Hydroxypropyl cellulose (HPC) was purchased from Aldrich and used as received.

6.2.2 Typical preparation of PS-nanocomposite latexes via dispersion polymerization using PS-MMT

A typical polymerization formulation is depicted in Table 1. The amount of PS-cationic used for surface modification of MMT, were 25%, 65% and 100% relative to the cation exchange capacity (CEC) of clay. PS-MMT (0.5g) was dispersed in 1mL of THF. After stirring for 10 min, the solution was added to the dispersion medium containing ethanol and water (85:15). HPC (0.015 g) was dissolved in ethanol (5 mL) and added to the above dispersion. The monomer phase was prepared by dissolving AIBN (0.004 g) in styrene monomer (10 g), and then purging with nitrogen for 20 min. The solution of PS-MMT/dispersion medium was first charged into the reactor, and then purged with nitrogen gas for 20 min. The reaction mixture was then heated to 75°C under continuous stirring, followed by the addition of the monomer phase all at once. Polymerization was carried out for 8 h. The reactor was then cooled down by immersion in an ice bath for 10 min. Small samples were regularly withdraws throughout the polymerization, with a syringe for analysis purposes.

Table 6.1: Formulations used for the preparation of PS-nanocomposites

Styrene	Clay		PS-cationic	
Mass (g)	Percentage clay relative to monomer (%)	Mass (g)	Percentage modification relative to CEC	Mass (g)
10	5	0.5	25	0.82
10	5	0.5	65	2.13
10	5	0.5	100	3.30
10	1	0.1	100	0.65
10	3	0.3	100	1.97
10	7	0.7	100	4.61
10	10	1	100	7.66

6.2.3 Characterizations

6.2.3.1 Small angle X-ray scattering (SAXS)

Small angle X-ray diffraction (SAXS) measurements were performed in a transmission configuration at 298 K. A copper rotating anode X-ray source (functioning at 4 kW), with a multilayer focusing Osmic monochromator giving high flux (10^8 photons/sec) and punctual collimation, was used. An image plate 2D detector was used. Scattering patterns were obtained, giving diffracted intensity as a function of the wave vector *q*. The calculation of the *q* values is described elsewhere.[35]

6.2.3.2 Transmission electron microscopy (TEM)

TEM was used to visualize the morphology of the clay particles in PS-clay nanocomposites at the nanometer level. Bright field TEM images were recorded using a LEO 912 transmission electron microscope, at an accelerating voltage of 120 kV. Prior to analysis the PS latex samples were dried, embedded in epoxy resin and cured for 24 h at

60 ºC. The embedded samples were then ultramicrotomed with a diamond knife on a Reichert Ultracut S ultra microtome at room temperature. This resulted in sections with a nominal thickness of ~100 nm. The sections were transferred from water at room temperature to 300-mesh copper grids, which were then transferred to the TEM apparatus.

TEM was also used to characterize the morphology of polymer latexes the samples were appropriately diluted to a concentration of $2.4x10^{-3}$ g/L before being applied to a carbon coated copper grid for TEM analysis.

6.2.3.3 Dynamic light scattering (DLS)

DLS was used to determine the particle size and particle size distribution of the latexes. Latex samples were prepared by diluting a few droplets of latex in deionized water. DLS measurements were carried out at 25 ºC on a Malvern-Nano instrument (Malvern instruments,USA) of 90º angle. The instrument was calibrated using nanosphere-size standards of polymer microsphereres in water, with a mean diameter of 60 nm.

6.2.3.4 Thermogravimetric analysis (TGA)

TGA was carried out using a TGA-50 SHIMADZU thermogravimetric instrument, with a TA-50 WSI thermal analyzer. Samples (10-15 mg) were degraded in a nitrogen atmosphere, using a flow rate of 50 mL/min and a heating rate of 20 °C/min.

6.2.3.5 Dynamic mechanical analysis (DMA)

Thermo-mechanical properties of PCNs were determined using a Physica MCR 501 apparatus (Anton Paar, Germany). Parallel-plate geometry (diameter 25 mm) was used, with a 1mm gap and a constant deformation strain of 0.1% and oscillation frequency of 1Hz. Measurements were from 145 ºC to - 25 °C, at cooling rate of -5 ºC/min, with a constant normal force of 5 N.

6.3 Results and discussion

6.3.1 Characterization of morphology and stability of PS-nanocomposites latexes

6.3.1.1 Conversions and particle sizes

Dispersion polymerization of styrene was carried out in the presence of PS-MMT, MMT was modified using different concentrations of PS-cationic (25%, 65% and 100% CEC respectively). Fig. 6.1 shows the conversion-time plots for the polymerization of styrene in dispersion polymerization with and without PS-MMT.

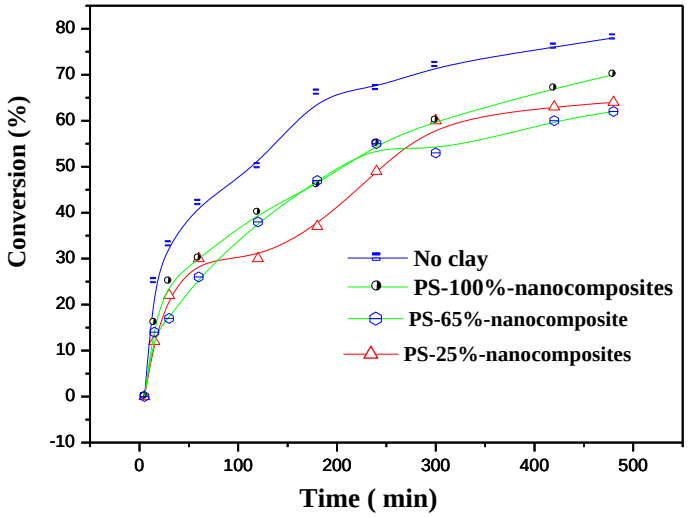

Fig 6.1: Plots of conversion versus time for PS-nanocomposites prepared.

The effect of the presence of inorganic particles on the polymerization rate and conversion has been reported in the literature.[36-38] In the general case, the addition of inorganic particles, such as SiO_2, TiO_2, $CaCO_3$ and Ag will reduce both the monomer conversion and propagation rate both in emulsion and suspension polymerizations.[39,40] Similar results were obtained in this study, the final conversions after 8 h of polymerization without and with 5wt% clay being 80% and 65%, respectively. It is believed that the reactivity of radicals and living polymers is lower in the presence of clay particles because of the adsorption of these living species onto the large nanoclay

surface.[38] This was also proven by Tong *et al.* [36] when they studied the kinetics of miniemulsion polymerization of styrene in the presence of organoclays, and found that the presence of organoclays in the polymerization medium increased the viscosity, thus lowered the reactivity of radicals and living polymer.

It was also found that the average particle size of the final dispersion measured by DLS, slightly decreased with the addition of clay, as seen in Fig. 6.2. As described earlier in Section 3.3.2 the presence of clay platelets in a polymerization system significantly affects the particle size of the final PS latex. Here it is also interesting to determine the effect of degree of clay modification on the particle size of the PS latex. Fig. 6.2 shows the effect of an increasing in the clay loading decreases on the particle sizes.

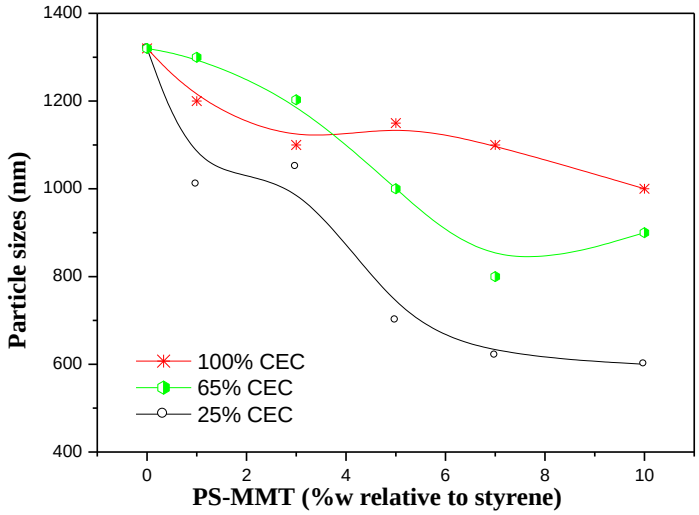

Fig 6.2 Particle sizes of PS-nanocomposites as a function of clay loading.

The average particle sizes of all the PS-nanocomposites synthesized were found to be decreased when the clay loading increases. However, the particle sizes of PS-nanocomposites prepared using clay modified with 25% and 65% PS-cationic decreased to greater extent than those of PS-nanocomposites prepared with 100% PS-cationic. A possible reason is the following: PS-MMT prepared using only 25% and 65% CEC gives the clay an amphiphilic character, with un-modified hydrophilic areas and modified hydrophobic patches, favoring the ability of partially modified PS-MMT to locate at the

surface of the PS particles. This seems lead to an enhanced degree of particles stabilization via Pickering stabilization, limiting the aggregation phenomena as the polymerization takes place. Similar results were reported by Yang *et al.*[41] who used PS and poly(2-(dimethyamino)ethyl methacrylate) (PS-PDMAEMA/clay) in Pickering suspension polymerization to produce PS latexes. The average PS particles size was also found to be decreasing with increasing the amount of PS-PDMAEMA/clay. Zhao and Samulski[13] also observed a similar effect of clay loadings on the particle size of PMMA prepared via dispersion polymerization in supercritical CO_2.

6.3.1.2 Morphology of PCNs latexes

TEM image of the PS-nanocomposites dispersion prepared in the presence of 5 wt% pristine clay is shown in Fig. 6.3 (a). The clay particles were found to be separated from the polymer latexes, and the clay was found to be aggregated in the water phase. The dispersion obtained after polymerization was unstable and phase separation occurred upon centrifugation at 5000 rpmfor 30 min (c.f. Fig. 6.3 b).

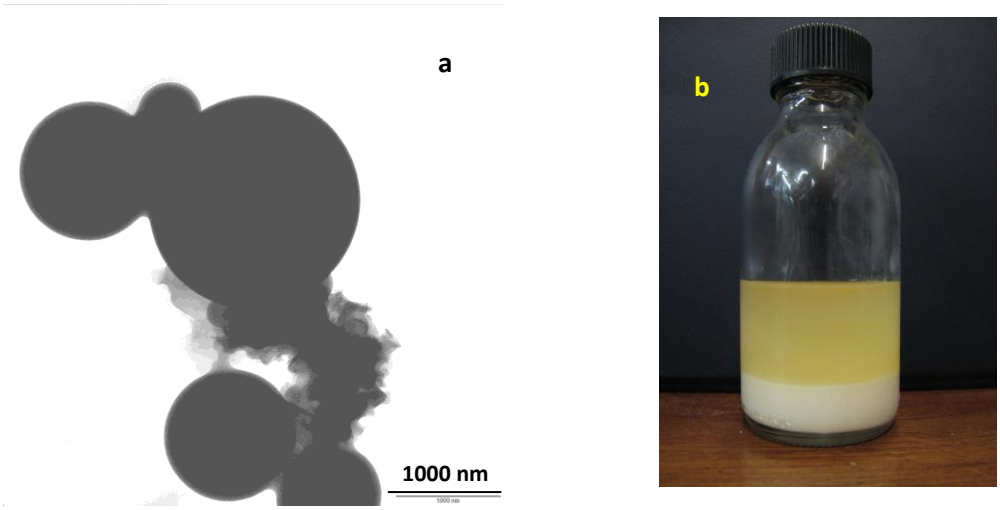

Fig. 6.3: TEM image of PS-nanocomposites prepared using 5 wt% unmodified clay (a), and photograph of PS-nanocomposites latex prepared using 5 wt% unmodified clay (b) (after centrifugation).

The particle size determined by DLS analysis was further confirmed by TEM analysis (Fig. 6.3). However, the particle sizes of the same PS latexes as measured by TEM were found to be slightly smaller than when determined by DLS. This is attributed to the different modes of analysis, although the same trends were obtained with both methods.

Fig. 6.4 (a, c) shows TEM images for PS-nanocomposites prepared using PS-25%-MMT and PS-65%-MMT, respectively. As expected, clay platelets were found to be located at the surface of the PS particles as indicated by the arrowhead in Fig. 6.4 (a). A partial surface modification of the clay surface yields organoclays with a moderate degree of hydrophobicity compared to when fully surface-modified. The resulting amphiphilic character of the partially modified clay constitutes a driving force to its adsorption onto the polymer particles as they form. The final PS latex however remained poorly stable as seen in Fig. 6.4 (b, d), due to an insufficient colloidal stability afforded by the partially modified PS-MMT organoclay that adsorbed onto the particles.

It is interesting to compare morphologies of particles prepared in the present study with those obtained by other researchers. Wu *et al*[42] prepared PS colloidal particles in suspension polymerization stabilized using PS-MMT, with PS brushes only at the edges of clay layers by Atom Transfer Radical Polymerization, ATRP. They observed a similar distribution of their partially modified PS-MMT on the surface of colloid particles. This behaviour was explained as follows: in PS-MMT the clay layers remained hydrophilic whereas PS brushes of the edges were hydrophobic, hence anchoring into the PS particles and leaving the negatively facing the polar dispersion medium.

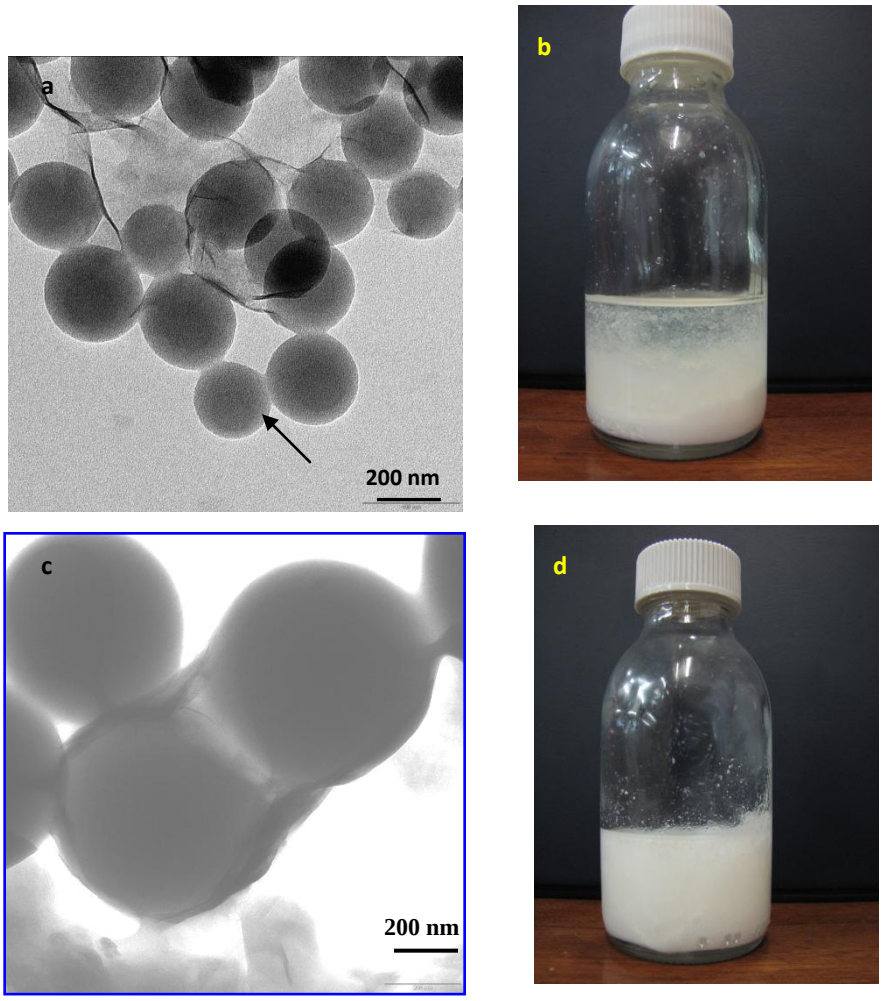

Fig. 6.4: TEM images of PS-nanocomposites latex containing 5 wt% clay loading, clay modified using different concentrations of PS-cationic: (a) 25% CEC and (c) 65% CEC. (b) and (d) are photographs of PS-nanocomposites latexes containing 5 wt% clay loading, clay modified using different concentrations of PS-cationic, respectively.

The thermodynamically driven adsorption of partially modified clay at the interface of multiphasic systems is controlled by its relative affinity for the immiscible phases present, as described by Pickering.[43]

Takahara *et al.* [44] prepared spherical silica particles with different hydrophobicity by surface modification with alkylsilane, and investigated the location of the particles in a mixture of water and oil. They found that the hydrophilic silica particles dispersed only in water due to surface hydroxyl groups. However, after fully reaction with an alkylsilane agent the hydrophobic silica particles dispersed in toluene. Only silica particles with partial modification of the external surface could locate at the interface between water and oil. It is interesting to note that although clay platelets in Fig. 6.4 were found to be located at the PS particles surface, they where however not encapsulated inside the polymer particles.

In order to gain more information about the effect of clay hydrophobicity on the morphology and stability of PS latex prepared via dispersion polymerization, the clay particles were fully pre-modified using PS-cationic at 100% CEC, and then used as stabilizer in dispersion polymerization of styrene. The majority of clay platelets were not visible in the TEM images of the PS latex obtained as illustrated in Fig. 6.5. However, some clay platelets were still remained visible at the surface of the polymer particles as indicated by the arrowhead.

Surprisingly, the final dispersion obtained from polymerization made from the 100% CEC modified clay was found to be stable, as no phase separation was observed (c.f. Fig. 6.5 c) after centrifugation at 4400 rpm for 30 min.

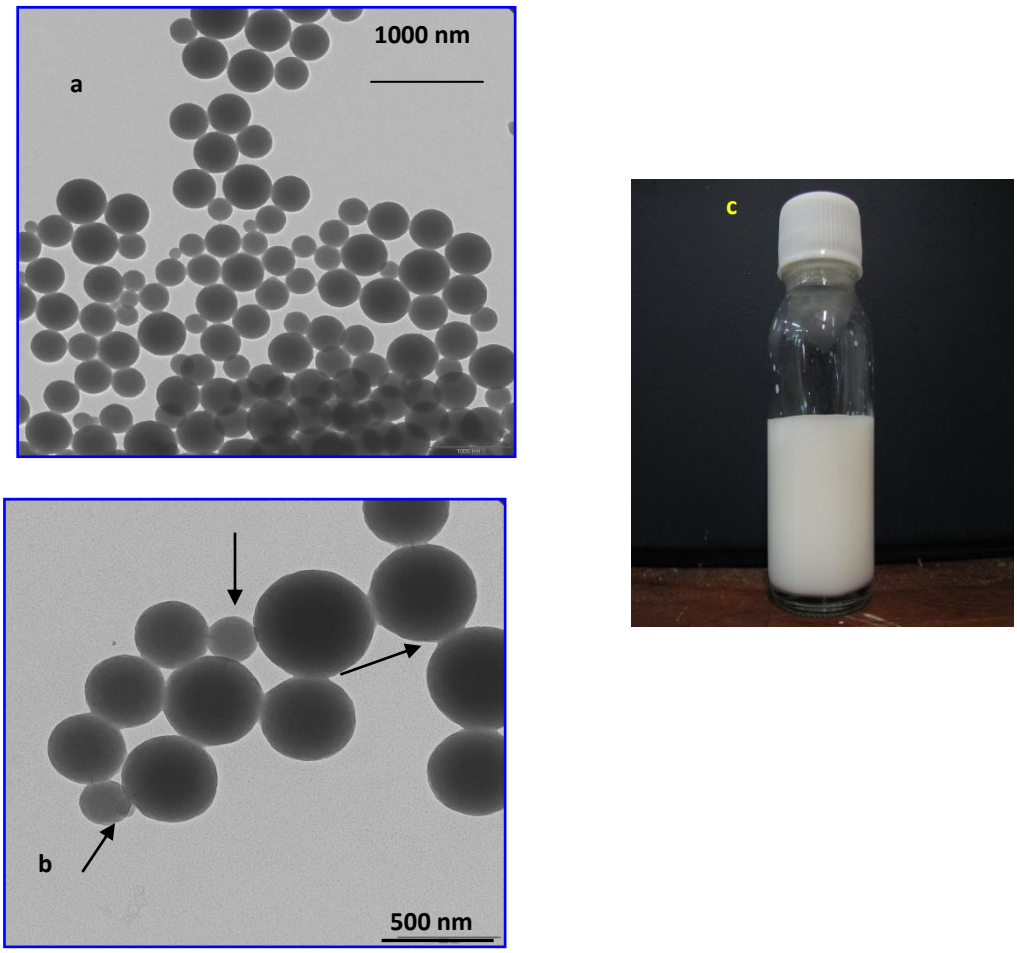

Fig. 6.5: TEM images of PS-nanocomposites latex containing 5 wt% clay loading, clay modified using 100% CEC of clay (a) at low magnification (b) at high magnification. (c) photograph of PS-nanocomposites latexes (after centrifugation)

In this case the PS-MMT clay platelets were highly hydrophobic hence had high affinity for styrene monomer and PS growing chains. As a result, the organoclay was encapsulated into the growing PS particles during the course of the dispersion polymerization. The inability to view by TEM clay nanoparticles embedded into polymer particles when sample are prepared directly from the dispersion medium has commonly been reported.[17,28] However, it is still possible to monitor the PCNs morphology by viewing the clay dispersion state after film formation, from thin slices of epoxy resin embedded pre-casted films.

Bourgeat-Lami and Lang.[14] successfully encapsulated silica particles inside a PS latex via dispersion polymerization; they also found that the success of encapsulation was highly dependent on the nature of the silica particles surface; the successful encapsulation was achieved only when silica was modified using MPTMS, otherwise encapsulation of unmodified silica particles failed to occur.

6.3.2 PS-nanocomposites material morphology and properties

6.3.2.1 The morphology of PCNs prepared via dispersion polymerization

The techniques most commonly used for characterizing of the nanocomposites morphologies are transmission electron microscopy (TEM) and X-ray diffraction (SAXS).

A : TEM analysis

TEM is an excellent qualitative analytical technique to monitor the extent of clay dispersion in a polymer matrix. Dry films of the PCNs material were prepared by removal of the dispersion phase, followed by preparing the dried powder obtained at 120ºC for 24 h. Fig. 6.6 shows TEM images for dried samples (film) of PS-nanocomposites containing 5% clay, clay was modified using different quantities of PS-cationic, 25% and 65% respectively.

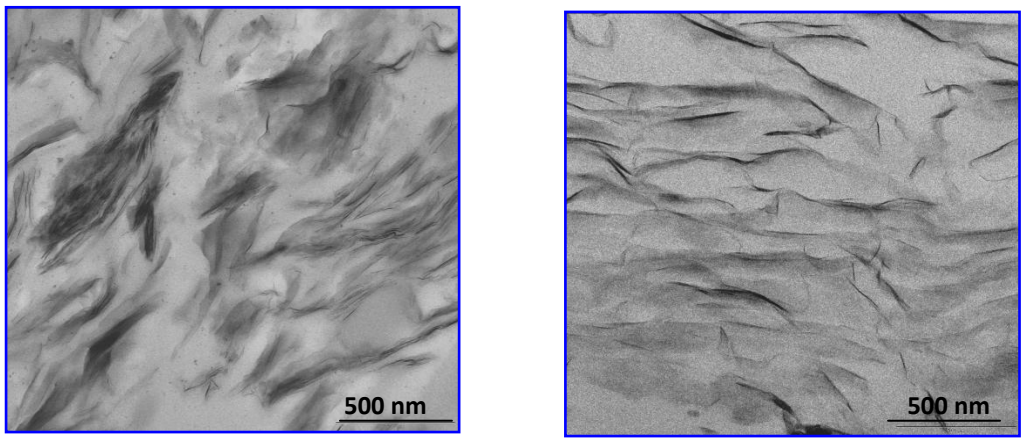

Fig. 6.6: TEM images of PS-nanocomposites containing 5 wt% clay loadings. The clay was modified using 65% (left) and 25% (right) of PS-cationic (mol% relative to clay CEC

Most of the clay platelets observed in TEM images of Fig 6.6 were of intercalated morphology, wherein the silicate layers were still closely packed with each other. Fig. 6.7 shows TEM image of PS-nanocomposites containing 5 wt% clay loadings, where the clay was modified using 100% PS-cationic.

Fig. 6.7: TEM images of PS-nanocomposites containing 5 wt% clay loadings, the clay was modified using 100% CEC

In opposition with the TEM image shown in Fig. 6.5 whereby the clay platelets were not visible, Fig. 6.7 demonstrates that clay particles were indeed embedded inside PS particles during dispersion polymerization process. Some clay layers were still found

closely packed with each other and appear as dark lines, while some individual clay layers were well distributed into the polymer matrix, which is typical of exfoliated/intercalated (i.e. partially exfoliated) structures.

B: SAXS analysis

The intercalation of the polymer chains into the clay galleries lead to an increase in the interlayer spacing relative to the original interlayer spacing relative to unmodified clay, which can be observed by Small Angle X-ray Scattering (SAXS) analysis. Fig 6.8 shows SAXS patterns of PS-nanocomposites prepared by dispersion polymerization using similar amount of PS-MMT (i.e. 5% wt), being modified with various quantities of PS-cationic modifier, 25% and 65% and 100% CEC respectively. The SAXS pattern of unmodified clay is included in the figure as a reference.

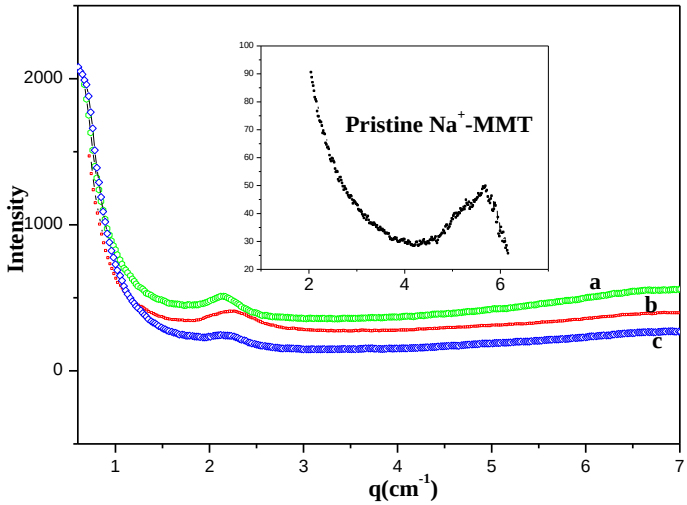

Fig 6.8: SAXS patterns for PS-nanocomposites prepared at 5 wt % clay loadings, clay was modified using different amount of PS-cationic: (a) 25% (b) 65% and 100% CEC of clay (c).

SAXS analysis of PCNs showed that all PCNs exhibited intercalated morphologies with a *d*-spacing between 2.60 and 3.12 nm. It is clear that the PCN prepared using 100% CEC exhibits broader and less intense diffraction peak with respect to those prepared using 65% and 25% CEC. The broadness of the diffraction peak suggests that a wide distribution of intermediate structures exist which is generally typical of semi-exfoliated

morphologies.[45] This is in good agreement with TEM results. The correlation between the degree of exfoliation and the degree of modification of the clay surface using PS-cationic was clearly established here. This was attributed to the impact compatibility between clay surface/monomer/polymer has on the degree of penetration of the polymer chains during conventional in situ polymerization.[1,46] The same driving force seem to be applying in polymerization in dispersion as also reported elsewhere.[13,29]

In order to study the effect of clay loadings on morphology of PCNs, a series of PCNs was prepared by dispersion polymerization of styrene using various amounts of PS-100%-MMT (see Fig 6.9).

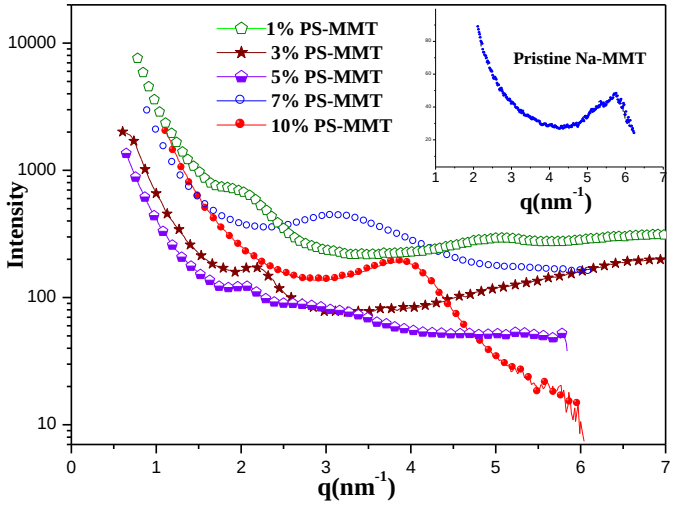

Fig 6.9: SAXS patterns for PS-nanocomposites prepared at different clay loadings

SAXS patterns showed that the morphology of the PCNs varied with the clay loading, different peaks patterns appearing depending on the amount of clay used. At low clay loadings between 1 to 5 wt%, a small diffraction peak corresponding to *d*=2.4 nm indicated that partially exfoliated morphologies were obtained. However, in the case of PCNs with 7 and 10 wt % clay, a broad diffraction peak was observed at higher q values (i.e. smaller *d*-spacing) indicating the formation of intercalated structure with a limited penetration of polymer chains inside the clay galleries. The clay loading is a known as being critical factor affecting the morphology and properties of PCNs.[12,47] Although it is

known that exfoliated structures can be easily obtained for clay loading lower than 10wt%,[48] there is however no universal rule relating to the way in which the percentage clay affects properties. Similar findings were obtained by Dong *et al*[49] who prepared PCNs of PS via dispersion polymerization in supercritical CO_2, an exfoliated structure was obtained at 1 wt % clay loadings and changed to be highly intercalated at 10wt% clay loading. In summary, the degree of modification seems to have a higher impact on the PCNs morphology relative to the clay loading.

6.3.2.2 Thermal stability of PS-nanocomposites

Fig. 6.10 shows TGA thermograms of PS-nanocomposites prepared by dispersion polymerization of styrene with various PS-MMT loadings, and for the neat polymer (i.e. with no clay). All PS-nanocomposites exhibited improved thermal stabilities relative to the neat polymer. The extent to which the thermal stability was improved did not correlate linearly to the clay loading. This is because the extraordinary thermal stability in PCNs is not only due to clay loading, but is also closely dependant on other factors such as the degree of interaction between the polymer matrix, the degree of dispersion of the clay nanofiller and the overall morphology.[46,50,51] For instance, nanocomposites synthesized using 10wt% clay loading were found to be thermally less stable than those prepared using 3 and 5wt% clay loading. The extent of thermal stabilities was found to be directly correlated to the structure of nanocomposites obtained (either intercalated or exfoliated) and not to the amount of clay incorporated into polymer.

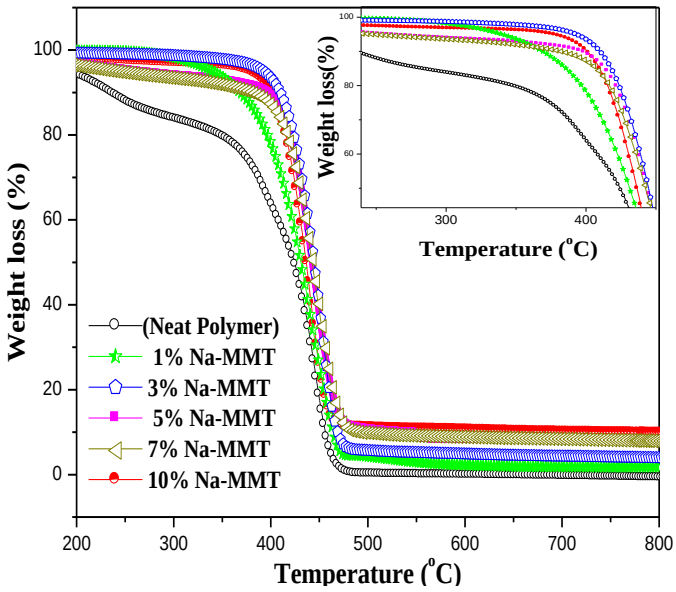

Fig. 6.10: TGA thermograms of PS-nanocomposites prepared with different PS-100%-MMT loadings. (The insert shows magnified PS standards and nanocomposites that are not clear in the main figure).

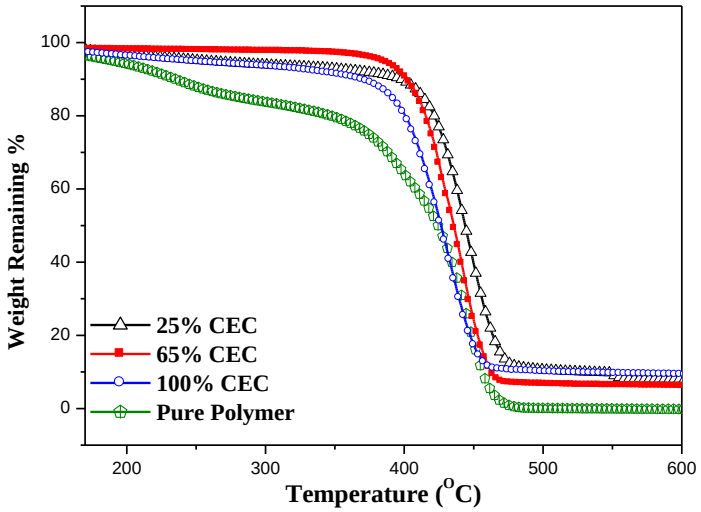

Fig. 6.11: Comparison of the thermal stability of three different nanocomposites at similar clay loading (5 wt %). The thermogram of neat PS is included as a reference.

Similar observations have been reported by several groups,[9,46,52] who explained this phenomenon as follows: in the case of the intercalated structure several stacked clay

layers might provide a more efficient thermal barrier between the decomposing zone and polymer matrix. In the present work, the amount of PS-cationic used to organically modify the clay can also have impact on the thermal stability. The lower thermal stability of PCNs prepared using 100% CEC PS-cationic relative to 25% CEC and 65% CEC PS-cationic may be also due to the presence of higher amount of the low molecular weight PS-cationic modifier inside clay galleries. Both effects (i.e. nanocomposites structure and amount of PS-cationic) are believed to contribute to changes in thermal stability of the PCNs.

Table 6.2 shows the effect of the organically modified clay on the molecular weight of the PS- nanocomposites. First of all, the synthesized polymers were found to all have a relatively high molecular weight with relatively broad polydispersity index (PDI).

Table 6.2: Effect of added organically on the average molecular weight, polydispersity of PS-nanocomposites

PS-cationic relative to CEC	Organoclay (wt % relative to styrene)	$\overline{M}_w \times 10^3$ (g/mol)	$\overline{M}_n \times 10^3$ (g/mol)	$\overline{M}_w / \overline{M}_n$
0	0	595	141	4.22
100%	1	467	116	4.0
100%	3	503	223	2.25
25%	5	407	131	3.1
65%	5	419	113	3.7
100%	5	411	106	3.87
100%	7	430	143	3.00
100%	10	392	137	2.86

This is commonly observed with polymers prepared via free radical polymerization in dispersion. The obtained molecular weight of the polymer matrix of the nanocomposites was found to be affected by the clay content. The M_w was found to decrease as the clay loading increased, which is a common trend in the preparation of PCNs via in situ free-radical polymerization in various media, including free radical polymerization inemulsion[10,46,53],in suspension[54]and in dispersion.[55] This has been explained due to hindrance of polymer chains growth by the clay platelets.[46] In the present case, molecular weights also underwent a slight decrease due to the presence of inorganic clay particles

on the polymerization systems, impeding the diffusion of initiator and monomer, as reported elsewhere.[56]

6.3.2.3 Thermo-mechanical properties of PS-nanocomposites

All nanocomposites that were synthesized exhibited higher storage modulus relative to that of the virgin copolymer, as shown in Table 6.3 below (where G^I is the storage modulus).

Table 6.3: T_g values and storage modules of nanocomposites

Sample	% clay	G^I x 10^7 (Pa)	T_g(ºC)
PS standard	0	3.00	98
PS-100%-nanocomposites	1	3.25	100
	5	5.00	115
	7	5.83	117
	10	7.00	111
PS-25%-nanocomposites	5	5.71	108
PS-65%-nanocomposites	5	7.00	108

Fig.6.12 shows the variation in storage modulus vs. temperature for pure PS and three different nanocomposites.

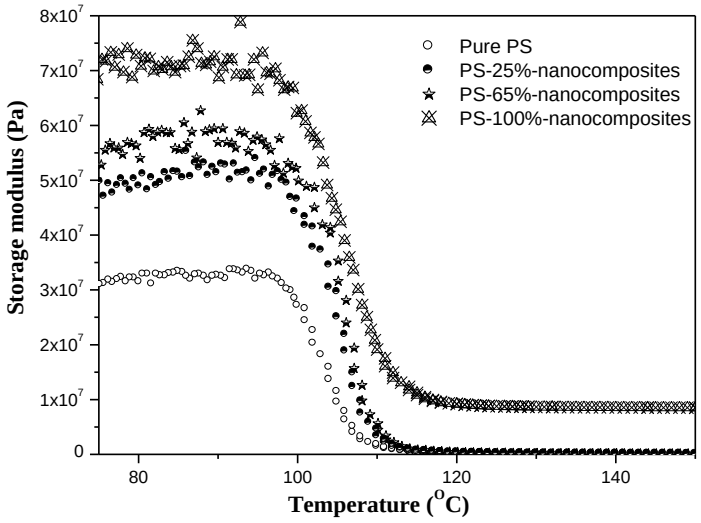

Fig. 6.12: Storage modulus as a function of temperature for pure PS and PS-nanocomposites.

The storage modulus of the plateau region below the T_g increased slightly as the clay loading increased as reported elsewhere.[48,53,57] The incorporation of MMTlead to increase in the storage modulus.[58]This is due to interactions between the polymer chains of the matrix and the silicate layers, which hinders the mobility of polymer segments near the filler interface.[1,59,60]In the present work the slight decreases in molecular weight did not counteract this effect on the storage modulus as it has been reported by Samakande*et al*for different PCNs system.[28]

Partially exfoliated PS-100%-nanocomposites showed a higher storage modulus than the intercalated PS-25%-nanocomposites, and PS-65%-nanocomposites. Similar results were reported by Xu*et al*.[53]who found that the exfoliated and partially exfoliated structure of poly (styrene-co-acrylonitrile) had a storage modulus higher than the intercalated structure of a similar copolymer due to a greater interfacial area between the clay particles and the polymer matrix.

Fig. 6.13 shows the change of loss modulus with temperature. The maximum point of the loss modulus peaks were used to determine the glass transition temperature (T_g)

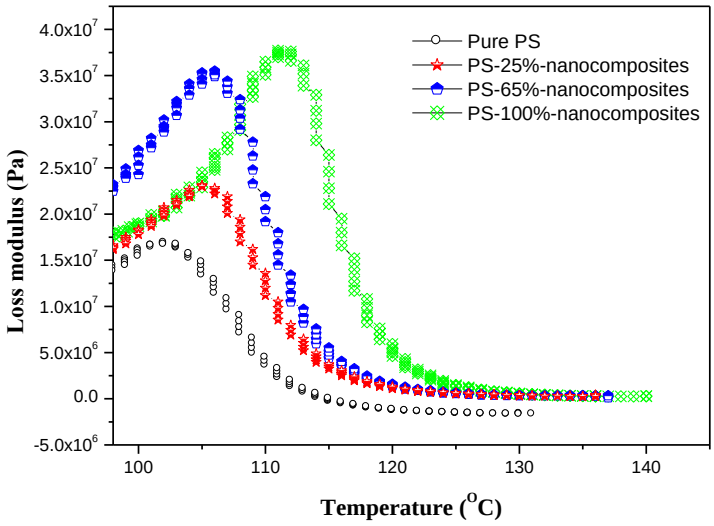

Fig. 6.13: Loss modulus as a function of temperature for pure PS and PS-nanocomposites with organoclays of various degree of modification.

Fig. 6.13 shows that the maximum of the loss modulus peaks for the nanocomposites shifted to higher temperature relative to that for the virgin polymer, indicating a shift of the glass transition temperature toward higher temperature. This is generally attributed to the restriction of the molecular chain motion of the polymer. The clay layers have been reported as acting in a similar way as cross-linking bridges in the nanocomposite systems, leading to the restriction of polymer chain motion.[53,59,61] TheT_g value increased slightly with semi-exfoliated structure (i.e. 100% CEC) relative to that for intercalated structures (i.e. 25% and 65% CEC), this is because the clay has a good dispersion in the semi-exfoliated nanocomposites, thus the sheets of the clay in this case can effectively restrain the movement of the PS chains and enhance the T_g as reported elsewhere.[1,62] Additionally, the quantity of compatibilizer used (i.e. PS-cationic) could also effect the T_g values, as the amount of PS-cationic increases the value of T_g increased. Many researches of other groups report on the effect of molecular weight on T_g values.[48,63,64] However, in the present study the slight decrease in the molecular weight could not cause any effect in the $T_g$due to the overall high molecular weight obtained.

Fig. 6.14 shows the variation of tan δ as a function of temperature for pure PS and PS-nanocomposites. All tan δ peaks of nanocomposites shifted to higher temperature relative to pure PS. T_g values were determined from the onset of tan δ peaks.

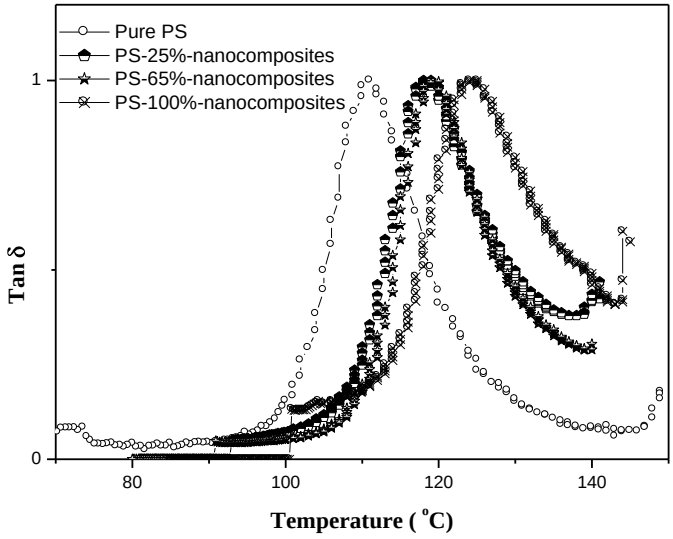

Fig. 6.14: Tan δ as a function of temperature for pure PS and PS-nanocomposites.

In Fig. 6.14 the tan δ peaks for the nanocomposites appear to be broader than the peak for the virgin copolymer. This can be ascribed to the occurrence of distribution of polymer chain mobility due to the presence of clay fillers.[59] The broadening of the tan δ peak is more pronounced with semi-exfoliated nanocomposites than with intercalated structures because of a higher inhomogeneity of the polymer chains environment throughout the PCNs material. The overall higher T_g of semi-exfoliated PCNs can be related to the relatively higher surface contact area of interaction between the polymer chains and the clay.

6.4 Conclusions

PS-nanocomposites were successfully synthesised in dispersion polymerization. The morphology of PCNs obtained was found to be strongly dependent on the degree of modification of the clay filler. The surface was pre-modified with various amounts of PS-cationic (25%, 65% and 100% CEC) via ion-exchange reaction. The clay particles were encapsulated into PS latex with a partially exfoliated structure at 100% CEC upon completion of polymerization process, and the final dispersion found to be stable for up

to 5 wt% of clay filler loading. Clay particles were distributed in between the dispersant phase and the particles in an intercalated structure when 25% and 65% CEC PS-cationic modified clay was used yielding an unstable final polymer dispersion. The thermal and mechanical properties of PS-nanocomposites were found to be dependent on both nanocomposites morphology, and clay loading.

6.5 References

1. Ray, S.; Okamoto, M. *Progress in Polymer Science* **2003,** 28, 1539-1641.

2. Alexandre, M.; Dubois, P. *Materials Science and Engineering: A* **2000,** 28, 1-63.

3. Fu, X.; Qutubuddin, S. *Materials Letters* **2000,** 42, 12-15.

4. Lebaron, P. C.; Wang, Z.; Pinnavaia, T. J. *Applied Clay Science* **1999,** 15, 11-29.

5. Fischer, H. *Materials Science and Engineering A* **2003,** 23, 763-772.

6. Bergaya, F.; Lagaly, G. *Applied Clay Science* **2001,** 19, 1-3.

7. Tiarks, F.; Landfester, K.; Antonietti, M. *Langmuir* **2001,** 17, 5775-5780.

8. Wang, D.; Zhu, J.; Yao, Q.; Wilkie, C. A. *Chemistry of Materials* **2002,** 14, 3837-3843.

9. Samakande, A.; Hartmann, P. C.; Cloete, V.; Sanderson, R. D. *Polymer* **2007,** 48, 1490-1499.

10. Xu, M.; Choi, Y. S.; Wang, K. H.; Kim, J. H.; Chung, I. *Macromolecular Research* **2003,** 11, 410-417.

11. Choi, Y. S.; Chung, I. J. *Macromolecular Research* **2003,** 11, 425-430.

12. Greesh, N.; Hartmann, P.; Sanderson, R. *Macromolecular Materials and Engineering* **2009,** 294, 206-212.

13. Zhao, Q.; Samulski, E. T. *Polymer* **2005,** 47, 663-671.

14. Bourgeat-Lami, E.; Lang, J. *Journal of Colloid and Interface Science* **1998,** 197, 293-308.

15. Landfester, K. *Angewandte Chemie International Edition* **2009,** 48, 4488-4507.

16. Voorn, D.; Ming, W.; Herk, A. V. *Macromolecular Symposia* **2006,** 245, 585-590.

17. Tong, Z.; Deng, Y. *Polymer* **2007,** 48, 4337-4343.

18. Mcdoland, C.; Devon, M. *Colloid and Interface Science* **2002,** 99, 181-213.

19. Micusík, M.; Bonnefond, A.; Reyes, Y.; Bogner, A.; Chazeau, L.; Plummer, C.; Paulis, M.; Leiza, J. *Macromolecular Reaction Engineering* **2010,** 4, 432-444.

20. Faucheu, J.; Gauthier, C.; Chazeau, L.; Cavaille, J.; Mellon, V.; Lami, B. *Polymer* **2010,** 51, 6-17.

21. Leelajariyakul, S.; Noguchi, H.; Kiatkamjornwong, S. *Progress in Organic Coatings* **2008,** 62, 145-161.

22. Steriet, N.; Landfester, K. *Macromolecular Materials and Engineering* **2007,** 292, 1111-1125.

23. Li, H.; Chen, H.; Xu, W.; Yuan, F.; Wang, J.; Wang, M. *Colloids and Surfaces A: Physicochemical and Engineering Aspects* **2005,** 254, 173-178.

24. Tiarks, F.; Landfester, K.; Antonietti, M. *Macromolecular Chemistry and Physics* **2001,** 202, 51-60.

25. Sun, Q.; Deng, Y.; L.Wang, Z. *Macromolecular Materials and Engineering* **2004,** 289, 288-295.

26. Huang, X.; Brittain, W. J. *Macromolecules* **2001,** 34, 3255-3260.

27. Negrete-Herrera, N.; Letoffe, J. M.; Putaux, J. L.; David, L.; Bourgeat-Lami, E. *Langmuir* **2004,** 20, 1564-1571.

28. Samakande, A.; Sanderson, R.; Hartmann, P. *Journal of Polymer Science Part A: Polymer Chemistry* **2008,** 46, 7114-7126.

29. Bourgeat-Lami, E.; Lang, J. *Journal of Colloid and Interface Science* **1999,** 210, 281-289.

30. Lee, J.; Ha, J.; Choe, S.; Lee, C.; Shim, S. *Journal of Colloid and Interface Science* **2006,** 298, 663-671.

31. Kim, O.; Lee, K.; Kima, K.; Lee, B.; Choe, S. *Polymer* **2006,** 47 1953-1959.

32. Horak, D. *Journal of Polymer Science Part A: Polymer Chemistry* **1999,** 37, 3785-3792.

33. Saenz, J. M.; Asua, J. M. *Journal of Polymer Science Part A: Polymer Chemistry* **1996,** 34, 1977-1992.

34. Paine, A.; Winnik, F. *Langmuir* **1989,** 5, 903-910.

35. Hartmann, P.; Dieudonne, P.; Sanderson, R. *Journal of Colloid and Interface Science* **2005,** 284, 289-297.

36. Tong, Z.; Deng, Y. *Macromolecular Materials and Engineering* **2008,** 293, 529-537.

37. Bon, S.; Colver, P. *Langmuir* **2007**, 8316-8322.

38. Tong, Z.; Deng, Y. *Industrial and Engineering Chemistry Research* **2006,** 45, 2641-2645.

39. Moustafa, A.; Hakim, A.; Mohamed, G. *Journal of Applied Polymer Science* **1997,** 63, 239-246.

40. Kim, J.; Kim, S.; Choi, H.; Juon, M. *Macromolecular Materials and Engineering* **1999,** 20, 450-452.

41. Yang, Y.; Zhang, J.; Liu, L.; Zhao, H. *Journal of Polymer Science Part A: Polymer Chemistry* **2007,** 45, 5759-5769.

42. Wu, Y.; Zhang, J.; Zhao, H. *Journal of Polymer Science Part A: Polymer Chemistry* **2008,** 47, 1535-1543.

43. Pickering, S. U. *Journal of the Chemical Society, Transactions* **1907,** 91 2001-2021.

44. Takahara, K.; Ikeda, S.; Ishino, S.; Tachi, K.; Ikeue, K.; Sakata, T.; Hasegawa, T.; Mori, H.; Matsurmura, M.; Ohtani, B. *Journal of the American Chemical Society* **2005,** 127, 6271-6281.

45. Morgan, A. B.; Gilman, J. W. *Journal of Applied Polymer Science* **2003,** 87, 1329-1338.

46. Greesh, N.; Hartmann, P.; Cloete, V.; Sanderson, R. *Journal of Polymer Science Part A: Polymer Chemistry* **2008,** 46, 3619-3628.

47. Wang, H.; Chang, K.; Chu, H. *Polymer International* **2005,** 54, 114-119.

48. Qutubuddin, S.; Fu, X. *Polymer* **2001,** 42, 807-813.

49. Dong, Z.; Liu, Z.; Zhang, J.; Han, B.; Sun, D.; Wang, Y.; Huang, Y. *Journal of Applied Polymer Science* **2004,** 94, 1194-1197.

50. Gilman, J. W. *Applied Clay Science* **1999,** 15, 31-49.

51. Pramoda, K. P.; Liu, T.; Liu, Z.; He, C.; Sue, H. *Polymer Degradation and Stability* **2003,** 81, 47-56.

52. Giannelis, P. E. *Advanced Materials* **1996,** 8, 29-40.

53. Xu, M.; Choi, Y. S.; Kim, Y. K.; Wang, K. H.; Chung, I. J. *Polymer* **2003,** 44, 6387-6395.

54. Yang, W.; Ko, T.; Wang, S.; Shin, P.; Chang, M.; Jiang, G. *Polymer Composites* **2008,** 29, 409-414.

55. Zhao, Q.; Samulski, E. T. *Polymer* **2006,** 47, 663-671.

56. Greesh, N.; Hartmann, P.; Sanderson, R. *Macromolecular Materials and Engineering* **2009,** 294, 787-794.

57. Kawasumi, M.; Hasegawa, N.; Kato, K.; Usuki, A.; Okada, A. *Macromolecules* **1997,** 30, 6333-6338.

58. Song, K.; Sand, G. *Clays and Clay Minerals* **2001,** 49, 119 -125.

59. Zhang, Y.; Lee, J.; Jang, H.; Nah, C. *Composites: Part B* **2004,** 35, 133-138.

60. Nalwa, H. S., Polymer/clay Nanocomposites. In *Encyclopedia of Nanoscience and Nanotechnology*, American Scientific Publishers: California, 2004; Vol. 8, pp 791-843.

61. Choi, Y. S.; Ham, H. T.; Chung, J. *Chemistry of Materials* **2004,** 16, 2522-2529.

62. Jan, I.; Lee, T.; Chiou, K.; Lin, J. *Industrial & Engineering Chemistry Research* **2005,** 44 2086-2090.

63. Kim, T. H.; Lim, S. T.; Lee, C. H.; Choi, H. J.; Jhon, M. S. *Journal of Applied Polymer Science* **2003,** 87, 2106-2112.

64. Tyan, H.; Wei, K.; Hsieh, T. *Journal of Polymer Science Part B: Polymer Physics* **2000,** 38, 2873-2878.

Preparation of Polystyrene Colloid Particles Armored by Clay Platelets via dispersion polymerization

Abstract

Polystyrene colloid particles armoured by montmorillonite clay (MMT) were prepared by dispersion polymerization. MMT was pre-modified with cationic amphiphilic block copolymer of poly(styrene-b-2hydroxyethyl acrylate) (PS-b-PHEA), and used as stabilizer. The impact of (PS-b-PHEA)-MMT loading on polymer particle size, monomer conversion, and on molecular weight were investigated. Transmission electron microscopy (TEM) showed that colloid PS particles with MMT layers at the surface can be observed, with particles sizes in the micrometer size range, that were fairly stable for clay loadings up to 5wt%. XRD and TEM revealed that nanocomposites materials at low clay loading yielded partially exfoliated structures, while intercalated structures were obtained at higher clay loading. The effect of PS-b-PHEA)-MMT loadings on thermal, thermo-mechanical and on melt flow properties of (PS-nanocomposites was investigated.

Preparation of Polystyrene Colloid Particles Armored by Clay Platelets via dispersion polymerization

7.1 Introduction

Most recent literature describes the stabilization of emulsion polymerization by various types of particles, such as inorganic or polymeric particles.[1-5] Furthermore, for environmental and economic reasons, the stabilization of emulsions by clay particles receives an increasing interest as it potentially allows formulating surfactant-free emulsion.[6-8] The focus of the present work is to obtain stable colloid polymer particles by polymerization in dispersion using clay as stabilizer.

Dispersion polymerization is a very useful method for the preparation of monodisperse polymer particles of micrometer size range. Owing to the simplicity of the process and to the wide variety of monomers that can be successfully polymerized, it has been already widely studied.[9-12] In dispersion polymerization, primary particles are generated from the precipitation of relatively large oligomeric species, and microspheres are subsequently growing by further absorption of oligomers and monomers from the medium. A short nucleation period and the uniform growth of the primary particles afford uniform-sized polymer particles.[13] The polymerization usually commences as a homogeneous solution of monomers, organic solvent, initiator and polymeric stabilizer.[14]

In dispersion polymerization a steric stabilizer is used to render the polymer dispersion obtained colloidally stable. The absence of such steric stabilizer yields aggregated macroscopic polymer particles of uncontrolled size.[15] The best steric stabilizers are amphiphilic di-block or graft copolymers, where one block has affinity for the polymer particle surface allowing it to bind itself to the particles by either physi- or chemi-sorption or even by incorporation in a growing particle. This “insoluble” block serves as

an anchor for the medium-soluble part of the polymer to the colloidal particles. The role of the soluble block of the stabilizer is to impart steric stabilization of the particles. For this reason, such blocks are referred to as the stabilizing moieties.[16] To date, most of those block copolymers have been synthesized using meticulous and time-consuming living ionic polymerizations.[17] New emerging living radical polymerization (LRP) techniques have been used to prepare block copolymers in readily easy upscalable way.

Controlled/living radical polymerization is a particularly useful technique for the preparation of well-defined polymer structures. The three main radical polymerization techniques capable of inducing living behaviour to growing chains are nitroxide-mediated polymerization (NMP),[18] atom transfer radical polymerization (ATRP),[19] and reversible addition-fragmentation chain transfer polymerization (RAFT).[20] In the present work, reverse iodine transfer polymerization (RITP) was used to synthesize amphiphilic block copolymer of poly(styrene-b-2-hydroxyethyl acrylate) PS-b-PHEA as described in Chapter 4.

Chapter 3 reported on the use of clay in the dispersion polymerization of styrene, the clay surface being pre-modified using 3-(trimethoxysilyl)propyl methacrylate (MPTMS). It was found that the particle size decreased and became more uniformly distributed as the clay loading increased, while the morphology of PS particles prepared without MPTMS-clay was found to be ill-defined, with large sizes and broad particles size distribution. Furthermore, the particles obtained were not completely stable and TEM images showed that most of the clay platelets were distributed in the dispersing phase.[21] Zhao and Samulsk.[22] also reported on the preparation of PMMA in the presence of clay using dispersion polymerization in supercritical CO_2 and concluded that clay not only functions as an inorganic filler but also as a stabilizer, although they did not mention that the polymer particles were armoured by clay platelets (i.e. clay platelets located on the surface of polymerparticles).

The overall negative charge and amphoteric rim of the clay particles are usually not sufficient to produce a stable aqueous clay dispersion, which is necessary to produce a stable polymer particle dispersion, and therefore some surfactants were introduced into

the systems.[23] Recently, some studies have been carried out on the use of polymer brushes on clay surfaces to obtain a stable emulsion polymerization system (i.e. armoured particles). It was found that introducing polymer brushes onto the surface of clay layers may be a convenient way to improve the self-assembly of clay particles at interfaces and to obtain stable colloidal particles.[24-26]

This study describes the use of the amphiphilic block copolymer (PS-b-PHEA) grafted onto clay surface (PS-b-PHEA)-MMT, as stabilizer to prepare PS colloidal particles via dispersion polymerization.It was proposed that the use of a block amphiphilic copolymer grafted onto clay as a stabilizerwould result in good stabilization, whereinthe PS segments adsorb onto the PS particle surface, while the PHEA segments anchored to the clay are dispersed into the dispersion medium, and provide steric stabilization for dispersion polymerization process. Accordingly, armoured latexes (i.e. where a polymer particle is completely covered with clay platelets) may be obtained.The effect of (PS-b-PHEA)-MMT clay filler loading on the particle size, molecular weight, conversion and thermal stability were studied, in addition thermo-mechanical and rheologicalproperties of the nanocomposites.

7.2 Experimental

7.2.1 Material

Styrene monomer was obtained from Aldrich. The stabilizers were removed by washing three times with a 3wt% potassium hydroxide aqueous solution. The initiator 2,2-azoisobutyronitrile (AIBN) was obtained from Aldrich and recrystallized from methanol before use. (PS-b-PHEA)-MMT was prepared according to procedure described in Section 5.2.5.

7.2.2 Preparation of PS colloidal particles stabilized by (PS-b-PHEA)-MMT

The polymerization of styrene was carried out in a 250 mL three-neck round bottom flask equipped with a baffle stirrer, a reflux condenser, a nitrogen inlet and rubber septum, at 75 ºC. In a typical procedure (PS-b-PHEA)-MMT (1−10 wt% relative to 10 g monomer)

was dispersed in 1 mL THF. After stirring for 10 min, the solution was added to a dispersion medium containing ethanol and water (85/15). The monomer phase was prepared by dissolving AIBN (0.004 g) in styrene monomer (10 g), and then flushed with nitrogen gas for 20 min. The solution of stabilizer/dispersion medium was first charged into the reactor, and then purged with nitrogen gas for 20 min. The reaction mixture was stirred and heated to 75°C, followed by the addition of the monomer phase all at once. The polymerization was carried out for 6 h. Upon completion of the reaction, the reactor was cooled down by immersion in a ice bath for 10 min. Small quantities of the dispersion were regularly sampled, throughout the polymerization, dried in a vacuum oven at 25°C for 24 h, and then analyzed by small angle x-ray scattering (SAXS), transmission electron microscopy (TEM), and thermogravimetric analysis (TGA).

The preparation of PS colloid particles stabilized by pure PS-b-PHEA was also carried out in similar way using different PS-b-PHEA concentrations.

7.2.3 Characterizations

TGA was carried out using a TGA-50 SHIMADZU thermogravimetric instrument, with a TA-50 WSI thermal analyzer, connected to a computer. Samples (10–15 mg) were degraded in a nitrogen atmosphere, using a flow rate of 50 ml/min and a heating rate of 20 °C/min.

Dynamic light scattering (DLS) was used to determine the particle size. Latex samples were prepared by diluting a few drops of the dispersion in deionized water. DLS measurements were carried out at 25 ºC on a Malvern-Nano instrument (Malvern instruments, USA) fixed at 90 degrees scattering angle. The instrument system was calibrated using nanosphere–size standards of polymer microsphereres in water, with a mean diameter of 60 nm.

Transmission electron microscopy (TEM) analysis was carried out at an accelerating voltage of 120 kV. Prior to analysis, samples of PCNs were stained with OsO_4, then embedded in epoxy resin and cured for 24 h at 60 ºC. The embedded samples were cut into slices of a nominal thickness of 100 nm, using an ultra-microtome with a diamond

knife on a Reichert Ultracut S ultra microtome, at room temperature. The sections were transferred from water at room temperature onto a 300-mesh copper grid. TEM analysis was also carried out on the latex to visualize the particles morphology on nanometer scale. Samples were prepared by diluting the latex in mixture of ethanol and water (85:15). The diluted samples were mounted on copper grids, which were then transferred into the TEM apparatus.

The size of the PS particles prepared via dispersion polymerization was determined by scanning electron microscopy (SEM), using a Leo® 1430VP scanning electron microscope. Prior to imaging, the samples were sputter-coated with gold. Samples were quantified by EDS analysis using an Oxford Instruments® 133keV detector and Oxford INCA software.

Gel permeation chromatography (GPC) was performed using a Waters 600E system controller equipped with a Waters 610 fluid unit pump, a Waters 410 differential refractometer as detector, and a column set of a PLgel 5 µm guard 50×7.5 mm and a PLgel 5 mm mixed-C 300×7.5 mm column (Polymer Laboratories, USA). Measurements were carried out at 30 ºC, using THF as eluent and a flow rate of 1 mL/min. The GPC column was first calibrated with 10 samples of polystyrene standards. Prior to analysis, samples were vigorously stirred in THF for a week, to ensure that all components were fully dissolved. The samples were then filtered five times through a 0.45-µm filter membrane.

Small angle X-ray diffractions (SAXS) measurements were performed at 298 K, in a transmission configuration. A copper rotating anode X-ray source (functioning at 4 kW) with a multilayer focusing "Osmic" monochromator giving high flux (10^8 photons/sec) and punctual collimation was used. An "image plate" 2D detector was used. Diffraction curves were obtained, giving diffracted intensity as a function of the wave vector *q*. The d spacing was calculated using the formula: $d = 2\pi/q$ (where q is the wave vector; associated with Bragg 's peak position).[27,28]

Thermomechanical properties of PCNs were determined using a Physica MCR 501 Rheometer (Anton Paar, Germany). For dynamic mechanical analysis (DMA) measurements, parallel-plate geometry (diameter 25 mm) was used, with a 1-mm gap distance and a constant strain of 0.1%. Measurements were carried out from 150 ºC to 20 ºC, at a cooling rate of -5 ºC/min, an oscillation frequency of 1 Hz, and a normal force of 5 N.

Frequency sweep measurements were performed using a Physica MCR 501 Rheometer (Anton Paar, Germany) in oscillatory mode, with parallel plate geometry (25 mm diameter). The measurements were carried out at 150 ºC, using an angular frequency range of 100-0.01 rad/sec, under a 10 N normal force. A constant strain of 0.1% was imposed, which was within the linear viscoelastic (LVE) range. Before conducting the measurements the samples were molded into circular discs at 150°C. The disc samples were 40 mm in diameter and sample thickness in the range 0.8-1.2 mm.

7.3 Results and Discussion

7.3.1 Dispersion polymerization of styrene using PS-b-PHEA

It is well known that diblock and triblock copolymers are effective stabilizers in heterophase polymerizations.[29] In order to examine the efficiency of PS-b-PHEA as stabilizer in dispersion polymerization, PS latexes were prepared by dispersion polymerization in alcoholic medium using PS-b-PHEA ($M_{n\ (SEC)}$ = 7.100 g/mol, polydispersity index =1.5, prepared via RITP) as stabilizer, following a similar procedure that has been used to produce PCNs in Section 7.2.2.

Fig. 7.1 displays SEM images of the PS particles prepared using various concentrations of PS-b-PHEA (1%, 3% 4% and 6% relative to monomer) by dispersion polymerization in a mixture of ethanol and water. Visual inspection of the spherical particles indicated that the PS-b-PHEA was a suitable stabilizer.

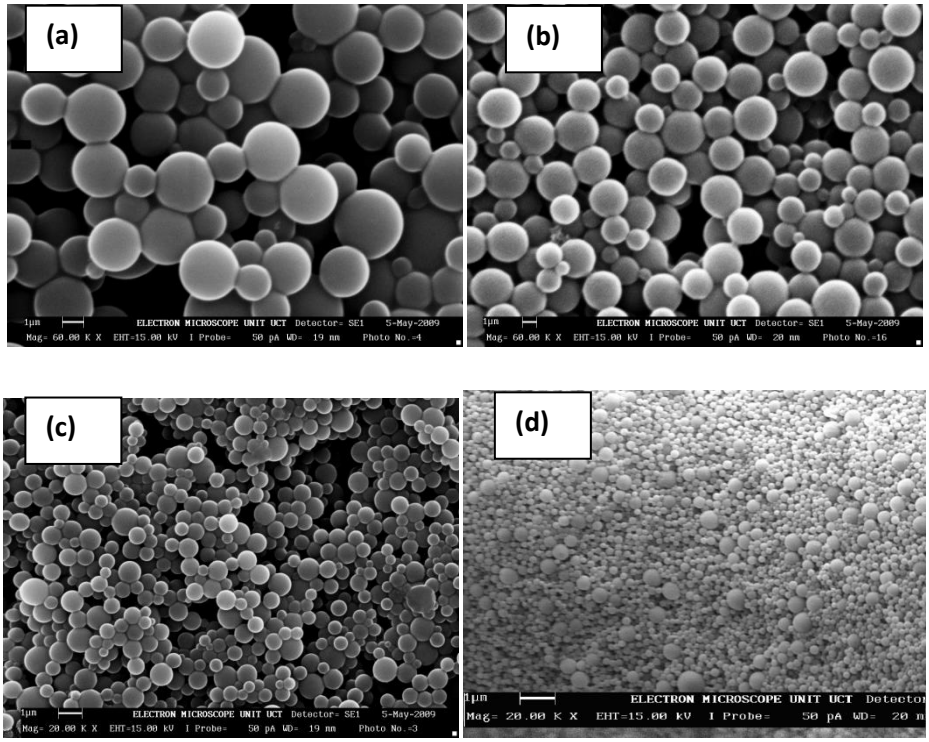

Fig. 7.1: SEM images of PS latex prepared using different concentrations of PS-b-PHEA: (a) 1%, (b) 3%, (c) 4% and (d) 6%, relative to monomer.

The average particle size varied within the range 0.8 −1.8 μm, depending on the concentration of the block copolymer. As the concentration of block copolymer increased (from 1 wt% to 6 wt% relative to monomer) the diameter of PS particles decreased from 1.8 to 0.8 μm. This is not a surprising result since the amount of stabilizer is a very important factor for stabilizing the produced nucleated particles and reducing the aggregation and coalescence between nucleated particles during the early stages of the growth process. Therefore, the number of formed nuclei increased with increasing PS-b-PHEA concentration which resulted in a large number of small particles. This tendency of decreasing particle size upon increasing stabilizer concentration has been observed by others.[15,30-32] The SEM images also show that monodisperse PS particles were obtained without coagulation for all the concentration range of PS-b-PHEA, confirming that the block copolymer of PS-b-PHEA is suitable for stabilization of PS in dispersion medium. PS-b-PHEA consists of a hydrophobic PS block and a hydrophilic PHEA block and

believed that it is located preferentially on the surface of the particles, with the PHEA segments providing steric stabilization of the polymer particles.

7.3.2 Dispersion polymerization of styrene using (PS-b-PHEA)-MMT

The (PS-b-PHEA)-MMT was synthesized as described in Section 5.2.5. Efforts were now directed at determining the efficiency of (PS-b-PHEA)-MMT as a stabilizer in dispersion polymerization.

7.3.2.1 Latex characterization

Dispersion polymerization in alcoholic medium (ethanol/water) of styrene was carried out in the presence of different concentrations of (PS-b-PHEA)-MMT as stabilizer. The monomer conversion was determined by a gravimetric method, taking the theoretical total solids content into consideration. The assumption was made was that the clay was uniformly distributed within the latex during sampling. Both rate of polymerization and monomer conversion were found to be decreased as the amount of (PS-b-PHEA)-MMT loading increased, as shown in Fig 7.2.

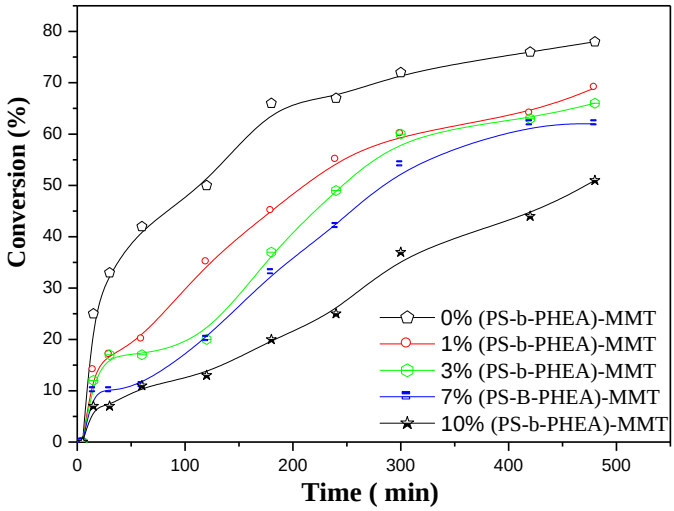

Fig. 7.2: Conversion versus time plots for PS-nanocomposites prepared.

According to Bon and Colver [33] who prepared polystyrene nanocomposites via miniemulsion polymerization using laponite clay as stabilizers, this phenomenon is explained as follows: when a radical is incident on a clay surface, it reacts irreversibly with the functionalities there, hence the more clay layers there are the greater are the chances of termination. They did however not give details of the species on the clay surface that are involved in the termination process. Also, Tong *et al* [34] observed a similar effect of clay loading on monomer conversion, however, they interpreted this due to the presence of organoclays in the polymerization medium enhance the viscosity, thus lowering the reactivity of radicals and growing chains, but this in contention. As mentioned a few articles have reported on the preparation of polymer-nanocomposites via dispersion polymerization in alcoholic medium,[35-38] however the effect of silicate loading on monomer conversion has not been reported.

Dispersion polymerization starts when the initiator decomposes and generates free radicals at elevated temperature.[39] In the presence of clay particles some initiator radicals could adsorb onto the clay surface. As the clay loading increases more initiator adsorbs into the clay surface and increases the chance of termination or simply decreases the initiator efficiency. Moreover, the presence of clay platelets in a polymerization system can hinder the growth of polymer chains, also leading to a decrease in monomer conversion. Increasing the amount of clay could also lead to restricted diffusion of monomer to the reaction side.[40]

Different results were reported by Yan *et al*.[41] who found that the conversion and the molecular weight of PS nanocomposites prepared in supercritical CO_2 increased significantly upon increasing the clay loading. They explained their results as follows: when the amount of organoclay in the system was low, stable gel systems could not be formed. Thus, the PS particles that were produced were not sufficiently stable and tended to coagulate. They could cease the polymerization process and cause lower conversion and molecular weights.

According to DLS measurements (Fig. 7.3) the presence of the clay particles also have significant effect on the particle size.

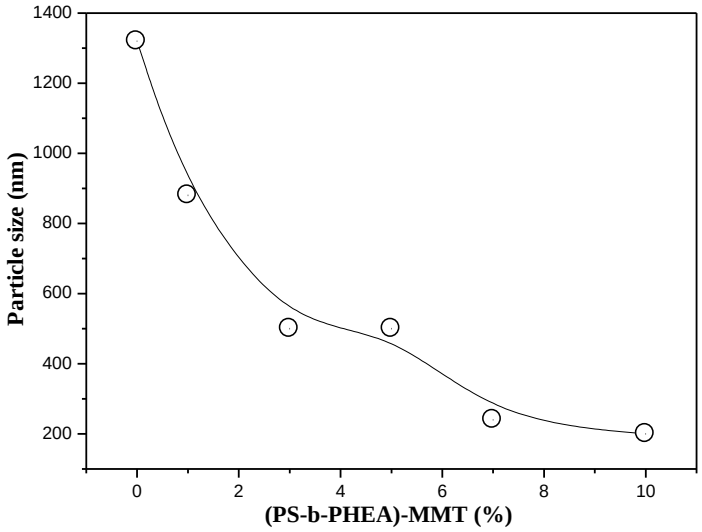

Fig. 7.3: Particle size of the PS-nanocomposites as a function of clay loading.

The particle size of PS-nanocomposites was found to decrease as the (PS-b-PHEA)-MMT clay loading increased. Yang *et al.*[25] also prepared PS colloid particles armoured by clay layers with mixed polymer brushes in suspension polymerization and observed that the clay loading had a similar effect on the particle size. Greesh *et al.*[21] observed similar results with PS-nanocomposites particles prepared via dispersion polymerization, using edgewise modified with MPTMS. This effect was explained by stabilization of the nucleated particles at the early stage of the polymerization brought about by adsorption of the partially modified clay.

7.3.2.2 Morphology of PS colloidal particles

TEM images of PS colloid particles stabilized by (PS-b-PHEA)-MMT obtained from dispersion polymerization are shown in Fig.7.4. Clay platelets were observed on the surface of the colloid particles, indicating that the PS was armoured by (PS-b-PHEA)-MMT.

The PS-b-PHEA block copolymer used as clay modifier is believed to play a decisive role in the ability of the clay to stabilize the polymer particles. The PS block affords clay areas of a great compatibility with the PS particle surface hence promoting their adsorption onto the surface of the growing PS particles during the dispersion polymerization. The second block of PHEA affords a good compatibility with the dispersing medium hence increasing the colloidal stability of the PS particles via steric stabilization.Fig. 7.4,a and 7.4,b shows TEM images of a PS-nanocomposite containing 3 wt% clay at different magnifications, and Fig 4.7,c shows TEM images of a PS-nanocomposite containing 7% clay loading.

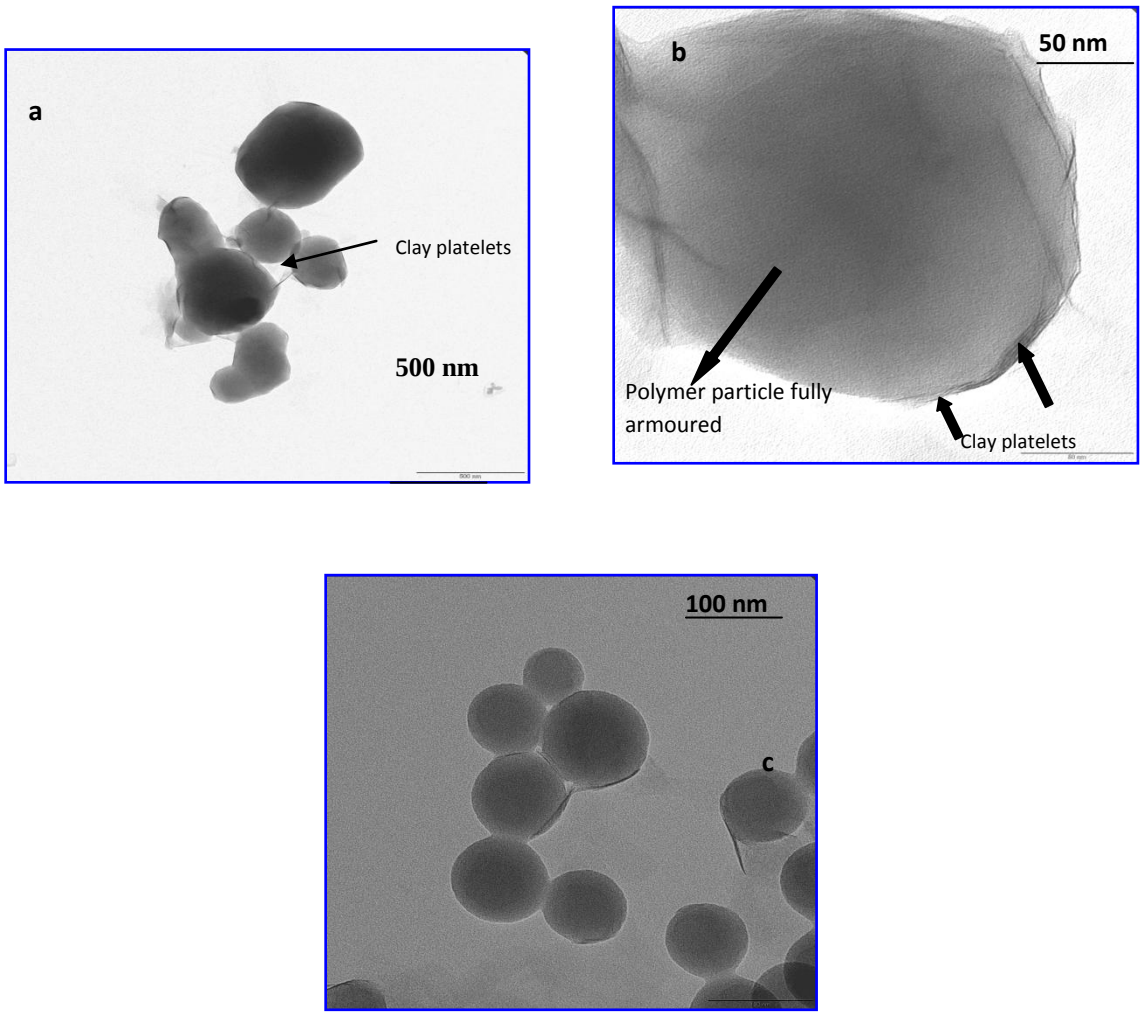

Fig.7.4: TEM images of a PS-nanocomposite latex at different clay loadings: 3 wt% clay, at low (a) and high (b) magnification, and 7 wt% clay (c).

The PS particles were found to be completely covered by clay platelets, With the increase of the amount of (PS-b-PHEA)-MMT added to the polymerization reaction, the size of PS colloid particles size decreased and particles distribution became more narrow as seen in Fig 7.4,c and confirmed by DLS results. Because of a faceting effect caused by the rigidity of the clay platelets the colloid particles are not perfectly spherical. It is interesting to note that on the TEM images, most particles are not isolated but rather tend to assemble together. This could be because PS-b-PHEA molecules are distributed on both sides of the clay surface, and two colloid particles share the same clay layers. The surface of the PS particles was also influenced by the amount of (PS-b-PHEA)-MMT loading, the PS particles becoming smoother as the clay loading increased. This could be

due to the difference in the degree of dispersion of the clay platelets. Stable PS particles were obtained for up to 5% clay loading. Such stability was not achieved when unmodified clay was used, as depicted in Section 6.3.1.2. This is due to the hydrophilic nature of pristine MMT clay, which does not have the capability to adsorb onto non polar surface such as PS particles. Unmodified MMT clay would hence remain dispersed in the water phase.

TEM analysis was performed to understand how (PS-b-PHEA)-MMT stabilizes PS particles. The PS samples were dried at only 40 °C (i.e. T lower than the T_g of the polymer) and then embedded into the epoxy resin and microtomed in order to try to monitor the degree of dispersion of the clay inside the PS particles. Fig.7.5 shows cross–sectional TEM images of the PS-nanocomposites prepared at 7wt% (PS-b-PHEA)-MMT loading, at low and high magnification. The PS particles are still visible; deformation had not occurred at this temperature. It is clearly visible that the clay platelets are located of the surface region of the latex particles, confirming the formation of armoured-like PS particles.

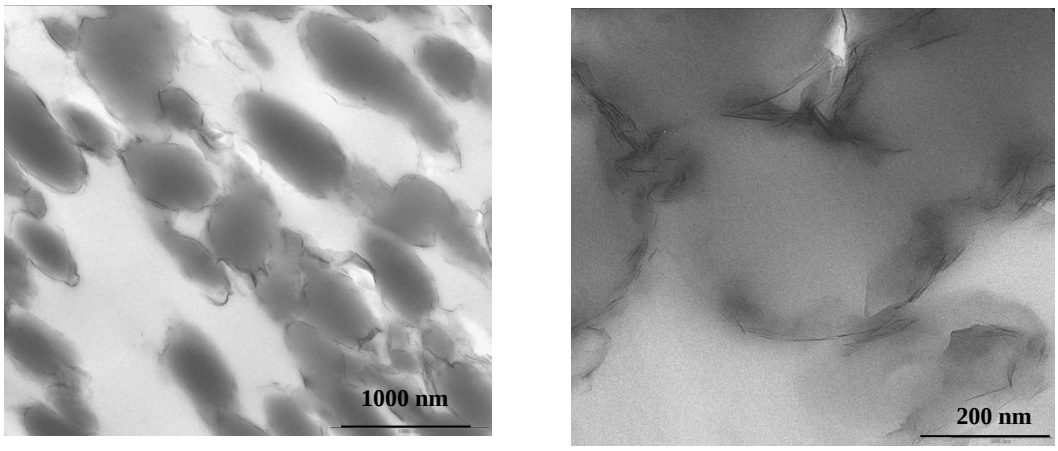

Fig. 7.5: TEM images of PS-nanocomposites prepared at 7 wt% clay loading, and film formation carried out at 40 °C.

To further prove the location of the clay layers on the surface of colloid particles, and understand the effect of PS-b-PHEA copolymer brushes on the stability of the colloid particles, the zeta potentials of (PS-b-PHEA)-MMT and PS colloid particles stabilized by

(PS-b-PHEA)-MMT were plotted as a function of pH in an ethanol/water as shown in Fig. 7.6.

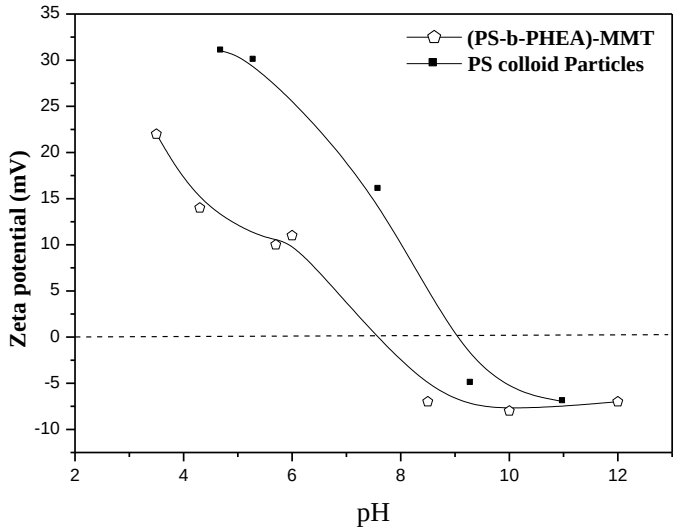

Fig. 7.6: Zeta potential versus pH curves obtained for (PS-b-PHEA) -MMT and PS colloid particles stabilized by (PS-b-PHEA) -MMT in ethanol/water.

Due to the negative charge on the surface of the clay layers, original clay has a negative zeta potential. The original sodium-montmorillonite (MMT) has a zeta potential of – 43.2 mV at pH 6.25.[42] At high pH the zeta potential of (PS-b-PHEA)-MMT, clay was found to be less negative than that of the unmodified MMT, this is due to nearly complete ion-exchange of counter ions from negative charges present at the MMT surface by PS-b-PHEA-cationic block copolymer. The modification of a clay surface using PS-b-PHEA changes the properties of the clay surface, after modification surprisingly the clay layers have a positive charged surface at low pH values. Zhang *et al* [43] reported that positive zeta potential observed for a solution of poly(2-dimethylamino)-ethyl methacrylate) brushes on the surface of clay layers (PDMAEM-MMT) at low pH values, they interrupted their results due to the protonation of amino groups under acidic conditions. Furthermore, positive zeta potential was also measured for poly(methyl methacrylate) PMMA colloidal particles with stabilized PDMAEM-MMT, due to the cationic nature of the PDMAEM. On the other hand, Wu *et al.*[44] prepared PS colloidal particles in

suspension polymerization using PS-MMT, the zeta potential was found to be negative in the range of pH value 2.0 to 9.0. In the present study although the observations of positive zeta potential at low pH values for PS-b-PHEA-MMT and PS colloidal particles were not quite understood, it can be concluded that the (PS-b-PHEA)-MMT located on the PS surface, and both (PS-b-PHEA)-MMT and PS show similar zeta potential profiles.

Based on these observations and the known mechanism of conventional radical polymerization in dispersion, the mechanism by which armoured PS particles are formed via polymerization in dispersion of styrene using (PS-b-PHEA)-MMT as stabilizer is proposed as in Scheme 7.1.

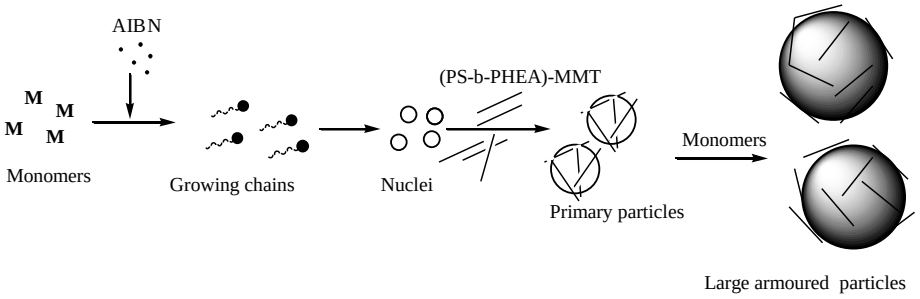

Scheme 7.1: Formation of PS armoured particles via dispersion polymerization.

The polymerization of styrene takes place homogeneously in dispersing medium until the polymer chains achieve a critical chain length and then precipitate. After particle nuclei are formed by aggregation of precipitated polymer chains, the PS block of the PS-b-PHEA copolymer bonded to clay (PS-b-PHEA)-MMT adsorbs onto the surface of the PS particle nuclei to prevent further aggregation. Then the polymerization continues within the particles through monomer diffusion from the dispersing medium to the particles. The presence of modified clay has rendered the mechanism of polymerization similar to a hybrid between polymerization in dispersion and in emulsion with Pickering stabilization.

7.3.2.3 Material characterization

(a) Morphology of nanocomposites materials

The distribution of clay around the polymer latex particles was characterized using TEM. Polymer particles were completely deformed after drying samples at 100 ºC. Fig. 7.7 shows TEM images of PS nanocomposites samples prepared at 7wt%, and 3wt% (PS-b-PHEA)-MMT clay loading levels.

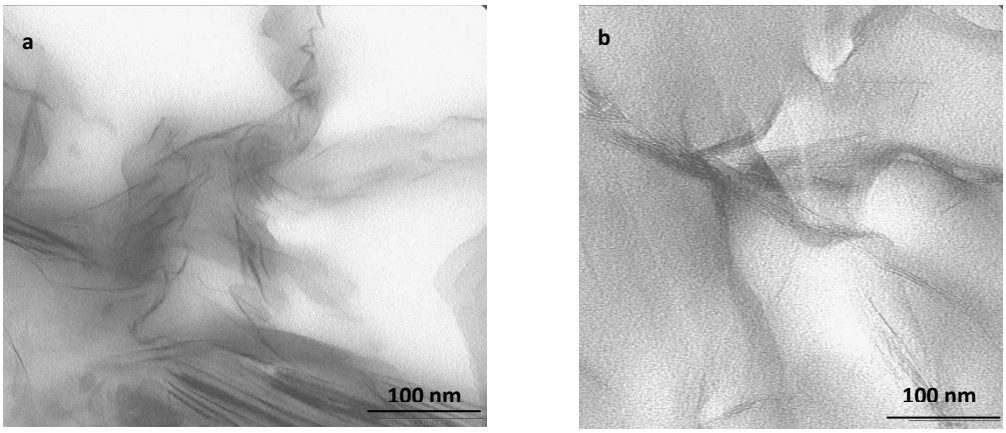

Fig. 7.7: TEM images of PS-nanocomposites at (a) 3 wt% clay loading and (b) 7 wt% clay loading.

The silicate layers can be seen as dark strips and the PS continuous matrix appear as relatively bright domains. Fig. 7.7 (a) depicts the TEM image of a PS-nanocomposite containing 3% (PS-b-PHEA)-MMT showing some of the clay platelets dispersed as single layers, while others remained stacked in an orderly manner, indicating a partially exfoliated structure. As the (PS-b-PHEA)-MMT loading increased, fewer individual layers and more clay layers were grouped together as seen in Fig 7.7 (b), indicating a lesser degree of exfoliation, and higher level of intercalation.

The SAXS patterns of the PS-nanocomposites are shown in Fig. 7.8. All synthesized nanocomposites were found to have broad diffraction peaks, shifted towards low q values relative to (PS-b-PHEA)-MMT, which is an indication of an increase in the *d*-spacing existing between the clay galleries.

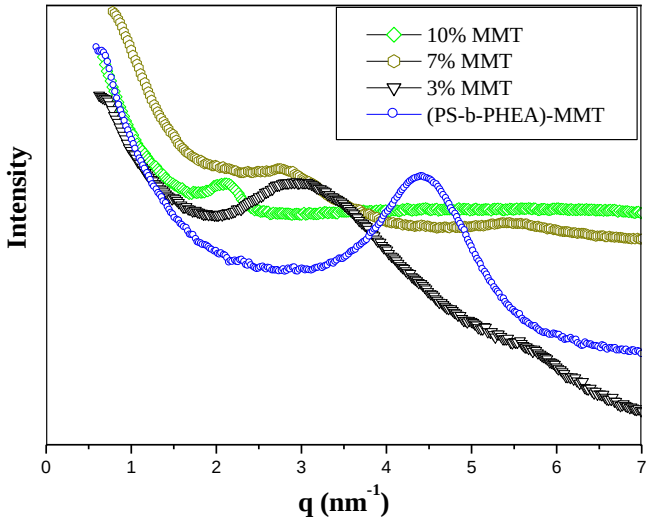

Fig. 7.8: SAXS patterns of PS-nanocomposites at different clay loadings.

The peak broadening was found to be more pronounced at low clay loading (i.e. 3% wt) and the diffraction peak became narrower again as the clay loading further increased (i.e. 10% wt). This is an indication that the morphology of the nanocomposites changed from semi-exfoliated to intercalated structure with increasing clay loadings.

The molecular weight and polydispersity indices of the PS matrix of the PCNs are shown in Table 7.1.

Table7.1: Effect of organoclay loading on the average molecular weight and polydispersity index of PS nanocomposites

Organoclay (wt % relative to styrene)	$\overline{M}_w \times 10^3$ (g/mol)	$\overline{M}_n \times 10^3$ (g/mol)	$\overline{M}_w / \overline{M}_n$
0	595	141	4.22
1	424	138	3.07
3	447	106	4.21
5	414	138	3.00
7	333	107	3.10
10	320	111	2.88

The general trend is a decrease in molecular weight and a decrease in polydispersities as the clay loading increases for the similar reasons explained previously (see Sections 3.3.2 and 6.3.2.2).

(b) Thermal stability of nanocomposites materials

The thermal stability of the nanocomposites and pure polymer were studied by TGA. Fig. 7.9 shows TGA thermograms and Table 7.2 shows temperatures for various % weight losses due to thermal decomposition.

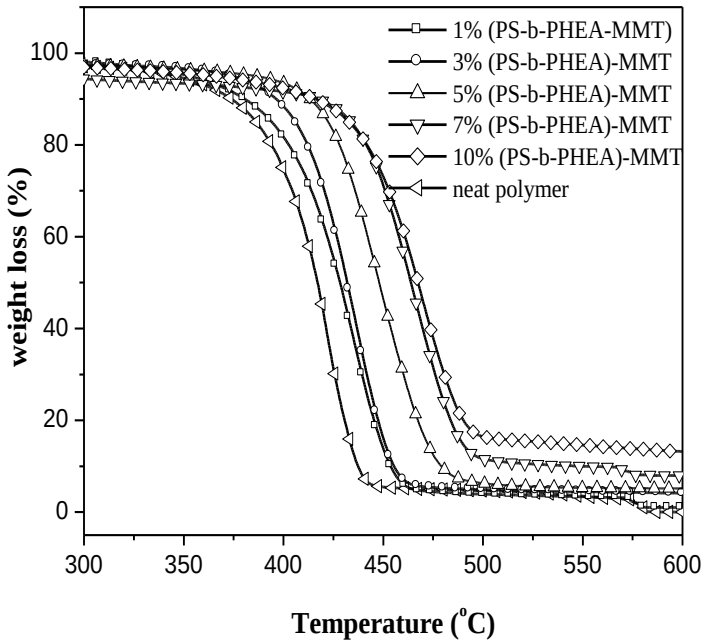

Fig. 7.9: TGA thermograms of PS-nanocomposites and neat polymer.

Table 7.2: TGA data for PS nanocomposites at various clay loadings

Organoclay (Feed) (wt%)	*$T_{10\%}$ °C	**$T_{50\%}$°C	% Clay i.e. % Char @ 600°C
0	373	416	0.00
1	381	427	1.08
3	395	432	3.10
5	416	448	5.20
7	430	461	8.11
10	430	467	11.02

$T_{10\%}$,$T_{50\%}$ and% clay: temperature at which 10% weight loss and 50% weight loss occurred, and experimental % clay as determined from the remaining char weight at 600ºC, respectively.

The improvement in thermal stability of polymers filled with nanoclay is generally attributed to the formation of a clay char that acts as a mass transport barrier and a thermal insulator between the bulk polymer and the surface where the combustion takes place.[45,46] Hindered diffusion of volatile decomposition products within the nanocomposite materials has also been attributed to the presence of delaminated clay sheets.[46] In addition, restricted thermal motion of polymer chains localized inside the clay galleries also promotes enhancement of thermal stability of PCNs.[47] TGA results in Fig. 7.9 show that the decomposition temperatures of PS were greatly affected by the clay content. PS-nanocomposites with 10 wt% and 7 wt% showed a large increase of the temperature of onset of degradation (i.e. + 60 ºC), relative to the neat polymer. In addition, the temperature at which 50% degradation occurs was found to be increased up to 90 ºC. The nanocomposites prepared using 1%, 3% and 5% clay loading also showed an improvement in thermal stability but to a lesser extent.

With reference to the TEM image in Fig. 7.4, and Fig 7.5 clay platelets were situated at the surface of the polymer particles forming armored particles. In this type of morphology clay platelets can act as super-heat barrier, enhancing the overall thermal stability of polymers to greater extant than neat polymer. Zhao and Samulsk[48] found that the temperature of maximum degradation rate of pure PS prepared by dispersion polymerization in supercritical CO_2, increases largely from 369 ºC to 419 °C for PS-nanocomposites with 13 wt% clay loading. The improvement in thermal stability for PS-nanocomposites prepared using (PS-b-PHEA)-MMT as stabilizer is significantly greater than that obtained when MPTMS-MMT was used in the dispersion polymerization with fully exfoliated structures as described in Section 3.3.3.2, indicating that the thermal stability is greatly dependent on the morphology of nanocomposites obtained.[21]

Table 7.2 and Fig 7.9 show that the percentage of clay (determined from the %Char at 600ºC) was found to be slightly higher than the theoretical clay percentage. Initially it was expected that %Char at 600 °C would be close to the initial clay percentage. This unexpected result is due to an incomplete conversion of monomer during the

polymerization. The conversion at the end of polymerization was found to be between 65–70% giving an experimental clay content that is slightly higher than expected.

(c) Mechanical properties of nanocomposites materials

DMA analysis was undertaken on PCNs samples to evaluate the effect of clay loading and degree of exfoliation on the thermo-mechanical properties. All nanocomposites exhibited enhanced storage moduli in the glassy state relative to neat PS prepared in similar temperature conditions as seen in Fig.7.10.

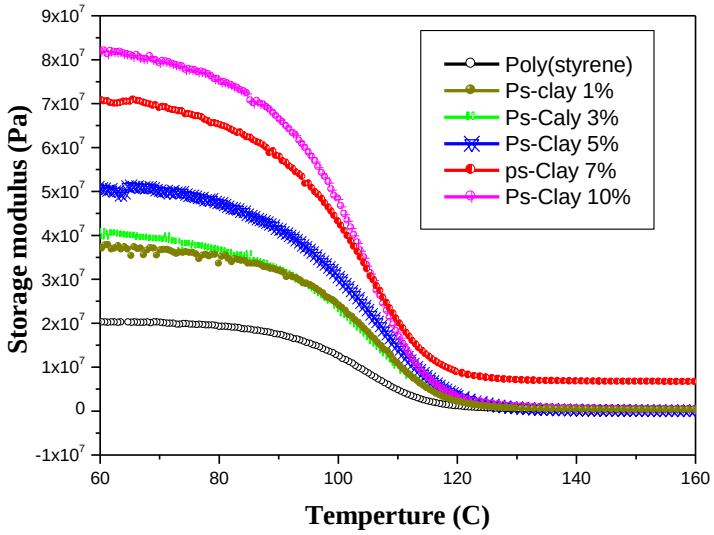

Fig.7.10: Storage modulus as a function of temperature of PS-nanocomposites prepared at different clay loadings.

The storage modulus (G') increased with increase in the clay content, which is in agreement with the literature.[49-51] This is due to the interaction between polymer and silicate layers at the interface, hindering the mobility of polymer segments at or near the interface, leading to an increase in storage modulus at temperature below the T_g.[46,49,52] Semi-exfoliated structures at low clay loading (i.e. < 5wt%) exhibited a lower storage modulus than the intercalated structures obtained at higher clay loading, which is in disagreement with literatures shows that exfoliated structures exhibited higher storage modulus than intercalated structure, due to homogeneous dispersion of clay and higher

interfacial area.[49,53,54] It is a known that the mechanical properties of nanocomposites materials depend on several factors such as: the filler type, filler loading, and nanocomposite morphology (i.e. the degree of filler distribution in the polymer matrix).[49,55-57] According to the results obtained in this study, the clay loading seem to be the main factor affecting the mechanical properties of PCNs, whatever the morphology of PCNs was.Below the T_g the enhancement of G' is clear for all PCNs. On the other hand, PCNs with high clay loading showed a greater increase in G' at high temperature compared to other PCNs at low clay loading. This is due to both mechanical reinforcement by the clay platelets and extended intercalation at high temperature. Interestingly, an increase of the storage modules plateau above the T_g was only observed for the highly filled nanocomposite with 10wt% organoclay. This could be due to the high content of clay leading to the percolation threshold between 7 and 10wt% clay loading.[46,58]

As shown in Fig. 7.11, the tan δ peaks for nanocomposites shifted to higher temperature with respect to virgin polymer, as the clay loading increased, in agreement with the literature.[49,57,59]

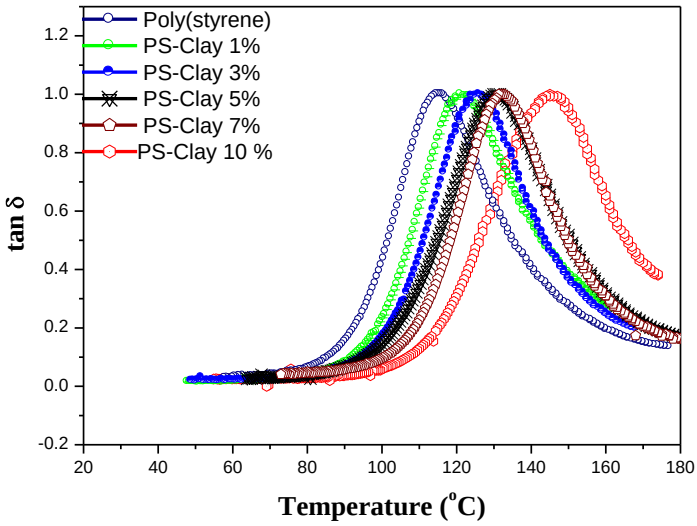

Fig. 7.11: Tan δ as a function of temperature for PS-clay nanocomposites prepared at different clay loadings.

This is also coupled to broadening of the tan δ peaks, which is generally attributed to a distribution of degrees of chain mobility restriction brought about by clay filler.[46,49,52]The glass transition temperature (T_g) of nanocomposites taken from the tan δ peaks was at a higher temperature than that for neat PS and increased slightly with increase in clay content, as seen in Fig.7.11 T_g of PCNs was greatly affected by the clay contents, PS-nanocomposites with 7 wt % and 10 wt %showed a large increase in T_g (i.e. + 30 °C) relative to the neat polymer. The reason for this is that the clay acts as a bridge between polymer chains, thus restricting polymer motion. It is worth to mention that, the low molecular weight block copolymer of PS-b-PHEA used as clay modifiers in this work, had not bring any effect on T_g values due to its low quantity relative to the PS matrix. In contrast Zhao *et al.* [48] prepared poly(methyl methacrylate)-clay nanocomposites via dispersion polymerization in the presence of poly (dimethylsioxane)-modified clay (PDMS-MMT) in supercritical carbon dioxide, and found an increase in T_g for PMMA/PDMS-clay nanocomposites of only 3 ºC (6% wt clay loading), due to the plasticizing effect of PDMS-MMT. Zhao *et al*[22] prepared the same polymer again but in the presence of fluorinated surfactant-modified clay (10F-clay) and compared the T_g values for both nanocomposites. They found that PMMA/PDMS-clay nanocomposites exhibited a limited increase in T_g compared to PMMA/10F-clay nanocomposites, because of the stronger plasticizing effect of PDMS chains than the fluorinated surfactant.

(d)Melt rheology of nanocomposite materials

Polymer melt rheological studies provide information that is similar to that of DMA and more importantly, also valuable information pertaining to the behaviour of a polymer under processing conditions prior to the formation of the final product.[60-64]

The melt rheological properties of PCNs are dependent on their molar mass, polydispersity index (PDI), clay loading and on the PCN morphology.[60,61,63,65-67] The complex viscosity of PCNs in rubbery state (at $T > T_g$) has been shown to be typically non-Newtonian in behaviour, as a result of the nanodispersion of the clay platelets.[65,68]

The storage and loss moduli have been reported to show non-terminal solid-like behaviour at low frequencies due to the presence of the clay platelets, while in the high frequency region monotonic increases in storage modulus (G') and loss modulus (G") are observed as clay loading increases.Depending on the material characteristics, the resultant response represents solid-like or liquid-like behavior.[60,61,63,69-72]Viscoelastic materials are referred as solid-like when G'>G", and as liquid-like when G'<G".Another important parameter related to the melt rheology of PCNs is the crossover frequencies (i.e. frequencies at which values of storage and loss moduli are equal), which can be related to the relaxation time of system.[73]

In order to determine the oscillation amplitude, i.e. the range within which the polymer structure is unaffected by deformation applied (the Linear Viscoelastic Range LVE), an amplitude sweep was performed at a constant frequency of 5Hz at 150°C. The LVE range corresponds to the range of amplitude sweep for which no changes in the storage and loss modulus are found. Fig 7.12 shows the effect of oscillation amplitude on the G', from 0.1 to 100% strain.

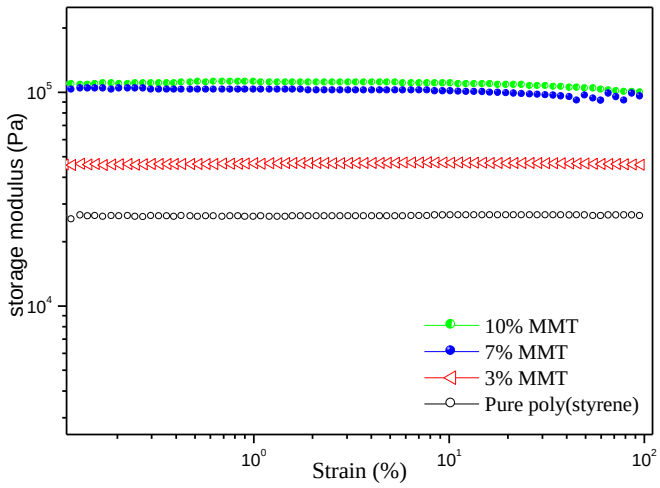

Fig 7.12: Strain amplitude sweeps for neat PS and PS-nanocomposites with different clay loadings at a constant oscillation frequency of 5 Hz at 150 °C.

Clearly the LVE range of the nanocomposites was not affected by the incorporation of clay, within the range 0.1–100% deformation strain range sweep. However, it is

noteworthy to note that none of the material tested exhibited any drop of G' within the amplitude strain range applied. On the other hand the storage modulus plateau was found to be increased with increasing clay content as reported elsewhere.[74] The subsequent frequency sweep measurements were hence carried out at 0.1% strain, which is within the reversible LVE of the materials.

Fig 7.13 depicts the change in storage modulus (a) and loss modulus (b) of PCNs with various clay loading, as a function of the angular frequency applied at a constant shear strain amplitude of 0.1% within the LVE range at T= 150 ºC. Both storage and loss moduli were found to increase monotonously with angular frequency as reported in elsewhere.[75-77] This is due to the fact that at low frequency, the time scale is large enough to unraveling of the entanglements due to the relaxation time being shorter than the deformation strain applied hence yielding an apparent low value of storage and loss moduli. On the other hand, when the polymer material isdeformed at higher frequencies the polymer chains relaxation time becomes higher than the strain frequency time scale, hence the apparent increase of G' and G".[76]

It was also observed that, there is a dramatic increase in both storage and loss modulus with clay loading, clearly showing that the presence of clay increases the stiffness of the material due to strong interaction between polymer and clay. [60-64,68,72] The effect of MMT content was found to be much higher at low frequencies than at high frequencies, and the increase of modulus at low frequencies is more pronounced in the storage modulus than in the loss modulus. This affect has been reported before by Krishnamoorti *et al,* [75]who described that a highly agglomerated system would show the existence of yield and high storage modulus at low frequencies, which varies minimally with frequency giving more solid-like response

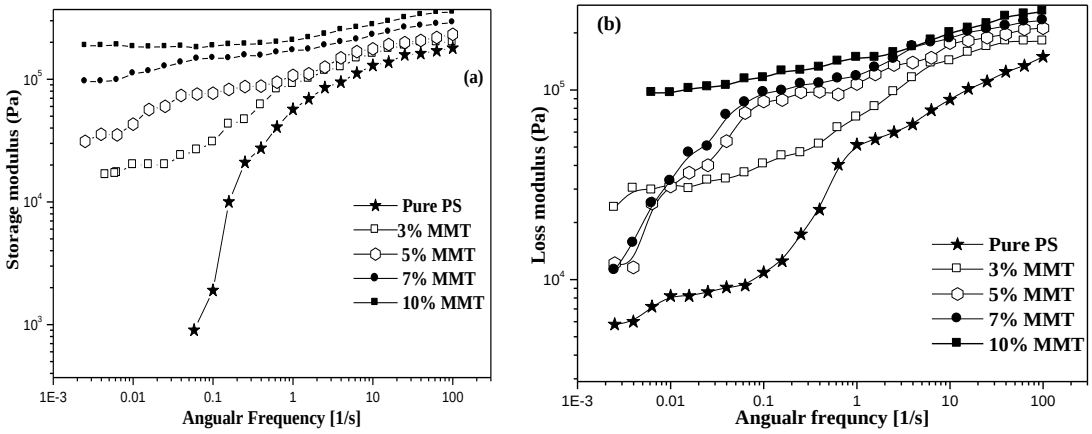

Fig. 7.13 (a) storage modulus, (b) loss modulus as a function of angular frequency for pure PS and PS-nanocomposites

In a similar manner, as the MMT content increases, a network-like structure is formed due to greater interactions between MMT, and as a result the storage modulus at low frequencies shows a dramatic increase. Thus, it can be said that the unique rheological response of the PS-nanocomposites is dominated by the degree of the formation of MMT network-like structure. The G' curve of the neat polymer did not show any low frequency plateau as did samples with higher clay loading. The reason for this is that in the case of PCNs, polymer and clay form an interconnected 3-dimensional network structure.[73,78] The 3-D network structure is a characteristic of highly filled polymers in which a percolated structure is formed. The plateau behavior has been reported to be an indication that PCNs act as solid-like viscoelastic materials in the frequency domain considered, or as viscoelastic fluids with infinitely long relaxation time.[79]

According to linear viscoelastic theory, in the terminal region (where frequency approaches 0), *G*' and *G*" are proportional to 2 and 1, respectively. In other words, the slopes of log(*G*') versus log(ω) and log(*G*") versus log(ω) at low frequencies (i.e. terminal zone) should be equal to 2 and 1, respectively.[60,61,66]

G' and G" crossover frequencies and corresponding relaxation times are reported in Table 7.3.The relaxation times of all PS-nanocomposites were found to be greater than that of

the neat PS, and for PCNs the relaxation time increases with clay loading. This is to be expected, since an increase in clay loading results in highly confined polymer chains; as such long-range relaxation processes take place over a longer period of time, this is was reported elsewhere.[69]

The terminal slope in the low frequency region was found to be decreased with the clay content as seen in Table 7.3,implying that, the flow properties in this region change to more solid-like type due to the addition of MMT, which promotes MMT- polymer interaction.[69]

Table 7.3: Slopes of log G' and log G" in the low-frequency region for PS-nanocomposites

Polymer	slope of G'	Slope of G"	* ω_c(rad/s)	**T (s)
PS	1.70	1.54	0.96	6.54
PS-3%	2.04	1.97	0.15	41.90
PS-5%	1.94	1.83	0.056	112.30
PS-7%	1.93	1.76	-	
PS-10%	1.63	1.73	-	

* ω_c =crossover angular frequency and **T = relaxation times calculated using the relation T = $2\pi/\omega$.

The terminal gradients of PS-nanocomposites decreased with an increase in clay loading, as reported by others.[63,72,80] The terminal gradients decreased from those typical of homopolymer behaviour, i.e. $G' \propto \omega^2$ and $G'' \propto \omega^1$, to levels where the solid-liquid behaviour dominates, here G' > G" at higher clay loadings, which is in agreement with literature.[81] The decreasing of terminal slopes indicating that, a transition of the slopes to a flattened behavior with an increase in the clay loading, that is, non-terminal behavior, is observed at low frequencies. Therefore, the low-frequency response is indicative of solid-like behavior with an increase in the amount of clay >5wt% clay loading, while at the lowest frequencies for clay loading below 5wt%, the response of the system exhibits

liquid-like behavior (*G"*> *G*'). It is very clear that MMT loading had a strong impact on the flow properties of PS-nanocomposites. At relatively high clay concentrations (such as 5 wt %), the distance between the clay layers is comparable to or even smaller than the size of a single layer of clay, this increases the frictional interactions between the MMT layers that form a percolating network giving the solid-like behaviour. Solar *et al*[79] who studied the viscoelastic behaviour of epoxy-clay nanocomposites, and reported that the change in the value of the terminal slope (the slope of G' at low frequencies) was found to be strongly dependent on the clay loadings.

The two moduli soon become equal and display nearly a plateau region, having higher *G*' than *G*". In this region, PCNs show solid-like behavior. This characteristic transition (from liquid-like to solid-like behavior) shifts to the low frequency region as the MMT loading increases. The crossover points occur at angular frequencies of 0.96, 0.15 and 0.05 rad/s for pure PS and PCN with 3% and 5% clay loadings, respectively. This is an indication of an increase of the relaxation time of the polymer chains as the clay loading increases as seen in Table 7.3, which consequently enlarge the frequency range for which the clay-containing materials exhibit a solid-like viscoelastic behaviour.[60,82] The terminal slopes and the absolute values of the dynamic moduli are related to the supermolecular structure of the PCNs. The higher the *G*' and the smaller the terminal slope, the more pronounced the intercalation of polymer chains between the silicate platelets and their tendency to form a three-dimensional superstructure. For more than 5 wt% clay loadings (*intercalated structure*), the nanocomposites did not exhibit any crossover between G' and G" even at very low angular frequency (cf. Table 7.3). The storage modulus (G'), which is an indication of the elastic character of material increases remarkably with clay loadings, due to a strong interaction between PS chains and clay.[83]Consequently the intercalated PCNs samples with % clay $\geq$ 5 wt% showed typical solid-like behaviour throughout the frequency range studied. This is in agreement with Hyun *et al.* [84] who studied the rheological properties of poly(ethylene oxide)/organoclay nanocomposites, and suggested that beyond a critical volume fraction, the tactoids and individual layers are incapable of rotating freely hence hindering a complete relaxation when subjected to

periodic shear. This incomplete relaxation due to the physical jamming or percolation leads to the presence of the solid-like behavior observed in intercalated nanocomposites.

The complex viscosity of PCNs with various clay loadings was determined at 150 ºC, using an angular frequency range of 100-0.1 rad/sec, and plotted in Fig 7.14 as a function of angular frequency.

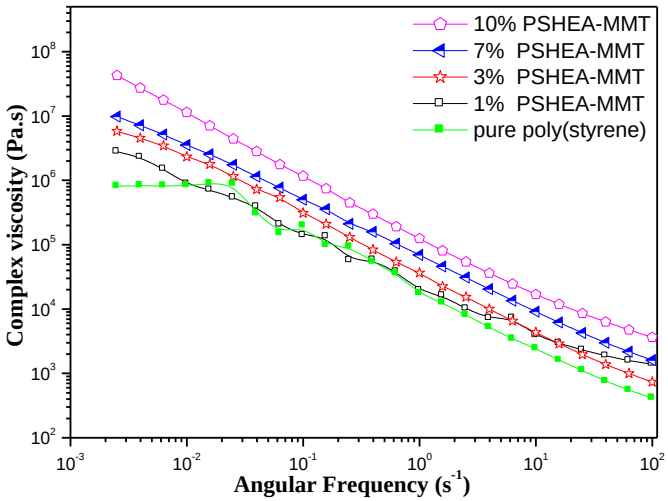

Fig 7.14: Complex viscosity of various PS-nanocomposites as a function of angular frequency at 150 °C.

PS and its nanocomposites showed high complex viscosities which decreased with an increase in the angular frequency, the complex viscosities of PCNs at temperature above T_g depends on number of factors: (i) molecular weight (ii) clay loadings and (iii) PCN morphology.[83,85] In this study an increase of complex viscosity with increasing clay content was observed although the nanocomposites had lower molecular weight than neat polymer, showing that the complex viscosity is dominated by the clay loadings for these PCNs series. For example PCN at 10 wt% shows higher complex viscosity than other nanocomposites despite of its intercalated structure and lower molar mass with respect to other PCNs. Such an increase in the complex viscosity with incorporation of clay has been reported to be caused by the occurrence of interaction between the dispersed clay filler and the polymer matrix.[73] Fig 7.14 shows also that all samples exhibited shear

thinning behaviour even that for neat polymer. The shear thinning in PCNs is not only due to disentanglement of polymeric chains under shear strain, but also due to the alignment of the clay platelets along the shearing planes.[73,86] A similar trend was observed by Krishnamoorti *et al* [87] for a series of intercalated poly(dimethyldiphenylsiloxane)/ silicate nanocomposites, and found that the more pronounced shear-thinning characteristic with increasing clay content is attributed to the ability of the clay to orient in the direction of shear under high shear stress or high angular frequencies.

7.4 Conclusions

The amphiphilic block copolymer of PS-b-PHEA has been successfully used as stabilizer compound in dispersion polymerization of styrene using AIBN as initiator. Spherical PS particles were obtained and the particle sizes decreased with an increase in the amount of block copolymer used. MMT clay layers pre-modified with the amphiphilic block copolymer PS-b-PHEA has also been used as a stabilizer in dispersion polymerization of styrene in alcoholic medium (ethanol/water). The average size of the PS colloid particles decreased with an increase in the amount of (PS-b-PHEA)-MMT used. PS colloid particles obtained were found to be armoured by (PS-b-PHEA)-MMT layers. Visually stable armoured colloidal polymer particles were obtained with up to 5% wt (PS-b-PHEA)-MMT. The corresponding nanocomposite cast film were found to be of partially exfoliated morphology at low clay loadings, and intercalated morphology as the clay loading increased, which was confirmed by SAXS and TEM. All nanocomposites were thermally more stable than the neat polymer, and the improvement in thermal stability was greatly affected by %clay loading. An increase in the storage modulus and the T_g of the PCNs was found and correlated to the clay loadings.The melt flow properties of PCNs was found to be strongly dependent on the clay loading, with a shift observed from liquid-like viscoelastic to solid-like viscoelastic behaviour as the clay content increased due to percolation of the clay network within the PS matrix taking place upon film formation above the T_g

7.5 References

1. Voorn, D.; Ming, W.; van Herk, A. M. *Macromolecular Symposia* **2006,** 245, 585-590.

2. Voorn, D.; Ming, W.; van Herk, A. M. *Macromolecules* **2006,** 39, 4654-4656.

3. Rieger, J.; Osterwinter, G.; Bui, C.; Stoffelbach, F.; Charleux, B. *Macromolecules* **2009,** 42, 5518-5525.

4. Thomson, M.; Manley, A.; Ness, J.; Schmid, S.; Cunningham, M. *Macromolecules* **2010,** 43 7958-7963.

5. Bourgeat-Lami, E.; Guimaraes, T.; Pereira, A.; Alves, G.; Moreira, J.; Putaux, J.; Santos, A. *Macromolecular Rapid Communications* **2010,** 31, 1874-1880.

6. Binks, B. P.; Lumsdon, S. O. *Langmuir* **2001,** 17, 4540-4547.

7. Guillot, S.; Bergaya, F.; Azevedo, C.; Warmont, F.; Tranchant, J. *Journal of Colloid and Interface Science* **2009,** 333, 563-569.

8. Micusík, M.; Bonnefond, A.; Reyes, Y.; Bogner, A.; Chazeau, L.; Plummer, C.; Paulis, M.; Leiza, J. *Macromolecular Reaction Engineering* **2010,** 4, 432-444.

9. Liu, J.; Gan, L.; Quek, C.; Gong, H.; Gan, L. *Journal of Polymer Science Part A: Polymer Chemistry* **1997,** 35, 3575-3585.

10. Tseng, C.; Lu, Y.; El-Aasser, M.; Vanderhoff, J. *Journal of Polymer Science, Part A: Polymer Chemistry* **1986,** 24, 347-354.

11. Ober, C.; Lok, K. *Macromolecules* **1987,** 20, 268-273.

12. Paine, A.; Winnik, F. *Langmuir* **1989,** 5, 903-910.

13. Kim, O.; Lee, K.; Kima, K.; Lee, B.; Choe, S. *Polymer* **2006,** 47 1953-1959.

14. Cho, S.; Ryu, J. H.; Jun, J. B.; Sun, K. D. *Colloid and Polymer Science* **2005,** 284, 266-275.

15. Lee, K.; Seo, H. *Korea Polymer Journal* **1998,** 6, 405-413.

16. Stark, H. *Physics Reports* **2001,** 351, 387-474.

17. Cho, Y.; Yang, J.; Lee, J. *Materials Science and Engineering A* **2004,** 24, 293-304.

18. Georges, M.; Vergin, R.; Kazmair, P.; Hamer, G. *Macromolecules* **1993,** 26, 2987-2995.

19. Wang, J.; Matyjaszewski, K. *Macromolecules* **1995,** 28, 7901-7911.

20. Moad, G.; Chiefari, J.; Chong, Y.; Krstina, J.; Mayadunne, R.; Postma, A.; Rizzardo, E.; Thang, S. *Polymer International* **2000,** 49, 993-1002.

21. Greesh, N.; Hartmann, P.; Sanderson, R. *Macromolecular Materials and Engineering* **2009,** 294, 206-212.

22. Zhao, Q.; Samulski, E. T. *Macromolecules* **2005,** 38, 7967-7971.

23. Negrete-Herrera, N.; Putaux, L.; David, L.; Bourgeat-Lami, E. *Macromolecules* **2006,** 39, 9177-9184.

24. Zhang, J.; Yang, Y.; Zhao, C.; Zhao, H. *Journal of Polymer Science, Part A: Polymer Chemistry* **2007,** 45, 5329-5338.

25. Yang, Y.; Zhang, J.; Liu, L.; Zhao, H. *Journal of Polymer Science Part A: Polymer Chemistry* **2007,** 45, 5759-5769.

26. Yang, Y.; Liu, L.; Zhang, J.; Li, C.; Zhao, H. *Langmuir* **2007,** 23, 2867-2873.

27. Lebaron, P. C.; Wang, Z.; Pinnavaia, T. J. *Applied Clay Science* **1999,** 15, 11-29.

28. Wang, H.; Chang, K.; Chu, H. *Polymer International* **2005,** 54, 114-119.

29. Jialanella, G.; Firer, E.; Piirma, I. *Journal of Polymer Science, Part A: Polymer Chemistry* **1992,** 30, 1925-1932.

30. Baines, F.; Dionisio, S.; Billingham, N. C.; Armes, S. *Macromolecules* **1996,** 29, 3096-3102.

31. Lee, J. M.; Shim, S. E.; Choe, S. *Industrial & Engineering Chemistry Research* **2006,** 12, 648-651.

32. Lee, J.; Ha, J.; Choe, S.; Lee, C.; Shim, S. *Journal of Colloid and Interface Science* **2006,** 298, 663-671.

33. Bon, S.; Colver, P. *Langmuir* **2007**, 8316-8322.

34. Tong, Z.; Deng, Y. *Macromolecular Materials and Engineering* **2008,** 293, 529-537.

35. Schmid, A.; Fujii, S.; Armes, S. P. *Langmuir* **2006,** 22, 4923-4927.

36. Bourgeat-Lami, E.; Lang, J. *Journal of Colloid and Interface Science* **1998,** 197, 293-308.

37. Percy, M.; Michailidou, V.; Armes, S. *Langmuir* **2003,** 19, 2072-2079.

38. Kim, S.; Lim, J.; Park, B.; Choi, H. *Macromolecular Chemistry and Physics* **2007,** 208, 514-519.

39. Shay, J. S.; English, R. J.; Spontak, R. J.; Balik, C. M.; Khan, S. A. *Macromolecules* **2000,** 33, 6664-6671.

40. Esfandiari, A.; Nazokdast, H.; Rashidi, A.; Yazdanshenas, M. *Journal of Applied sciences* **2008,** 8, 545-561.

41. Yan, C.; Ma, L.; Yang, J. *Journal of Applied Polymer Science* **2005,** 98, 22-28.

42. Kaya, A.; Yukselen, Y. *Journal of Hazardous Materials* **2005,** 120, 119-126.

43. Zhang, J.; Chen, K.; Zhao, H. *Journal of Polymer Science Part A: Polymer Chemistry* **2008,** 46, 2632-2639.

44. Wu, Y.; Zhang, J.; Zhao, H. *Journal of Polymer Science Part A: Polymer Chemistry* **2008,** 47, 1535-1543.

45. Wang, J.; Du, J.; Zhu, J.; Wilkie, C. A. *Polymer Degradation and Stability* **2002,** 77, 249-252.

46. Ray, S.; Okamoto, M. *Progress in Polymer Science* **2003,** 28, 1539-1641.

47. Blumstein, A. *Journal of Polymer Science, Part A: Polymer Chemistry* **1965,** 3, 2653-2661.

48. Zhao, Q.; Samulski, E. T. *Polymer* **2006,** 47, 663-671.

49. Tjong, S. C. *Materials Science and Engineering* **2006,** 53, 73-197.

50. Qutubuddin, S.; Fu, X. *Polymer* **2001,** 42, 807-813.

51. Kawasumi, M.; Hasegawa, N.; Kato, K.; Usuki, A.; Okada, A. *Macromolecules* **1997,** 30, 6333-6338.

52. Xu, M.; Choi, Y. S.; Kim, Y. K.; Wang, K. H.; Chung, I. J. *Polymer* **2003,** 44, 6387-6395.

53. Zhao, C.; Qin, H.; Gong, F.; Feng, M.; Zhang, S.; Yang, M. *Polymer Degradation and Stability* **2005,** 87 183-189.

54. Li, H.; Yu, Y.; Yang, Y. *European Polymer Journal* **2005,** 41, 2016-2022.

55. Khan, A.; Shamsi, M.; Choi, T. *Computational Materials Science* **2009,** 45, 257-265.

56. Dong, Y.; Bhattacharyya, D. *Composites: Part A* **2008,** 39, 1177-1191.

57. Pavlidoua, S.; Papaspyrides, C. *Progress in Polymer Science* **2008,** 33, 1119-1198.

58. Maiti, P.; Nam, P.; Okamoto, M. *Macromolecules* **2002,** 35, 2042-2049.

59. Xu, M.; Choi, Y. S.; Wang, K. H.; Kim, J. H.; Chung, I. *Macromolecular Research* **2003,** 11, 410-417.

60. Krishnamoorti, R.; Giannelis, P. *Macromolecules* **1997,** 30, 4097- 4102.

61. Ren, J.; Silva, A.; Krishnamoorti, R. *Macromolecules* **2000,** 33, 3739-3746.

62. Moad, G.; Rizzardo, E.; Solomon, J.; Willing, I. R. *Macromolecular Rapid Communications* **1984,** 5, 793-798.

63. Okada, K.; Mitsunaga, T.; Nagase, Y. *Korea-Australia Rheology Journal* **2003,** 15, 43-50.

64. Meincke, O.; Hoffmann, B.; Dietrich, C.; Friedrich, C. *Macromolecular Chemistry and Physics* **2003,** 204, 823-830.

65. Fornes, T. D.; Yoon, P. J.; Keskkula, H.; Paul, D. *Polymer* **2001,** 42, 9929-9940.

66. Galgali, G.; Ramesh, C.; Lele, A. *Macromolecules* **2001,** 34, 852-858.

67. Xu, M.; Choi, Y. S.; Kim, Y. K.; Wang, K. H.; Chung, I. J. *Polymer* **2003,** 44, 6387-6395.

68. Zhao, J.; Morgan, B.; Harris, D. *Polymer* **2005,** 46, 8641-8660.

69. Lim, T.; Lee, H.; Choi, J.; Jhon, S. *Journal of Polymer Science Part B: Polymer Physics* **2003** 41, 2052-2061.

70. Ma, Y.; Tong, F.; Xu, B.; Fang, P. *Polymer Degradation and stability* **2007,** 92, 1439-1445.

71. Moraes, P.; Santos, M.; Oliveira, C.; Souza, T.; Amaral, M.; Valera, S. *Macromolecular Symposia* **2006,** 245, 106-115.

72. Kim, T. H.; Lim, S. T.; Lee, C. H.; Choi, H. J.; Jhon, M. S. *Journal of Applied Polymer Science* **2003,** 87, 2106-2112.

73. Lee, M.; Park, J.; Gupta, K.; Bhattachary, N. *Journal of Macromolecular Science: Part B: Physics* **2007,** 46, 261-273.

74. Zhong, W.; Qiao, X.; Sun, K.; Zhang, G.; Chen, X. *Journal of Applied Polymer Science* **2006,** 99, 1523-1529.

75. Krishnamoorti, R.; Yurekli, K. *Colloid and Interface Science* **2001,** 6, 464-470.

76. Mishra, J.; Hwanga, K.; Ha, C. *Polymer* **2005,** 46, 1995-2002

77. Kim, T.; Lim, T.; Lee, H.; Choi, H.; Jhon, S. *Journal of Applied Polymer Science* **2003,** 87, 2106-2112.

78. Lotti, C.; Branciforti, S.; Alves, M.; Liberman, S.; R.Bretas. *European Polymer Journal* **2008,** 44, 1346-1357.

79. Solar, L.; Nohales, A.; Muno-zespi, R.; Lopez, D.; Gomez, C. *Journal of Polymer Science: Part B: Polymer Physics* **2008,** 46, 1837-1844.

80. Ma, H. Y.; Tong, L. F.; Xu, Z. B.; Fang, Z. P. *Polymer Degradation and Stability* **2007,** 92, 1439-1445.

81. Zhao, J.; Morgan, A. B.; Harris, J. D. *Polymer* **2005,** 46, (20), 8641-8660.

82. Zidelkheir, B.; Boudjemaa, S.; Abdel-Goad, M.; Djellouli, B. *Iranian Polymer Journal* **2006,** 15, 645-653.

83. Sohn, J.; Lee, C. H.; Lim, S. T.; Kim, T. H.; Choi, H. J.; Jhon, M. S. *Journal of Materials Science* **2003,** 38 1849-1852.

84. Hyun, Y.; Lim, S.; Choi, H.; Jhon, M. *Macromolecules* **2001,** 34, 8084-8093.

85. Samakande, A.; Sanderson, R.; Hartmann, P. *Polymer* **2009,** 50, 42-49

86. Park, B.; Kim, T.; Choi, H.; Lee, J. *Journal of Macromolecular Science: Part B: Physics* **2007,** 46, 341-354.

87. Krishnamooti, R.; A.Vaia, R.; Giannelis, E. P. *Chemistry of Materials* **1996,** 8, 1728-1737.

Conclusions and Recommendations

8.1 Conclusions

- Fully exfoliated PS/clay nanocomposites were successfully synthesized for the first time via dispersion polymerization in polar medium (ethanol/water). The particle size and molecular weight of the PS/clay nanocomposites were affected by the MPTMS-clay loading. The particles size decreased and the distribution narrowed as the clay loading increased. Exfoliated structures were obtained at low clay loading, while intercalated structures predominated at increasing clay loading. All synthesized PS/clay nanocomposites were found to be thermally more stable than the neat PS. Intercalated, high clay loading PCNs were found to be thermally more stable than exfoliated structures with low clay loading. The prepared nanocomposites also exhibited enhanced mechanical properties which were dependent on the extent of clay dispersion.

- Controlled /living polymerization of styrene and HEA via RITP was successfully achieved. Homopolymers of controlled molecular weights and with relatively narrow molecular weight distributions were prepared. The reaction kinetic profile of the RITP process for styrene was found to be different from HEA. In RITP of HEA the inhibition time is much shorter than the one observed for styrene, the mechanism of styrene in RITP was found to be more complicated than HEA. The structure of polymer produced was confirmed by various analytical techniques (^{1}H-NMR, FT-IR and MALDI-TOF), and found to be in

good agreement with the expected structure (A-M_n-I). RITP can be used for the synthesis of functional PS-I and PHEA-I polymers of controlled molecular weights. Finally, from a PS-I macroinitiator (capped with iodine), and upon addition of a second monomer the amphiphilic block copolymer PS-b-PHEA was successfully synthesized via RITP, illustrating the living nature of the process. This is the first report on the synthesis of this kind of diblock copolymers by such a straightforward controlled radical polymerization method, RITP. The successful formation of the block copolymer PS-b-PHEA was confirmed by GPC and further analyzed using HPLC in toluene/DMF systems.

- Low molecular weights of PS-cationic were successfully synthesized by a simple reaction between PS-I and DMEA. Analysis by FT-IR, ^{1}H-NMR and MALDI-TOF indicated the replacement of iodine from the PS end chains by a quaternary ammonium group. The PS-cationic was successfully ion exchanged at the surface of MMT, as was confirmed by SAXS analysis showing that increasing the PS-cationic concentration caused an increase in *d*-spacing from 1.14 nm (for virgin MMT) up to 1.93 nm for PS-MMT. Furthermore TGA indicated that the complete ion-exchange was never obtained even with excess of PS-cationic this is due to bulkiness of the oligomeric PS-cationic. The attachment between PS-cationic and clay was found to be strongly dependent on the polarity of the modification medium, the modification of clay by PS-cationic was only successful in polar medium (THF),and was unsuccessful in non-polar solvent (toluene). The cationic block (PS-b-PHEA)-cationic was also obtained by reaction of (PS-b-PHEA)-I with TEA. The interaction of(PS-b-PHEA)-cationic with claywas found to be occurring via both ion-exchange process and adsorption. (PS-b-PHEA)-cationic can adsorb

onto the surface of the clay galleries in several ways: by formation of H-bonding, Van der Waals forces, and ion exchange. These interactions lead to an increase in the basal spacing relative to pristine MMT (1.14 nm for virgin MMT up to 2.09 nm for modified clay).

- PS-nanocomposites in dispersion polymerization were successfully synthesised using PS-MMT as stabilizers, the morphology of nanocomposites obtained was found to be strongly dependent on the hydrophobicity of clay. The clay particles were simply modified with different amounts of PS-cationic (25%, 65% and 100% CEC) via ion-exchange reaction. The clay particles were encapsulated into PS latex with partially exfoliated structure at 100% CEC, and the final latex is stable up to 5% wt of clay in the polymer. While the clay particles were distributed in between water phase and oil phase with intercalated structures at 25% and 65% CEC, with unstable final polymer latex due to insufficient colloidal stability afforded by partially modified PS-MMT that adsorbed onto the particles. The particle sizes of PS-nanocomposites were also affected by the degree of modification and clay loadings, the particle sizes were generally decreasing with clay loading, however the particle size of PS-nanocomposites prepared using clay modified with 25% and 65% CEC of PS-cationic decreased to greater extent than that of PS-nanocomposites prepared with clay modified with 100% CEC PS-cationic. The thermal stability of PS-nanocomposites was found be directly correlated to the morphology of nanocomposites obtained and not to the amount of clay incorporated. On the other hand thermo-mechanical properties and the T_g of PS-nanocomposites were found to be strongly dependent on both: nanocomposites morphology, and clay loading.

- Clay layers modified by amphiphilic copolymer (PS-b-PHEA)-MMT were successfully used as efficient stabilizers in dispersion polymerization of styrene in alcoholic medium. The average size of PS colloid particles decreased with an increase of (PS-b-PHEA)-MMT concentrations. PS colloid particles armored by clay layers modified by PS-b-PHEA whereas the PS particles were completely covered by clay platelets, stable polymer latex were obtained up to 5 wt% (PS-b-PHEA)-MMT. The nanocomposites were of partially exfoliated morphology at low clay loadings, and changed to intercalated morphology as the clay loading increased. All nanocomposites were thermally more stable than the pure polymer, the improvement in thermal stability was greatly effected by clay content. Thermo-mechanical properties of nanocomposites were enhanced with respect to pure polymer. The melt flow properties of PCNs was found to be strongly dependent on the clay loading, with shift observed from liquid-like viscoelastic to solid-like viscoelastic behaviour as the clay content increased due to percolation of the clay network within the PS matrix taking place upon film formation above T_g.

8.2 Recommendations for future work

- Synthesize polymers and block copolymers with different molecular weight range using RITP, and study the effect of molecular weights on terms of MMT modification and dispersion polymerization stability.
- Synthesize block copolymers of PS-b-HEA with different composition in order to study the effect of different copolymer composition on the efficiency of block copolymer stabilization.

- Study of the kinetics of the dispersion polymerization in the presence of MMT. Study of kinetics of polymerization is useful for the academic understanding of the reaction process and for industrial PCN preparation.

- The on line coupling of TEM and XRD insitu so as to look at the changing morphology of the nanocomposites with conversion. Such a study will provide vital information about the PCN formation, hence factors that affect PCN formation.

- Study the effect of the time needs for monomer diffusion inside MMT galleries.